UNCOVERING THE ROLE OF EAF1 IN THE REGULATION OF LIPID SYNTHESIS AND MEMBRANE COMPOSITION IN *SACCHAROMYCES CEREVISIAE*

Sarah Laframboise

Thesis submitted to the University of Ottawa
in partial Fulfillment of the requirements for a Doctorate in Philosophy, Biochemistry, Specializing in Human and Molecular Genetics.

Department of Biochemistry, Microbiology and Immunology
Faculty of Medicine
University of Ottawa

Abstract

The yeast lysine acetyltransferase NuA4 has been implicated in regulating various aspects of metabolism, including a poorly defined role in lipid homeostasis. While classically known to acetylate histones, regulating gene expression, NuA4 also targets several non-histone proteins for acetylation. Here, I use a combination of functional genomics and fluorescent microscopy to define a novel role for NuA4 in regulating phospholipid availability for organelle morphology. First, I characterized that disruption of the NuA4 complex resulted in 70% of cells displaying deformed nuclei and nearly 50% of cells exhibiting high levels of vacuolar fragmentation. Interestingly, the deformed nuclei appeared to occur at all stages of the cell cycle, indicating an underlying dysregulation of lipids driving phospholipid metabolism. With deletion or mutation of additional genes involved in phospholipid synthesis, I was able to partially rescue nuclear deformation but not vacuolar fragmentation. To investigate the cause of these phenotypes further, I probed whether there could be a defect in a critical autophagy process known as piecemeal microautophagy of the nucleus (PMN). PMN acts to selectively degrade excess nuclear membrane into the vacuole and is performed at the nuclear-vacuole junction (NVJ). Interestingly, cells deficient in NuA4 also showed severe defects in the formation of NVJ and the function of PMN. To determine the cause of these defects, I sought to determine if these phenotypes were due to an uncharacterized relationship between NuA4 and Pah1, an enzyme that converts phosphatidic acid into diacylglycerol, which favours the accumulation of lipid droplets over phospholipids that are used for membrane expansion. NuA4 subunit Eaf1 was required for Pah1 localization to the inner nuclear membrane, and artificial tethering of Pah1 to the nuclear membrane rescued nuclear flare and vacuole fragmentation defects but not defects related to the formation of NVJs. Mutation of a candidate NuA4 acetylation site on Pah1 also resulted in aberrant Pah1 localization and defects in membrane morphology and NVJ. This work defines a critical role for NuA4 modification of Pah1 in the regulation of lipid pools that define the characteristics and function of organelle membranes. Given the high level of conservation of NuA4 with the human Tip60 complex, as well as Pah1 with human lipin, this work is highly relevant to human disease.

Authorship

Manuscript #1:

Laframboise, SJ*, Deneault, LD, Denoncourt, A, Downey, M, Baetz, K,. (2024) ***Uncovering the role of the yeast lysine acetyltransferase NuA4 in the regulation of nuclear shape and lipid metabolism.*** *Molecular and Cellular Biology*. 44:7,273-288, https://doi.org/10.1080/10985549.2024.2366206

Manuscript #2 (Appendix B)

Walden, EA, Fong, RY, Pham, TT, Knill, H, **Laframboise, SJ*,** Huard, S, Harper, ME, Baetz, K. (2020) ***Phenomic screen identifies a role for yeast lysine acetyltransferase NuA4 in the control of Bcy1 subcellular localization, glycogen biosynthesis, and mitochondrial morphology.*** *PLOS Genetics*. 2020;16(11): e1009220. http://dx.doi.org/10.1371/journal.pgen.1009220.

Manuscript #3 (Appendix C)

Laframboise, SJ*, Bailey, T, Dang, A, Rose, M, Zhou, Z, Berg, M, Holland, S, Abdul, SA, El-Sahli, S, Boucher, DM, Fairman, G, Deng, J, Shaw, K, Noblett, N, D'Addario, A, Empey, M, Sinclair, K. (April 2023) ***Analysis of financial challenges faced by graduate students in Canada****. Biochemistry and Cell Biology*. 101:326-260 (2023). dx.doi.org/10.1139/bcb-2023-0021

Acknowledgements

Thanking everyone who has played a part in my graduate school journey seems impossible, but here it goes:

To begin, I would like to honour and remember the late Dr. Marie Öhman who took a chance on a Canadian exchange student and welcomed me into her lab as an undergraduate student at Stockholm University. Your legacy inspired me to continue on to pursue a career in science, and I am forever grateful for your kindness.

Next, to my supervisor, Dr. Kristin Baetz. Thank you for your leadership and guidance over the last six years. Not only did you mold me into the scientist that I am today, but also the person and leader that I am now. Thank you for giving me the space to explore my passions and for inspiring my love for science communication. I look forward to continuing to run into you professionally in the future! To all the past members of the Baetz Lab, Dr. Eugene Fletcher, Dr. Elizabeth Walden, Kevin Mercurrio, Sangavi Sivananthan, Lauren Deneault, Dr. Jessica Gosse and Dr. Sylvain Huard, thank you for the countless memories, it is these that I will miss the most.

To Dr. Michael Downey, thank you for welcoming me into your lab and your invaluable support in the completion of my PhD. And a big thanks to the members of the Downey lab, including Dr. Amanda Bentley-DeSousa, Kanchi Baijal, Alix Denoncourt, Liam McCarthy, Cameron Gibson and others. Additionally, I would like to thank Dr. Mary-Ellen Harper and Dr. Damien D'Amours for their guidance and support as members of my Thesis Advisory Committee.

I had the unique experience and immense honour of become a national voice for graduate students in Canada over the last few years. From representing graduate student in the House of Commons, the Senate, in rallies, on the media and talk shows, this work gave my graduate experience a deeper meaning, and opened my eyes up to a career I never knew existed. I would like to additionally thank my incredible team at Support Our Science, Dr. Marc Johnson, Dr. Courtney Robichaud, Dr. Andrea Wishart, Kaitlin Kharas, and many others, for your friendship and leadership. Additionally, to my team at the Ottawa Science Policy Network for trusting in and creating a platform for science policy at the University of Ottawa. Collectively, these efforts resulted in nearly $3.5 Billion dollars in funding that will directly increase salaries for graduate students and postdoctoral scholars in Canada. I will forever be grateful to all those who have followed, supported and engaged with us over the last several years!

Finally, to my biggest cheerleaders: my friends and family.

To my mom, thank you for pretending to understand my PhD and for the countless phone calls of support. You blindly follow me into every battle I enter, and I am eternally grateful for you. To the rest of my family – my dad, step-dad, uncle Kenny, my brothers: Carter, Jake (and Alexa), Owen, Aiden, and many others – thank you for believing in me and supporting me from a far. You have all inspired and supported my love for science for as long as I can remember. I may not come from a family of scientists, but you all show that I come from a family that knows the value of hard work. It is this determination that truly got me through my PhD. To my in-laws, thank you for never batting an

eye when I go deep into explaining a scientific topic on the news, and for always supporting my continued education over all these years.

To my friends, Michael and Brittany, thank you for making Ottawa a home. I am so grateful for your unwavering support of my PhD. Thank you for knowing when I needed a night out, a proofread and/or a hug. To my best friend, Renata, you may be 14228 kilometers away but you have been there for me every step of the way. Thank you for helping me with my computer science and math homework 12 years ago, and making me actually learn calculus. I couldn't have done graduate school without it, or you. To the countless other graduate students, peers, friends, and teammates I have had the pleasure of knowing through this degree, thank you for your support, kindness and friendship.

To my partner, Chase. You should receive an honorary doctorate for your contribution to this work. Thank you of pushing me when I needed, being a shoulder to cry on, and for literally holding my hand as I finished my last experiments. On my hardest days, you always give me a reason to smile and I am the luckiest person alive to have you as a partner for life. And finally, to our crazy dog Billie. Your endless energy always gives me a reason to enjoy the outdoors. There's nothing like the unconditional love of a dog to brighten your day.

Table of Contents

List of Figures

List of Tables

List of Abbreviations

ACC	acetyl-CoA carboxylase
AcK	acetyl-lysine
AMP	Adenosine monophosphate
AMPK	AMP activated kinase
ATP	adenosine triphosphate
BiFC	BiFluorescent Complementation Assay
CDK1	Cyclin-dependent kinase-1
CDP-DAG	Cytidine diphosphate diacylglycerol
CMAC	CellTracker Blue CMAC (7-amino-4-chloromethylcoumarin)
CPC	chromosome passenger complex
CRISPR	clustered regularly interspaced short palindromic repeats
DAG	diacylglycerol
Dgk1	diacylglycerol kinase
DMA	deletion mutant array
DNA	deoxyribonucleic acid
DSB	double stranded breaks
dsDNA	double stranded DNA
EAF1	Esa1p-associated factor
EM	electron microscopy
ER	endoplasmic reticulum
G3P	glycerol-3-phosphate
GEF	guanine nucleotide exchange factor
GFP	green fluorescent protein
GNAT	GCN5-related N-acetyltransferases
GPAT	glycerol-3-phosphate acyltransferase
HAT	histone acetyltransferase
HDAC	histone deacetylase
HMG	high mobility group
ICRE	inositol/choline-responsive elements
IDRs	intrinsically disordered regions
INM	inner nuclear membrane
Ino3	inositol-3-phosphate synthase
K	lysine
KAT	lysine acetyltransferase
KDAC	lysine deacetylase
LC-MASS	Lipid chromatography-mass spectrometry
LD	lipid droplets
LPA	lysophosphatidic acid
LPAAT	lysophosphatidic acid acyltransferase
mRNA	messenger RNA
MYST	MOZ, Ybf2, Sas2, and Tip60
NAD^+	nicotinamide adenine dinucleotide
NATs	Nt-acetyltransferases
NE	nuclear envelope
NHEJ	non-homologous end joining
NPC	nuclear pore complex
NS	nitrogen starvation
Nt	N-terminal
NuA4	nucleosomal acetyltransferase of histone H4

NVJ	nuclear-vacuole junction
OD	optical density
ONM	outer nuclear membrane
PA	phosphatidic acid
Pah1	phosphatidic acid phosphatase
PAM	protospacer adjacent motif
PC	phosphatidylcholine
PHD	plant homeodomain
PE	phosphatidylethanolamine
PI	phosphatidylinositol
PI-4-P	phosphatidylinositol-4-phosphate
PKA	protein kinase A
PKC	protein kinase C
Plc1	phospholipase C
PLD	phospholipase D
PMN	Piecemeal Microautophagy of the Nucleus
PS	phosphatidylserine
PTM	post translational Modification
Q	glutamine
R	arginine
rDNA	ribosomal DNA
RFP	red fluorescent protein
RNA	ribonucleic acid
RP	regulation of phosphorylation
RPLs	reconstituted proteoliposomes
S	Serine
SAC	spindle assembly checkpoints
SAGA	Spt-Ada-Gcn5 acetyltransferase
SC	synthetic complete
SE	steryl esters
SGA	Synthetic Genetic Array
T	threonine
TAG	triacyclglycerols
TINTIN	Trimer Independent of NuA4 involved in Transcription Interactions with Nucleosomes
Tip60	tat interactive protein 60 kDa/KAT5/human NuA4
WT	wild type
VC	C-terminal half of Venus fluorescent protein
VLCFA	Very Long Chain Fatty Acids
VN	N-terminal half of Venus fluorescent protein
YEATS	Yaf9, ENL, AF9, Taf14 and Sas5
YNB	Yeast nitrogen base
YP	yeast extract peptone media
YPD	yeast extract peptone dextrose media

Chapter 1

Introduction

1.1 Introduction to Lysine Acetylation

Post translational modifications (PTMs) are common cellular mechanism that expands the variety of protein species, thereby enhancing functional diversity.[1] This diversity is essential to the cell's ability to quickly respond to internal and external factors.[2] While several other types of PTMs exist and are actively investigated, such as phosphorylation, glycosylation, acylation and ubiquitination[1], acetylation remains one of the most prevalent PTMs.[3,4] There are two prominent types of acetylation that can occur on a protein, characterized by the location of acetylation on lysine (K), N-terminal (Nt) acetylation or the Nε lysine acetylation.[4] Nt modifications can occur co- or post-translationally and are catalyzed by Nt-acetyltransferases (NATs).[4-6] Alternatively, the Nε lysine acetylation (herein referred to as lysine acetylation and depicted in **Figure 1.1**) occurs on the side chains of protein lysine residues and, unlike Nt acetylation, is reversible.[7] Adding an acetyl group onto lysine changes the electrostatic properties of the protein by preventing lysine positive charge.[7]

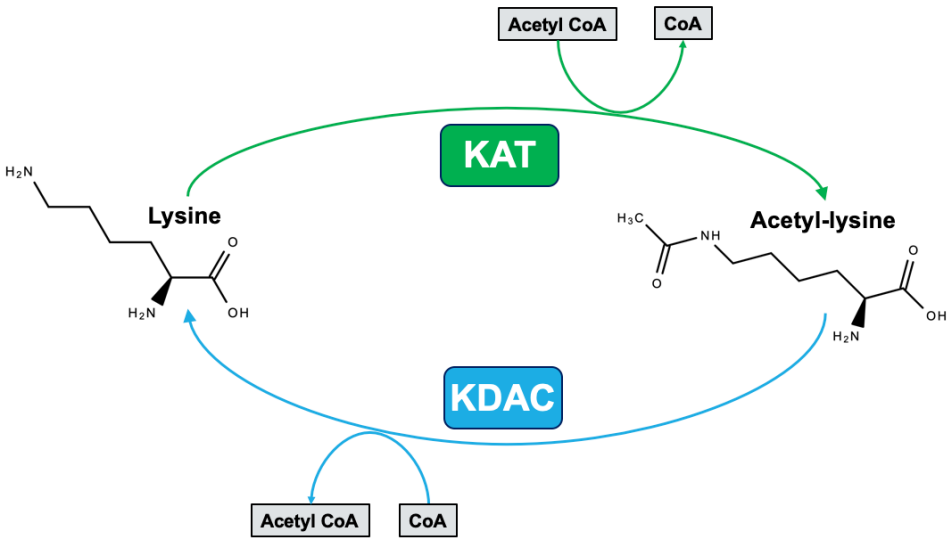

Figure 1.1 - Schematic representation of lysine acetylation and de-acetylation.

Lysine acetyltransferase (KAT) enzymes add acetyl groups onto lysine residues at the N-terminal nitrogen residue. This causes a change in the structure and charge of the residue, which utilizes acetyl-CoA. Alternatively, lysine deacetylase (KDAC) catalyzes CoA into Acetyl CoA by reversing the covalent lysine acetylation. Amino acid structures were created through www.chemspider.com.

Early studies of acetylation began investigating histone targets[8,9] and the enzymes catalyzing this reaction, which became known as histone acetyltransferases (HATs).[8] Acetylation on histones causes conformational changes resulting from a change in charge on the lysine residue that allows for improved access of the DNA to transcriptional machinery.[10] Therefore, high levels of histone acetylation typically leads to increased levels of transcription.[4] Additionally, the acetylation of histones also allows for them to be bound by proteins containing a bromodomain, a YEATS domain (Yaf9, ENL AF9, Taf14, Sas5), or a plant homeodomain (PHD).[11-13] However, it was later shown that lysine acetylation was not only restricted to histones but could occur on lysine residues within proteins.[7] Given this diverse set of targets, the name of the catalyzing enzymes was changed to lysine acetyltransferases (KATs).[14]

KATs are further broken down into three distinct families: (1) the GCN5-related N-acetyltransferases (GNAT) family,[15,16] (2) the MOZ, Ybf2, Sas2 and Tip60 (MYST) family,[17] and (3) the p300/CBP (CREB-binding protein) family.[18] Most KATs function in multi-protein complexes containing many subunits that guide the complex's catalytic capabilities and are involved in transportation to specific substrates. The actions of KATs are countered by lysine deacetylases (KDACs), which can remove acetyl groups from lysine residues (outlined in **Figure 1.1**). There are four distinct classes of KDACs based on substrate dependence, homology, and localization. Class I, II and IV are Zn^{2+}-dependent aminohydrolases and mainly localize to the nucleus and cytoplasm, while Class III, also known as sirtuins, require NAD^+ for its catalytic function.[14,19,20] The opposing actions of KATs and KDACs tightly regulate a cell's complex lysine acetylation profile.

1.1.1 Evolving research on non-histone protein acetylation targets

Acetylation of proteins results in the change in function of a protein because it alters the protein's stability, hydrophobicity or localization.[7,21] Given that lysine is also a target for several other forms of PTMs (such as ubiquitylation or SUMOylation), acetylation can block other PTMs from occurring, causing additional functional consequences.[22] While there are thousands of identified protein targets of acetylation identified in several systems (from *Escherichia coli* to *Homo sapiens*), only a handful have been functionally analyzed.[23,24] As a result, we are only starting to get a picture of the diverse role that protein acetylation plays in the cell. Some of the first proteins discovered to be acetylation were high mobility group (HMG) proteins 14 and 17 in 1981[25] and p300-mediated acetylation on p53 in 1997.[26] Since then, expansive mass spectrometry-based proteomics has continued to expand the list of non-histone protein targets of acetylation.[14,27]

Both KATs and KDACs have become increasingly relevant as therapeutic targets since their deregulation has been shown to underlie many diseases, most notably cancer [28], neurodegeneration [29], and diabetes.[30] As additional acetylation targets are uncovered, further work must be done to characterize the significance and function of non-histone acetylation. Identifying the biological outcome of acetylation on these non-histone targets will assist in understanding why KATs and KDACs contribute to disease and how they can be used in therapeutics.

1.2 Tip60, a human lysine acetyltransferase

Tip60, a Tat (trans-activator of transcription)-interactive protein 60 kDa in size, remains one of the best characterized MYST proteins, known for its role in DNA damage response and transcription.[31] True to its namesake, TIP60 was first isolated as an HIV-1 Tat interactive protein but was quickly discovered to have HAT activity on histones H2A, H3 and H4.[32-34] Tip60 exists primarily as a stable protein complex with 18 subunits, summarized and compared to NuA4 for homology in

Table 1 and **Figure 1.2**. Further work uncovered Tip60-mediated acetylation of several transcription factors, such as androgen receptor (AR),[35] upstream binding transcription factor (UBF),[36] myelocytomatosis oncogene c (c-Myc),[37] and kinase Ataxia Telangiectasia mutated (ATM).[38] The name Tip60 remains widely accepted, however, recent efforts to simplify the naming systems of KATs have denoted it as KAT5 to reflect its broader role in acetylation.[39]

Tip60 has several functions, both through its epigenetic regulation of gene expression and its non-histone protein targets of acetylation. In addition to the links between Tip60 and metabolism (outlined below), the following is a highlight of Tip60 functions (also found in **Figure 1.2D**):

1.2.1 Tip60 and Chromosome Segregation

Segregation of chromosomes is an essential process of mitosis and is highly regulated through various checkpoints that aim to ensure there is no DNA damage and that spindle attachments are assembled appropriately (governed by spindle assembly checkpoints, SACs). Aurora B serine/threonine kinase is the catalytic subunit of the chromosome passenger complex (CPC), which governs chromosome segregation through spindle and microtubule attachments.[40] As a result, Aurora b plays a vital role in the progression into mitosis, ensuring chromosome segregation occurs smoothly and error-free. [41] It has recently been shown that Tip60 acetylates Aurora B at K215, preventing it from dephosphorylation and sustaining its actions. This acetylation required Tip60 to be phosphorylated and activated by the cyclin-dependent kinase (CDK1)-cyclin B complex at Ser90.[40]

1.2.2 Tip60 and p53

The transcription factor p53 is one of the most studied human proteins. This is because over 50% of human cancers exhibit a mutation in the *p53* gene.[42] Primarily, p53 acts as a tumour suppressor. Upon DNA damage, p53 is activated through several PTMs, including acetylation by Tip60, among several other acetyltransferases.[43] Tip60-dependent acetylation occurs at K120 within

the DNA-binding domain of p53. This modification allows for p53 to transcriptionally active genes associated with cell cycle arrest and apoptosis.[44] Given the diverse roles of p53 in regulating cancer, Alzheimer's disease, and other aging-related diseases, Tip60's regulation of p53 is of high clinical significance.

1.3 *Saccharomyces cerevisiae* as a model organism to study lysine acetylation

Saccharomyces cerevisiae, commonly known as budding or brewer's yeast, provides a comprehensive and robust model to study acetylation, given its proven role as a model organism for genetic analysis. As the first eukaryotic organism to have its DNA fully sequenced,[45] *S. cerevisiae* has been fundamental to our understanding of genetics. Nearly 31% of all protein-coding *S. cerevisiae* DNA shows high levels of homology to mammalian sequences.[46] As a single-celled organism, approximately 5μm in size, *S. cerevisiae* contains a nucleus and several membrane-bound organelles. *S. cerevisiae* are known for their quick and simple growth requirements, which make it incredibly easy for them to work within a lab setting.[47] Under optimal conditions, yeast cells divide every 90 minutes through a process known as budding, which involves the budding of a daughter cell that is genetically identical to the mother cell.[47] Once the process of transformations was successfully defined to introduce *Escherichia coli* plasmids into *S. cerevisiae*, and later the integration of homologous recombination to integrate DNA fragments into the *S. cerevisiae* genome, *S. cerevisiae* became widely accepted as a model organism for genetic studies.[47-49]

Notably, KAT and KDAC complexes show a high degree of conservation between yeast and mammals, with acetylated lysines being more conserved across species than their non-acetylated counterparts.[50-52] In *S. cerevisiae*, there are 10 KDACs (Hda1, Hos1, Hos2, Hos3, Hst1, Hst2, Hst3, Hst4, Rpd3 and Sir2), 8 confirmed KATs (Eco1, Elp3, Esa1, Gcn5, Hat1, Rtt109, Sas2 and Sas3), and 6 putative KATs (Hp12, Hp13, Lys20, Lys21, Spt10 and Taf1).[23] Large-scale protein-wide

assessments and acetylome studies have identified over 2000 acetylated proteins,[2,51,53] however, only a handful have been studied for their functional consequences.

Further, *S. cerevisiae* provides a robust model to perform large-scale screening since the creation of several collections of yeast strains, most notably the deletion mutant array (DMA),[54,55] the overexpression collection,[56] and the green fluorescent protein (GFP)-tagged collection.[57] These collections allowed for the characterization of gene/protein functions through Synthetic Genetic Array (SGA) analysis, allowing for investigating query strains by generating multi-mutant collections.[58,59] The resulting combination provides for the interpretation of genetic interactions between genes of interest and has significantly contributed to our understanding of cellular functions and interactions.[58,59] SGA analysis has increased our knowledge of KATs and KDACs by providing insight into interactions with each other and other genes/proteins. For example, SGA unveiled the dynamic relationship between the KAT NuA4 and the KDAC Rpd3 in response to DNA double-stranded breaks.[60] Additionally, SGA can provide, for the first time, valuable findings on the role of mutations on the *in vitro* proteome of the cell. By deleting the KDAC *RPD3* in combination with the GFP-tagged yeast collection, there were drastic changes in the localization of the GFP-tagged proteins.[61] This revolutionized our understanding of acetylation as a modulator of protein localization and function.

1.4 The yeast lysine acetyltransferase, NuA4

The Nucleosomal Acetyltransferase of histone 4, referred to as NuA4, is the only essential KAT in *S. cerevisiae*.[62] It was named for its predominant role in acetylating Histone H4.[63] However, NuA4 has now been linked to several metabolic proteins,[64,65] lipid regulatory pathways,[66] growth defects,[67] and stress response[68] in yeast. The NuA4 complex is a member of the MYST KAT family and is comprised of 13 subunits, including the catalytic component, Esa1, 5 components essential to

cell viability, Act1, Arp4, Epl1, Swc4, and Tra1, as well as 7 others (not required for cell viability), Eaf1, Eaf3, Eaf5, Eaf6, Eaf7, Yaf9, and Yng2.[62,69,70] Importantly, Esa1 is homologous to human Tip60, which also functions in a complex known as the Tip60 complex.[71] The 12 other subunits of the yeast NuA4 complex also have mammalian homologs, highlighting the high level of conservation of this complex between species.[69] [69] As such, studies investigating NuA4 in yeast can provide meaningful insight into the function and role of Tip60 in human disease states.[69]

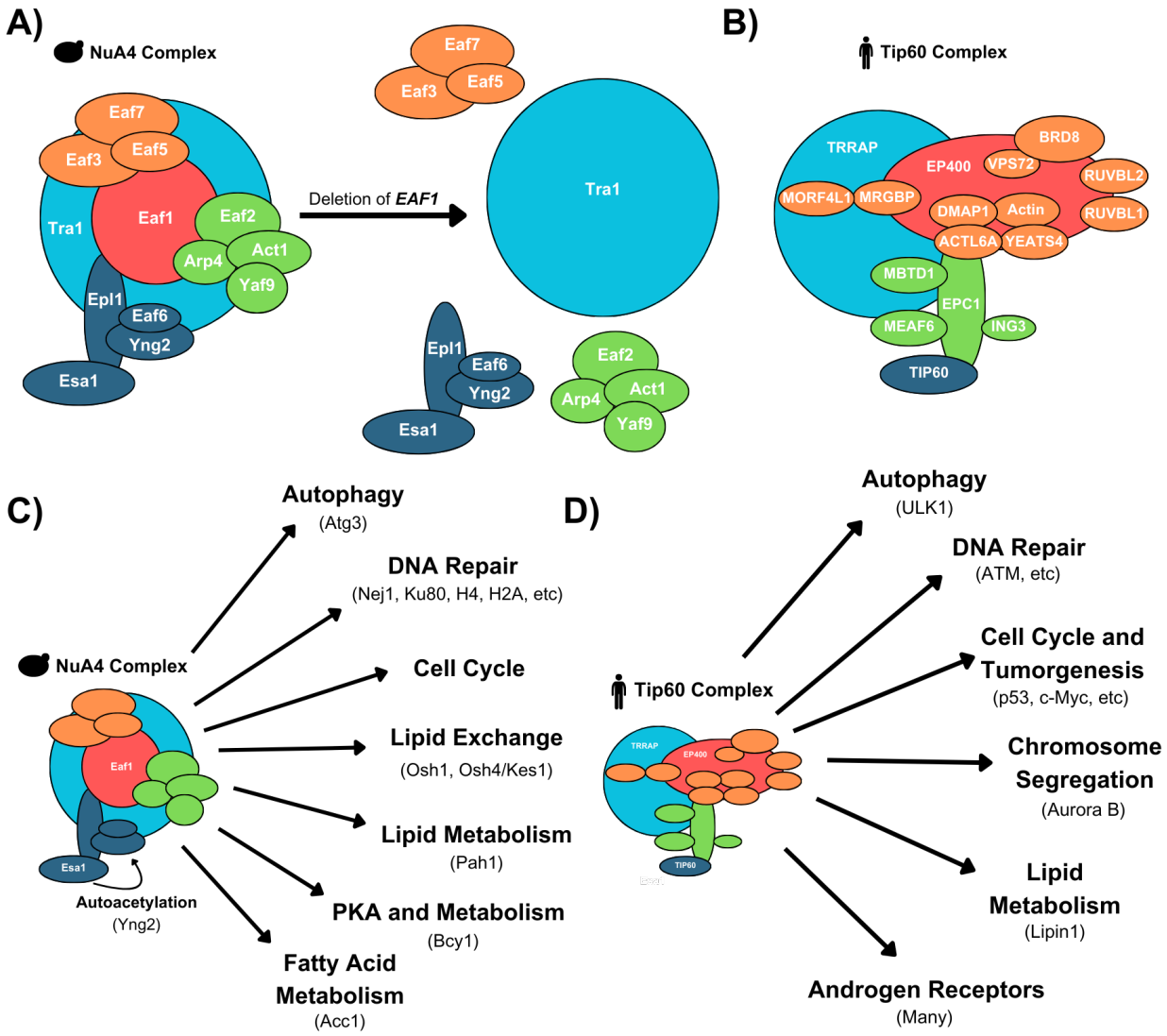

Figure 1.2 – Structure and function of NuA4 and Tip60.

A) Labelled complex of the yeast lysine acetyltransferase NuA4. All 13 subunits are denoted, including the catalytic component, Esa1. As an essential subunit, *ESA1* cannot be deleted, however deletion of the scaffolding subunit *EAF1* results in the dissociation of the complex, a reduction in Esa1 activity and a reduction in the acetylation of NuA4 complex acetylation targets. **B)** Labelled complex of the human Tip60 complex. **C)** Schematic displaying the various cellular mechanisms that NuA4 takes part in. Below, in brackets, is the specific target of NuA4 acetylation that it modulates this pathway through. **D)** Schematic displaying the various cellular mechanisms that Tip60 takes part in. Below, in brackets, is the specific target of Tip60 acetylation that it modulates this pathway through.

The NuA4 complex is comprised of 4 separate subcomplexes (**Figure 1.2A**). Firstly, the piccolo complex, or the catalytic submodule, includes subunits Esa1, Yng2, Eaf6 and Epl1.[72,73] As such, this portion completes the catalytic function of acetylation but is unable to interact with transcription factors, making it unable to localize to its location of function.[74,75] Second is the **T**rimer **I**ndependent of **N**uA4 involved in **T**ranscription **I**nteractions with **N**ucleosomes, referred to as the TINTIN subcomplex, comprising of Eaf3, Eaf5 and Eaf7.[76] While TINTIN can act both with or without the complete NuA4 complex, its main role is to aid in NuA4 interaction with nucleosomes through methylated histone H3.[77] On its own, TINTIN can block the incorporation of new histones and promote the recycling of nucleosomes following elongation by RNA polymerase II.[77,78] The third NuA4 subcomplex is comprised solely of Tra1, the largest subunit of the NuA4 complex, which is shared with the SAGA complex. Given its size, Tra1 serves as a platform for interacting with transcription factors in the NuA4 and SAGA complexes.[79,80] Tra1 is most commonly described as an activator target, assisting with the localization of NuA4 and SAGA complexes to specific loci.[81] Finally, the core of NuA4 is made up of the remaining subunits, Act1, Swc4, Yaf9, Arp4 and Eaf1, which connect the other three groups together.[70,82]

While it is known that these 4 subcomplexes form the overall holo complex structure of NuA4, the details of this dynamic remain an active area of research. In recent years, advancements in cryo-electron microscopy (EM) have provided significant details on NuA4 structure in *S. cerevisiae.*[83] For example, cryo-EM uncovered that Elp1 plays a large role in maintaining the connection between

NuA4's catalytic and core subcomplexes.[84] As a bridge, the C-terminal tail region of Elp1 interacts directly with the core module of NuA4 through a tight binding between Elp1 and Eaf1. At its N-terminal, Elp1 connects to the FAT domain of Tra1.[84] Cryo-EM confirmed that NuA4 exists in two major modules: the KAT and TRA modules. While the KAT module is involved in binding the nucleosome, the TRA modules remain in close proximity and act as an activator surface for the complex. Given the advancements in techniques in this area, further research will elucidate the structure of NuA4 and its association with the nucleosome.

Table 1 – Components of the yeast lysine acetyltransferase, NuA4 and the human Tip60 complex.

Yeast Protein	Human Ortholog	Role in the yeast, NuA4 complex	Role in the human, Tip60 complex
Esa1	TIP60	Piccolo Complex (NuA4 catalytic submodule)	Acetyltransferase Complex
Yng2	ING3	Piccolo Complex (NuA4 catalytic submodule)	PHD finger domain, growth inhibitor, apoptosis
Eaf6	MEAF6/ FLJ11730	Piccolo Complex (NuA4 catalytic submodule)	
Epl1	Epc1/2	Piccolo Complex (NuA4 catalytic submodule)	Transcription control, silencing
Eaf3	Mrg15/X	TINTIN Complex (NuA4 interaction with nucleosomes)	Chromo domain, senescence
Eaf5	BRD8	TINTIN Complex (NuA4 interaction with nucleosomes)	
Eaf7	MrgBP	TINTIN Complex (NuA4 interaction with nucleosomes)	
Tra1	TRRAP	Platform for NuA4/SAGA interaction with transcription factors.	PIKK domain, component of Hat complexes
Act1	Actin	NuA4 Core	ATPase, cytoskeleton
Swc4	DMAP1	NuA4 Core	
Yaf9	YEATS4	NuA4 Core	
Arp4	BAF53a	NuA4 Core	Actin related, DNA repair
Eaf1	EP400 (not homologous but shares some similarity)	NuA4 Core	
Eaf1/Swr1	P400/Domino		SWI2/SNF2-like ATPase
Vps72	VPS72/Yl-1	Subunit of SWR1	Chromatin remodelling
Brd8/TRCp120	BRD8	Subunit of SWR1	
--	MSL3		
Sas5 and Taf14	YEATS2	SAS complex, INO80, SWI/SNF and NuA3 complexes	
Rvb1/2	RuvBL1/2	No role in NuA4	Helicase/ATPase?

--	MBTD1		
Sas5 and Taf14	MLLT1/3	SAS complex, INO80, SWI/SNF and NuA3 complexes	

Since *ESA1* is an essential gene, the temperature-sensitive mutant *esa1*^{ts} (*esa1-L254P*), which inactivates the encoded subunit at high temperatures, reducing acetylation activity, may be used to investigate the role of NuA4.[70,85,86] Another method to manipulate *ESA1* without causing secondary effects throughout the cell is to use the "anchor-away" model, *AA-ESA1*, which pulls Esa1 from the nucleus and anchors it in the cytoplasm.[87] Studies show that *AA-ESA1* causes no difference in cell growth or viability in *AA-ESA1* compared to WT.[88] This model is ideal when one is studying only nuclear phenotypes and/or functions since targeting *ESA1* to the cytoplasm can cause its own effects. Alternatively, the deletion of the non-essential *EAF1* can also serve as an easier and more efficient model since Eaf1 functions exclusively within the NuA4 complex.[62,89,90] As a scaffolding subunit in the core module of NuA4, deletion of *EAF1* results in dissociation of the NuA4 complex and reduction of Esa1 targeting (**Figure 1.2A**).[84,89] Therefore, *eaf1*Δ strains are useful models for investigating the consequences of NuA4 dysfunction.[62,65,66,89-91]

In addition to NuA4's role in histone acetylation, it is widely accepted that NuA4 is also involved in the acetylation of a variety of non-histone/protein targets. Mapping of NuA4's genetic interactions has provided a deeper understanding of clusters of NuA4 activity, many of which remain unexplored. This role ranges from metabolism (described in further detail below) to mRNA transport, DNA damage, and cell cycle. Additional functions of NuA4 and its interactors are summarized here and in **Figure 1.2C**:

1.4.1 NuA4 and DNA repair

NuA4's role in DNA repair is multi-faceted and well-documented, especially in relation to DNA double-stranded breaks (DSBs). DSBs can be repaired either through non-homologous end

joining (NHEJ) or homologous recombination (HR).[92] NuA4 is specifically recruited to the site of DSBs,[93] where NuA4-dependent acetylation on H4 and H2A facilitates the incorporation of the H2A.Z histone variant into nucleosomes in response to DNA damage.[94] This specifically marks the nucleosome for DNA damage and is a fundamental step in DNA repair.[94] Beyond histones, NuA4 also actively recruits several chromatin remodelers and influences the selectivity of the DNA repair pathways. For example, by acetylating Nej1 and Ku80 at DNA breaks, NuA4 inhibits NHEJ, thereby promoting DNA end resection and favouring homologous recombination repair.[95]

1.4.2 NuA4 auto-acetylation

Autoacetylation sites have been identified on nearly all of the NuA4 complex subunits. Most significantly occurring on Yng2 and Epl1.[86] Acetylation of Yng2 is important for the stability and function of the subunit and impacts the overall function of NuA4.[60] Autoacetylation sites have also been found directly on Esa1[96]and are conserved on Tip60,[97] impacting its activity and function.[98]

1.4.3 NuA4 and autophagy

Autophagy is the cell's natural ability to recycle materials through lysosomal (in most mammalian cells) or vacuolar (in most eukaryotic cells) degradation. In particular, this process plays a protective role in the cell and aims to get rid of harmful proteins or injured organelles throughout the cell's life cycle.[99] Defects in autophagy are highly relevant to cancer and aging research since this is highly related to recycling and removing damaged cellular products.[100-102] Given the role of protein acetylation in regulating autophagy,[103] Tip60 has been investigated with great interest by autophagy researchers. Notably, glycogen synthase kinase-3 (GSK3) phosphorylates Tip60 upon depletion of growth factors and ER stress, activating Tip60.[104] This requires prior phosphorylation of Tip60 by cyclin-dependent kinase 1 (CDK1). Tip60 then acetylates the protein kinase ULK1, activating autophagy.[104,105] Ulk1's yeast homolog is Atg1, an upstream component of the autophagy machinery

and a key regulator in selective autophagy in yeast.[106] GSK3-activated Tip60 also induces autophagy through acetylation of RUBCNL/Pacer, which facilitates the recruitment of the HOPS complex to the autophagosome, promoting maturation and clearance of lipid droplets.[107] Similarly, GSK1-activated Tip60 also acetylates p62/SQSTM1, enhancing p62's ability to bind ubiquitylated proteins and promote autophagy.[108]

While several autophagy proteins exist in yeast, NuA4's role in autophagy is mainly related to the acetylation of the autophagy protein Atg3 under nitrogen starvation.[109] Acetylation on Atg3 is found at K19 and K48 and has been found to be dependent on Esa1. This acetylation promotes Atg3 interaction with Atg8 and directly promotes autophagy. Therefore, impeding the acetylation of Atg3 caused a defect in autophagy.[109] All of the described autophagy pathways are depicted in **Figure 1.3.**

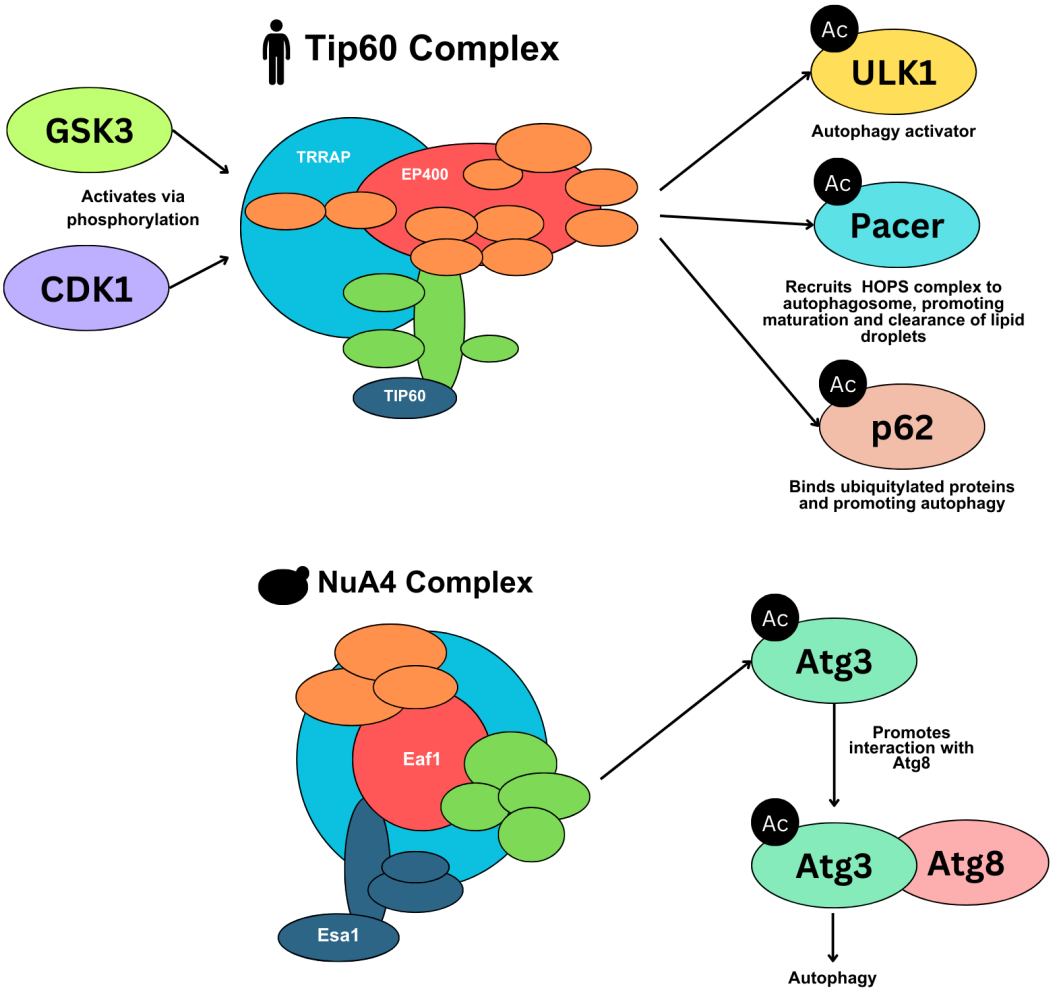

Figure 1.3 – Summary of Tip60 and NuA4 complex's roles in autophagy pathways.
The top panel describes Tip60's role in regulating autophagy in humans. First, Tip60 must be phosphorylated and activated by cyclin-dependent kinase 1 (CDK1) and glycogen synthase kinase-3 (GSK3). Tip60 was then described to acetylate the protein kinase ULK1, RUBCNL/Pacer and p62/SQSTM1. All of which promote autophagy. In yeast (bottom panel), NuA4 is known to acetylate the autophagy gene, Atg3, which promotes its interaction with Atg8 and its role in autophagy.

1.5 NuA4-dependent acetylation is tightly linked to lipid metabolism and biosynthesis

Previous work by the Baetz lab and others has established a role for NuA4 in regulating the expression of the inositol-3-phosphate synthase genes, *INO1*,[66,67] the oxysterol binding protein Osh1 (unpublished), ergosterol (submitted to G3), and the activity and location of the Acetyl-CoA Carboxylase protein, Acc1.[91] There is growing evidence that NuA4 may have a role in regulating the phosphatidic acid phosphatase Pah1, contributing to the delicate balance between lipid storage and phospholipid biosynthesis.[110]

1.5.1 An overview of lipid metabolism in yeast

Lipids, small organic biomolecules, have become increasingly studied for their involvement in human diseases. This heightened interest in studying lipids led to a need for a classification system. In 2005, the International Lipid Classification and Nomenclature Committee developed a "*Comprehensive Classification System of Lipids*" that involved defining lipids into 8 different categories: fatty acyls, glycerolipids, glycerophospholipids, sphingolipids, sterol lipids, prenol lipids, saccharolipids and polyketides.[111] Lipids can serve a multitude of roles in the cell. Primarily, they are an energy source, but they can also serve as structural elements of the cell envelope and organelles, act as a signaling molecule, or even as a mediator of membrane fusion and apoptosis.[112-115]

Yeast provides an ideal model organism for studying lipid metabolism due to the high level of conservation with humans.[116,117] Additionally, the nature of deletion sets and the flexibility and customization of growth conditions make the metabolism pathways easy to manipulate in practice.[118-120] Yeast lipid metabolism is characterized by the balance between lipid synthesis, storage and utilization. In excess, high levels of lipids can cause lipotoxicity, causing corresponding signalling,

stress response, and cell death.[121] To counter this, lipids are often stored in lipid droplets (LD) as an energy reservoir that can be utilized for energy production or the creation of more complex lipids, such as membrane phospholipids.[119] LDs are comprised of triacylglycerols (TAG) cores, a layer of steryl esters (SE) with a phospholipid monolayer.[122]

1.5.2 Pah1 is a central component of lipid metabolism.

As a central component of the lipid synthesis pathway, phosphatidic acid (PA) sits at a critical crossroad between lipid droplet formation and phospholipid production (**Figure 1.4**).[123] In one direction, PA can be dephosphorylated by the yeast phosphatidic acid phosphatase (Pah1) to create diacylglycerol (DAG), which is subsequently modified by the DAG acyltransferase to form triacylglycerol (TAG).[124,125] Alternatively, PA can be processed into CDP-DAG, which is a precursor to the membrane phospholipids, phosphatidylinositol (PI), phosphatidylserine (PS), phosphatidylethanolamine (PE) and phosphatidylcholine (PC).[123,126,127] PI production requires the addition of inositol, which is derived from glucose and processed by inositol-3-phosphate synthase (Ino1). PI is essential in promoting vacuole fusion through the production of PI(3,5)P by the PI 3-kinase Vps34 and DAG through phospholipase C, Plc1.[128]

Regulation of PA is vital to establishing a balance between the production of lipid droplets and membrane phospholipids. Initial pools of PA can be produced mainly through two methods. The most common is through glycerol-3-phosphate (G3P), an intermediate in the glycolysis pathway.[129] G3P can be subsequently acylated by glycerol-3-phosphate acyltransferase (GPAT) to create lysophosphatidic acid (LPA) and then by lysophosphatidic acid acyltransferase (LPAAT) to create PA. Alternatively, PA can be made by the digestion of PC by phospholipase D (PLD) (Summarized in **Figure 1.4A**).[129]

Pah1 is a critical regulator of PA, and this is highlighted by the phenotypes that are seen upon its deletion. As the primary function of Pah1 is to convert PA into DAG, *pah1*Δ cells have increased

levels of PA and corresponding decreases in DAG and TAG, its derivative.[130-132] Through regulation of PA levels, Pah1 also acts as a repressor of the transcription factor Opi1, a transcriptional repressor of phospholipid synthesis genes, such as *CHO1, INO1* and other phospholipid metabolic genes containing inositol/choline-responsive elements (ICREs) in their promotor regions (**Figure 1.4B**).[133,134] These genes are transcriptionally activated through Ino2 and Ino4, forming a heterodimer and binding ICRE-related genes' promotors.[135-137] When PA is low, Opi1 translocates into the nucleus, binds Ino2, and represses transcription of phospholipid metabolic genes.[134,138] In the context of a *pah1*Δ*,* increased levels of PA inhibit Opi1. As a result, there is a further increase in the synthesis of phospholipid genes.[67,125,133]

*pah1*Δ mutants exhibit an expansion of the nuclear/ER membrane, show sensitivity to fatty-acid-induced toxicity, and have defects in lipid droplet formation.[125,126,139,140] Additionally, *pah1*Δ mutants exhibit growth defects on non-fermentable carbon sources and at high temperatures,[130,132,141] are hypersensitive to oxidative stress,[142] have shortened life spans,[142] and have defects in cell wall integrity,[143,144] autophagy[142,145,146] and vacuole fusion.[147] Interestingly, the deletion of the DAG kinase (Dgk1), which counteracts Pah1 activity converting DAG into PA, can rescue nuclear flares, the expression of phospholipid synthesis genes, and lipid droplet numbers,[148,149] but not the defects in vacuole fusion.[150]

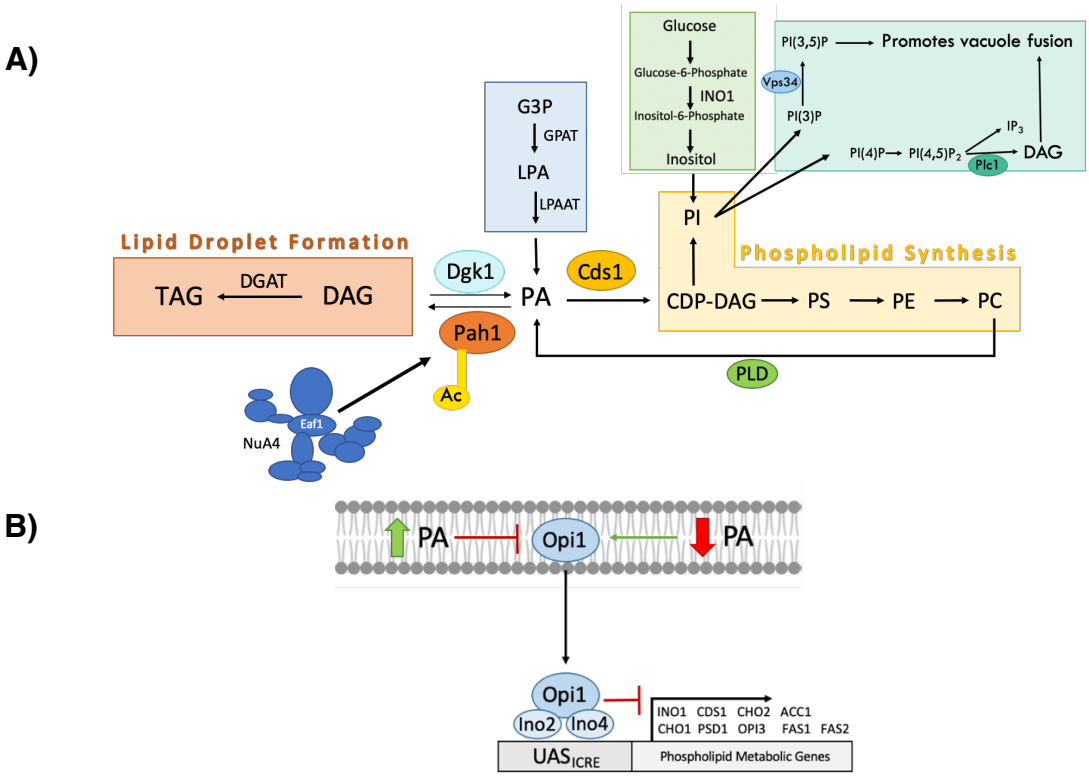

Figure 1.4 - Schematic diagram for lipid metabolism in yeast.
A) Simplified pathway for PA production, membrane lipid synthesis and lipid droplet formation. B) Role of PA as a repressor of Opi1 transcriptional repression of phospholipid metabolic genes. The figure is adapted from Dacquay *et al.* [66].

1.5.3 Pah1 location, function and regulation through phosphorylation

Pah1 function is entirely dependent on its localization. Since it lacks a transmembrane domain, Pah1 interacts with members through PA.[151] Therefore, Pah1 can bind to the membrane when PA is present and execute its function. Pah1 is located in the cytosol in its inactive state, and only through posttranslational modification, primarily phosphorylation and dephosphorylation, can Pah1 be shuttled to the nuclear/endoplasmic reticulum (ER).[130,152] Pah1 is phosphorylated through several protein kinases, such as cell cycle kinase, Cdc28 (Cdk1)-cyclin B complex,[153] Pho85p-Pho80p,[154] Hsl1 kinase,[155] protein kinase A (PKA),[156] and protein kinase C (PKC).[157] This process of Pah1 modulation through phosphorylation is summarized in **Figure 1.5**. Through mass spectrometry, it was found that this phosphorylation activity centralized on seven Ser/Thr-Pro motifs (Ser-110, Ser-114, Ser-168, Ser-

602, Thr-723, Ser-744, and Ser-748) within Pah1.[124,153] A summary of these sites and their corresponding kinase activity can be found in **Figure 1.6**.

For Pah1 to bind to the nuclear/ER membrane, it must first be dephosphorylated by Nem1-Spo7, a protein phosphatase complex located in the nuclear/ER membrane.[125,158] Notably, both Nem1, the catalytic subunit, and Spo7, the regulator subunit, are required for Pah1 function.[158] In fact, deletion of *NEM1* or *SPO7* results in many of the same phenotypes at deletion of *PAH1* itself (such as expansion of the nuclear/ER membrane, decreases in TAG and LDs, temperature sensitivity, and defects in autophagy).[125,131,146,152,159] Pah1 has several domain regions that play various roles in its function and location. Nem1-Spo7 interacts with Pah1 through its acidic tail, as well as directly through several phosphorylation sites within intrinsically disordered regions (IDRs),[121,160] many of which are regulated through the regulation of phosphorylation (RP) domain.[160] Pah1 can be dephosphorylated to interact directly with the nuclear/ER membrane, and interaction occurs through Pah1's N-terminal amphipathic helix, which specifically recognizes PA in the membrane.[151,161] Interestingly, mutations at all seven sites to alanine residues on Pah1, rendering them non-phosphorylatable, bypass the requirement for dephosphorylation by Nem1-Spo7 and cause enhanced Pah1 activity.[124,153]

Additional domains on Pah1 include the HAD-like domain containing the D*X*D*X*(T/V) catalytic motif, which must form a catalytic core through interaction with the N-LIP domain. The C-terminal of the HAD-like domain is the WRDPLVDID domain, which is also required for enzymatic activity.[162,163] Non-phosphorylated Pah1, either through lack of phosphorylation or following dephosphorylation by Nem1-Spo7, is readily degraded through 20S proteasomal degradation.[164,165] Figure 1.5 summarizes these domains and their relation to the Pah1 function.

In summary, Pah1 is heavily regulated by phosphorylation and dephosphorylation. These modifications manipulate Pah1's location from the cytosol to the nuclear membrane. Recent research suggests that the binding of Pah1 to PA in the nuclear/ER membrane is a "hop" and a "scoot" along

the membrane to additional PA molecules within the membrane that converts into DAG.[166] While this seems the energetically favourable model, Pah1 is found at various other membranes in the cell, such as the nuclear-vacuole junction,[126] the inner nuclear membrane,[167] and lipid droplets.[161,168] This suggests that physiological conditions within the cell must promote Pah1 to shift from a "scoot" across the membrane to a "hopping" mode at various membrane locations.[166] Future work on specific Pah1 mutations and post-translational modifications could shed light on the movement of Pah1 between membranes and continues to be an active area of investigation.

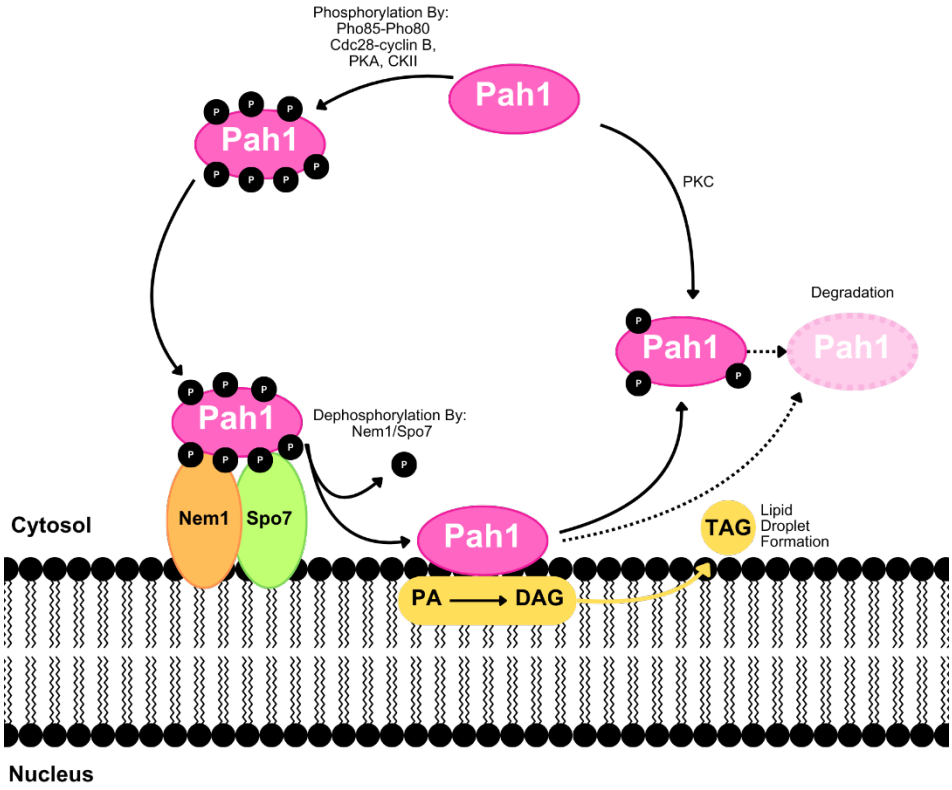

Figure 1.5 – Graphical representation of Pah1 localization to the nuclear membrane mediated by phosphorylation and dephosphorylation.
Pah1 is inactive in the cytosol. Upon dephosphorylation by Nem1/Spo7, Pah1 is recruited to the nuclear membrane, which converts PA into DAG, facilitating the production of lipid droplets. Pah1 can also be shuttled to proteasomal degradation. The graphic is adapted from Han et al. [169] and Park *et al.* [162]

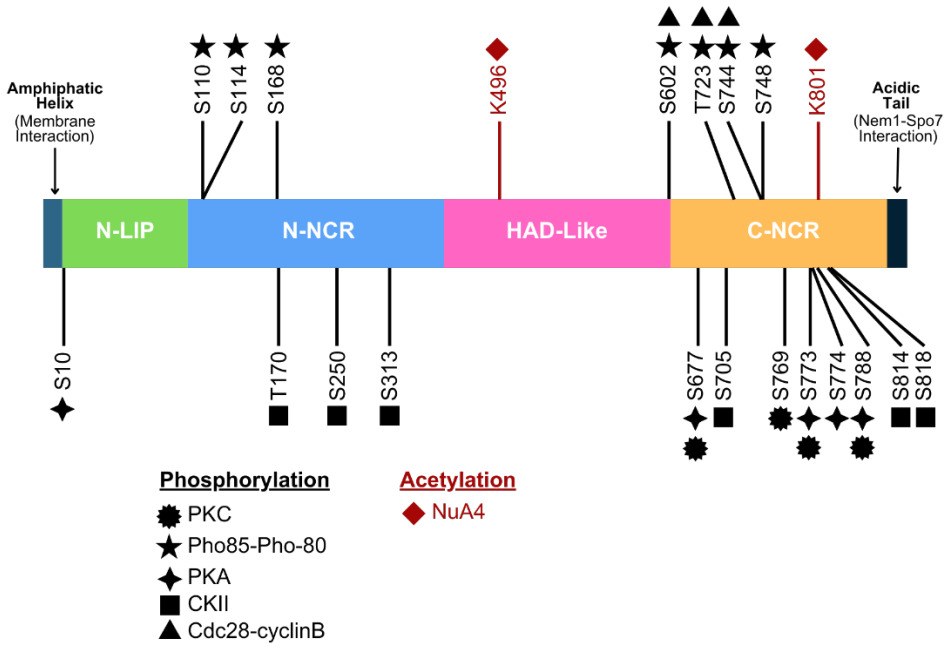

Figure 1.6 – Domains and phosphorylation sites of Pah1.
Regions of Pah1 are shown (from left to right), the amphipathic helix required for association with the nuclear membrane (dark blue), the N-LIP (green), the N-terminal non-conserved region, N-NCR (light blue), the HAD-like domain required for PAP activity, the C-terminal non-conserved region, C-NCR (orange), and the acidic tail required for association with Nem1-Spo7. All phosphorylation sites are labelled in black, where S indicates a serine residue and T indicates a threonine residue. Acetylation sites are labelled in red, and K indicates a lysine residue. All enzymes responsible for the corresponding site mutations are indicated through a series of shapes and labelled below the diagram. Phosphorylation data is summarized and adapted from Park *et al.* [162] and acetylation data is from Li *et al.* [110].

1.5.4 Tip60-dependent regulation of Lipin

Similar to the high level of conservation between yeast *ESA1* and mammalian *Tip60* (see **Sections 1.2** and **1.4**), yeast *PAH1* is highly conserved in higher eukaryotes, including the human *Lpin1* gene.[170-175] The *Lpin1* gene was first discovered and isolated in a mutant mouse strain with fatty liver dystrophy (fld).[176,177] The corresponding protein, lipin 1, exists in two protein isoforms (lipin-1α and lipin-1β) from alternative mRNA splicing of the *Lpin1* gene.[171] lipin 1, lipin 2 and lipin 3 make up the human lipin family.[172] All are characterized by their PAP1 enzyme activity and D*X*D*X*T motif within the C-LIP domain of Pah1.[130,172] These various lipin proteins have unique physiological roles in mammals and contribute to PAP activity in different regions of the body.[172] For example, lipin 1 is responsible for nearly all PAP activity in skeletal muscle, the heart, and adipose tissues.[172,178,179]

Similarly to Pah1 in yeast, lipins do not have transmembrane domains, are inactive in the cytosol, and are active when bound through PA to membranes such as the ER, mitochondria and autophagosomes (or lysosomes).[124,125,180]

A study on mice with reduced Tip60 function (homozygous mice for the *Tip60*^{S86A} allele containing a serine to alanine mutations at S86, with 50% reduced Tip60 activity), herein referred to as *Tip60*$^{SA/SA}$ mice, found that these mice had significantly reduced body weight.[110] This was paired with inhibited milk supply and TAG production in female mice, both of which indicate significant impairment of TAG production in *Tip60*$^{SA/SA}$ mice. Upon investigation into the root of this impairment, Tip60 was found to exclusively acetylate lipin 1 and no other enzymes involved in TAG biosynthesis pathway.[110] While 9 acetylation sites were identified on lipin 1, Lys425 and Lys595 were found to be the most important sites with the largest impact on activity and the highest level of conservation (shown in **Figure 1.7**). Lipid chromatography-mass spectrometry (LC-MASS) also showed that *Tip60*$^{SA/SA}$ mice had elevated PA and decreased DAG levels compared to WT mice.[110] These lipotypes are summarized in comparison to other NuA4 and Tip60 mutants in **Table 2**. Since the function of lipin 1 is to convert PA into DAG, this finding further illustrates the relationship between Tip60 and lipin 1. Interestingly, acetylation of lipin 1 did not have an impact on its PAP activity but rather assisted in lipin 1 translocation to the ER. Further, this Tip60-mediated acetylation of lipin 1 was found to be countered by the HDAC, sirtuin 1.[110]

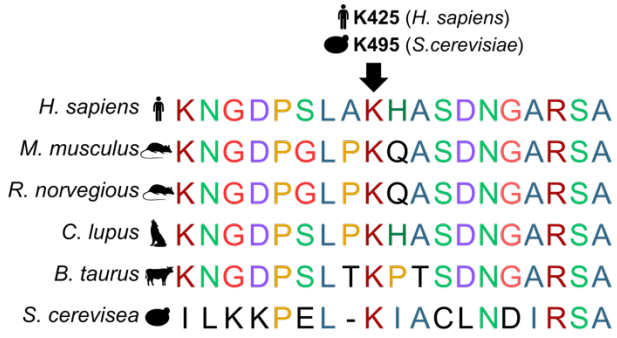

Figure 1.7 – Sequence alignment of the conserved NuA4-dependent acetylation site on lipin/Pah1. An arrow denotes K425 in *H. sapiens* and K495 in *S. cerevisiae.* This figure is adapted from Li *et al.* [110]

1.5.5 NuA4-dependent acetylation of Pah1

Two NuA4 subunits, *EAF7* and *YNG2,* have been shown to have genetic interactions with Pah1, the first being a positive genetic interaction (where the combination of genetic mutations alleviates a defect seen in a single mutant alone, indicating that the two genes function in the same pathways) and the latter being a synthetic lethality (where the combination of genetic mutations results in cell death, while each mutant alone has no affect).[60,181] Like human lipin 1, NuA4-dependent acetylation sites were also detected on Pah1 at Lys^{496} and Lys^{801}.[110] Lys^{496} is conserved as Lys^{425} on lipin1. Additionally, only *ESA1* was required for TAG accumulation out of eight essential acetyltransferases. A plasmid carrying *PAH1* with Lys^{496} and Lys^{801} mutated to arginine was expressed in a *pah1*Δ strain, resulting in reduced TAG accumulation.[110] While these results suggest that NuA4 plays a role in the regulation of TAG accumulation through Pah1, the functional consequences of this acetylation have not been further investigated or understood. As exemplified in both mice and yeast models, it remains unclear how NuA4/Tip60-dependent acetylation of Pah1/lipin 1 regulates the localization to the nucleus and ER.

Table 2 – Summary of NuA4 and Tip60 mutants and their effect on global lipid levels.

Genotype	***TIP60$^{SA/SA}$***	***pah1*Δ**	***eaf1*Δ**	***esa1-ts***
Source	Li *et al.* [110]	Karanasios *et al.* [151]	Pham *et al.* [91] & Walden *et al.* Unpublished	Walden *et al.* Unpublished
TAG	Down ~ 50%	Down	Up	Up
DAG	Down ~ 50%	Down	Up (NS)	Down (NS)
LPA			Up (unpublished)	UP (unpublished)
PA	Up ~ 40%	Up	No change	No change
CDP-DAG			Up (unpublished)	UP (unpublished)
PI	Up	Up	Down (NS)	Down
PG	Up			
PC	No change	Down	Down	Down
PS			Down (NS)	Down (NS)
PE	No change	Up	Down	Down (NS)

EE		Up	Up	Up
ERG		Down		

1.5.6 Lipin-related human diseases

The regulation of lipid storage is a critical factor in metabolic diseases, such as obesity and lipodystrophy (a family of medical conditions characterized by abnormal fat distribution resulting in insulin resistance and hypertriglyceridemia).[171,182,183] Since lipins have a central role in the regulation of TAG storage, the lipin family is a regular suspect in disease states associated with impaired and accumulated TAG production. Several diseases have been identified due to a mutation to *LPIN1* in both mice and humans and are generally referred to as Lipin 1 deficiency diseases.[184] First, a glycine to arginine mutation at Gly^{84} within the N-LIP domain of mouse Lipin was found to cause lipodystrophy and neuropathy.[171] More recently, mutations in human lipin-1 have been found and characterized by acute rhabdomyolysis, myalgia, and myoglobinuria.[185,186] Presenting within the first 7 years of life, these conditions are mainly accompanied by muscle pain and weakness.[184] Studies in both mice and humans have shown that phenotypes associated with lipin 1 deficiencies result from either/or both of the PAP products (i.e. DAG, TAG and LD formation) or the accumulation of PA and related shuffling of lipids.[184,187]

1.5.7 NuA4 regulation of phospholipid homeostasis through Sec14 signaling

Multiple studies have suggested a role for NuA4 in regulating phospholipid homeostasis. To begin, NuA4 mutants have been identified to have an Opi- phenotype, characterized by an excessive level of inositol.[188,189] The role of Opi1 in modulating the expression of phospholipid metabolism genes is summarized in **Section 1.5.2** and **Figure 1.4**. To summarize, a loss of Opi1 leads to overexpression of ICRE genes, including *INO1,* causing increased inositol.[134] NuA4, despite binding to the promotor of INO1, is not required for its activation, indicating that NuA4 must interact in another way. NuA4 has a negative genetic interaction with temperature-sensitive mutants of *SEC14*.[66]

Sec14 is an essential protein located at the Golgi and is involved in the lipid transfer of PI and PC between membranes.[190] In fact, deletion or mutation of NuA4 subunits results in an exacerbated growth defect in *sec14-1^{ts}* cells.[66] RNA-sequencing of *sec14-1^{ts} eaf1*Δ cells showed that of all the ICRE genes, *INO1* was most significantly upregulated along with *FAS1* and *FAS2,* while *CDS*1 was significantly downregulated.[66] This research indicates that NuA4 acts as a positive regulator of fatty acid biosynthesis.

1.5.8 NuA4 regulation of Acc1 and Fatty Acid Synthesis

Acetyl-CoA connects several metabolic pathways and can be created from glucose, fatty acids, and the catabolism of amino acids. Not only is it used as a substrate for the acetylation of proteins,[2] but the shuttling of acetyl-CoA is central to the adaptability of metabolism in the cell, allowing for a variation in response when "fed" or "starved".[191] For example, under "fed" conditions where glucose is abundant, acetyl-CoA is shuttled away from the mitochondria, generating fatty acids, sterols and other lipids, and perpetuating acetylation of histones and the activation of gene expression.[191-193] In "starved" states, cells shift from growth to survival. Acetyl-CoA, in this case, will become oxidized at the mitochondria to produce ATP, resulting in a decline in the level of acetyl-coA in the nucleus and cytosol, as well as an induction of autophagy.[194,195] Importantly, the levels of acetylation in the cell are tightly linked to the metabolic state of the cell. Further work in yeast has shown that when yeast cells are starved, there is a dramatic alternation of the global levels of histone acetylation, explicitly allowing for a shift in the expression of specific genes and directing metabolism towards fatty acid oxidation when acetyl-CoA is low.[196] It's clear that there is a tight link between metabolism and lysine acetylation through acetyl-CoA.

As the fate-determining step of acetyl-CoA to lipogenesis, acetyl-CoA carboxylase (ACC) converts acetyl-CoA into malonyl-CoA.[197-199] In yeast, there are two main ACC proteins: the cytosolic

Acc1 and the mitochondrial Hfa1.[197,200,201] Numerous mechanisms regulate Acc1's activity. Most relevant to this work, mRNA levels of *ACC1* mRNA are upregulated when PA is high through modulation of the Opi1 repressor and Ino2/Ino4 transcriptional activator complex.[202,203] Acc1 is also subject to phosphorylation by the AMP-activated protein kinase, AMPK, also known as Snf1 in yeast.[198,204,205] Snf1/AMPK is highly linked to metabolic conditions, and Snf1/AMPK activity is increased when the cell is starved. This leads to increased phosphorylation on Acc1, reducing its activity and corresponding fatty acid metabolism.

Interestingly, previous work in the Baetz lab has shown high levels of acetyl-CoA and reduced Acc1 activity in NuA4 mutants.[68,91] Additionally, there are changes in Acc1 localization compared to WT cells, in both an *eaf1*Δ and an *esa1-ts* mutant shifted to 37°C. While WT cells show "punctate and rod-like structures", NuA4 mutants displayed diffuse localization.[91] Further, NuA4 was also shown to negatively regulate Snf1 through acetylation of one of its inhibitory subunits, Sip2.[206] It was recently found that Snf1/AMPK is only responsible for some of NuA4's regulation of Acc1.[91] Most notably, this appeared to be specifically through genes involved in the elongation of Very Long Chain Fatty Acids (VLCFA) and sphingolipid synthesis.[91] While further work is needed to determine the mechanism behind this regulation, this work highlights a tight relationship between NuA4 and lipid metabolism.

1.6 Pah1 as a regulator of nuclear shape

1.6.1 Regulation of the Yeast Nuclear Shape

Most nuclei are spherical in nature, and yeast are no exception. While yeast lack the nuclear filament protein lamin found in higher eukaryotic cells to regulate nuclear shape, there are several lamin-associated proteins with yeast homologs that can be found at the yeast nuclear envelope (NE), such as Man1, Msp3 and Doa10.[207-210] A high level of internal organization breaks up the yeast nuclei

into distinct structural elements, mainly the NE, the nuclear pore complex (NPC), and the nucleolus. The NE consists of two distinct lipid bilayers, an inner and outer membrane herein referred to as the INM and ONM. The INM plays an important role as an anchor point for several types of chromatin (most notably rDNA) through tethering proteins.[208,211,212] The NPCs are gatekeeps between the nucleoplasm and the cytoplasm, facilitating the transfer of key proteins and RNAs.[213] In some cases, deletion of NPCs, such as *NUP84,* can lead to small outgrowths of the nuclear membrane.[214,215] Finally, the yeast nucleolus produces ribosomes and takes on a distinct crescent shape while occupying about a third of the nucleus.[216,217] The nucleolus is anchored to the nuclear periphery through specific regions on the INM.[218]

While the regulation of nuclear size and shape remains an active area of research, we do know that there is a link between the ratio of nuclear to cellular volume (N:C volume).[219] This is consistent with other higher eukaryotes but is less understood in yeast. Importantly, studies have shown that DNA content does not determine nuclear size.[220,221] Given the defects in nuclear shape seen upon deletion of key lipid metabolism genes, such as *PAH1* and *SPO7*, significant research has investigated the role that lipids play in shaping the nucleus of the yeast cells.[222] In particular, studies in these mutants have shown that there is a direct link between the *availability* of NE and the *ability of* the NE to expand. If the nuclear scales gradually throughout the cell cycle, it's natural to think that NE would expand accordingly. However, it was shown that NE can expand independently of cell size, and nuclear volume can remain unimpacted during cases of NE expansion.[222]

To summarize, there are many reasons for irregular nuclear shape. Most commonly, deformations and/or extensions of the nucleus are due to:

1. **Mitotic Arrest** – It's important to note that since yeast undergo closed mitosis, the nucleus must naturally expand to allow for chromosome segregation. The expansion of the NE tightly links the process of lipid metabolism to the cell cycle. However, a delay in cell cycle

progression can cause normal expansion of the NE to continue unchecked. This results in an abundance of nuclear membrane with nowhere to go.[223,224] While the progression of mitosis stalls out, the nucleus continues to expand asymmetrically, resulting in an extension from one side of the cell referred to as a "nuclear flare".[225] By projecting this nuclear membrane as a flare in a "membrane sink", the cell can maintain intranuclear organization, causing minimal disruption to the cell's DNA.[225] These types of nuclear flares occur distinctly adjacent to the nucleolus and are thought to be due to a specific make-up of the NE at this location that allows for expansions to occur.[224,226] Further research indicates that Golgi-associated vesicle trafficking is needed to confine the NE expansion to the area surrounding the nucleolus.[227] Cells with an interruption of vesicle trafficking (such as in cells with deletion of *ARL1* and *SYS1)* exhibited multiple flares and an increase in NE but maintained the N:C volume.[227]

2. **Manipulation of Pah1** – As outlined in **Section 1.5.2**, Pah1 acts as a mediator between lipid droplet formation and membrane phospholipid synthesis.[125,152] Any inhibition of Pah1 increases the total level of phospholipids and a single flare from the NE adjacent to the nucleolus. These flares look very similar to that seen in a mitotic flare because the mechanism (an overproduction of NE phospholipids) is the root cause of the flare.[222,224]
3. **Piecemeal Microautophagy of the Nucleus (PMN)** – As described in **Section 1.7.3**, PMN is the cell's natural ability to digest excess nuclear by inserting a teardrop-like piece of the NE directly into the vacuole.[228] Unlike mitotic flares, nuclear extensions here are not confined to the location on the NE adjacent to the nucleolus.[224,228,229] In cases where PMN is inhibited (such as that seen in a variety of autophagy gene deletions), nuclear deformations can occur in an attempt to insert NE into the vacuole but instead extend around the nucleus.[230]

1.7 Pah1 and the yeast vacuole

1.7.1 Vacuole Fusion and Morphology

In addition to regulating nuclear shape, lipid availability is a key regulator of vacuolar morphology and fusion. Known for its ability to "recycle" cell content, this lysosome-like organelle is critical to regulating several cell trafficking pathways.[231] Yeast vacuole fusion pathways are highly conserved in organelles and vesicles in higher eukaryotes. Therefore, vacuoles can be used as a model for studying membrane fusion defects that underlay many human diseases such as diabetes, lipodystrophy, neurodegenerative disease and some types of cancers.[232]

Recent studies have aimed at understanding the fundamental role of regulatory lipids in determining the fusogenic ability of the vacuole membrane and the localization of vital components of the fusion process. There are four distinct stages of vacuole fusion: priming, tethering/docking and fusion (**Figure 1.8A**). [231,232] The first priming stage signals the beginning of a new round of fusion, which is initiated by hydrolysis of ATP by Sec18 and releases it from the vacuole membrane. This allows Sec18 to use Sec17 as a wedge to dissociate the two inactive *cis*-SNARE complexes. In its inactive state, PA is bound to Sec18 on the vacuole membrane. Therefore, a reduction in PA levels is also required to release Sec18 from the vacuole membrane. At this point, the vacuole will tether to another vacuole through a process driven by the interaction between Ypt7 and the HOPS complex (**Figure 1.8A and B**). SNAREs from opposing vacuoles will interact and form a complex, bringing the vacuolar membranes closer together. This contact creates a disc called the boundary vertex. It is here that high levels of DAG are required to facilitate the mixing of vacuole content through either a fusion pore or intermediate mixing known as Hemifusion.[231,232]

A growing list of lipids and lipid modifiers have been identified as being required for vacuole fusion. Through the purification of vacuoles, PI3P, $PI(4,5)P_2$, ergosterol and DAG were shown to be needed for vacuole fusion.[233] Later, minimal lipid requirements for vacuole fusion were determined

using reconstituted proteoliposomes (RPLs).[234,235] This verified previous findings but also identified PE and PA for vacuole fusion, specifically for the assembly of SNARE complexes. Additionally, PA is required to interact directly with Sec18 and the HOPS subunit Vps39. Although these are all the lipids required for vacuole fusion, additional lipids, such as PI4P, are also involved in this process and help establish equilibrium between fusion and fission events.[234]

It is well characterized that lipids are required to regulate trafficking pathways. For example, upon deletion of *PAH1,* vacuoles lack several components necessary for fusion, including the PI3P-kinase Vps34, the HOPS subunit Vps39, Mon1-Ccz1, and Ypt7.[147,236] These molecules are all linked through the Rab cascade model for the endolysosomal pathway. PI3P produced by Vps34 recruits the Ypt7 guanine nucleotide exchange factor (GEF), Mon1-Ccz1, which recruits and activates Ypt7.[236,237] It is not clear how Pah1 recruits Vps34 to the vacuole, although it is thought to be partly due to hyperacidification of vacuoles due to an upregulation of V-ATPase genes in a *pah1*Δ mutant.[238] Additionally, the role of Pah1 in establishing the levels of PA also drastically impacts PA binding to Sec18. Inhibition of Pah1 activity inhibits PA-bound Sec18 from detaching from the vacuole membrane and binding SNAREs.[239] PA has also been shown to bind Vam7, which could lead to many other downstream effects of PA on vacuole fusion.[240]

A)

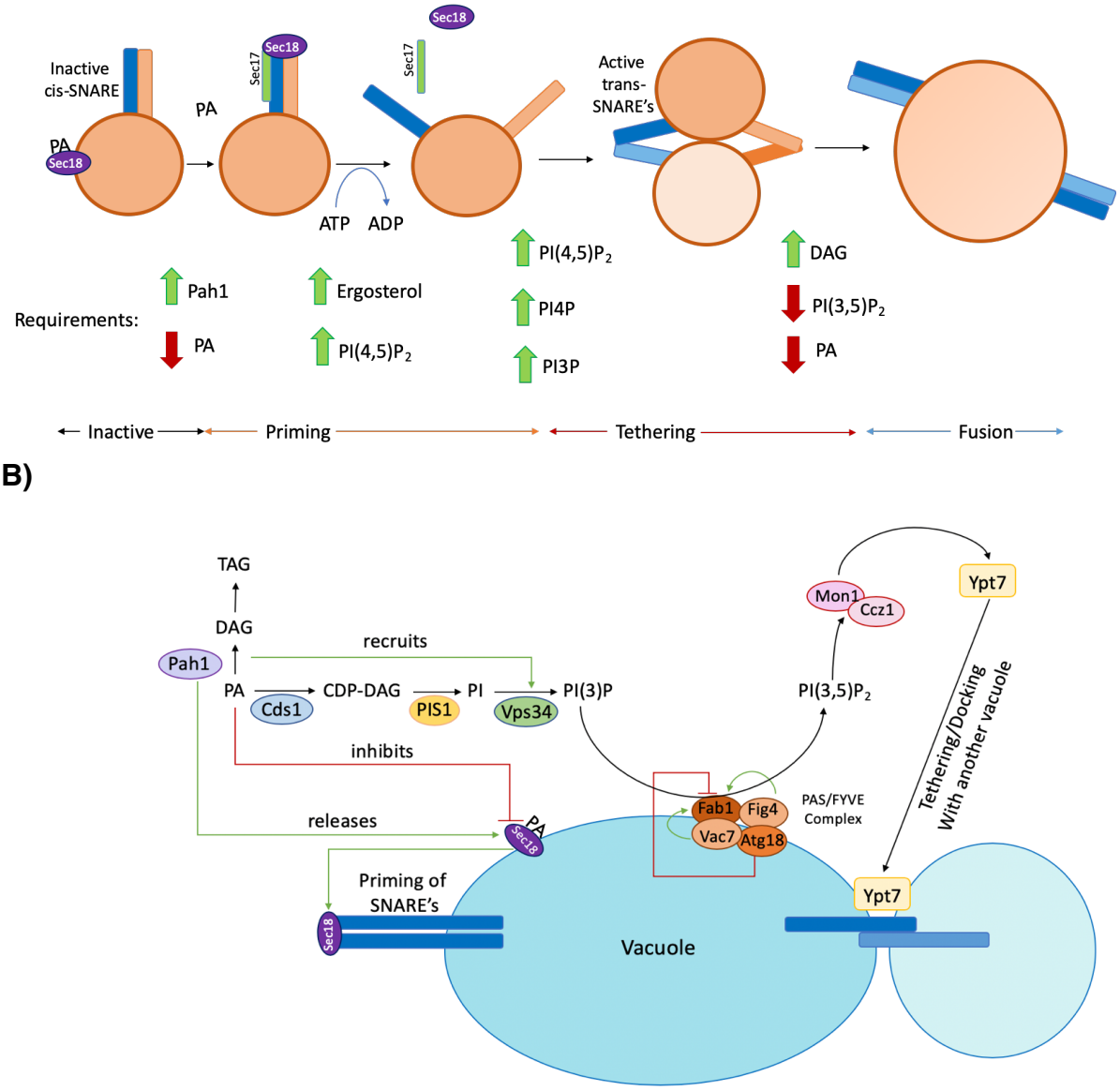

Figure 1.8 - A schematic representing the process of vacuolar fusion in yeast.
A) Fusion of the vacuoles in a yeast cell occurs through priming, tethering and fusion stages. This requires transient levels of lipids to facilitate fusion. **B)** Summary of proteins required for vacuole fusions and their relationship to lipids. The interconnected nature of these processes allows for tight regulation of vacuole fusion.

1.7.2 Lipid Metabolism at the Nuclear Vacuole Junction (NVJ)

Membrane contact sites are vital to facilitate timely communication between organelles during changes in metabolic conditions. First discovered in yeast, the nuclear-vacuole junction (NVJ) is a vital membrane contact site connecting the vacuole with the nuclear ER.[229] A few years later, a membrane contact site between the ER and endosomes was homologous in mammals, containing many conserved lipid transfer proteins and mechanisms.[241,242] In yeast, the NVJ is formed through

direct interaction between the nuclear protein, Nvj1, and the vacuolar protein, Vac8.[229] Nvj1 binds to specific regions within the nuclear ER through its N-terminus, while the C-terminus binds directly to Vac8.[243,244] Nvj1 has several other binding partners which are involved in lipid metabolism. For example, the oxysterol-binding protein Osh1 can be found in the late Golgi and the NVJ, interacting with the cytoplasmic region of Nvj1 through its ankyrin region.[245,246] Additionally, the enoyl-CoA reductase Tsc13 accumulates at the NVJ and interacts with Nvj1 through its transmembrane domain.[247,248] Other relevant proteins localizing to the NVJ are summarized in **Figure 1.9** and **Table 3**.

Upon glucose deprivation, the NVJ expands to facilitate inter-organelle communication.[249,250] Remarkably, the ability of the NVJ to expand is an indicator of cell viability, marking cells as quiescent. Cells that cannot generate NVJs are more likely to become senescent, failing to enter proper cell functioning upon returning to normal glucose conditions.[251] By expanding the NVJ contact site, this surface provides a site for the production of LD in an Mdm1-dependent manner.[252] Under glucose deprivation, Pah1*-GFP (a fusion carrying the D298A D400A mutant that allows it to bind to the membrane without requiring dephosphorylation) was found to localize transiently to the NVJ, co-localize with LDs.[126,165] The location of LDs to the NVJ may facilitate the transfer of LDs to the vacuole, where they are degraded, as seen in lipophagy.[253] The role of Pah1 in this process is still an area of research. However, it is known that Pah1 continues to localize to the NVJ upon deletion of *NVJ1*, indicating that the NVJ is not required for targeting Pah1.

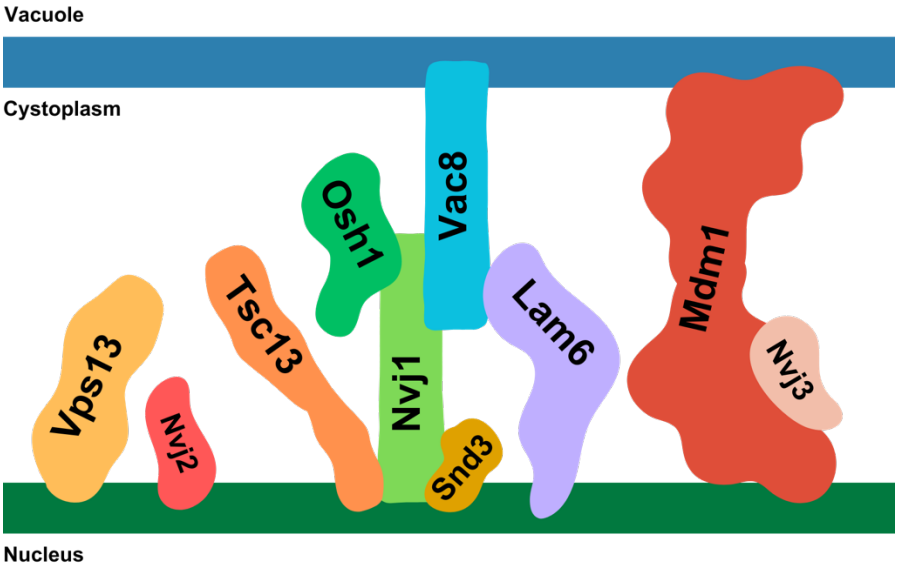

Figure 1.9– Summarization of metabolic proteins localized to the NVJ in yeast.
Protein descriptions are listed in **Table 3**, and information expands on the work by Kohler and Büttner [254].

Table 3 – Summary of the role and function of metabolic proteins localized to the NVJ.

Proteins Localization to the NVJ	Interacts Through	Role
Osh1	Nvj1	Binds ergosterol and PI(4)P, transferring lipids between membranes.[255]
Tsc13	Nvj1	
Nvj2	Nucleus	Lipid-binding protein involved in ceramide transfer.[256]
Mdm1	Vacuole	Tethers to the vacuole via PX-domain, promotes LD biogenesis via localized FA activation.[257]
Nvj3	Mdm1	
Lam6	Vac8	Mediates sterol-enriched lipid microdomains on the vacuolar membrane, expands contact site interaction under glucose limitation.[258,259]
Vps13	Nucleus	Transiently enriched at the NVJ, involved in phospholipid transport.[260,261]
Snd3	Nvj1	Regulator of the NVJ, responds to glucose signalling.[262]
Lam6	Nucleus and Vac8	Sterol transporter, recruited when glucose is limiting.[258]

1.7.3 Piecemeal Microautophagy of the Nucleus (PMN)

PMN is the primary function of the yeast NVJ.[228,263] PMN is a specific type of microautophagy involving the selective degradation of nuclear material into the vacuole.[230] This process is typically induced by starvation and is structurally maintained by the NVJ. The formation of PMN blebs is regulated by stress-inducible Nvj1.[250] Once the junction between Nvj1 and Vac8 is made, excessive

nuclear membrane extends into the vacuole and pinches off from the nucleus as the vacuole fuses around it. A summary of the stages in this process can be found in **Figure 1.10**. Both Nvj1 and Vac8 are required for PMN, and deletions of either are devoid of NVJs altogether.[224,229] For PMN to occur, remodelling of the nuclear membrane is required. Both Tsc13 and the oxysterol-binding protein, Osh1, are involved in this process and allow PMN to occur properly.[245,247,250,263] The remodelling that occurs at the NVJ during PMN requires TAG to be stored in LDs as a source of autophagosomal membrane. Cells defective in TAG synthesis, such as mutants of the Pah1, typically are defective in PMN.[146] When this process is dysregulated, the nucleus will continue to extend around the vacuole and appear "flared", as is further described in **Section 1.6.1**.[224]

As a form of microautophagy, PMN also requires a suite of autophagy genes.[230] However, several proteins involved with vacuole fusion (such as Vph1, LMA1 and Vtc proteins) are not necessary for PMN function, indicating that the fusion of vacuoles seen in PMN is not classic homotypic fusion.[230]

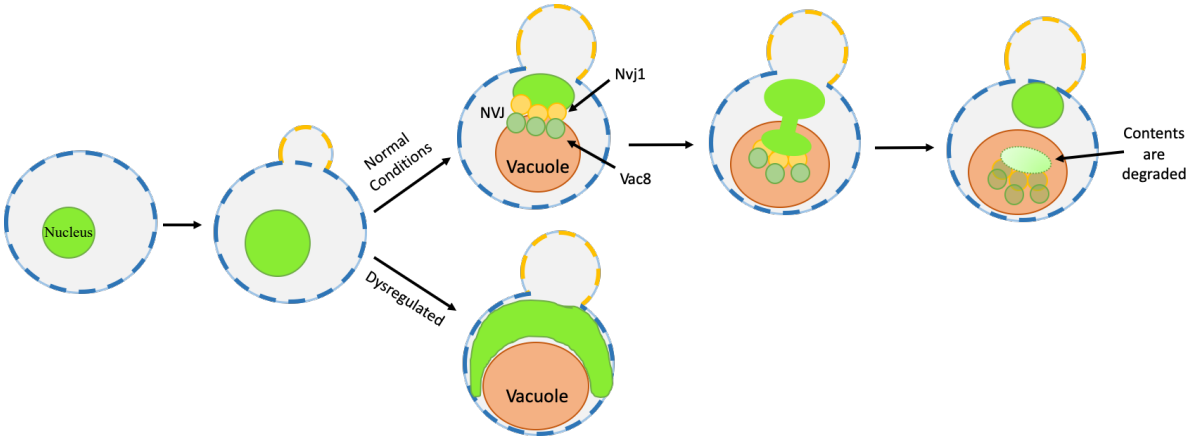

Figure 1.10 – Schematic diagram of Piecemeal Microautophagy of the nucleus (PMN).
Under normal conditions, PMN will endocytose excess nuclear membrane and recycle its contents. If this process is dysregulated, or the NVJ is compromised, then the nucleus will extend around the vacuole in an attempt to create a contact site with the vacuole. This results in a type of nuclear flare.

1.8 Motivations:

The last 20 years have re-defined our understanding of lysine acetylation as we continue to discover novel non-histone protein targets whose acetylation alters their localization and function. This thesis sought to further investigate the connection between NuA4 and lipid metabolism, exploring how this relationship influences organelle morphology. **The following motivating factors drove this work:**

1. **Discovery of nuclear dysregulation in the NuA4 mutant, *eaf1*Δ** - Previous work in the Baetz lab identified Acs2-GFP in high-content microscopy screen of *eaf1*Δ cells expressing GFP-tagged proteins.[65] While typically nuclear, Acs2-GFP in an *eaf1*Δ showed an irregular nuclear structure. This brought many questions surrounding how NuA4 could be regulating nuclear share and morphology.
2. **NuA4's important role in the regulation of lipid metabolism** – The yeast lysine acetyltransferase, NuA4, has been implicated in a variety of lipid metabolism pathways.[66,67,91] Most recently, the Baetz lab described the role of NuA4 in the regulation of ergosterol and Acc1.[65,91] While described in detail in the **Introduction**, NuA4 is also tightly linked to autophagy and the regulation of gene expression. Since these pathways have underlying roles in regulating nuclear shape, structure, and function, this probed further investigation into the mechanisms driving nuclear morphology.
3. **Deletion of *PAH1* results in nuclear flares and vacuolar fragmentation –** Pah1, a key regulator of lipid droplet formation and phospholipid membrane synthesis (described in **Section 1.5.2**), is well known for its role in maintaining nuclear shape (described in **Section 1.6.1**). In fact, deletions of *PAH1* result in a unique nuclear phenotype called a nuclear flare, as well as severe fragmentation of the vacuole.[222,147,236] The nuclear dysregulation and vacuolar

fragmentation we saw upon deletion of *EAF1* was very similar to that seen upon deletion of *PAH1*. However, these phenotypes appeared more severe in *eaf1*Δ cells than in *pah1*Δ cells.

4. **An undefined relationship between NuA4 and Pah1** - Previous research found that NuA4 directly acetylated Pah1; however, the functional consequences remained unclear.[110] This motivated my investigation to further define the role of acetylation on Pah1 localization and function. This is compounded by the fact that this recent study also showed that mice with reduced Tip60 (the human homology of NuA4) activity (described in **Section 1.5.4**) have impaired fat accumulation. This was proven to be a direct result of impaired acetylation of lipin 1 (the human homolog of Pah1). Given these results, it was clear there is a functional consequence of NuA4/Tip60-dependent acetylation of Pah1/lipin 1. While this was investigated in the context of lipid droplet and fatty acid accumulation, there was a need for further investigation into the specific role of the NuA4-Pah1 relationship in regulating organelle morphology.

1.9 Hypothesis:

This thesis explores the intricate relationship between NuA4 and lipid metabolism, focusing on its impact on organelle morphology. I hypothesize that NuA4 regulates lipid metabolism through both direct mechanisms, such as the acetylation of Pah1, and indirect pathways that remain undefined. These regulatory roles influence nuclear shape, vacuolar structure, and broader organelle organization. Understanding this relationship has the potential to inform clinically relevant insights into Tip60's role in human diseases involving lipid dysregulation.

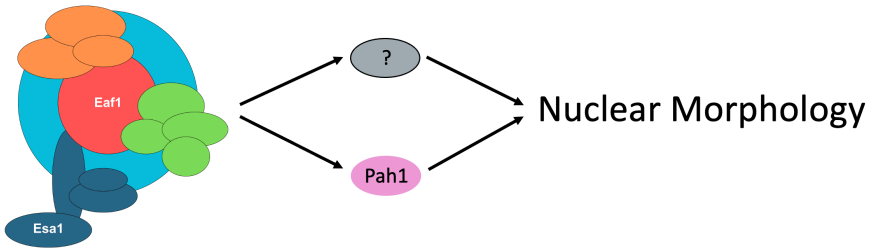

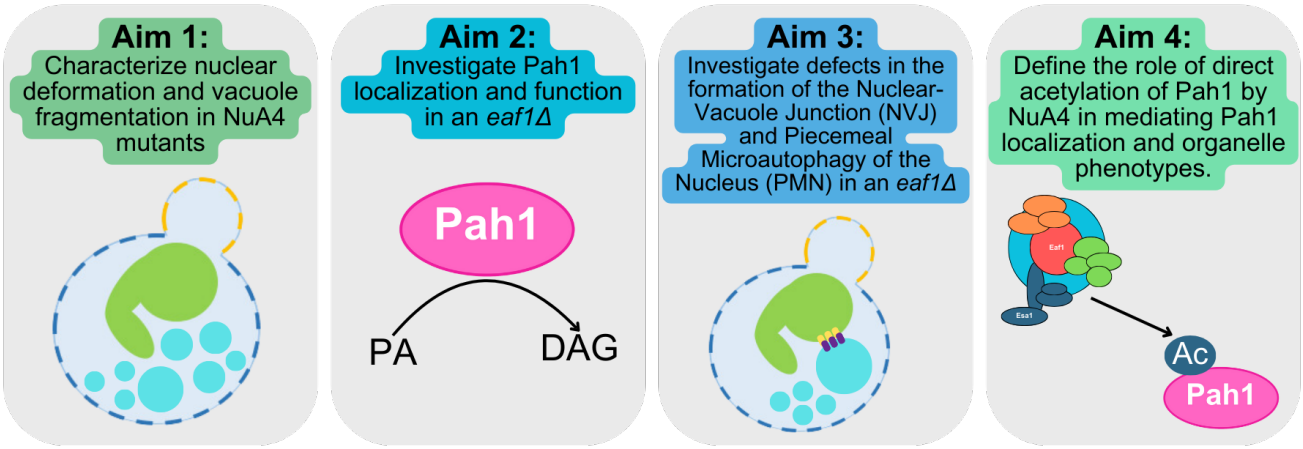

Chapter 2

Manuscript #1 - Uncovering the role of the yeast lysine acetyltransferase NuA4 in the regulation of nuclear shape and lipid metabolism

Sarah Jane Laframboise[1,2], Lauren Deneault[1,2], Alix Denoncourt[2,3], Michael Downey[2,3,*], & Kristin Baetz[1,2,4,*]

[1]Department of Biochemistry, Microbiology and Immunology, Faculty of Medicine, University of Ottawa
[2]Ottawa Institute of Systems Biology
[3]Department of Cellular and Molecular Medicine, Faculty of Medicine, University of Ottawa
[4]Department of Biological Sciences, Faculty of Science, University of Calgary

*Co-corresponding Author: Dr. Kristin Baetz, kristin.baetz@ucalgary.ca
X (Twitter): @DrKristinBaetz
LinkedIn: linkedin.com/in/kristin-baetz-3b45a134

*Co-corresponding Author: Dr. Michael Downey, mdowne2@uottawa.ca
X (Twitter): @downeyuottawa

2.1 Author contributions

This work was executed, analyzed, written and prepared for publication by S.J.L.. Each Figure was produced by S.J.L.. L.D. contributed to cell counting in Figure 2.4 and 2.5. A.D. performed an experiment during revisions that was not used in the final publication. S.J.L., M.D. and K.B performed conceptualization, methodology, and review & editing of the final draft for publication. K.B. & M.D. provided supervision, resources, project administration and funding acquisition.

2.2 Abstract

Here, we report a novel role for the yeast lysine acetyltransferase NuA4 in regulating phospholipid availability for organelle morphology. Disruption of the NuA4 complex results in 70% of cells displaying nuclear deformations and nearly 50% of cells exhibiting vacuolar fragmentation. Cells deficient in NuA4 also show severe defects in the formation of nuclear-vacuole junctions (NVJ), as well as a decrease in piecemeal microautophagy of the nucleus (PMN). To determine the cause of these defects we focused on Pah1, an enzyme that converts phosphatidic acid into diacylglycerol, favouring accumulation of lipid droplets over phospholipids that are used for membrane expansion. NuA4 subunit Eaf1 was required for Pah1 localization to the inner nuclear membrane and artificially tethering of Pah1 to the nuclear membrane rescued nuclear deformation and vacuole fragmentation defects, but not

defects related to the formation of NVJs. Mutation of a NuA4-dependent acetylation site on Pah1 also resulted in aberrant Pah1 localization and defects in nuclear morphology and NVJ. Our work suggests a critical role for NuA4 in organelle morphology that is partially mediated through the regulation of Pah1 subcellular localization.

Keywords: NuA4; acetylation; lipid metabolism; nuclear deformation; vacuole fragmentation

2.3 Introduction

One of the most common types of post translational modification (PTM) is acetylation, the reversible addition of acetyl groups onto lysine residues. Our work focuses on the *Saccharomyces cerevisiae* lysine acetyltransferase complex NuA4 - the yeast homolog of the mammalian Tip60 complex. NuA4 is comprised of 13 subunits, including the catalytic component, Esa1, and the scaffolding unit, Eaf1.[70,72,89,90,264] Esa1 is homologous to human Tip60 and 12 of the additional subunits in the yeast NuA4 complex have mammalian homologs found in the Tip60 complex, demonstrating conservation between species.[69] Since *ESA1* is an essential gene, the temperature sensitive mutant *esa1*^{ts}, which inactivates the encoded subunit at high temperatures, is commonly used to investigate the role of NuA4.[70,85,86] Alternatively, deletion of the non-essential *EAF1* results in dissociation of the NuA4 complex and reduction of Esa1 targeting. Therefore, *eaf1*Δ strains are useful models for investigating the consequences of NuA4 dysfunction.[62,65,66,89-91]

NuA4 action has been linked to several pathways related to lipid regulation,[66,91,64,65] growth control,[67] and the stress response[68] in yeast. Previous work in mice has identified an essential role for Tip60 in regulating triacylglycerol (TAG) accumulation and lipid droplet size.[110] This role is believed to be mediated by Tip60 acetylation of phospholipid phosphohydrolase, lipin 1, which results in translocation of lipin 1 to the endoplasmic reticulum (ER). In yeast, mutants of NuA4 also display decreased TAG accumulation and lipid droplets.[66,110] The yeast homolog of lipin 1, Pah1, is also an important enzyme in the lipid synthesis pathway, as it converts the key metabolite phosphatidic acid

(PA) into diacylglycerol (DAG), which is subsequently modified by the DAG acetyltransferase to form TAG. TAG is then packaged and stored in lipid droplets. Alternatively, PA can be processed into CDP-DAG, which is a precursor to many membrane phospholipids (**Summarized in Fig. 2.1A**).[123,126,127,130] Two NuA4-dependent acetylation sites have been identified on Pah1, and lysine to arginine mutations at these two sites, in tandem, resulted in a reduction in lipid droplet formation.[110] However, the individual contributions of each site, the functional consequences of this regulatory circuit for Pah1 localization, and the downstream consequences for organelle homeostasis are not clear.

Regulation of PA, and in particular the function of Pah1, is important to establish a balance between the production of lipid droplets and membrane phospholipids. For example, in *pah1*Δ cells there is an increase in total phospholipids resulting in extensions of the nuclear membrane (known as nuclear flares),[125,222] and a corresponding decrease in TAG accumulation.[148,265] This gross dysregulation of underlying lipids causes additional defects in vacuole fusion,[147] autophagy[146], and cell wall integrity.[143] Importantly, these phenotypes are rescued upon deletion of *DGK1,* which encodes an enzyme functioning in opposition to Pah1, converting DAG into PA.[148,150] Collectively, the available data highlight the importance of PA and DAG levels in modulating the balance between phospholipid production and lipid droplet formation.

In this study, we report that NuA4 mutants display abnormal organelle phenotypes such as nuclear deformation and vacuolar fragmentation. Additionally, we identified defects in nuclear-vacuole junction (NVJ) formation and piecemeal microautophagy of the nucleus (PMN), which provides a secondary mechanism for nuclear deformation in NuA4 mutants. By targeting Pah1 to the nuclear membrane, we were able to rescue nuclear deformation and vacuole fragmentation defects in *eaf1*Δ cells, but not NVJ and PMN defects. Finally, we provide evidence that these phenotypes are caused in part by misregulation of Pah1 subcellular localization mediated by acetylation at K496.

2.4 Materials and Methods

Cell Culture

A list of all strains used in this work can be found in Supplemental Table 2. This study uses the BY4741 (S288C) yeast strain background. Strains were made through PCR-mediated insertion/deletion[266] and confirmed through PCR. All strains were grown in either YPD media (1% yeast extract, 2% peptone, 2% dextrose), SC media (6.7g/litre of YNB with ammonium sulfate, lacking indicated amino acids) or NS media (1.7g/litre of YNB without ammonium sulfate). Yeast were cultured in the indicated media at 30°C unless otherwise stated. Yeast were grown overnight before being diluted to an OD600 of 0.1 in the morning and allowed to grow to mid-log phase (OD600 of 0.5-0.8) for experiments. For induction of PMN, cells were grown to mid-log phase, washed with water, and resuspended in NS media to grow for four hours.

Serial Dilution Dot Assays

Cultures were grown to mid-log phase in YPD media and diluted to an OD600 of 1.0. They were then further diluted into OD600's of 0.1, 0.001, and 0.0001. 5 μL of each serial dilution was placed onto YPD plates in descending order across each row. This was repeated three times for all query strains. Representative images are shown.

Microscopy

Yeast cells were prepared by growing them to mid-log phase (OD600 0.5-0.8) in necessary media to maintain plasmids. If CellTracker Blue *CMAC* (7-amino-4-chloromethylcoumarin) (Invitrogen C2110) was used, it was added to cells in liquid media at a concentration of 10 mM for 15 mins. Cells were spun down and the pellet resuspended in SC media for imaging.

All representative images were captured with Zeiss Axio-ObserverZ1-LSM 880-AiryScan confocal microscope driven by the Zen Black 2.3 software. The Laser Scanning microscope is a Zeiss LSM880 confocal microscope, outfitted with a 63X/1.4 NA objective (in combination with Immersion

oil 518F 37C). Images were captured using the Airyscan detector (sequential, unidirectional scanning, Z-stack of 0.2 μm slice thickness).

See below the relevant settings used to image each type of fluorophore:

- *For Venus:* Argon laser at 514 nm (2 %), with filter: BP 495-550 + LP 570, pixel dwell: 8.04 $x10^{-7}$
- *For GFP:* Argon laser at 488nm (2 %), with filter: BP 495-550 + LP 570, pixel dwell: 8.04 $x10^{-7}$
- *For CellTracker Blue CMAC:* Diode laser at 405-30nm (2.9 %), with filter: BP 420-480 + LP605 + LP 570, pixel dwell: 8.04 $x10^{-7}$
- *For RFP and mCherry*: Diode laser 561nm (2 %), with filter: BP 495-550 + LP 570, pixel dwell: 8.04 $x10^{-7}$

Raw images went through subsequent Airyscan processing before being used for the surface rendering.

Fluorescence intensities of Venus fluorescence and PA/DAG mCherry biosensors were measured using the "plot profile" plugin of Fiji to generate a profile of fluorescence intensity across the cell (centred on the nucleus or punctate when relevant). This was repeated for the indicated "n" replicates. All replicates were plotted on the graph with the mean of all lines plotted in black.

When indicated, images for quantification were done on Leica fluorescent microscope (DMI6000; Leica Microsystems) equipped with a Hamamatsu camera, DG4 light source (Sutter Instruments) and Volocity 4.3.2 software (Perkin Elmer), or on the Axio-Obsersever7 (Zeiss) driven by Zen 3.2.

Illumination: HXP 120

Camera: sCMOS ORCA-Flash LT

Objective: 63x/NA 1.4

Filters:

- *GFP channel:* Ex: BP 450/50, FT: 480, EM: BP 510/50, exposure time: 5 sec, Light intensity
- *CellTracker Blue CMAC:* Ex: G365, FT: 395 nm, EM: BP 445/50, exposure time: 3 sec, Light intensity
- *Mcherry or RFP:* Ex: BP 550/25, FT: 570, EM: BP 605/70, exposure time: 10 sec, Light intensity

3D Images

Surface rendering was performed using Imaris 9.8 (Bitplane, Oxford Instruments), with the following settings:

- Background subtraction- LS (Largest surface) set at: 0.2 μm, without smoothing
- Objects smaller than 0.2 μm were filtered out.

Western Blots

Yeast strains were grown overnight at 30°C in 25 mL of YPD media and diluted the next morning into 50 mL cultures at an OD600 of 0.2. Cells were harvested at mid-log phase and whole cell extracts were collected. Cells were centrifuged at 4°C, washed with water, and centrifuged again to remove any trace of culture media. Finally, pellets were flash frozen in liquid nitrogen and stored at -80°C. Pellets were thawed on ice and 1x the pellet volume of lysis buffer (20 mM HEPES pH 7.4, 0.1% Tween 20, 2 mM $MgCl_2$, 300 mM NaCl, protease inhibitor [P-8215; Sigma]) was added. Equal volume of glass beads (Fisher 35–5350) were added to the mixture, which was then lysed by bead beating method 5 times for 1 minute with a 1 minute rest on ice in between. Whole cell extracts were collected and quantified using Bradford assay.

A standard curve for each protein was performed to determine the optimal amount of protein to be loaded on TGX quantitative gels for western blot. This was loaded onto a 10% Mini-PROTEAN

TGX Precast Protein gels (Bio-Rad 4561033) and run in 1X SDS-PAGE running buffer at 120V for about an hour and a half. Once completed, the gel was activated and visualized under UV. The gel then was transferred onto nitrocellulose membrane (Bio-Rad 1620112) using the semi-dry transfer method. Total protein was imaged under UV. Blocking was performed in 5% milk in TBS-T (tris-buffered saline + 1% Tween 20) for 1 hour before incubation overnight with 1:1000 dilution of anti-GFP primary antibody (Sigma-Aldrich 11874460000) or anti-mCherry (Abcam ab125096) in 5% milk TBS-T. Blots were then washed 3 times in TBS-T for ten minutes each, incubated for 1 hour with 1:5000 dilution of anti-mouse secondary antibody in 5% milk TBS-T and washed again three times. Blots were visualized with Clarity Western ECL (Bio-Rad 170-5061) and imaged with Bio-Rad's ChemiDoc system.

CRISPR-Cas9 Acetylation Mimics

Pah1 point mutations at Lysine 496 (K496) were created by CRISPR-Cas9. This protocol is adapted from Dicarlo et al. [267] The Cas9 plasmid, p415-TEF1p-Cas9-CYC1t,[267] was transformed into Pah1-3xGFP strains and maintained on SC-LEU media.

A PAM sequence, selected from a list from Dicarlo *et al.* [267] to target the surrounding area of Pah1-K496, was cloned into the guide RNA plasmid, p426-SNR52p-NotI(gRNA)-SUP4t by PCR. The resulting plasmid was treated with DPN1, transformed into DH5α *E.coli* to amplify, and then confirmed through sequencing at the TCAG facility at SickKids, Toronto. Double-stranded DNA (dsDNA) that matched the cleaved area and contained the mutations at K496, as well as the NGG PAM site, were created by annealing two single-stranded oligos at 100°C and then slowly decreasing the temperature.

The guide RNA plasmid and the dsDNA were transformed into the strains and selected for on SC-LEU-URA. Positive colonies were collected for genomic DNA extraction. A PCR product was

generated from the mutation area and sent for sequencing at the TCAG Facility at SickKids, Toronto to confirm the mutation site.

Mutagenesis of BiFC Pah1-VC plasmid

Pah1-K496Q-VC, Pah1-K496R-VC, Pah1-K801Q-VC and Pah1-K801R-VC plasmids were generated via Mutagenesis service from Genscript USA Inc.

Gibson Assembly

Mlp1-VC and Nup2-VC plasmids were assembled via Gibson assembly service provided by the University of Ottawa's Genome Editing and Molecular biology (GEM) Facility following standardized protocols.

Statistical Analysis

GraphPad Prism was used to perform all statistical analyses. A 2-way ANOVA was used to compare all data with more than two groups. The means of individual pairs were compared by Tukey's multiple comparison test. P values are indicated in Figure legends.

2.5 Results

NuA4 mutants exhibit nuclear deformation and vacuole fragmentation

We were motivated to determine if NuA4 mutants display nuclear deformations, as a previous high-content microscopy screen determined that *eaf1*Δ cells expressing a GFP-tagged nucleoplasmic protein, Acs2-GFP, indicated abnormal nuclear morphology.[65] Nuclear deformations, or an expansion of the nuclear membrane,[224] can be observed using a nucleoplasmic fluorescence marker, such as Acs2-GFP, that is not bound to chromatin. We continued to use Acs2-GFP, in combination with nuclear membrane marker Nup49-RFP, to assess nuclear morphology in wildtype (WT), *pah1*Δ, and NuA4 mutant cells. We also monitored vacuole morphology using CellTracker Blue CMAC (7-amino-4-chloromethylcoumarin), which stains the vacuole lumen. As expected, nuclear deformations

were detected in 7.1% of WT cells (**Fig. 2.1B and C, Supplemental Video 2.1**) and 26.5% of *pah1*Δ cells (**Fig. 2.1C**).[125,148] In NuA4 mutants, nuclear deformations were detected in 69.8% of *eaf1*Δ cells (**Fig. 2.1 B and C, Supplemental Video 2.2 and 2.3**) and in 32.4% of *esa1-L254P* mutants, which are temperature sensitive (**Supplemental Fig. 2.1A and B**).[85] These nuclear deformations were seen in all stages of the cell cycle, and exhibited a vastly different profile than those seen in mitotic arrest induced by nocodozole treatment (**Supplemental Fig. 2.2**). We were surprised that *eaf1*Δ cells had rates of nuclear deformations substantially higher than *pah1*Δ cells, which suggests that NuA4 may impact nuclear morphology through both Pah1-dependent and Pah1-independent pathways. Even more surprising was the observation that deletion of *PAH1* partially rescued nuclear deformation phenotypes of *eaf1*Δ cells (**Fig. 2.1C**). This observation suggests that in NuA4 mutants, Pah1 in part promotes nuclear deformations, even though it normally functions to prevent them.

Given their important role in the production of phospholipids (**outlined in Fig. 2.1A**), we asked if deleting *DGK1* and *INO1*, or introduction of a temperature sensitive mutation of the essential gene *CDS1, cds1-ts*[268], could rescue nuclear deformation of *eaf1*Δ cells in a manner similar to how these mutations rescue phenotypes associated with deletion of *PAH1*. [132,148,265] While the single mutants maintained WT levels of nuclear deformations, double deletions with *eaf1*Δ partially rescued the increase in nuclear deformations seen in *eaf1*Δ single mutant cells (**Fig. 2.1C**). This result suggests that increased nuclear deformations in *eaf1*Δ cells are caused in part by a flux into membrane phospholipid synthesis.

Next, we examined the consequences of lipid dysregulation at the level of vacuolar morphology. Cells were considered to have fragmented vacuoles if they contained five or more vacuolar lobes, with CMAC being used to stain the vacuolar lumen. With this classification, 48.5% of *eaf1*Δ cells (**Fig. 2.1B and D**) and 32.4% of *esa1-L254P*^{ts} cells shifted to a non-permissive temperature (**Supplemental Fig. 2.1A and C**) had fragmented vacuoles, compared to only 4.8% of

WT cells (**Fig. 2.1B and D**). This defect was significantly greater than the 9.1% observed in a *pah1*Δ strain. Unlike nuclear deformations, the phospholipid membrane enzyme mutants tested (*pah1*Δ, *dgk1*Δ, *ino1*Δ and *cds1-ts*) were unable to rescue vacuole fragmentation in *eaf1*Δ cells (**Fig. 2.1D**). Interestingly, a previous study showed that the deletion of *DGK1* was also unable to rescue the vacuolar defects seen in *pah1*Δ.[150] Together our work indicates that *eaf1*Δ and *esa1-L254P*^{ts} cells have nuclear deformations stemming from dysregulation of phospholipid synthesis, while vacuole fragmentation defects are most likely caused by a disruption of an alternative pathway.

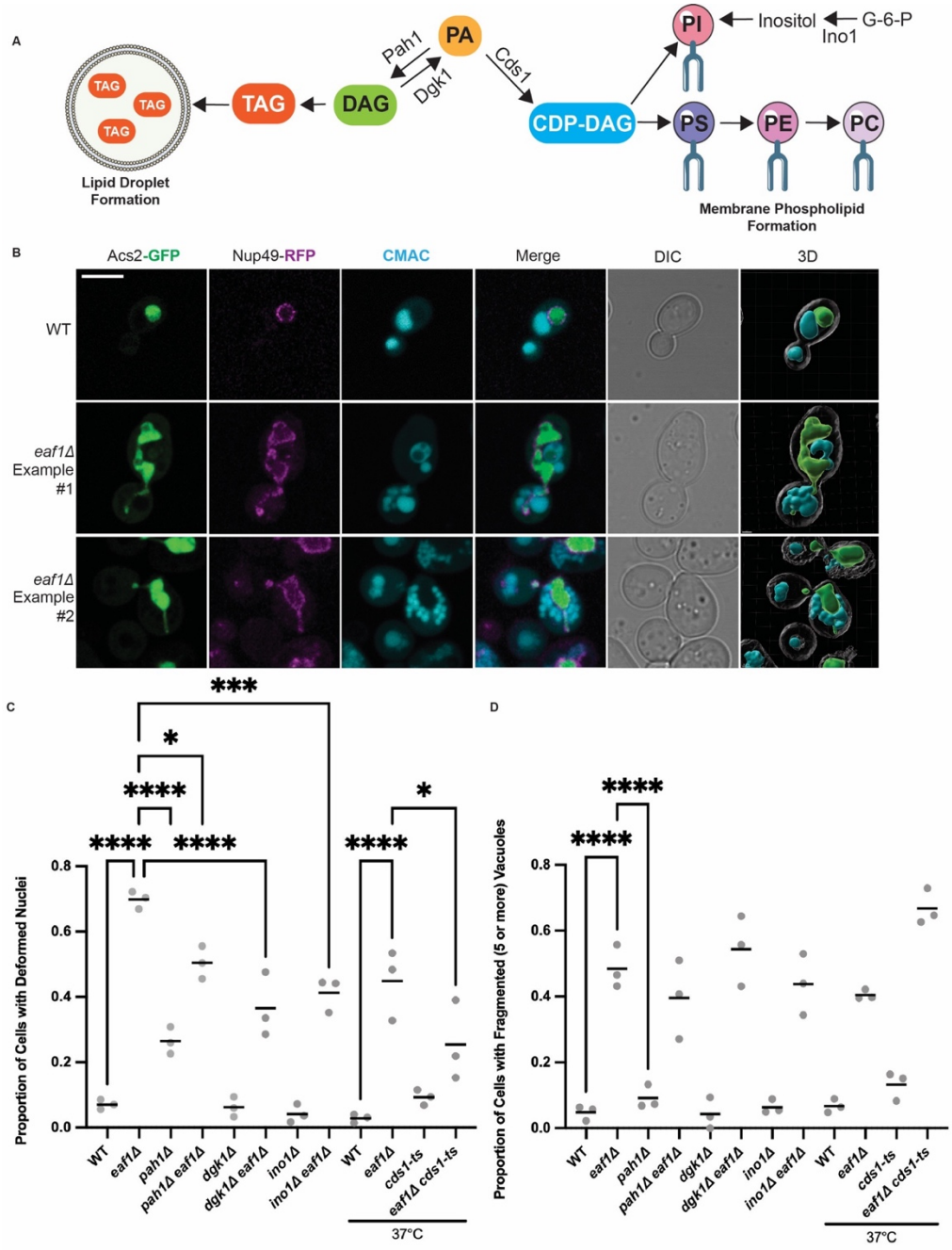

Figure 2.1 – Deletion of *EAF1* results in nuclear deformation and vacuole fragmentation.
A) Simplified diagram of yeast lipid synthesis showing the diversion of phosphatidic acid (PA) into two main pathways; one producing lipid droplets, and the other producing membrane phospholipids (PS, phosphatidylserine. PE, phosphatidylethanolamine. PC, phosphatidylcholine. PI, phosphatidylinositol). DAG, diacylglycerol. TAG, triacylglycerol. CDP-DAG, cytidine diphosphate diacylglycerol. G-6-P, glucose-6-phosphate. (B) Representative images showing nuclear deformation and vacuole fragmentation in WT and *eaf1*Δ cells expressing *ACS2-GFP*, *NUP49-RFP* (YKB 4972 and YKB 4863) and stained with CMAC. 3D reconstruction of cells was done using Imaris software. Scale bar = 5 µm. Images presented are representative of three biological replicates. (C) Proportion of total cells with deformed nuclei was quantified through visual analysis of cells. This was repeated for three biological replicates, counting at least 100 cells for each. (D) Proportion of total cells with fragmented vacuoles (i.e. having 5 or more vacuolar lobes), was quantified by visually counting the number of vacuoles per cell. Grey dots represent three biological replicates of at least 100

cells for each. Horizontal bars represent the mean. For C and D, an ANOVA analysis was performed using Tukey's multiple comparison test. *p≤0.05, **p≤0.01, ***p≤0.001, ****p<0.0001, ns = not significant, p>0.05. Relevant statistical significance bars are shown, additional comparisons can be found in Supplemental Table 2.1.

Loss of Pah1 at the inner nuclear membrane in eaf1Δ cells

We next sought to understand how NuA4, which is largely nuclear,[269] could be impacting Pah1 activity and nuclear morphology. Active Pah1 is localized to both the inner and outer nuclear membrane (INM and ONM) where it converts PA into DAG.[167] DAG is subsequently further metabolized into TAG and packaged into lipid droplets.[126,270] To investigate Pah1 localization inside the nucleus, we sought to determine if disruption of NuA4 impacted the subcellular localization of Pah1 to the INM using a BiFluorescent Complementation (BiFC) assay. This same assay had previously been used to detect Pah1 localization to the INM.[167] Pah1 was expressed from a plasmid as a fusion with half of the Venus fluorescent protein (indicated as VC), while the INM protein Nup60 or nucleoplasmic protein Pus1 was expressed from a second plasmid as a fusion with the other half of Venus (indicated as VN) (**Fig. 2.2A**). If the two proteins interact, the full Venus protein is brought together and can be visualized via fluorescence microscopy. In both WT and *eaf1*Δ cells expressing Pah1-VC and Pus1-VN constructs, a Venus signal was detected indicating a pool of Pah1-VC within the nucleoplasm (**Fig. 2.2B**). In WT cells expressing Pah1-VC and Nup60-VN a signal was detected on the INM. In *eaf1*Δ cells, however, the interaction between Pah1-VC and Nup60-VN at the INM is lost, despite appropriate expression of Pah1-VC (**Supplemental Fig. 2.3**). Further, deletion of *EAF1* did not abolish Nup2-VC or Mlp1-VC interaction with Nup60-VN at the INM, suggesting that disruption of NuA4 is not causing gross mislocalization of INM proteins (**Supplemental Fig. 2.4**). Together, our BiFC work indicates that Eaf1 is required for INM localization of Pah1-VC.

If Pah1 localization to the INM is decreased in *eaf1*Δ cells, we predicted we may also see changes in PA and DAG at this location. To test this hypothesis, we next assessed the levels of INM PA and

DAG using the previously validated plasmid-encoded biosensors NLS-Opi1-Q2-mCherry (NLS-PA), and 2XNLS-Cla+Clb mCherry (NLS-DAG).[271] Despite the fact that the expression of both biosensors was reduced in *eaf1*Δ cells (**Supplemental Fig. 2.5**), we were able to make important conclusions about INM PA and DAG pools.[271] In both WT and *eaf1*Δ cells, the NLS-PA biosensor displayed diffuse nucleoplasmic signal (**Fig. 2.2C**). This is consistent with previous results from Romanauska et al.[167] showing that under WT conditions PA is present at lower levels at the INM in comparison to the PA-rich plasma membrane. Only with specific dysregulation of the lipid metabolism pathways, such as that seen in a *cds1-ts* mutant or oleic acid treatment, were they able to detect NLS-PA biosensor enrichment at the INM.[167] PA that accumulates may be quickly shuttled into phospholipid synthesis. In contrast, the NLS-DAG biosensor detected DAG at the INM in both WT and *eaf1*Δ cells (**Fig. 2.2C**). Further, we did not observe nucleoplasmic accumulation of the DAG biosensor, which would be expected in cases of decreased DAG at the INM.[167] This suggests that some Pah1 remains active despite its reduction at the INM of *eaf1*Δ cells as measured by BiFC. Alternatively, *eaf1*Δ cells could be compensating for decreased Pah1 activity by altering other lipid metabolism pathways.

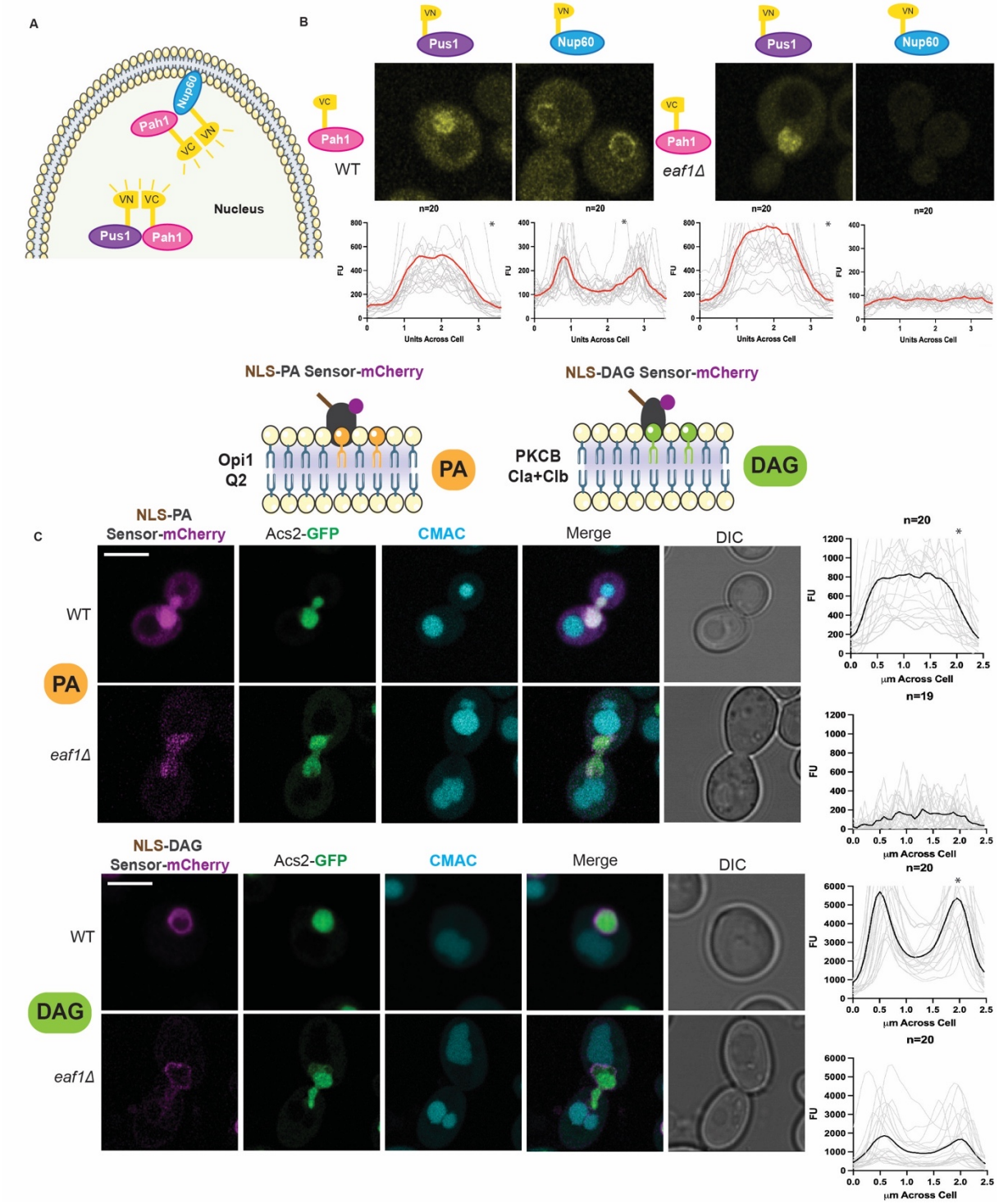

Figure 2.2 – Loss of Pah1 at the INM upon deletion of *EAF1*, with no change in nuclear Phosphatidic Acid (PA) and INM Diacylglycerol (DAG).

(A) Schematic diagram for a BiFluorescent Complementation Assay (BiFC) shows the interaction between two protein fragments, each encoding half of the Venus fluorescent protein. Upon interaction, they form the whole Venus that can be visualized using a fluorescence microscope. (B) Pah1 INM localization is dependent on *EAF1*. BiFC experiment with WT or *eaf1*Δ cells expressing Pah1-VC and Nup60-VN (YKB 4977 and YKB 4978) or Pus1-VN (YKB 4975 and YKB 4976) was assessed. Scale bar = 5 μm. (C) Live imaging of WT and *eaf1*Δ cells expressing genomically integrated *ASC2*-GFP and the plasmid-based NLS-Q2-mCherry biosensor (YKB 5182 and YKB 5183) (top panel) or NLS-DAG-mCherry biosensor (YKB 5184 and YKB 5185) (bottom

panel) and stained with CMAC to mark the vacuoles. Scale bar = 5 μm. Images presented are representative of three biological replicates. Line graphs for (B) and (C) were generated by measuring the fluorescence intensity value of pixels across the nucleus of the cell, using Plot Profile in ImageJ Software. Red/black lines indicate the average for the indicated number of cells, and the grey lines show each cell profile. n = the number of randomly selected cells. FU = Fluorescence Units.
***** Indicates that that y-axis has been cropped to facilitate comparison of strains.

Artificially targeting Pah1 to the nuclear membrane rescues eaf1Δ nuclear deformations and vacuole fragmentation

If nuclear deformations or vacuole fragmentation defects displayed in *eaf1*Δ cells are due to decreased localization of Pah1 to the nuclear membrane, we predicted that artificially targeting Pah1 to the nuclear membranes may rescue these defects. To explore this possibility, we took advantage of the fact that Pah1 localization is primarily modulated through phosphorylation via protein kinases such as Pho85-Pho80, Cdc28-cyclin B and PKA.[125,154,156] However, Pah1 is only dephosphorylated by one phosphatase complex known as Nem1-Spo7. As illustrated in **Fig. 2.3A, top panel**, Nem1-Spo7 dephosphorylation of Pah1 is required for Pah1 association with PA on the nuclear membrane where it converts it to DAG.[123,151,161,166] Under normal conditions, Pah1 remains inactive in the cytoplasm and is only active when dephosphorylated and bound to the nuclear membrane.[140]

We used a previously established approach that exploits this regulatory system to modulate the subcellular localization of Pah1.[151] Pah1-7A-GFP, wherein 7 phosphorylated serine residues are replaced with alanine, artificially binds to the nuclear membrane.[151] Conversely, Pah1-7A-AH3A-GFP contains an additional mutation in Pah1's alpha helix, rendering it unable to bind at this location (**Fig. 2.3A bottom panel**).[151] Therefore, these constructs allow for examination of two distinct scenarios where Pah1 is either active and bound to the nuclear membrane (Pah1-7A-GFP), or a control scenario where this tethering does not occur (Pah1-7A-AH3A-GFP). WT and *eaf1*Δ cells expressing the Nab2-NLS-mCherry construct (nucleoplasm marker) were transformed with plasmids expressing either Pah1-7A-GFP or Pah1-7A-AH3A-GFP and stained with CMAC to mark the vacuole. Consistent with previous literature, both Pah1-7A-GFP and Pah1-7A-AH3A-GFP showed a low level of disperse

cytosolic signal in both WT and *eaf1*Δ cells (**Supplemental Fig. 2.6A**).[126,151] Wild-type *PAH1* is still present in these cells and all Pah1-GFP fusions were expressed in WT and *eaf1*Δ cells (**Supplemental Fig. 2.6B**). WT cells expressing Pah1-7A-GFP or Pah1-7A-AH3A-GFP had low levels of nuclear deformations (**Fig. 2.3B and C**) and fragmented vacuoles (**Fig. 2.3B and D**). In *eaf1*Δ cells, tethering of Pah1 to the nuclear membrane with Pah1-7A-GFP resulted in a greatly reduced nuclear deformations and fragmented vacuoles compared to *eaf1*Δ cells expressing the Pah1-7A-AH3A-GFP control (**Fig. 2.3B, C and D**). These results suggest that the changes in subcellular localization of Pah1 observed in *eaf1*Δ mutants have important consequences for membrane homeostasis.

Defect in the formation of the Nuclear-Vacuole Junction (NVJ) and Piecemeal Microautophagy of the Nucleus (PMN) in an eaf1Δ

If unregulated nuclear membrane growth was the only reason for nuclear deformations in *eaf1*Δ cells, we would anticipate *pah1*Δ and *eaf1*Δ cells to have similar levels of these structures. In contrast, *eaf1*Δ cells had higher levels of deformations than *pah1*Δ cells. Moreover, deletion of *PAH1* in *eaf1*Δ cells partially suppressed the phenotype (**Fig. 2.1**). As defects in piecemeal microautophagy of the nucleus (PMN) also contribute to nuclear deformation,[224] we next sought to determine if NuA4 also impacts this pathway.

PMN, sometimes referred to as nucleophagy, selectively degrades and recycles portions of the nucleus into the vacuole under carbon or nitrogen limiting conditions.[228,272] The first step of PMN is the formation of the nuclear vacuole junction (NVJ), which occurs via an interaction between the vacuolar protein Vac8 and the nuclear protein Nvj1 (**Fig. 2.4A**).[229,255,273,274] Pah1 localizes to the NVJ and participates in lipid remodelling required for PMN.[126]

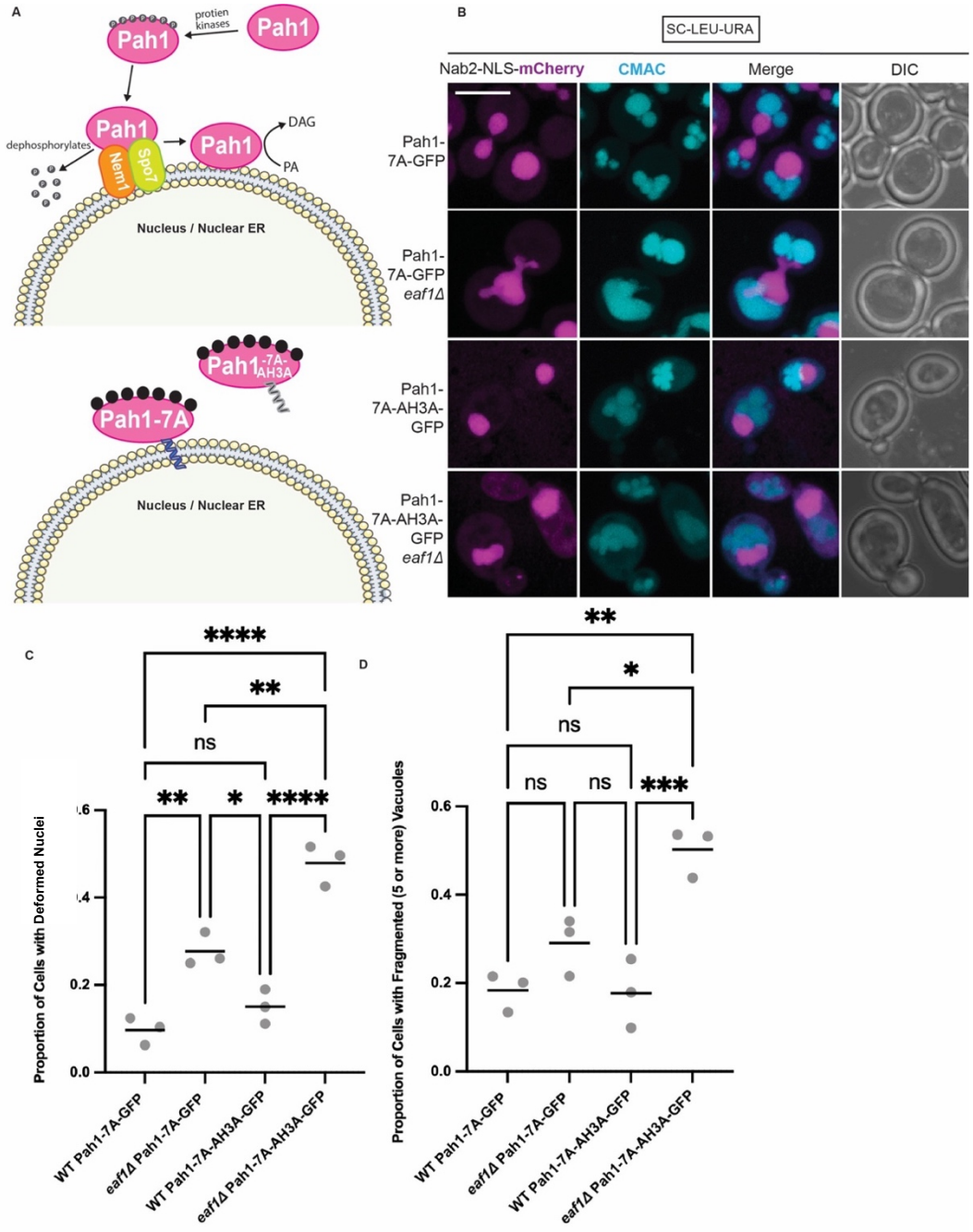

Figure 2.3 – Targeting Pah1 to the nuclear membrane with Pah1-7A-GFP rescues nuclear deformation and vacuole fusion defects.

(A) Graphic depicting the interaction of Pah1-7A and Pah1-7A-AH3A with the nucleus/nuclear ER (NER). (B) Merged Z-stack images showing WT and *eaf1Δ* Pah1-7A-GFP (YKB 5198 and YKB 5199) as well as WT and *eaf1*Δ Pah1-7A-AH3A-GFP (YKB 5200 and YKB 5201), with Nab2-NLS mCherry to visualize the nucleus, and the vacuole stained with CMAC. Scale bar = 5 µm. Images presented are representative of three biological replicates. (C) Proportion of cells with deformed nuclei. Cells were quantified by observing a nuclear extension versus a round nuclei. (D) Proportion of cells with fragmented (5 or more) vacuoles. Cells were quantified by visually counting the number of vacuoles per cell. For C and D, an ANOVA analysis was performed using Tukey's multiple comparison test. Cells were counted by investigating the full Z-stack of cells. Grey dots

represent three biological replicates of at least 100 cells for each. Horizontal bars represent the mean. *p≤0.05, **p≤0.01, ***p≤0.001, ****p<0.0001, ns = not significant, p>0.05.

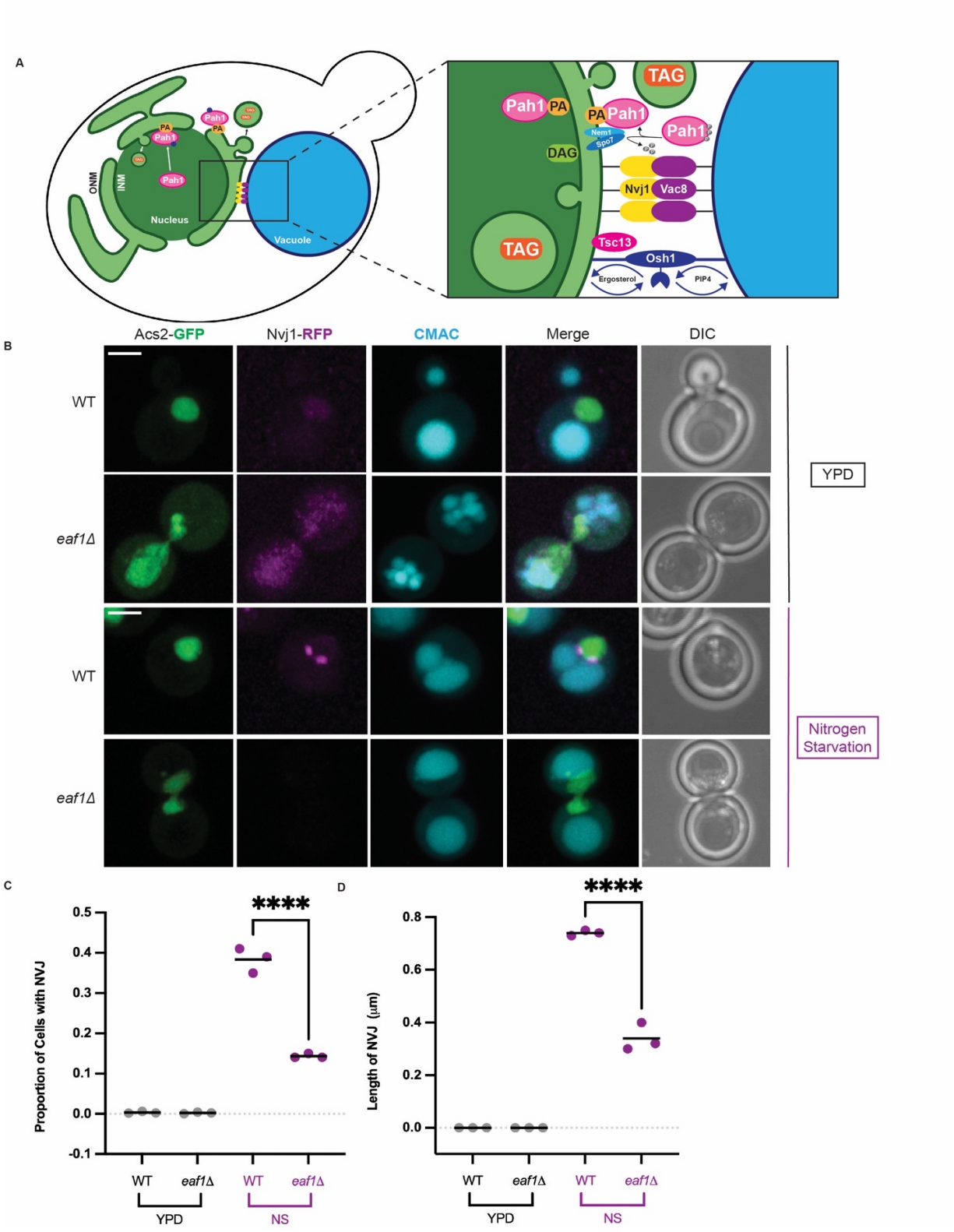

Figure 2.4 – Deletion of *EAF1* results in a decrease in nuclear vacuole junction (NVJ) formation.

(A) Graphic depicting the proteins and complex lipid metabolism that occurs at the NVJ. (B) Nitrogen starvation-induced NVJs are reduced in *eaf1*Δ cells. WT and *eaf1*Δ cells expressing genomically integrated *NVJ1-RFP* (YKB 5123 and YKB 5134) were grown to log phase in YPD at 30°C prior to shifting into nitrogen starvation (NS) media for four hours and staining with CMAC to visualize vacuoles. Images presented are representative of three biological replicates of at least 200 cells counted for each. Scale bar = 5 μm. (C) Proportion of cells with an NVJ, counted visually by assessing the presence or absence of Nvj1-RFP punctae within the cell. (D) The length of the NVJ was measured using a line tool on ImageJ. 20 cells were measured for each strain and performed in triplicate. For both C and D, ANOVA analysis was performed using Tukey's multiple comparison test. Grey and purple dots represent three biological replicates. Horizontal bars represent the mean. ****$p<0.0001$, ns = not significant, $p>0.05$. Relevant statistical significance bars are shown, additional comparisons can be found in Supplemental Table 2.1.

First, we used Nvj1-RFP to visualize the formation of NVJ punctae localized between the nucleus (Acs2-GFP) and vacuole (CMAC) following nitrogen starvation. We found that *eaf1*Δ cells had a significant defect in the formation of the NVJ and a decrease in the size of those NVJs that did form (**Fig. 2.4B, C and D**). Next, we measured PMN using Nab2-NLS-mCherry to mark the nucleus of the cell, and carefully dissected the Z-stack to measure the number of NLS-Nab2-mCherry PMN blebs within the CMAC-labelled vacuole.[275] We identified 37.5% of WT cells with a PMN bleb fully engulfed in the vacuole after four hours of nitrogen starvation (**Fig. 2.5A and B, Supplemental Video 2.4**). In contrast, only 7.6% of *eaf1*Δ cells had PMN blebs within the vacuole (**Fig. 2.5B**). Interestingly, in *eaf1*Δ mutants, there were several instances where Nab2-NLS-mCherry extended in nuclear extensions around the vacuole (**Fig. 2.5A, Middle Panel**), or was squeezed between vacuolar lobes (**Fig. 2.5A, Bottom Panel**). However, 3D reconstruction of these cells confirmed that these extensions of the nucleus did not enter the vacuole itself (**Supplemental Video 2.5 and 2.6**).

In a complementary approach, we used a GFP-Rosella construct fused to the nuclear localization signal of Nab35.[276] Under nutrient replete conditions, the GFP-Rosella-Nab35 fusion protein localizes to the nucleus where both GFP and Rosella can be visualized. After 24 hrs of nitrogen starvation, the GFP-Rosella-Nab35 proteins are engulfed in PMN blebs. Once in the vacuole, the GFP is digested leaving only the Rosella signal visible within the vacuole lumen.[276] Following nitrogen starvation, the WT strain expressing *GFP-Rosella-NAB35* showed GFP and Rosella signal in

the nucleus, and Rosella signal in the vacuole (**Fig. 2.5C**), indicating successful induction of PMN. However, in *eaf1*Δ cells GFP and Rosella signal only co-localized in the nucleus, with no detection of Rosella in the vacuoles (**Fig. 2.5C**). Therefore, disruption of the NuA4 complex results in defects in PMN. Interestingly, unlike the nuclear deformations and vacuole fragmentation phenotypes (**Fig. 2.3**), PMN defects observed in *eaf1*Δ were not rescued by artificial tethering of Pah1 to the nuclear membrane (**Supplemental Fig. 2.7)**. Moreover, *EAF1* was not required for interaction of Pah1 with Nvj1 and Vac8, as measured using a BiFC assay **(Supplemental Fig. 2.8)**. Therefore, despite having NVJ and PMN defects, NuA4 disruption does not impact the localization of Pah1 to the NVJ. Thus, NuA4's impact on these processes appears to be independent of Pah1.

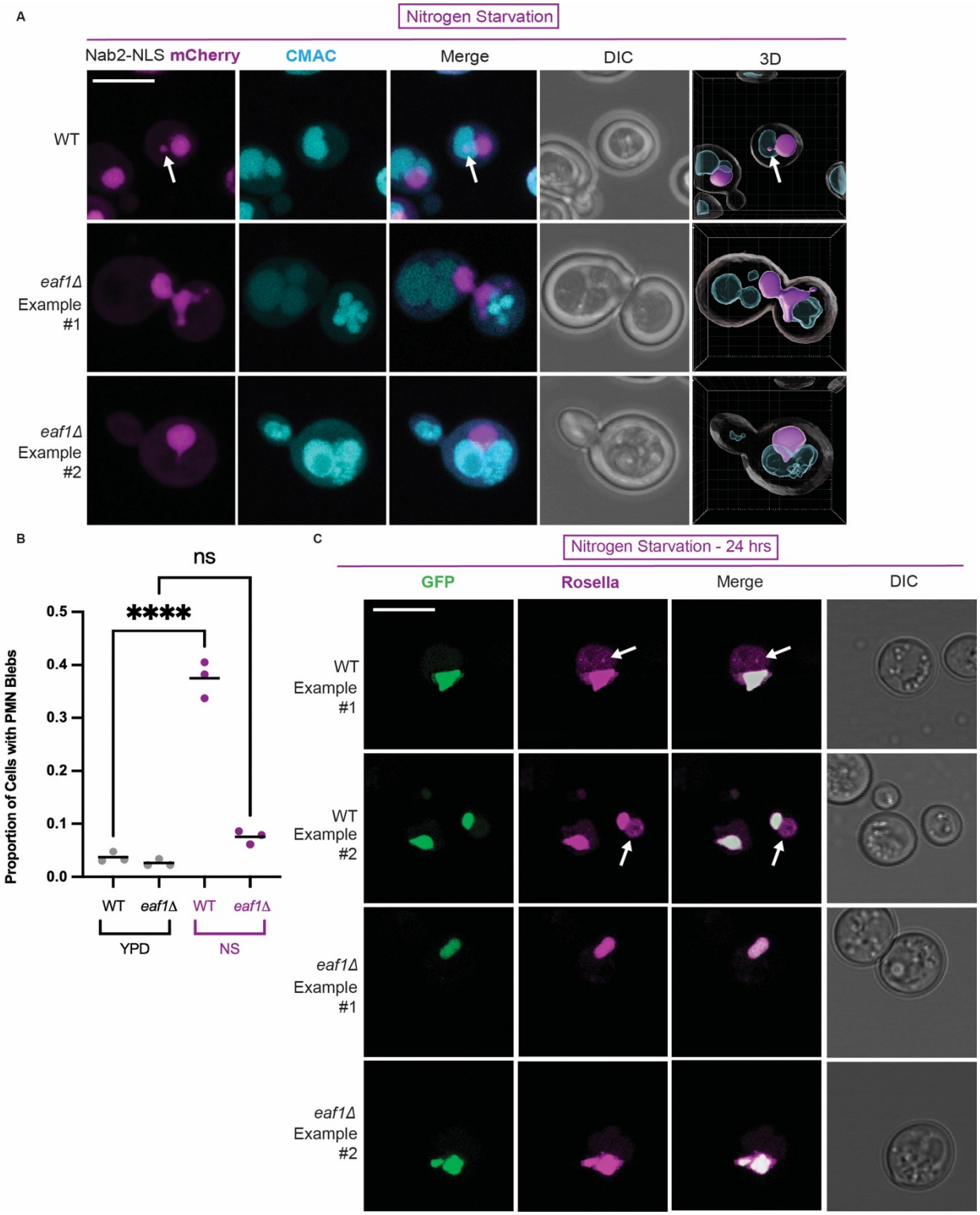

Figure 2.5 – Deletion of *EAF1* results in decreased piecemeal microautophagy of the nucleus (PMN). (A) WT and *eaf1*Δ cells (YKB 5186 and YKB 5187) with Nab2-NLS-mCherry to visualize the nucleus and CMAC staining the vacuole. Cells were grown to log phase in nutrient-rich media and then transferred into nitrogen starvation media. Merged Z-stack images show the formation of PMN structures, indicated by a white arrow, following four hours of nitrogen starvation. 3D projection of Z-stacks using Imaris software shows PMN blebs entering the vacuole in WT cells. In *eaf1*Δ cells with nuclear extensions wrapping around or between vacuolar lobes were detected. Scale bar = 5 μm. Arrows indicate presence of a PMN bleb entering the vacuole.

(B) Cells were grown in either YPD or switched to nitrogen starvation (NS) media for four hours. The proportion of cells with PMN were carefully counted by investigating the full Z-stack of cells. If there was a clear bleb of Nab2-NLS mCherry that entered the vacuole, a cell was counted as having PMN. Under nitrogen starvation, *eaf1*Δ cells have a significant reduction in PMN compared to WT. ANOVA analysis was performed using Tukey's multiple comparison test. Grey and purple dots represent three biological replicates, counting at least 200 cells for each. Horizontal bars represent the mean. Relevant statistical significance bars are shown, additional comparisons can be found in Supplemental Table 2.1. ****$p<0.0001$, ns = not significant, $p>0.05$. (C) WT and *eaf1*Δ cells expressing a GFP-Rosella construct fused to the nuclear localization signal from Nab35 (YKB 5188 and YKB 5189), were grown to mid-log phase and switched to nitrogen starvation media for 24 hours prior to imaging. Arrows highlight Rosella signal in the vacuole, indicating active PMN. Scale bar = 5 μm.

Pah1-K496 impacts Pah1 localization to the INM

Pah1 is primarily localized to the cytosol, where it remains inactive, with a small proportion that is localized to the nuclear membrane and NVJ where it performs its catalytic function.[126,130,151,161] The balance of Pah1 localization is directly linked to its functional activity. As our work suggests NuA4 regulates the localization of Pah1 to the nuclear membrane, we next explored if this effect is mediated by Pah1 acetylation. Previous work has detected NuA4-dependent acetylation of Pah1 at K496 and K801. K496 was shown to be conserved amongst mammals and yeast, while tandem mutation of K496 and K801 to arginine resulted in decreased lipid droplet formation.[110] To investigate the functions of these two sites individually, we started by employing a modified BiFC assay. Lysine sites mutated to glutamine (Q) were used as an acetylation mimic. Lysine to arginine (R) mutations where used to prevent acetylation.[277] We constructed a series of four point mutants in the Pah1-VC bait protein (Pah1-K496Q-VC, Pah1-K496R-VC, Pah1-K801Q-VC and Pah1-K801R-VC), and confirmed their expression via western blot (**Supplemental Fig. 2.3**). We then assessed whether those mutations impacted Pah1-VC's interaction with Pus1-VN (nucleoplasm marker) or Nup60-VN (INM marker). While Pah1-K801Q-VC and Pah1-K801R-VC interacted with both markers, we were unable to detect interactions between Pah1-K496Q-VC or Pah1-K496R-VC with either Pus1-VN or Nup60-VN (**Fig. 2.6).** This suggests that Pah1-K496 may impact its subcellular localization to the nucleus and the INM.

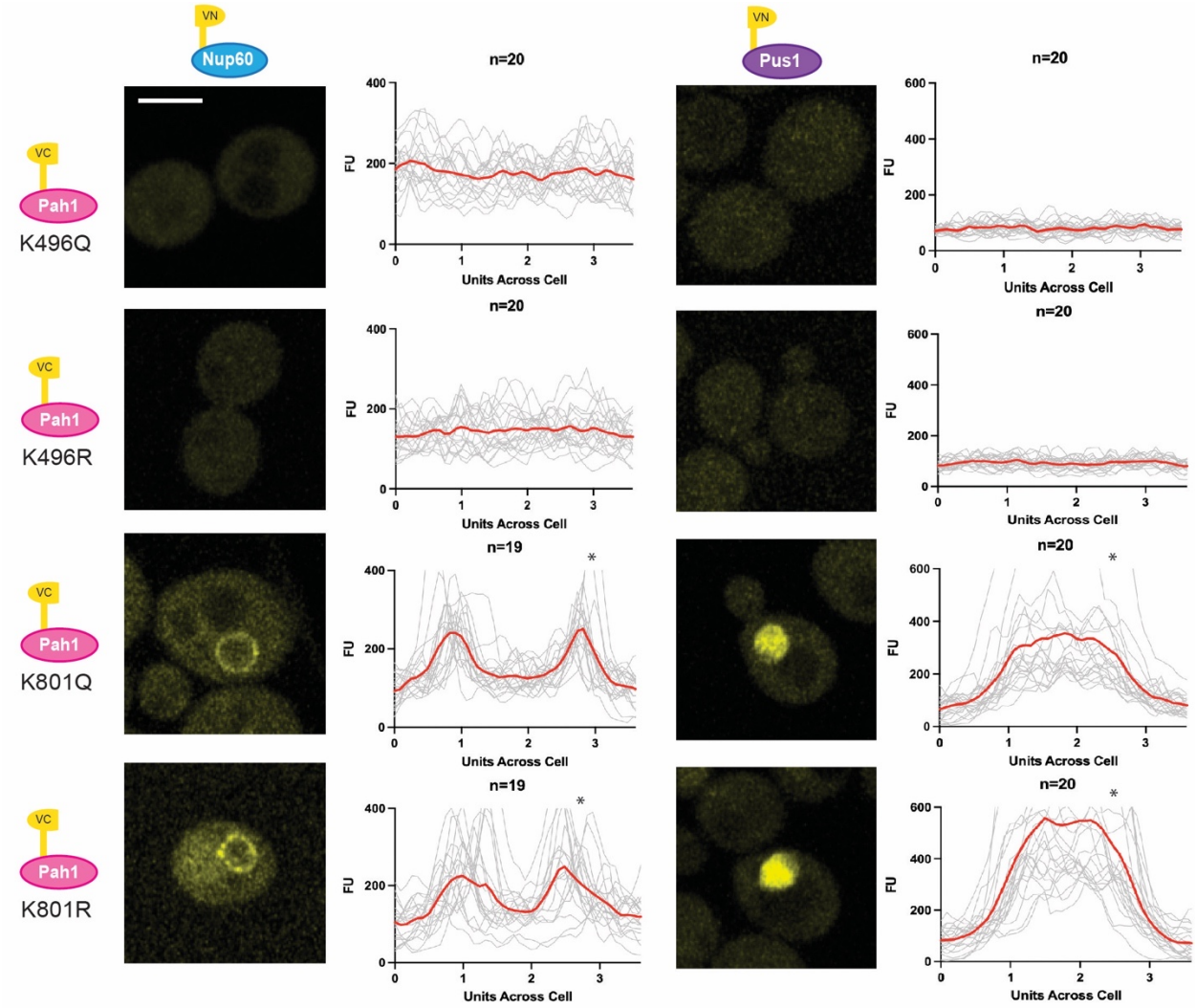

Figure 2.6 – Mutations at Pah1-K496 result in a loss of Pah1-VC interaction with Pus1-VN and Nup60-VN. BiFC interaction between Pah1-K496Q-VC, Pah1-K496R-VC, Pah1-K801Q-VC, and Pah1-K801R-VC with both Nup60-VN (on left) and Pus1-VN (on right) (YKB 5206 – YKB 5213) were visualized using fluorescence microscopy. Scale bar = 5 µm. Line graphs were generated by measuring the fluorescence intensity value of pixels across the nucleus of the cell using Plot Profile in ImageJ Software. The grey lines show individual cell profiles and the red line indicate the average across all measured cells. n = the number of randomly selected cells. FU = Fluorescence Units. * Indicates that that y-axis has been cropped for easy comparison of strains.

To further investigate Pah1-K496 as a potential site involved in the subcellular nuclear localization of Pah1, we introduced mutations in genomically integrated *PAH1-3xGFP* using CRISPR-Cas9.[267] As expected, in WT cells Pah1-3xGFP showed cytosolic localization (**Fig. 2.7A**).[161] In *eaf1*Δ cells, Pah1-3xGFP localized to small punctate dots in a small percentage of cells but otherwise showed cytosolic localization. However, Pah1-K496R-3xGFP and Pah1-K496Q-3xGFP in both WT and *eaf1*Δ were mislocalized, possibly to the plasma membrane/ER (**Fig. 2.7A)**. We also

performed a western blot to confirm the protein levels of Pah1-3xGFP and were surprised to see a high level of degradation of Pah1-3xGFP in *eaf1*Δ as well as isoforms with higher apparent molecular weight (**Supplemental Fig. 2.9**). Given the high levels of phosphorylation of Pah1 by multiple protein kinases (outlined in **Fig. 2.3A**), it is possible that the loss of NuA4 is causing Pah1 to be hyperphosphorylated and sent to proteasomal degradation. Additionally, in growth assays, *pah1-K496Q* cells had a significant growth defect compared to the moderate growth defects observed for *eaf1*Δ and *pah1-K496R* cells (**Fig. 2.7B**).

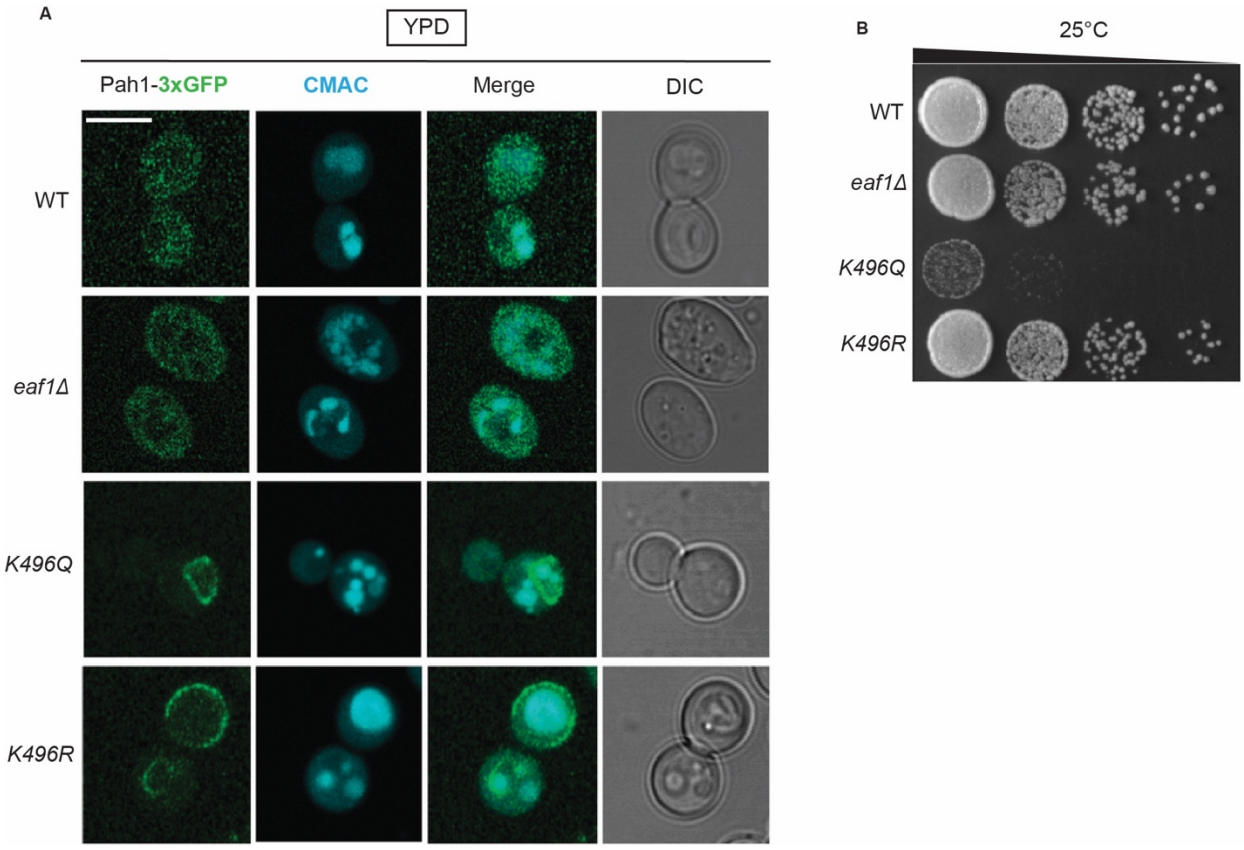

Figure 2.7 - Pah1-K496 confers changes in Pah1 localization.
(A) Single sliced Z-stack images showing Pah1-3xGFP localization, and vacuoles labelled with CMAC in the WT *PAH1-3xGFP* (YKB 4993), *eaf1*Δ *PAH1-3xGFP* (YKB 4994), *PAH1-K496Q-3XGFP* (YKB 5130) and *PAH1-K496R-3XGFP* (YKB 5131) strains. Scale bar = 5 µm. (B) Dot assays showing growth of WT *PAH1-3xGFP* (YKB 4993), *eaf1*Δ *PAH1-3xGFP* (YKB 4994), *PAH1-K496Q-3XGFP* (YKB 5130) and *PAH1-K496R-3XGFP* (YKB 5131) after a period of 48 hours at 25°C.

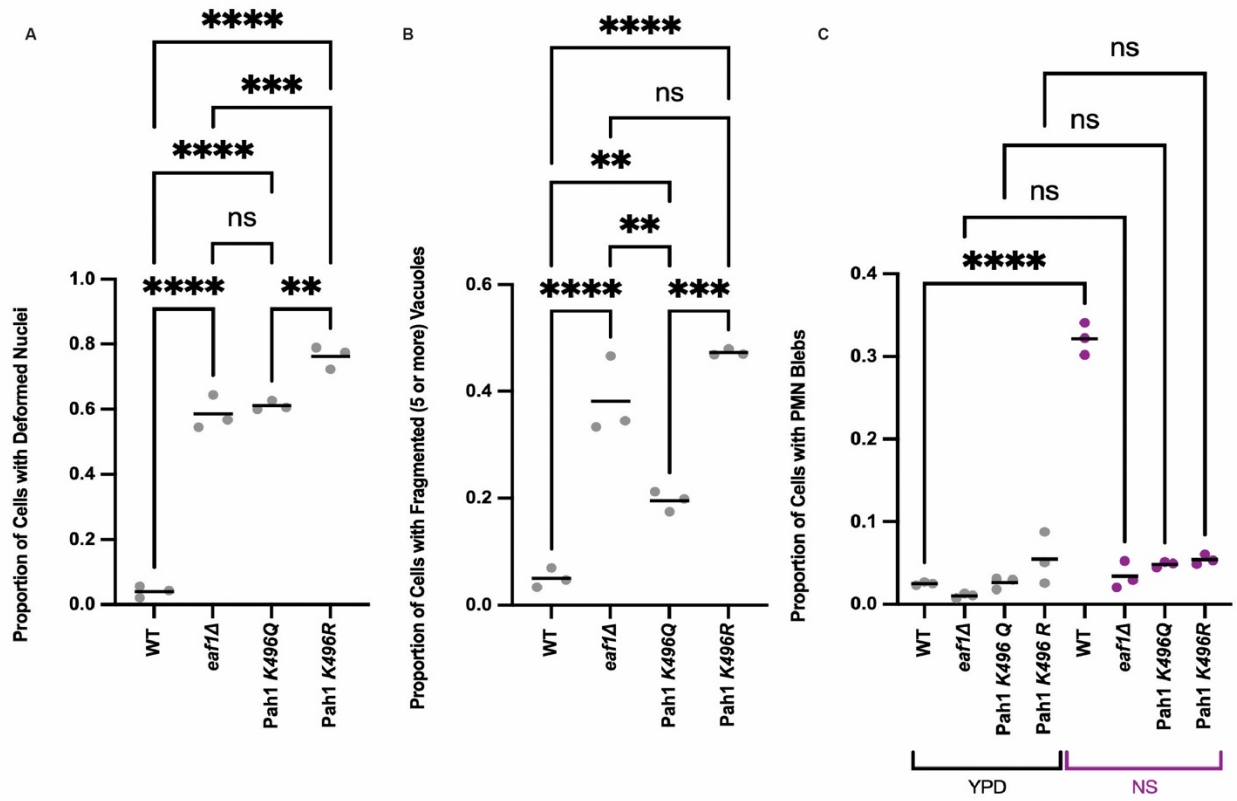

Figure 2. 8 - Pah1-K496 mutation results in increased nuclear deformation, vacuole fragmentation and defects in piecemeal microautophagy of the nucleus.
(A) Proportion of WT (YKB 5190), *eaf1*Δ (YKB 5191)*, PAH1-K496Q* (YKB 5192), and *PAH1-K496R* (YKB 5193) cells expressing Pah1-3xGFP and Nab2-NLS-mCherry were accessed for nuclear deformation. (B) Proportion of cells with fragmented (5 or more) vacuoles quantified by visually counting the number of vacuoles per cell. (C) Proportion of cells with PMN blebs. Cells were grown in either YPD or switched to nitrogen starvation (NS) media for four hours. If there was a clear bleb of Nab2-NLS mCherry that entered the vacuole, a cell was counted as having PMN. For A, B and C, an ANOVA analysis was performed using Tukey's multiple comparison test. Cells were counted by investigating the full Z-stack of cells. Grey and purple dots represent three biological replicates of at least 100 cells for each. Horizontal bars represent the mean. **p≤0.01, ***p≤0.001, ****p<0.0001, ns = not significant, p>0.05. Relevant statistical significance bars are shown, additional comparisons can be found in Supplemental Table 2.1.

We hypothesized that if NuA4 was mediating its effects through acetylation of Pah1-K496, nuclear deformations, vacuole fragmentation and PMN defects detected in *eaf1*Δ cells would be recapitulated in *pah1-K496R* cells. Interestingly, both *pah1-K496Q* and *pah1-K496R* cells had high levels of nuclear deformations and defects in PMN, similar to *eaf1*Δ cells (**Fig. 2.8A and C**). For vacuole fragmentation, *pah1-K496R* cells had fragmentation levels similar to that of *eaf1*Δ cells, while

pah1-K496Q cells had levels closer to that of WT cells (**Fig. 2.8B**). Our results suggest that mutations at K496 lead to phenotypes generally similar to that of *eaf1*Δ.

2.6 Discussion

The functional consequences of Pah1 acetylation and the role of NuA4 in regulating phospholipid availability for membranes has remained unclear. In this study we identify changes in organelle morphology upon deletion of *EAF1*, the scaffolding subunit of the NuA4 complex, including nuclear deformation and vacuole fragmentation (**Fig. 2.1**). We further identified significant defects in NVJ formation and function of PMN in *eaf1*Δ cells (**Fig. 2.4 and 5**). Importantly, all nuclear deformation and vacuole fragmentation phenotypes are recapitulated by Pah1 mutation at lysine residue K496 (**Fig. 2.8**), a known site of NuA4-acetylation. Together, our data suggest that Pah1 K496 directs multiple aspects of Pah1 function to coordinate organelle membrane homeostasis.

Pah1 is typically inactive in the cytoplasm but is activated by dephosphorylation by Nem1-Spo7, allowing it to localize to the nucleus to perform its function (**Summarized in Fig. 2.3A**).[123,124,166] Using a BiFC assay, we were able to visualize a subpopulation of Pah1 in the nucleoplasm, but not the INM, upon deletion of *EAF1* (**Fig. 2.2B**). Recent work from our lab showed that there are no changes in global levels of PA in NuA4 mutants.[91] In agreement with this, we did not detect PA accumulation at the INM of *eaf1*Δ cells (**Fig. 2.2C**). Thus, we suggest that transient PA that accumulates due to mislocalization of Pah1 is quickly converted to phospholipids that can drive membrane expansions associated with nuclear deformations. Since DAG is the substrate for Pah1, we were surprised to detect this lipid species at the INM. It is possible that DAG synthesis is maintained in part via a subpool of Pah1 that localizes to the INM but is not detectable by our BiFC assay. Alternatively, DAG accumulation could be explained by activation of compensatory mechanisms in *eaf1*Δ cells.

While we have shown that nuclear deformations in *eaf1*Δ are partially caused by an influx of PA driving the production of membrane phospholipids, there remains a portion of nuclear deformations that were not rescued by decreasing membrane phospholipid synthesis via mutation of *DGK1*, *INO1* or *CDS1* (**Fig. 2.1C**). Therefore, we explored alternative pathways that regulate nuclear shape. We focused on the NVJ,[229,250] an important membrane contact site between the nucleus and the vacuole that promotes a selective autophagy process, PMN, and digests excess nuclear membrane that could be contributing to deformations.[228,250,278] Interestingly, we found that upon deletion of *EAF1* there are severe defects in the formation of the NVJ (**Fig. 2.4B and C**) and subsequent PMN (**Fig. 2.5**). It is tempting to think that the level of vacuole fragmentation seen in our NuA4 mutants (**Fig. 2.1B and D, Supplemental Fig. 2.1**) could be the cause of NVJ dysfunction. However, previous work from Krick *et al.* [230] showed that PMN can still occur in vacuoles lacking fusion machinery. Further, *eaf1*Δ cells have large, fused vacuoles upon nitrogen starvation (**Fig. 2.4B**), indicating that they retain the machinery for vacuole fusion. NVJ and PMN defects are also not due to defects in localization of Pah1 adjacent to the NVJ,[126] as our BiFC studies indicate that Pah1 interaction with Nvj1 and Vac8 are not disrupted in *eaf1*Δ cells (**Supplemental Fig. 2.8**). One possibility is that NuA4 may be involved in regulating the core autophagy machinery involved in PMN. For example, NuA4 is a known regulator of Atg3 through direct acetylation at 3 different sites.[103,109] Conversely, NuA4 could impact the stability and/or formation of the NVJ itself, as NuA4 has been shown to interact with Vac8 through Eaf1.[279]

Finally, cells lacking *EAF1* also have vacuolar fragmentation defects (**Fig. 2.1B and D**) that are rescued by artificial recruitment of Pah1 to the nuclear membrane (**Fig. 2.3B and D**). This rescue was surprising given that *pah1*Δ cells do not have increased vacuolar fragmentation. It is possible that forced localization of Pah1 to the nuclear membrane initiates a nuclear-vacuole feedback response that

is not active under physiological conditions. This result highlights unknown complexities in nuclear-vacuole communication.

Since previous studies identified two potential NuA4 acetylation sites on Pah1, K496 and K801, we sought to determine if these sites influence Pah1 subcellular location. Mutation of K496, but not K801, to either Q or R prevented Pah1-VC localization to the nucleus and INM (**Fig. 2.6**), redistributed Pah1-3xGFP to organelle membranes (**Fig. 2.7A**), and decreased PMN (**Fig. 2.8C**). While both Pah1-K496R and Pah1-K496Q displayed increased nuclear deformation and vacuole fragmentation, the defects displayed by the K496Q mutant were significantly lower than the K496R mutant (**Fig. 2.8A and B**). Since both mutants showed similar phenotypes, we cannot discount that these mutations are not affecting Pah1 functions beyond acetylation. Alternatively, we suggest that dynamic acetylation and deacetylation is critical to maintain Pah1 localization and other functions related to lipid metabolism and organelle membrane homeostasis. As such, dynamic regulation of Pah1 by lysine deacetylases should be an active area of future investigation.

2.7 Acknowledgements

We thank Siniossoglou Lab at the University of Cambridge and the Köhler lab at the Medical University of Vienna for providing plasmids used in this work. We would like to acknowledge that all fluorescent microscopy images were generated in the Cell Biology and Image Acquisition (CBIA) Core Facility at the University of Ottawa. Additionally, Gibson assembly was performed by the University of Ottawa's Genomic Editing and Molecular biology (GEM) core.

This work was supported by the Canadian Institutes of Health Research (CIHR; http://www.cihr-irsc.gc.ca/e/193.html) Grant (MOP-142403) to KB; and a Natural Sciences and Engineering Research Council of Canada (NSERC, https://www.nserccrsng.gc.ca/index_eng.asp) Discovery Grant to MD. SJL was supported by NSERC in the form of a Postgraduate Scholarship Award, and through the Collaborative Research and Training Experience (CREATE) program 'SynBioApps'.

2.8 Disclosure statement

The authors declare no competing financial interests.

2.9 Data availability statement

Raw figure data are available on Figshare: https://figshare.com/s/0448d63faeb05ded3d0b (DOI: 10.6084/m9.figshare.25576950). Additional data is available upon request to corresponding authors.

Chapter 3

General Discussion

3.1 Overview of Thesis Work

Over the past few decades, our understanding of the functions of NuA4 and Tip60 has significantly expanded. It is now widely accepted that lysine acetyltransferases play a vital role in acetylating proteins, with targets ranging vastly in function. This thesis specifically adds novel intel into the relationship between NuA4 and the regulation of phospholipid metabolism in *Saccharomyces cerevisiae.* The primary manuscript in **Chapter 2** of this thesis identifies novel phenotypes in a NuA4 mutant, offering a deeper understanding of the role of lysine acetylation in modulating lipid metabolism within organelle membranes. This work dissects the regulatory pathways influenced by NuA4, highlighting both Pah1-dependent and independent mechanisms.

The first aim of this work was to characterize nuclear deformations and vacuolar defects seen in NuA4 mutants. Using a variety of imaging techniques, we were able to determine that the nuclear deformations were, in fact, abnormalities in the nuclear membrane that were much more severe than those seen upon deletion of other lipid metabolism genes. This included the deletion of *PAH1,* which is well characterized for its unchecked phospholipid synthesis. Further, deletions of *EAF1,* in tandem with these other lipid metabolism genes, could only rescue some of the nuclear and vacuolar defects. This signifies that there is likely a Pah1-dependent and independent mechanism involved.

To further investigate Pah1, I used previously established BiFC assays and fluorescent biosensors to assess the location and function of Pah1 in *eaf1*Δ cells. This showed very clearly that Pah1 was mislocalized in *eaf1*Δ cells and was not found at the INM. Interestingly, artificially targeting Pah1 to the nuclear membrane with Pah1-7A-GFP (and its counterpart as a control Pah1-7A-AH3A-GFP) was able to rescue some of the nuclear deformations and vacuolar fragmentation seen in *eaf1*Δ

cells. Both of these results highlight the important role of Pah1 localization and its corresponding function at the nuclear membrane. In *eaf1*Δ cells, this localization was essential to rescue defects in nuclear and vacuole morphology.

To investigate the Pah1-independent mechanisms for *eaf1*Δ phenotypes, I explored the role of the NVJ and the function of the PMN as regulators of excess nuclear membrane. Using fluorescence microscopy, I determined that when induced with nitrogen starvation, *eaf1*Δ cells had significant defects in the ability to form NVJs compared to WT cells. When the NVJ did form in *eaf1*Δ cells, they were significantly smaller than WT NVJs. This corresponded with a similar defect in the functioning of PMN, which was assessed using two fluorescence microscopy techniques. The consequence of these defects is highly important for *eaf1*Δ cells since they have an abundance of nuclear membrane phospholipids. If it is unable to recycle and digest the excess membrane, it can build up and cause further deformations of the nuclear membrane.

Since the functional consequences of NuA4-dependent acetylation on Pah1 remained uncharacterized, we finally sought to determine the role of this acetylation in the context of this work. I began by generating a series of mutations at the two known acetylation sites on Pah1 within my previously used BiFC system. This allowed me to specifically assess changes in localization to the INM and the nucleoplasm as a result of these mutations. This showed that mutations at K496 on Pah1 impacted its location to the nucleus entirely. Therefore, I generated integrated CRISPR-Cas9 acetylation mutations of Pah1 at K496. Interestingly, there were changes in Pah1 localization in both Q and R mutations at this site, in comparison to WT cells, while K496Q exhibited a distinct growth defect. Further, mutations at K496 also exhibited increases in nuclear deformation, vacuolar fragmentation and defects in PMN, similar to that seen in *eaf1*Δ cells.

3.2 Implications for NuA4/Tip60 research and human disease

The relationship described in this work between NuA4 and Pah1 builds on findings directly from a mice-Tip60 model, as described by Li *et al.* [110]. Both NuA4 and Pah1 are highly conserved in higher eukaryotes and have been active areas of research.

3.2.1 Lipid Dysregulation and Human Disease

Given the vital role of NuA4 and Tip60 in the regulation of the balance between lipid droplet formation and phospholipid synthesis, this study is highly relevant to lipid storage more broadly. This could be extended to diseases such as diabetes and lipodystrophy. Understanding the role of Tip60/NuA4 in these pathways could open up new treatment options for diseases associated with the accumulation of fatty acids.

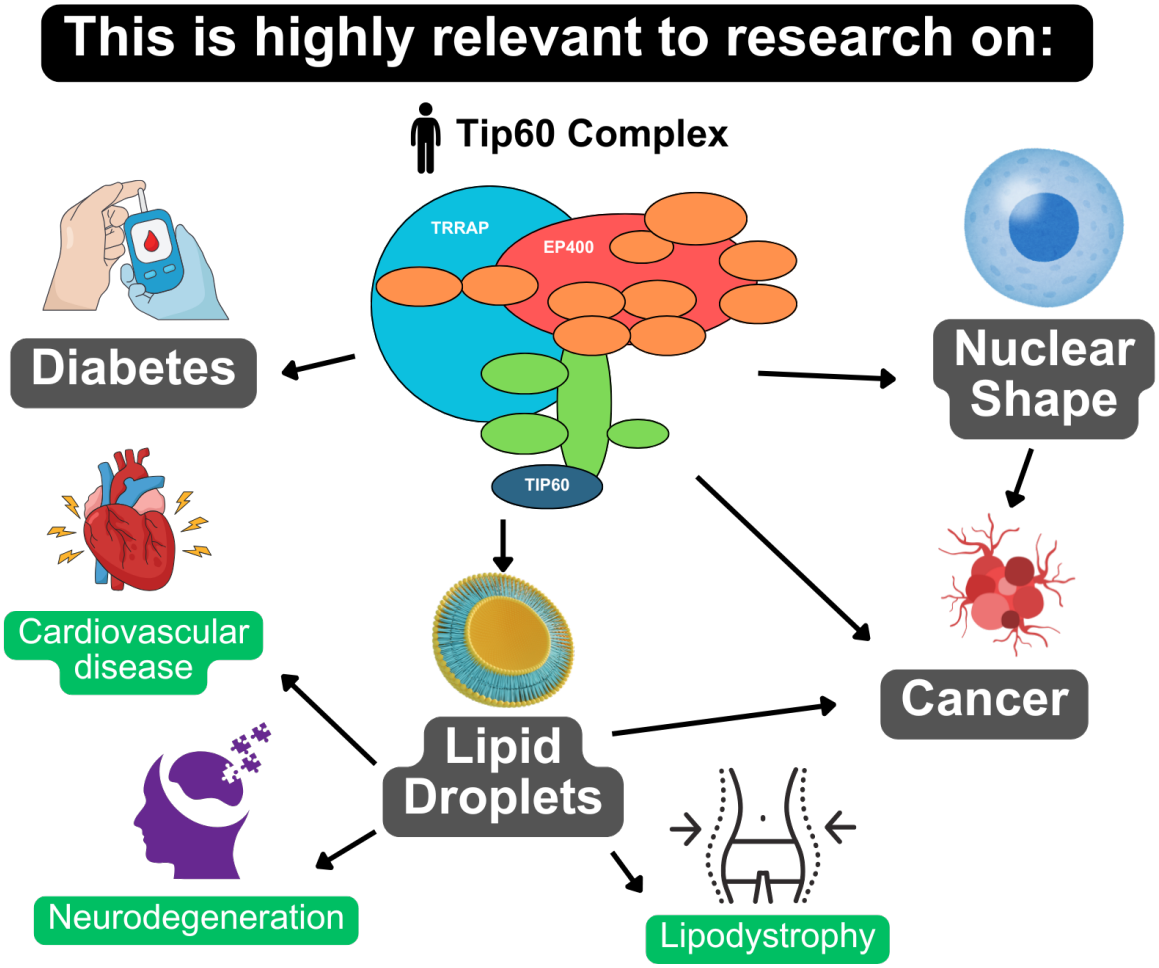

3.2.1.1 NuA4, Tip60 and Diabetes

Tip60 has been highly investigated for its role in diabetes.[280-282] Primarily, NuA4/Tip60 is a positive regulator of insulin secretion.[283] Additionally, research in **Appendix B** shows the role of NuA4 in directly regulating glucose and glycogen. It has also been found that Esa1 acetylates and positively regulates the phosphoenolpyruvate carboxykinase, Pck1.[64] These results were conserved in humans.[64] It is clear that Tip60/NuA4 have a conserved and important role in diabetes through regulation of gluconeogenesis.

3.2.1.2 NuA4, Tip60 and Lipid Droplets

Previous work in our lab showed that upon deletion of *EAF1*, cells exhibited a reduction in the lipid droplet content, measuring fluorescent intensity per area.[66] However, further investigation found that the number of foci (representing a lipid droplet) per cell was actually increased in *eaf1*Δ cells (unpublished data). More investigation is needed into the role of Tip60/NuA4 in lipid droplet formation, given its diverse role in human health. For example, lipid droplets play a role in the following diseases:

- **Lipodystrophy** – This rare disease is hallmarked by a loss of fat in regions of the body.[182] While there are several underlying causes, they centralize on the regulation of phosphatidic acid, lipid droplet biogenesis and the formation of adipose tissues.[284]
- **Neurodegeneration** – Lipid droplets were originally observed in Alzheimer's disease patients.[285] There are now several genetic markers associated with lipid droplet biogenesis that are classified as risk factors for Alzheimer's disease,[286] most notably the APOE4 allele.[287]
- **Cardiovascular disease** – Lipid droplets in the heart are of clinical significance as they occur in cardiomyocytes and macrophage foam cells.[288] Generally, TAG and lipid

droplets play a cardioprotective role in cardiomyocytes. However, the turnover rate is highly clinically relevant, as accumulation can lead to diseases such as diabetes, heart failure and cardiomyopathy.[288,289] In macrophage foam cells, the accumulation of cholesterol-rich lipid droplets is the primary feature of atherosclerosis.[290]

- **Cancer** – Several types of cancers exhibit an accumulation of lipid droplets.[291] Functionally, they provide lipids for membrane formation in proliferating cancer cells and can act in cell signalling, promoting communication between tumours and their environment.[291] Additionally, lipid droplets can protect against hypoxia and radiation therapy by combatting ROS damage.[292]

3.2.1.3 NuA4, Tip60 and Nuclear Shape

This work provides valuable insights into regulating nuclear shape, size and structure. As previously outlined in **Section 1.6.1**, the exact mechanisms regulating nuclear shape and size are poorly understood. In this work, we have seen a complex and multi-faceted cause for nuclear deformations that extends our understanding of the role of lipid metabolism in perpetuating nuclear shape. At its core, nuclear deformations in NuA4 mutants are caused by several different mechanisms, some of which are directly related to lipid metabolism through Pah1 and some not. This opens up our understanding of this complex regulatory system and brings to light the connectedness of lipid metabolism with the cell cycle and autophagy processes.

When extended to a human context, defects in the nuclei seen in yeast are more complex to understand. Since cell division and the regulatory mechanisms behind cell shape are quite different, it can be easy to assume that there are no translatable findings. However, yeast can provide us with an uninhibited ability to access nuclear shape and size in the absence of a regulatory system. Since the underlying lipid metabolism functioning is relatively conserved, this could help to understand cases in mammalian cells where nuclear structure goes awry. In fact, altered nuclear size and shape are

considered to be primary indicators of disease states and cancers.[293] Further investigation into the root cause of nuclear dysregulation in NuA4 could help understand this dynamic regulation and its drivers.

3.2.1.4 NuA4, Tip60 and Cancer

Tip60 has been highly studied for its role in human cancers, most notably in lung, colon, prostate and breast cancer.[10,294-296] Since Tip60 plays such an important role in cell cycle progression, DNA repair, transcription and gene expression, a lack of Tip60 can both promote and suppress the development of cancers. Therefore, Tip60 is a common target for investigation into potential cancer therapies.[297] For example, 1,2-bis(isothiazol-5-yl) disulfane (NU9056) was found to inactivate Tip60, decrease its corresponding acetylation of histone and non-histone targets, and inhibit the progression of prostate cancer cell lines.[10] However, the opposite is seen in breast cancer, where Tip60 protects the cells from double-stranded breaks.[295] Here, Tip60 activators are investigated for clinical treatment in an effort to re-introduce Tip60 to the nucleus.[295]

Studies in yeast have significantly increased our understanding of the role of Tip60 in human cancers. For example, work investigating NuA4 in yeast helped to understand its transcriptional regulation of the proto-oncogene MYC, which is commonly over-expressed in cancer cell lines.[298] Further, yeast has been fundamental in understanding Tip60/NuA4's role in DNA breaks and repair.[299-301] This work is directly applicable to human cancer models and has grown our understanding of the role of Tip60 in these processes.

3.3 Future Investigation and Additional Roles for NuA4 in Lipid Metabolism

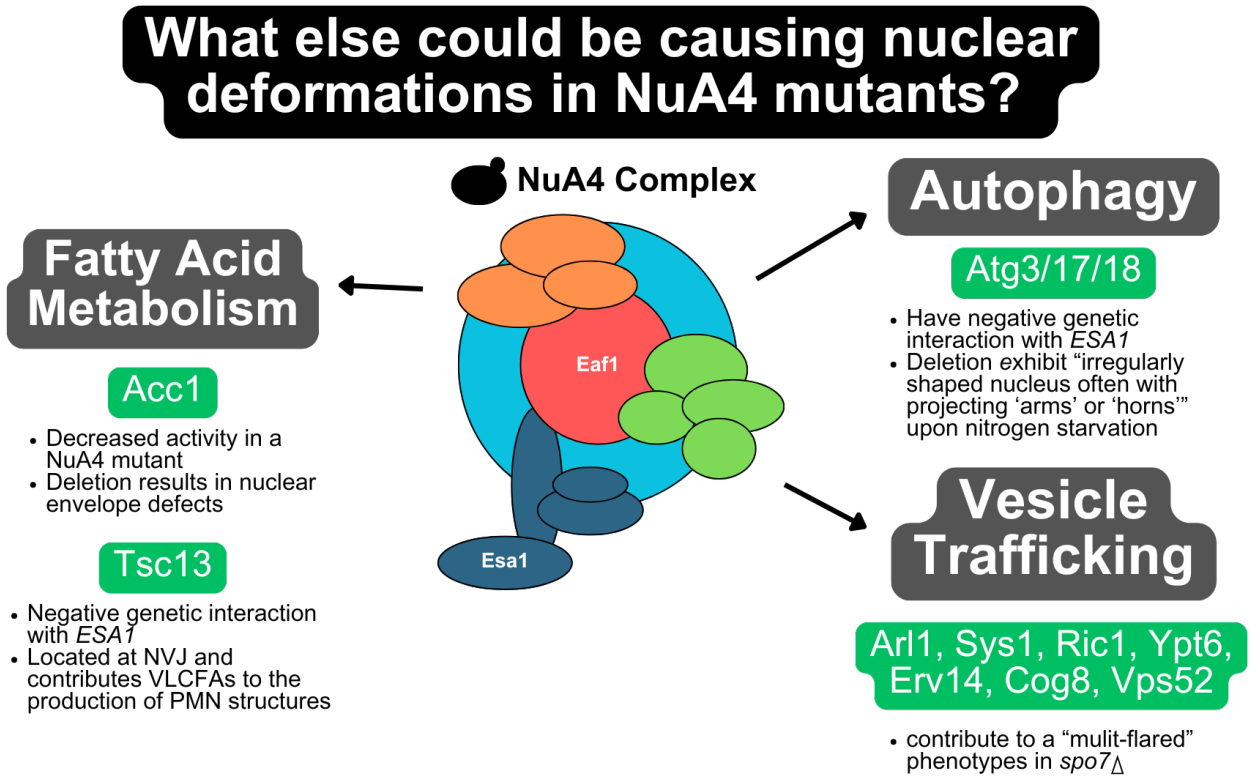

Future investigation surrounding this work should investigate the role of NuA4 more broadly in the context of nuclear flares, vacuole fusion, and formation of the NVJ. Given that our results indicate that NuA4's regulation of Pah1 does not solely account for the phenotypes seen in this body of work, understanding these phenotypes both holistically and independently will help shed light on the role of NuA4 in lipid metabolism. In particular, here are potential pathways to investigate further understand the specific phenotypes displayed in this thesis, including additional targets of NuA4-acetylation that may be involved:

3.3.1 NuA4 and Fatty Acid Metabolism, Acc1

Recent work in the Baetz lab has characterized defects in the activity of Acc1 in NuA4 mutants, accompanied by increased Acetyl-CoA levels.[91] Specifically, Acc1 commits fatty acid metabolism towards VLCFAs.[197] Deletions of *ACC1* result in alterations of the nuclear envelope,

directly due to aberrant VLCFA synthesis.[302] This becomes further relevant to this body of work upon examination of the NVJ and the role of VLFCAs at this contact site. As explained in **Section 1.7.2**, Tsc13 is a fatty acid elongase highly enriched at the NVJ.[247] It is specifically targeted to the NVJ to contribute VLCFAs to producing PMN structures.[248] Interestingly, *TSC13* also has a negative genetic interaction with *ESA1*.[181] Given these overlaps, future research should investigate the presence of VLCFAs at the NVJ in NuA4 mutants and the role of Acc1 and Tsc13 in mediating these lipid populations as it relates to the formation of the NVJ and function of PMN.

It is possible that NuA4's role in regulating Acc1 may contribute to a percentage of nuclear deformations (and potentially other organelle dysregulation phenotypes). A comprehensive analysis of the levels of nuclear deformations, vacuole fragmentation and PMN in Acc1 mutants would help to understand similarities in these phenotypes seen in *eaf1*Δ cells. By performing these in double deletion backgrounds with *eaf1*Δ, we will also be able to assess whether these phenotypes converge on the same or parallel pathways. Further, accessing the role of NuA4-mediated acetylation on Acc1 in modulating these phenotypes would help determine the specific role of NuA4 in this pathway.

3.3.2 NuA4 and Vesicle Trafficking

As described in **Section 1.6.1**, vesicle trafficking is required to specifically confine the region of a nuclear flare. This effect can be studied in *spo7*Δ, where the cell has a single nuclear flare adjacent to the nucleolus. Interestingly, a subset of vesicle trafficking mutants exacerbated the multi-flared phenotype seen in a *spo7*Δ but otherwise did not exhibit flares alone.[227] The following list of these mutants also have interactions with Esa1:

- *ARL1* – synthetic growth defect[60]
- *SYS1* – negative genetic[181]
- *RIC1* – synthetic growth defect[60]

- *YPT6* – synthetic growth defect,[62] synthetic growth lethality[60]
- *ERV14* – negative genetic[181]
- *COG8* – synthetic lethality[62]
- *VPS52* – synthetic lethality[60]

Given the high levels of deformations in the nucleus seen in NuA4 mutants, as shown in this body of work, and the prevalence of multiple flares in these mutants, it remains possible that defects in vesicle trafficking could be impacting the nuclei' ability to compartmentalize flares to the nucleolar region. Further, in an analysis of genetic interactors, NuA4 was found to be genetically mapped to 15 genes (including COG8 and YPT6 listed above) related to vesicle trafficking. All of these genes had strong genetic interactions with deletions of *EAF1* and *ESA1*.[62] Investigation of the relationship between NuA4 and vesicle trafficking genes could provide further explanation for their role in nuclear flares, in addition to vacuolar morphology.

3.3.3 NuA4 and Autophagy

3.3.3.1 Atg3, Atg17 and Atg18

NuA4's role in autophagy is not well-defined. However, NuA4 has several interactors that could provide insight into nuclear dysregulation and additional phenotypes seen in a NuA4 mutant. At the top of this list are Atg3, Atg17 and Atg18. All of which, upon deletion, exhibit "irregularly shaped nucleus often with projecting 'arms' or 'horns'" upon nitrogen starvation, and have negative genetic interactions with Esa1.[181,303] While all three are required for the functioning of PMN, it is possible that this could provide insight into the specific role of PMN-related deformations of the nucleus in *eaf1*Δ cells. Atg3 is directly acetylated by NuA4, promoting its interaction with Atg8 and promoting autophagy.[109] Therefore, further research should investigate the relationship between NuA4 and other yeast ATG genes, such as Atg17 and 18. For example, Tip60 has been shown to

acetylate human ULK1, promoting autophagy.[109] ULK1's yeast homology is Atg1, which functions in a complex with Atg17 as a regulatory subunit.[304] In particular, investigating the levels of PMN in mutants of *ATG3, ATG 17* and *ATG18,* alone and in combination with *eaf1*Δ, would aid in understanding the role these autophagy proteins play in PMN and whether that function is modulated by NuA4.

3.3.3.2 Role of NuA4 in Additional Types of Autophagy in Yeast

Given the high level of metabolic activity and lipid transfer at the NVJ,[126] and the defects in the NVJ upon deletion of *EAF1,* it would be interesting to investigate lipophagy in NuA4 mutants further. Lipophagy is a form of microautophagy where the vacuole engulfs and degrades LDs.[305] We know Pah1's role at the NVJ is to participate in the production of LDs, and its partitioning of this activity to the NVJ suggests a shift in metabolic priorities requiring this process to align with the vacuolar membrane.[126] Similarly, could NuA4 play a role in mitophagy, the degradation of mitochondria? It was shown that the Nem1/Spo7-Pah1 axis was required for mitophagy following activation via TORC1.[146] It would be interesting to explore whether NuA4 mutants have defects in lipophagy and mitophagy, and, if so, is it dependent on Pah1?

The regulation of mechanisms, such as lipophagy, could play an essential role in the balance of lipid droplets and phospholipid membranes. This balance plays a vital role in regulating nuclear morphology and is the underlying mechanism for some of the dysregulation seen in a NuA4 mutant. A comprehensive analysis of overlapping genetic and physical interactions between these pathways could help to understand if NuA4 plays a role in the catabolic pathways. Some genes of interest would be triacylglycerol lipases, *TGL3, TGL4,* and *TGL5,* as well as steryl ester lipases, *TGL1, YEH1* and *YEH2.*[306-308]

3.3.4 NuA4's Direct Interaction with Vac8

Interestingly, Eaf1 has a positive genetic interaction with Vac8[309] and has been shown to physically interact through yeast two-hybrid.[279] Given Vac8's fundamental role in the NVJ, investigating this interaction further could be of great interest to the work in this thesis as it could provide valuable insights into the defects in the formation of the NVJ in NuA4 mutants. Further, Vac8 has several other functions in relation to vacuolar biogenesis[279] and could shed light on the vacuole fragmentation seen in NuA4 mutants.

3.3.5 NuA4 and the Vacuole

This work identified a significant defect in vacuole fusion in NuA4 mutants. This phenotype was not rescued by the deletion of proteins involved in the flux of PA into membrane phospholipids, but it was partially rescued by targeting Pah1 to the nuclear membrane through Pah1-7A-GFP. However, the exact mechanisms behind these defects aren't fully elucidated in this body of work. While it is possible that vacuole defects are a by-product of defects in vesicle trafficking (outlined above), there are several possibilities for NuA4 to play a role directly in the vacuole fusion process, both through Pah1 and independently. Further research investigating the vacuolar fusion pathway (outlined in **Section 1.7.1**) would help identify the mechanism behind these severe vacuolar phenotypes in NuA4 mutants.

3.3.6 NuA4 and the Inner Nuclear Membrane (INM)

This work identified a loss of Pah1 to the INM in NuA4 mutants (**Chapter 2**). This raises a larger question about the larger context of metabolism at the INM. Future research investigating the loss of other key proteins at the INM would be interesting to get a larger picture of changes within the nucleus. To do this, BiFC could be employed in a screen to look for the loss of interaction of key proteins to the nucleoplasm and INM. This would allow for the identification of clusters of protein from distinct cellular processes that are changing in NuA4 mutants.

3.3.7 Additional Investigations:

3.3.7.1 Regulation of the localization of KATs

It is generally assumed that KATs are localized to the nucleus to be in close proximity to chromatin, given their role in histone acetylation. However, when considering an evolving role for KATs in the acetylation of proteins, does this mean that KATs are active outside of the nucleus as well? Esa1, for example, is categorized as a nuclear protein by Huh *et al.* [209] but not much is known about NuA4's localization outside of the nucleus. The mechanisms regulating NuA4 localization within the cell could be just as crucial as NuA4 activity itself and shed light on transient NuA4 activity. Tip60 is also considered to be predominantly nuclear, however, it has been shown to localize to the cytoplasm, where it is particularly involved in interleukin-9 (IL-9) signalling and cytokine promotion through interaction with interleukin-9-reception (IL-9R) and its downstream transcription factor, signal transducer and activator of transcription 3 (STAT3).[310,311] Further, it was recently found that breast cancer tumour cells had a predominantly cytoplasmic expression of Tip60, which suggests that the lack of Tip60 in the nucleus could be contributing to tumorigenesis.[295] However, the mechanisms behind the nuclear-cytoplasmic movement of Tip60 are unknown. It is hypothesized that this shuttling could rely on internal or external stimuli, such as cytokines and hormones.[312] Understanding these dynamics could assist in our understanding of non-histone acetylation by KATs. Further, how can we identify microdomains of active KATs in yeast cells?

3.3.7.2 Functional consequences of dysregulated nuclei

While much research has investigated the causes and mechanisms behind nuclear flares and deformation, less is understood about the functional consequences of dysregulated nuclei in yeast. Mechanistic research has examined the role of the nuclear and cytosolic volume ratio as a cause for flares, as the cell aims to maintain this ratio and cause minimal disruptions. In this work, it is interesting to see that despite having significant defects in their nuclear structure, yeast cells with this

phenotype are largely viable and have minimal consequences. Investigating this in a larger context would be very interesting, especially extrapolated to a human/mammalian context where there are additional mechanisms in place specifically to regulate nuclear shape, and the dysregulation of nuclear shape is indicative of severe disease states.

Chapter 4

Overall Conclusion

In conclusion, this work sheds new light on the complex regulatory roles of NuA4 in phospholipid metabolism in *Saccharomyces cerevisiae.* Notably, our findings underscore both Pah1-dependent and independent mechanisms for NuA4 regulation of nuclear and vacuole morphology. This work characterizes novel changes in the localization of Pah1 in NuA4 mutants and further describes the role of direct NuA4-dependent acetylation on Pah1. Additionally, this investigation revealed significant defects in the formation of the NVJ and the corresponding function of PMN in NuA4 mutants. Overall, this thesis advances our understanding of NuA4's role in lipid metabolism and its implications for cellular regulation and diseases. Future research directions include exploration of NuA4's involvement in fatty acid metabolism, autophagy, vesicle trafficking and vacuole fusion, allowing for deeper insight into the complex network of lipid regulatory pathways.

References

1. Gil, J., Ramírez-Torres, A., and Encarnación-Guevara, S. Lysine acetylation and cancer: A proteomics perspective. J Proteomics. 2017;*150*:(297-309. 10.1016/j.jprot.2016.10.003.
2. Choudhary, C., Weinert, B.T., Nishida, Y., Verdin, E., and Mann, M. The growing landscape of lysine acetylation links metabolism and cell signalling. Nature Reviews Molecular Cell Biology. 2014;*15*:(536-550. 10.1038/nrm3841.
3. Weinert, B.T., Iesmantavicius, V., Moustafa, T., Schölz, C., Wagner, S.A., Magnes, C., Zechner, R., and Choudhary, C. Acetylation dynamics and stoichiometry in Saccharomyces cerevisiae. Mol Syst Biol. 2014;*10*:(716. 10.1002/msb.134766.
4. Drazic, A., Myklebust, L.M., Ree, R., and Arnesen, T. The world of protein acetylation. Biochimica et Biophysica Acta (BBA) - Proteins and Proteomics. 2016;*1864*:(1372-1401. https://doi.org/10.1016/j.bbapap.2016.06.007.
5. Brown, J.L., and Roberts, W.K. Evidence that approximately eighty per cent of the soluble proteins from Ehrlich ascites cells are Nalpha-acetylated. Journal of Biological Chemistry. 1976;*251*:(1009-1014. https://doi.org/10.1016/S0021-9258(17)33793-6.
6. Helsens, K., Van Damme, P., Degroeve, S., Martens, L., Arnesen, T., Vandekerckhove, J., and Gevaert, K. Bioinformatics Analysis of a Saccharomyces cerevisiae N-Terminal Proteome Provides Evidence of Alternative Translation Initiation and Post-Translational N-Terminal Acetylation. Journal of Proteome Research. 2011;*10*:(3578-3589. 10.1021/pr2002325.
7. Glozak, M.A., Sengupta, N., Zhang, X., and Seto, E. Acetylation and deacetylation of non-histone proteins. Gene. 2005;*363*:(15-23. 10.1016/j.gene.2005.09.010.
8. Allfrey, V.G., Faulkner, R., and Mirsky, A.E. ACETYLATION AND METHYLATION OF HISTONES AND THEIR POSSIBLE ROLE IN THE REGULATION OF RNA SYNTHESIS. Proc Natl Acad Sci U S A. 1964;*51*:(786-794. 10.1073/pnas.51.5.786.
9. Gershey, E.L., Vidali, G., and Allfrey, V.G. Chemical studies of histone acetylation. The occurrence of epsilon-N-acetyllysine in the f2a1 histone. J Biol Chem. 1968;*243*:(5018-5022.
10. Coffey, K., Blackburn, T.J., Cook, S., Golding, B.T., Griffin, R.J., Hardcastle, I.R., Hewitt, L., Huberman, K., McNeill, H.V., Newell, D.R., et al. Characterisation of a Tip60 Specific Inhibitor, NU9056, in Prostate Cancer. PLOS ONE. 2012;*7*:(e45539. 10.1371/journal.pone.0045539.
11. Filippakopoulos, P., and Knapp, S. The bromodomain interaction module. FEBS Lett. 2012;*586*:(2692-2704. 10.1016/j.febslet.2012.04.045.
12. Schulze, J.M., Wang, A.Y., and Kobor, M.S. Reading chromatin: insights from yeast into YEATS domain structure and function. Epigenetics. 2010;*5*:(573-577. 10.4161/epi.5.7.12856.
13. Zeng, L., Zhang, Q., Li, S., Plotnikov, A.N., Walsh, M.J., and Zhou, M.-M. Mechanism and regulation of acetylated histone binding by the tandem PHD finger of DPF3b. Nature. 2010;*466*:(258-262. 10.1038/nature09139.
14. Narita, T., Weinert, B.T., and Choudhary, C. Functions and mechanisms of non-histone protein acetylation. Nature Reviews Molecular Cell Biology. 2019;*20*:(156-174. 10.1038/s41580-018-0081-3.
15. Vetting, M.W., LP, S.d.C., Yu, M., Hegde, S.S., Magnet, S., Roderick, S.L., and Blanchard, J.S. Structure and functions of the GNAT superfamily of acetyltransferases. Arch Biochem Biophys. 2005;*433*:(212-226. 10.1016/j.abb.2004.09.003.

16. Salah Ud-Din, A.I., Tikhomirova, A., and Roujeinikova, A. Structure and Functional Diversity of GCN5-Related N-Acetyltransferases (GNAT). Int J Mol Sci. 2016;*17*:(10.3390/ijms17071018.
17. Utley, R.T., and Côté, J. The MYST family of histone acetyltransferases. Curr Top Microbiol Immunol. 2003;*274*:(203-236. 10.1007/978-3-642-55747-7_8.
18. Ogryzko, V.V., Schiltz, R.L., Russanova, V., Howard, B.H., and Nakatani, Y. The transcriptional coactivators p300 and CBP are histone acetyltransferases. Cell. 1996;*87*:(953-959. 10.1016/s0092-8674(00)82001-2.
19. Guedes-Dias, P., and Oliveira, J.M.A. Lysine deacetylases and mitochondrial dynamics in neurodegeneration. Biochimica et Biophysica Acta (BBA) - Molecular Basis of Disease. 2013;*1832*:(1345-1359. https://doi.org/10.1016/j.bbadis.2013.04.005.
20. Gallinari, P., Marco, S.D., Jones, P., Pallaoro, M., and Steinkühler, C. HDACs, histone deacetylation and gene transcription: from molecular biology to cancer therapeutics. Cell Research. 2007;*17*:(195-211. 10.1038/sj.cr.7310149.
21. Figlia, G., Willnow, P., and Teleman, A.A. Metabolites Regulate Cell Signaling and Growth via Covalent Modification of Proteins. Developmental Cell. 2020;*54*:(156-170. 10.1016/j.devcel.2020.06.036.
22. Shvedunova, M., and Akhtar, A. Modulation of cellular processes by histone and non-histone protein acetylation. Nature Reviews Molecular Cell Biology. 2022;*23*:(329-349. 10.1038/s41580-021-00441-y.
23. Downey, M., and Baetz, K. Building a KATalogue of acetyllysine targeting and function. Briefings in Functional Genomics. 2016;*15*:(109-118. 10.1093/bfgp/elv045.
24. Choudhary, C., Kumar, C., Gnad, F., Nielsen, M.L., Rehman, M., Walther, T.C., Olsen, J.V., and Mann, M. Lysine acetylation targets protein complexes and co-regulates major cellular functions. Science. 2009;*325*:(834-840. 10.1126/science.1175371.
25. Sterner, R., Vidali, G., and Allfrey, V.G. Studies of acetylation and deacetylation in high mobility group proteins. Identification of the sites of acetylation in high mobility group proteins 14 and 17. Journal of Biological Chemistry. 1981;*256*:(8892-8895. https://doi.org/10.1016/S0021-9258(19)52481-4.
26. Gu, W., and Roeder, R.G. Activation of p53 Sequence-Specific DNA Binding by Acetylation of the p53 C-Terminal Domain. Cell. 1997;*90*:(595-606. https://doi.org/10.1016/S0092-8674(00)80521-8.
27. Kim, S.C., Sprung, R., Chen, Y., Xu, Y., Ball, H., Pei, J., Cheng, T., Kho, Y., Xiao, H., Xiao, L., et al. Substrate and Functional Diversity of Lysine Acetylation Revealed by a Proteomics Survey. Molecular Cell. 2006;*23*:(607-618. https://doi.org/10.1016/j.molcel.2006.06.026.
28. Singh, B.N., Zhang, G., Hwa, Y.L., Li, J., Dowdy, S.C., and Jiang, S.-W. Nonhistone protein acetylation as cancer therapy targets. Expert Review of Anticancer Therapy. 2010;*10*:(935-954. 10.1586/era.10.62.
29. Saha, R.N., and Pahan, K. HATs and HDACs in neurodegeneration: a tale of disconcerted acetylation homeostasis. Cell Death & Differentiation. 2006;*13*:(539-550. 10.1038/sj.cdd.4401769.
30. Iyer, A., Fairlie, D.P., and Brown, L. Lysine acetylation in obesity, diabetes and metabolic disease. Immunology & Cell Biology. 2012;*90*:(39-46. 10.1038/icb.2011.99.
31. Sapountzi, V., Logan, I.R., and Robson, C.N. Cellular functions of TIP60. Int J Biochem Cell Biol. 2006;*38*:(1496-1509. 10.1016/j.biocel.2006.03.003.

32. Kamine, J., Elangovan, B., Subramanian, T., Coleman, D., and Chinnadurai, G. Identification of a cellular protein that specifically interacts with the essential cysteine region of the HIV-1 Tat transactivator. Virology. 1996;*216*:(357-366. 10.1006/viro.1996.0071.
33. Yamamoto, T., and Horikoshi, M. Novel substrate specificity of the histone acetyltransferase activity of HIV-1-Tat interactive protein Tip60. J Biol Chem. 1997;*272*:(30595-30598. 10.1074/jbc.272.49.30595.
34. Kimura, A., and Horikoshi, M. Tip60 acetylates six lysines of a specific class in core histones in vitro. Genes Cells. 1998;*3*:(789-800. 10.1046/j.1365-2443.1998.00229.x.
35. Gaughan, L., Logan, I.R., Cook, S., Neal, D.E., and Robson, C.N. Tip60 and Histone Deacetylase 1 Regulate Androgen Receptor Activity through Changes to the Acetylation Status of the Receptor*. Journal of Biological Chemistry. 2002;*277*:(25904-25913. https://doi.org/10.1074/jbc.M203423200.
36. Halkidou, K., Logan, I.R., Cook, S., Neal, D.E., and Robson, C.N. Putative involvement of the histone acetyltransferase Tip60 in ribosomal gene transcription. Nucleic Acids Res. 2004;*32*:(1654-1665. 10.1093/nar/gkh296.
37. Patel, J.H., Du, Y., Ard, P.G., Phillips, C., Carella, B., Chen, C.J., Rakowski, C., Chatterjee, C., Lieberman, P.M., Lane, W.S., et al. The c-MYC oncoprotein is a substrate of the acetyltransferases hGCN5/PCAF and TIP60. Mol Cell Biol. 2004;*24*:(10826-10834. 10.1128/mcb.24.24.10826-10834.2004.
38. Sun, Y., Jiang, X., Chen, S., Fernandes, N., and Price, B.D. A role for the Tip60 histone acetyltransferase in the acetylation and activation of ATM. Proc Natl Acad Sci U S A. 2005;*102*:(13182-13187. 10.1073/pnas.0504211102.
39. Ghobashi, A.H., and Kamel, M.A. Tip60: updates. Journal of Applied Genetics. 2018;*59*:(161-168. 10.1007/s13353-018-0432-y.
40. Mo, F., Zhuang, X., Liu, X., Yao, P.Y., Qin, B., Su, Z., Zang, J., Wang, Z., Zhang, J., Dou, Z., et al. Acetylation of Aurora B by TIP60 ensures accurate chromosomal segregation. Nature Chemical Biology. 2016;*12*:(226-232. 10.1038/nchembio.2017.
41. Varshney, N., Rani, A., Kashyap, D., Tiwari, D., and Jha, H.C. (2022). Chapter 10 - Aurora kinase: An emerging potential target in therapeutics. In Protein Kinase Inhibitors, M.I. Hassan, and S. Noor, eds. (Academic Press), pp. 261-322. https://doi.org/10.1016/B978-0-323-91287-7.00028-4.
42. Ozaki, T., and Nakagawara, A. Role of p53 in Cell Death and Human Cancers. Cancers (Basel). 2011;*3*:(994-1013. 10.3390/cancers3010994.
43. Reed, S., and Quelle, D. p53 Acetylation: Regulation and Consequences. Cancers. 2014;*7*:(30-69. 10.3390/cancers7010030.
44. Tang, Y., Luo, J., Zhang, W., and Gu, W. Tip60-Dependent Acetylation of p53 Modulates the Decision between Cell-Cycle Arrest and Apoptosis. Molecular Cell. 2006;*24*:(827-839. https://doi.org/10.1016/j.molcel.2006.11.021.
45. Goffeau, A., Barrell, B.G., Bussey, H., Davis, R.W., Dujon, B., Feldmann, H., Galibert, F., Hoheisel, J.D., Jacq, C., Johnston, M., et al. Life with 6000 genes. Science. 1996;*274*:(546, 563-547. 10.1126/science.274.5287.546.
46. Botstein, D., Chervitz, S.A., and Cherry, J.M. Yeast as a model organism. Science. 1997;*277*:(1259-1260. 10.1126/science.277.5330.1259.

47. Vanderwaeren, L., Dok, R., Voordeckers, K., Nuyts, S., and Verstrepen, K.J. Saccharomyces cerevisiae as a Model System for Eukaryotic Cell Biology, from Cell Cycle Control to DNA Damage Response. Int J Mol Sci. 2022;*23*:(10.3390/ijms231911665.
48. Hinnen, A., Hicks, J.B., and Fink, G.R. Transformation of yeast. Proc Natl Acad Sci U S A. 1978;*75*:(1929-1933. 10.1073/pnas.75.4.1929.
49. Eckert-Boulet, N., Rothstein, R., and Lisby, M. Cell biology of homologous recombination in yeast. Methods Mol Biol. 2011;*745*:(523-536. 10.1007/978-1-61779-129-1_30.
50. Beltrao, P., Albanèse, V., Kenner, L.R., Swaney, D.L., Burlingame, A., Villén, J., Lim, W.A., Fraser, J.S., Frydman, J., and Krogan, N.J. Systematic functional prioritization of protein posttranslational modifications. Cell. 2012;*150*:(413-425. 10.1016/j.cell.2012.05.036.
51. Henriksen, P., Wagner, S.A., Weinert, B.T., Sharma, S., Bacinskaja, G., Rehman, M., Juffer, A.H., Walther, T.C., Lisby, M., and Choudhary, C. Proteome-wide analysis of lysine acetylation suggests its broad regulatory scope in Saccharomyces cerevisiae. Mol Cell Proteomics. 2012;*11*:(1510-1522. 10.1074/mcp.M112.017251.
52. Weinert, B.T., Wagner, S.A., Horn, H., Henriksen, P., Liu, W.R., Olsen, J.V., Jensen, L.J., and Choudhary, C. Proteome-Wide Mapping of the Drosophila Acetylome Demonstrates a High Degree of Conservation of Lysine Acetylation. Science Signaling. 2011;*4*:(ra48-ra48. doi:10.1126/scisignal.2001902.
53. Downey, M., Johnson, J.R., Davey, N.E., Newton, B.W., Johnson, T.L., Galaang, S., Seller, C.A., Krogan, N., and Toczyski, D.P. Acetylome profiling reveals overlap in the regulation of diverse processes by sirtuins, gcn5, and esa1. Mol Cell Proteomics. 2015;*14*:(162-176. 10.1074/mcp.M114.043141.
54. Giaever, G., Chu, A.M., Ni, L., Connelly, C., Riles, L., Véronneau, S., Dow, S., Lucau-Danila, A., Anderson, K., André, B., et al. Functional profiling of the Saccharomyces cerevisiae genome. Nature. 2002;*418*:(387-391. 10.1038/nature00935.
55. Giaever, G., and Nislow, C. The yeast deletion collection: a decade of functional genomics. Genetics. 2014;*197*:(451-465. 10.1534/genetics.114.161620.
56. Douglas, A.C., Smith, A.M., Sharifpoor, S., Yan, Z., Durbic, T., Heisler, L.E., Lee, A.Y., Ryan, O., Göttert, H., Surendra, A., et al. Functional analysis with a barcoder yeast gene overexpression system. G3 (Bethesda). 2012;*2*:(1279-1289. 10.1534/g3.112.003400.
57. Huh, W.-K., Falvo, J.V., Gerke, L.C., Carroll, A.S., Howson, R.W., Weissman, J.S., and O'Shea, E.K. Global analysis of protein localization in budding yeast. Nature. 2003;*425*:(686-691. 10.1038/nature02026.
58. Tong, A.H.Y., Evangelista, M., Parsons, A.B., Xu, H., Bader, G.D., Pagé, N., Robinson, M., Raghibizadeh, S., Hogue, C.W.V., Bussey, H., et al. Systematic Genetic Analysis with Ordered Arrays of Yeast Deletion Mutants. Science. 2001;*294*:(2364-2368. doi:10.1126/science.1065810.
59. Costanzo, M., Baryshnikova, A., Bellay, J., Kim, Y., Spear, E.D., Sevier, C.S., Ding, H., Koh, J.L.Y., Toufighi, K., Mostafavi, S., et al. The Genetic Landscape of a Cell. Science. 2010;*327*:(425-431. 10.1126/science.1180823.
60. Lin, Y.Y., Qi, Y., Lu, J.Y., Pan, X., Yuan, D.S., Zhao, Y., Bader, J.S., and Boeke, J.D. A comprehensive synthetic genetic interaction network governing yeast histone acetylation and deacetylation. Genes Dev. 2008;*22*:(2062-2074. 10.1101/gad.1679508.
61. Chong, Yolanda T., Koh, Judice L.Y., Friesen, H., Kaluarachchi Duffy, S., Cox, Michael J., Moses, A., Moffat, J., Boone, C., and Andrews, Brenda J. Yeast Proteome Dynamics from Single Cell

Imaging and Automated Analysis. Cell. 2015;*161*:(1413-1424. https://doi.org/10.1016/j.cell.2015.04.051.
62. Mitchell, L., Lambert, J.-P., Gerdes, M., Al-Madhoun, A.S., Skerjanc, I.S., Figeys, D., and Baetz, K. Functional Dissection of the NuA4 Histone Acetyltransferase Reveals Its Role as a Genetic Hub and that Eaf1 Is Essential for Complex Integrity. Molecular and Cellular Biology. 2008;*28*:(2244-2256. 10.1128/mcb.01653-07.
63. Eberharter, A., John, S., Grant, P.A., Utley, R.T., and Workman, J.L. Identification and Analysis of Yeast Nucleosomal Histone Acetyltransferase Complexes. Methods. 1998;*15*:(315-321. https://doi.org/10.1006/meth.1998.0635.
64. Lin, Y.Y., Lu, J.Y., Zhang, J., Walter, W., Dang, W., Wan, J., Tao, S.C., Qian, J., Zhao, Y., Boeke, J.D., et al. Protein acetylation microarray reveals that NuA4 controls key metabolic target regulating gluconeogenesis. Cell. 2009;*136*:(1073-1084. 10.1016/j.cell.2009.01.033.
65. Walden, E.A., Fong, R.Y., Pham, T.T., Knill, H., Laframboise, S.J., Huard, S., Harper, M.E., and Baetz, K. Phenomic screen identifies a role for the yeast lysine acetyltransferase NuA4 in the control of Bcy1 subcellular localization, glycogen biosynthesis, and mitochondrial morphology. PLoS Genet. 2020;*16*:(e1009220. 10.1371/journal.pgen.1009220.
66. Dacquay, L., Flint, A., Butcher, J., Salem, D., Kennedy, M., Kaern, M., Stintzi, A., and Baetz, K. NuA4 Lysine Acetyltransferase Complex Contributes to Phospholipid Homeostasis in Saccharomyces cerevisiae. G3 Genes|Genomes|Genetics. 2017;*7*:(1799-1809. 10.1534/g3.117.041053.
67. Huang, J., Mousley, C.J., Dacquay, L., Maitra, N., Drin, G., He, C., Ridgway, N.D., Tripathi, A., Kennedy, M., Kennedy, B.K., et al. A Lipid Transfer Protein Signaling Axis Exerts Dual Control of Cell-Cycle and Membrane Trafficking Systems. Dev Cell. 2018;*44*:(378-391.e375. 10.1016/j.devcel.2017.12.026.
68. Rollins, M., Huard, S., Morettin, A., Takuski, J., Pham, T.T., Fullerton, M.D., Côté, J., and Baetz, K. Lysine acetyltransferase NuA4 and acetyl-CoA regulate glucose-deprived stress granule formation in Saccharomyces cerevisiae. PLoS Genet. 2017;*13*:(e1006626. 10.1371/journal.pgen.1006626.
69. Doyon, Y., Selleck, W., Lane, W.S., Tan, S., and CôTé, J. Structural and Functional Conservation of the NuA4 Histone Acetyltransferase Complex from Yeast to Humans. Molecular and Cellular Biology. 2004;*24*:(1884-1896. 10.1128/mcb.24.5.1884-1896.2004.
70. Allard, S. NuA4, an essential transcription adaptor/histone H4 acetyltransferase complex containing Esa1p and the ATM-related cofactor Tra1p. The EMBO Journal. 1999;*18*:(5108-5119. 10.1093/emboj/18.18.5108.
71. Doyon, Y., Selleck, W., Lane, W.S., Tan, S., and Côté, J. Structural and functional conservation of the NuA4 histone acetyltransferase complex from yeast to humans. Mol Cell Biol. 2004;*24*:(1884-1896. 10.1128/mcb.24.5.1884-1896.2004.
72. Chittuluru, J.R., Chaban, Y., Monnet-Saksouk, J., Carrozza, M.J., Sapountzi, V., Selleck, W., Huang, J., Utley, R.T., Cramet, M., Allard, S., et al. Structure and nucleosome interaction of the yeast NuA4 and Piccolo–NuA4 histone acetyltransferase complexes. Nature Structural & Molecular Biology. 2011;*18*:(1196-1203. 10.1038/nsmb.2128.
73. Selleck, W., Fortin, I., Sermwittayawong, D., Côté, J., and Tan, S. The Saccharomyces cerevisiae Piccolo NuA4 histone acetyltransferase complex requires the Enhancer of Polycomb A domain and chromodomain to acetylate nucleosomes. Mol Cell Biol. 2005;*25*:(5535-5542. 10.1128/mcb.25.13.5535-5542.2005.

74. Boudreault, A.A., Cronier, D., Selleck, W., Lacoste, N., Utley, R.T., Allard, S., Savard, J., Lane, W.S., Tan, S., and Côté, J. Yeast enhancer of polycomb defines global Esa1-dependent acetylation of chromatin. Genes Dev. 2003;*17*:(1415-1428. 10.1101/gad.1056603.
75. Huang, J., and Tan, S. Piccolo NuA4-catalyzed acetylation of nucleosomal histones: critical roles of an Esa1 Tudor/chromo barrel loop and an Epl1 enhancer of polycomb A (EPcA) basic region. Mol Cell Biol. 2013;*33*:(159-169. 10.1128/mcb.01131-12.
76. Rossetto, D., Cramet, M., Wang, A.Y., Steunou, A.L., Lacoste, N., Schulze, J.M., Côté, V., Monnet-Saksouk, J., Piquet, S., Nourani, A., et al. Eaf5/7/3 form a functionally independent NuA4 submodule linked to RNA polymerase II-coupled nucleosome recycling. Embo j. 2014;*33*:(1397-1415. 10.15252/embj.201386433.
77. Bhat, W., Ahmad, S., and Côté, J. TINTIN, at the interface of chromatin, transcription elongation, and mRNA processing. RNA Biol. 2015;*12*:(486-489. 10.1080/15476286.2015.1026032.
78. Cheng, X., and Côté, J. A new companion of elongating RNA Polymerase II: TINTIN, an independent sub-module of NuA4/TIP60 for nucleosome transactions. Transcription. 2014;*5*:(e995571. 10.1080/21541264.2014.995571.
79. Sharov, G., Voltz, K., Durand, A., Kolesnikova, O., Papai, G., Myasnikov, A.G., Dejaegere, A., Ben Shem, A., and Schultz, P. Structure of the transcription activator target Tra1 within the chromatin modifying complex SAGA. Nature Communications. 2017;*8*:(1556. 10.1038/s41467-017-01564-7.
80. Grant, P.A., Schieltz, D., Pray-Grant, M.G., Yates, J.R., 3rd, and Workman, J.L. The ATM-related cofactor Tra1 is a component of the purified SAGA complex. Mol Cell. 1998;*2*:(863-867. 10.1016/s1097-2765(00)80300-7.
81. Cheung, A.C.M., and Díaz-Santín, L.M. Share and share alike: the role of Tra1 from the SAGA and NuA4 coactivator complexes. Transcription. 2019;*10*:(37-43. 10.1080/21541264.2018.1530936.
82. Wang, X., Ahmad, S., Zhang, Z., Côté, J., and Cai, G. Architecture of the Saccharomyces cerevisiae NuA4/TIP60 complex. Nature Communications. 2018;*9*:(1147. 10.1038/s41467-018-03504-5.
83. Ji, L., Zhao, L., Xu, K., Gao, H., Zhou, Y., Kornberg, R.D., and Zhang, H. Structure of the NuA4 histone acetyltransferase complex. Proceedings of the National Academy of Sciences. 2022;*119*:(10.1073/pnas.2214313119.
84. Zukin, S.A., Marunde, M.R., Popova, I.K., Soczek, K.M., Nogales, E., and Patel, A.B. Structure and flexibility of the yeast NuA4 histone acetyltransferase complex. eLife. 2022;*11*:(e81400. 10.7554/eLife.81400.
85. Clarke, A.S., Lowell, J.E., Jacobson, S.J., and Pillus, L. Esa1p Is an Essential Histone Acetyltransferase Required for Cell Cycle Progression. Molecular and Cellular Biology. 1999;*19*:(2515-2526. 10.1128/mcb.19.4.2515.
86. Mitchell, L., Huard, S., Cotrut, M., Pourhanifeh-Lemeri, R., Steunou, A.L., Hamza, A., Lambert, J.P., Zhou, H., Ning, Z., Basu, A., et al. mChIP-KAT-MS, a method to map protein interactions and acetylation sites for lysine acetyltransferases. Proceedings of the National Academy of Sciences. 2013;*110*:(E1641-E1650. 10.1073/pnas.1218515110.
87. Haruki, H., Nishikawa, J., and Laemmli, U.K. The Anchor-Away Technique: Rapid, Conditional Establishment of Yeast Mutant Phenotypes. Molecular Cell. 2008;*31*:(925-932. 10.1016/j.molcel.2008.07.020.

88. Hodges, A.J., Plummer, D.A., and Wyrick, J.J. NuA4 acetyltransferase is required for efficient nucleotide excision repair in yeast. DNA Repair. 2019;*73*:(91-98. 10.1016/j.dnarep.2018.11.006.
89. Auger, A.A., Galarneau, L., Altaf, M., Nourani, A., Doyon, Y., Utley, R.T., Cronier, D., Allard, S.P., and CôTé, J. Eaf1 Is the Platform for NuA4 Molecular Assembly That Evolutionarily Links Chromatin Acetylation to ATP-Dependent Exchange of Histone H2A Variants. Molecular and Cellular Biology. 2008;*28*:(2257-2270. 10.1128/mcb.01755-07.
90. Cheng, X., Auger, A., Altaf, M., Drouin, S., Paquet, E., Utley, R.T., Robert, F., and Côté, J. Eaf1 Links the NuA4 Histone Acetyltransferase Complex to Htz1 Incorporation and Regulation of Purine Biosynthesis. Eukaryotic Cell. 2015;*14*:(535-544. 10.1128/ec.00004-15.
91. Pham, T., Walden, E., Huard, S., Pezacki, J., Fullerton, M.D., and Baetz, K. Fine-tuning acetyl-CoA carboxylase 1 activity through localization: functional genomics reveals a role for the lysine acetyltransferase NuA4 and sphingolipid metabolism in regulating Acc1 activity and localization. Genetics. 2022. 10.1093/genetics/iyac086.
92. Hustedt, N., and Durocher, D. The control of DNA repair by the cell cycle. Nat Cell Biol. 2016;*19*:(1-9. 10.1038/ncb3452.
93. Downs, J.A., Allard, S., Jobin-Robitaille, O., Javaheri, A., Auger, A., Bouchard, N., Kron, S.J., Jackson, S.P., and Côté, J. Binding of chromatin-modifying activities to phosphorylated histone H2A at DNA damage sites. Mol Cell. 2004;*16*:(979-990. 10.1016/j.molcel.2004.12.003.
94. Altaf, M., Auger, A., Monnet-Saksouk, J., Brodeur, J., Piquet, S., Cramet, M., Bouchard, N., Lacoste, N., Utley, R.T., Gaudreau, L., and Côté, J. NuA4-dependent acetylation of nucleosomal histones H4 and H2A directly stimulates incorporation of H2A.Z by the SWR1 complex. J Biol Chem. 2010;*285*:(15966-15977. 10.1074/jbc.M110.117069.
95. Ahmad, S., Côté, V., Cheng, X., Bourriquen, G., Sapountzi, V., Altaf, M., and Côté, J. Antagonistic relationship of NuA4 with the non-homologous end-joining machinery at DNA damage sites. PLOS Genetics. 2021;*17*:(e1009816. 10.1371/journal.pgen.1009816.
96. Xu, P., Li, C., Chen, Z., Jiang, S., Fan, S., Wang, J., Dai, J., Zhu, P., and Chen, Z. The NuA4 Core Complex Acetylates Nucleosomal Histone H4 through a Double Recognition Mechanism. Molecular Cell. 2016;*63*:(965-975. https://doi.org/10.1016/j.molcel.2016.07.024.
97. Yang, C., Wu, J., and Zheng, Y.G. Function of the active site lysine autoacetylation in Tip60 catalysis. PLoS One. 2012;*7*:(e32886. 10.1371/journal.pone.0032886.
98. Dubey, S., Gupta, H., and Gupta, A. (2023). Autoacetylation-mediated phase separation of TIP60 is critical for its functions. Cold Spring Harbor Laboratory.
99. Shabkhizan, R., Haiaty, S., Moslehian, M.S., Bazmani, A., Sadeghsoltani, F., Saghaei Bagheri, H., Rahbarghazi, R., and Sakhinia, E. The Beneficial and Adverse Effects of Autophagic Response to Caloric Restriction and Fasting. Adv Nutr. 2023;*14*:(1211-1225. 10.1016/j.advnut.2023.07.006.
100. Li, Z., and Rasmussen, L.J. TIP60 in aging and neurodegeneration. Ageing Res Rev. 2020;*64*:(101195. 10.1016/j.arr.2020.101195.
101. Menzies, F.M., Fleming, A., and Rubinsztein, D.C. Compromised autophagy and neurodegenerative diseases. Nature Reviews Neuroscience. 2015;*16*:(345-357. 10.1038/nrn3961.
102. Ravikumar, B., Sarkar, S., Davies, J.E., Futter, M., Garcia-Arencibia, M., Green-Thompson, Z.W., Jimenez-Sanchez, M., Korolchuk, V.I., Lichtenberg, M., Luo, S., et al. Regulation of

Mammalian Autophagy in Physiology and Pathophysiology. Physiological Reviews. 2010;*90*:(1383-1435. 10.1152/physrev.00030.2009.
103. Hamaï, A., and Codogno, P. New Targets for Acetylation in Autophagy. Science Signaling. 2012;*5*:(pe29-pe29. doi:10.1126/scisignal.2003187.
104. Lin, S.Y., Li, T.Y., Liu, Q., Zhang, C., Li, X., Chen, Y., Zhang, S.M., Lian, G., Liu, Q., Ruan, K., et al. GSK3-TIP60-ULK1 signaling pathway links growth factor deprivation to autophagy. Science. 2012;*336*:(477-481. 10.1126/science.1217032.
105. Nie, T., Yang, S., Ma, H., Zhang, L., Lu, F., Tao, K., Wang, R., Yang, R., Huang, L., Mao, Z., and Yang, Q. Regulation of ER stress-induced autophagy by GSK3β-TIP60-ULK1 pathway. Cell Death & Disease. 2016;*7*:(e2563-e2563. 10.1038/cddis.2016.423.
106. Turco, E., Fracchiolla, D., and Martens, S. Recruitment and Activation of the ULK1/Atg1 Kinase Complex in Selective Autophagy. J Mol Biol. 2020;*432*:(123-134. 10.1016/j.jmb.2019.07.027.
107. Cheng, X., Ma, X., Zhu, Q., Song, D., Ding, X., Li, L., Jiang, X., Wang, X., Tian, R., Su, H., et al. Pacer Is a Mediator of mTORC1 and GSK3-TIP60 Signaling in Regulation of Autophagosome Maturation and Lipid Metabolism. Molecular Cell. 2019;*73*:(788-802.e787. 10.1016/j.molcel.2018.12.017.
108. You, Z., Jiang, W.-X., Qin, L.-Y., Gong, Z., Wan, W., Li, J., Wang, Y., Zhang, H., Peng, C., Zhou, T., et al. Requirement for p62 acetylation in the aggregation of ubiquitylated proteins under nutrient stress. Nature Communications. 2019;*10*:(5792. 10.1038/s41467-019-13718-w.
109. Yi, C., Ma, M., Ran, L., Zheng, J., Tong, J., Zhu, J., Ma, C., Sun, Y., Zhang, S., Feng, W., et al. Function and Molecular Mechanism of Acetylation in Autophagy Regulation. Science. 2012;*336*:(474-477. doi:10.1126/science.1216990.
110. Li, T.Y., Song, L., Sun, Y., Li, J., Yi, C., Lam, S.M., Xu, D., Zhou, L., Li, X., Yang, Y., et al. Tip60-mediated lipin 1 acetylation and ER translocation determine triacylglycerol synthesis rate. Nature Communications. 2018;*9*:(10.1038/s41467-018-04363-w.
111. Fahy, E., Subramaniam, S., Murphy, R.C., Nishijima, M., Raetz, C.R.H., Shimizu, T., Spener, F., Van Meer, G., Wakelam, M.J.O., and Dennis, E.A. Update of the LIPID MAPS comprehensive classification system for lipids. Journal of Lipid Research. 2009;*50*:(S9-S14. 10.1194/jlr.r800095-jlr200.
112. Escribá, P.V., González-Ros, J.M., Goñi, F.M., Kinnunen, P.K.J., Vigh, L., Sánchez-Magraner, L., Fernández, A.M., Busquets, X., Horváth, I., and Barceló-Coblijn, G. Membranes: a meeting point for lipids, proteins and therapies. Journal of Cellular and Molecular Medicine. 2008;*12*:(829-875. 10.1111/j.1582-4934.2008.00281.x.
113. Henderson, C.M., and Block, D.E. Examining the Role of Membrane Lipid Composition in Determining the Ethanol Tolerance of Saccharomyces cerevisiae. Applied and Environmental Microbiology. 2014;*80*:(2966-2972. 10.1128/aem.04151-13.
114. Rego, A., Trindade, D., Chaves, S.R., Manon, S., Costa, V., Sousa, M.J., and Côrte-Real, M. The yeast model system as a tool towards the understanding of apoptosis regulation by sphingolipids. FEMS Yeast Res. 2014;*14*:(160-178. 10.1111/1567-1364.12096.
115. Grillitsch, K., Connerth, M., Köfeler, H., Arrey, T.N., Rietschel, B., Wagner, B., Karas, M., and Daum, G. Lipid particles/droplets of the yeast Saccharomyces cerevisiae revisited: lipidome meets proteome. Biochim Biophys Acta. 2011;*1811*:(1165-1176. 10.1016/j.bbalip.2011.07.015.
116. Nielsen, J. Systems biology of lipid metabolism: From yeast to human. FEBS Letters. 2009;*583*:(3905-3913. 10.1016/j.febslet.2009.10.054.

117. Petranovic, D., Tyo, K., Vemuri, G.N., and Nielsen, J. Prospects of yeast systems biology for human health: integrating lipid, protein and energy metabolism. FEMS Yeast Res. 2010;*10*:(1046-1059. 10.1111/j.1567-1364.2010.00689.x.
118. Santos, A.X., and Riezman, H. Yeast as a model system for studying lipid homeostasis and function. FEBS Lett. 2012;*586*:(2858-2867. 10.1016/j.febslet.2012.07.033.
119. Klug, L., and Daum, G. Yeast lipid metabolism at a glance. FEMS Yeast Research. 2014;*14*:(369-388. 10.1111/1567-1364.12141.
120. de Kroon, A.I.P.M. Lipidomics in research on yeast membrane lipid homeostasis. Biochimica et Biophysica Acta (BBA) - Molecular and Cell Biology of Lipids. 2017;*1862*:(797-799. https://doi.org/10.1016/j.bbalip.2017.02.007.
121. Rockenfeller, P., and Gourlay, C.W. Lipotoxicty in yeast: a focus on plasma membrane signalling and membrane contact sites. FEMS Yeast Res. 2018;*18*:(10.1093/femsyr/foy034.
122. Athenstaedt, K. (2010). Neutral Lipids in Yeast: Synthesis, Storage and Degradation. In (Springer Berlin Heidelberg), pp. 471-480. 10.1007/978-3-540-77587-4_35.
123. Carman, G.M., and Han, G.-S. Fat-regulating phosphatidic acid phosphatase: a review of its roles and regulation in lipid homeostasis. Journal of Lipid Research. 2019;*60*:(2-6. 10.1194/jlr.s087452.
124. O'Hara, L., Han, G.-S., Peak-Chew, S., Grimsey, N., Carman, G.M., and Siniossoglou, S. Control of Phospholipid Synthesis by Phosphorylation of the Yeast Lipin Pah1p/Smp2p Mg2+-dependent Phosphatidate Phosphatase. Journal of Biological Chemistry. 2006;*281*:(34537-34548. 10.1074/jbc.m606654200.
125. Santos-Rosa, H., Leung, J., Grimsey, N., Peak-Chew, S., and Siniossoglou, S. The yeast lipin Smp2 couples phospholipid biosynthesis to nuclear membrane growth. The EMBO Journal. 2005;*24*:(1931-1941. 10.1038/sj.emboj.7600672.
126. Barbosa, A.D., Sembongi, H., Su, W.-M., Abreu, S., Reggiori, F., Carman, G.M., and Siniossoglou, S. Lipid partitioning at the nuclear envelope controls membrane biogenesis. Molecular Biology of the Cell. 2015;*26*:(3641-3657. 10.1091/mbc.e15-03-0173.
127. Pillai, A.N., Shukla, S., and Rahaman, A. An evolutionarily conserved phosphatidate phosphatase maintains lipid droplet number and ER morphology but not nuclear morphology. Biology Open. 2017;*6*:(1629-1643. 10.1242/bio.028233.
128. Flick, J.S., and Thorner, J. Genetic and biochemical characterization of a phosphatidylinositol-specific phospholipase C in Saccharomyces cerevisiae. Molecular and Cellular Biology. 1993;*13*:(5861-5876. 10.1128/mcb.13.9.5861.
129. Bond, P. Phosphatidic acid: biosynthesis, pharmacokinetics, mechanisms of action and effect on strength and body composition in resistance-trained individuals. Nutrition & Metabolism. 2017;*14*:(10.1186/s12986-017-0166-6.
130. Han, G.-S., Wu, W.-I., and Carman, G.M. The Saccharomyces cerevisiae Lipin Homolog Is a Mg2+-dependent Phosphatidate Phosphatase Enzyme*. Journal of Biological Chemistry. 2006;*281*:(9210-9218. 10.1074/jbc.m600425200.
131. Han, G.-S., Siniossoglou, S., and Carman, G.M. The Cellular Functions of the Yeast Lipin Homolog Pah1p Are Dependent on Its Phosphatidate Phosphatase Activity*. Journal of Biological Chemistry. 2007;*282*:(37026-37035. https://doi.org/10.1074/jbc.M705777200.
132. Fakas, S., Qiu, Y., Dixon, J.L., Han, G.-S., Ruggles, K.V., Garbarino, J., Sturley, S.L., and Carman, G.M. Phosphatidate Phosphatase Activity Plays Key Role in Protection against Fatty Acid-

induced Toxicity in Yeast. Journal of Biological Chemistry. 2011;*286*:(29074-29085. 10.1074/jbc.m111.258798.
133. Han, G.-S., and Carman, G.M. Yeast PAH1-encoded phosphatidate phosphatase controls the expression of CHO1-encoded phosphatidylserine synthase for membrane phospholipid synthesis. Journal of Biological Chemistry. 2017;*292*:(13230-13242. 10.1074/jbc.m117.801720.
134. Greenberg, M.L., Reiner, B., and Henry, S.A. Regulatory mutations of inositol biosynthesis in yeast: isolation of inositol-excreting mutants. Genetics. 1982;*100*:(19-33. 10.1093/genetics/100.1.19.
135. Lopes, J.M., Schulze, K.L., Yates, J.W., Hirsch, J.P., and Henry, S.A. The INO1 promoter of Saccharomyces cerevisiae includes an upstream repressor sequence (URS1) common to a diverse set of yeast genes. J Bacteriol. 1993;*175*:(4235-4238. 10.1128/jb.175.13.4235-4238.1993.
136. Schüller, H.J., Richter, K., Hoffmann, B., Ebbert, R., and Schweizer, E. DNA binding site of the yeast heteromeric Ino2p/Ino4p basic helix-loop-helix transcription factor: structural requirements as defined by saturation mutagenesis. FEBS Lett. 1995;*370*:(149-152. 10.1016/0014-5793(95)00818-t.
137. Schwank, S., Ebbert, R., Rautenstrauss, K., Schweizer, E., and Schüller, H.J. Yeast transcriptional activator INO2 interacts as an Ino2p/Ino4p basic helix-loop-helix heteromeric complex with the inositol/choline-responsive element necessary for expression of phospholipid biosynthetic genes in Saccharomyces cerevisiae. Nucleic Acids Res. 1995;*23*:(230-237. 10.1093/nar/23.2.230.
138. Wagner, C., Dietz, M., Wittmann, J., Albrecht, A., and Schüller, H.J. The negative regulator Opi1 of phospholipid biosynthesis in yeast contacts the pleiotropic repressor Sin3 and the transcriptional activator Ino2. Mol Microbiol. 2001;*41*:(155-166. 10.1046/j.1365-2958.2001.02495.x.
139. Adeyo, O., Horn, P.J., Lee, S., Binns, D.D., Chandrahas, A., Chapman, K.D., and Goodman, J.M. The yeast lipin orthologue Pah1p is important for biogenesis of lipid droplets. J Cell Biol. 2011;*192*:(1043-1055. 10.1083/jcb.201010111.
140. Han, G.S., and Carman, G.M. Yeast PAH1-encoded phosphatidate phosphatase controls the expression of CHO1-encoded phosphatidylserine synthase for membrane phospholipid synthesis. J Biol Chem. 2017;*292*:(13230-13242. 10.1074/jbc.M117.801720.
141. Irie, K., Takase, M., Araki, H., and Oshima, Y. A gene, SMP2, involved in plasmid maintenance and respiration in Saccharomyces cerevisiae encodes a highly charged protein. Mol Gen Genet. 1993;*236*:(283-288. 10.1007/bf00277124.
142. Park, Y., Han, G.S., Mileykovskaya, E., Garrett, T.A., and Carman, G.M. Altered Lipid Synthesis by Lack of Yeast Pah1 Phosphatidate Phosphatase Reduces Chronological Life Span. J Biol Chem. 2015;*290*:(25382-25394. 10.1074/jbc.M115.680314.
143. Lussier, M., White, A.-M., Sheraton, J., Di Paolo, T., Treadwell, J., Southard, S.B., Horenstein, C.I., Chen-Weiner, J., Ram, A.F.J., Kapteyn, J.C., et al. Large Scale Identification of Genes Involved in Cell Surface Biosynthesis and Architecture in Saccharomyces cerevisiae. Genetics. 1997;*147*:(435-450. 10.1093/genetics/147.2.435.
144. Ruiz, C., Cid, V.J., Lussier, M., Molina, M., and Nombela, C. A large-scale sonication assay for cell wall mutant analysis in yeast. Yeast. 1999;*15*:(1001-1008. 10.1002/(sici)1097-0061(199907)15:10b<1001::Aid-yea400>3.0.Co;2-t.

145. Park, Y., Stukey, G.J., Jog, R., Kwiatek, J.M., Han, G.S., and Carman, G.M. Mutant phosphatidate phosphatase Pah1-W637A exhibits altered phosphorylation, membrane association, and enzyme function in yeast. J Biol Chem. 2022;*298*:(101578. 10.1016/j.jbc.2022.101578.
146. Rahman, M.A., Mostofa, M.G., and Ushimaru, T. The Nem1/Spo7–Pah1/lipin axis is required for autophagy induction after TORC 1 inactivation. The FEBS Journal. 2018;*285*:(1840-1860. 10.1111/febs.14448.
147. Sasser, T., Qiu, Q.-S., Karunakaran, S., Padolina, M., Reyes, A., Flood, B., Smith, S., Gonzales, C., and Fratti, R.A. Yeast Lipin 1 Orthologue Pah1p Regulates Vacuole Homeostasis and Membrane Fusion. Journal of Biological Chemistry. 2012;*287*:(2221-2236. 10.1074/jbc.m111.317420.
148. Han, G.-S., O'Hara, L., Carman, G.M., and Siniossoglou, S. An Unconventional Diacylglycerol Kinase That Regulates Phospholipid Synthesis and Nuclear Membrane Growth. Journal of Biological Chemistry. 2008;*283*:(20433-20442. 10.1074/jbc.m802903200.
149. Han, G.-S., O'Hara, L., Siniossoglou, S., and Carman, G.M. Characterization of the Yeast DGK1-encoded CTP-dependent Diacylglycerol Kinase. Journal of Biological Chemistry. 2008;*283*:(20443-20453. 10.1074/jbc.m802866200.
150. Miner, G.E., Starr, M.L., Hurst, L.R., and Fratti, R.A. Deleting the DAG kinase Dgk1 augments yeast vacuole fusion through increased Ypt7 activity and altered membrane fluidity. Traffic. 2017;*18*:(315-329. 10.1111/tra.12479.
151. Karanasios, E., Han, G.-S., Xu, Z., Carman, G.M., and Siniossoglou, S. A phosphorylation-regulated amphipathic helix controls the membrane translocation and function of the yeast phosphatidate phosphatase. Proceedings of the National Academy of Sciences. 2010;*107*:(17539-17544. 10.1073/pnas.1007974107.
152. Siniossoglou, S. A novel complex of membrane proteins required for formation of a spherical nucleus. The EMBO Journal. 1998;*17*:(6449-6464. 10.1093/emboj/17.22.6449.
153. Choi, H.S., Su, W.M., Morgan, J.M., Han, G.S., Xu, Z., Karanasios, E., Siniossoglou, S., and Carman, G.M. Phosphorylation of phosphatidate phosphatase regulates its membrane association and physiological functions in Saccharomyces cerevisiae: identification of SER(602), THR(723), AND SER(744) as the sites phosphorylated by CDC28 (CDK1)-encoded cyclin-dependent kinase. J Biol Chem. 2011;*286*:(1486-1498. 10.1074/jbc.M110.155598.
154. Choi, H.-S., Su, W.-M., Han, G.-S., Plote, D., Xu, Z., and Carman, G.M. Pho85p-Pho80p Phosphorylation of Yeast Pah1p Phosphatidate Phosphatase Regulates Its Activity, Location, Abundance, and Function in Lipid Metabolism. Journal of Biological Chemistry. 2012;*287*:(11290-11301. 10.1074/jbc.m112.346023.
155. Khondker, S., Han, G.-S., and Carman, G.M. Protein kinase Hsl1 phosphorylates Pah1 to inhibit phosphatidate phosphatase activity and regulate lipid synthesis in Saccharomyces cerevisiae. Journal of Biological Chemistry. 2024;*300*:(10.1016/j.jbc.2024.107572.
156. Su, W.-M., Han, G.-S., Casciano, J., and Carman, G.M. Protein Kinase A-mediated Phosphorylation of Pah1p Phosphatidate Phosphatase Functions in Conjunction with the Pho85p-Pho80p and Cdc28p-Cyclin B Kinases to Regulate Lipid Synthesis in Yeast. Journal of Biological Chemistry. 2012;*287*:(33364-33376. 10.1074/jbc.m112.402339.
157. Su, W.-M., Han, G.-S., and Carman, G.M. Cross-talk Phosphorylations by Protein Kinase C and Pho85p-Pho80p Protein Kinase Regulate Pah1p Phosphatidate Phosphatase Abundance in

Saccharomyces cerevisiae*. Journal of Biological Chemistry. 2014;*289*:(18818-18830. https://doi.org/10.1074/jbc.M114.581462.
158. Su, W.-M., Han, G.-S., and Carman, G.M. Yeast Nem1-Spo7 Protein Phosphatase Activity on Pah1 Phosphatidate Phosphatase Is Specific for the Pho85-Pho80 Protein Kinase Phosphorylation Sites. Journal of Biological Chemistry. 2014;*289*:(34699-34708. 10.1074/jbc.m114.614883.
159. Xu, X., and Okamoto, K. The Nem1-Spo7 protein phosphatase complex is required for efficient mitophagy in yeast. Biochem Biophys Res Commun. 2018;*496*:(51-57. 10.1016/j.bbrc.2017.12.163.
160. Stukey, G.J., Han, G.-S., and Carman, G.M. Phosphatidate phosphatase Pah1 contains a novel RP domain that regulates its phosphorylation and function in yeast lipid synthesis. Journal of Biological Chemistry. 2023;*299*:(105025. 10.1016/j.jbc.2023.105025.
161. Karanasios, E., Barbosa, A.D., Sembongi, H., Mari, M., Han, G.-S., Reggiori, F., Carman, G.M., and Siniossoglou, S. Regulation of lipid droplet and membrane biogenesis by the acidic tail of the phosphatidate phosphatase Pah1p. Molecular Biology of the Cell. 2013;*24*:(2124-2133. 10.1091/mbc.e13-01-0021.
162. Park, Y., Han, G.S., and Carman, G.M. A conserved tryptophan within the WRDPLVDID domain of yeast Pah1 phosphatidate phosphatase is required for its in vivo function in lipid metabolism. J Biol Chem. 2017;*292*:(19580-19589. 10.1074/jbc.M117.819375.
163. Park, Y., Stukey, G.J., Jog, R., Kwiatek, J.M., Han, G.-S., and Carman, G.M. Mutant phosphatidate phosphatase Pah1-W637A exhibits altered phosphorylation, membrane association, and enzyme function in yeast. Journal of Biological Chemistry. 2022;*298*:(101578. 10.1016/j.jbc.2022.101578.
164. Hsieh, L.-S., Su, W.-M., Han, G.-S., and Carman, G.M. Phosphorylation Regulates the Ubiquitin-independent Degradation of Yeast Pah1 Phosphatidate Phosphatase by the 20S Proteasome. Journal of Biological Chemistry. 2015;*290*:(11467-11478. 10.1074/jbc.m115.648659.
165. Pascual, F., Hsieh, L.S., Soto-Cardalda, A., and Carman, G.M. Yeast Pah1p phosphatidate phosphatase is regulated by proteasome-mediated degradation. J Biol Chem. 2014;*289*:(9811-9822. 10.1074/jbc.M114.550103.
166. Kwiatek, J.M., and Carman, G.M. Yeast phosphatidic acid phosphatase Pah1 hops and scoots along the membrane phospholipid bilayer. J Lipid Res. 2020;*61*:(1232-1243. 10.1194/jlr.RA120000937.
167. Romanauska, A., and Köhler, A. The Inner Nuclear Membrane Is a Metabolically Active Territory that Generates Nuclear Lipid Droplets. Cell. 2018;*174*:(700-715.e718. 10.1016/j.cell.2018.05.047.
168. Wolinski, H., Hofbauer, H.F., Hellauer, K., Cristobal-Sarramian, A., Kolb, D., Radulovic, M., Knittelfelder, O.L., Rechberger, G.N., and Kohlwein, S.D. Seipin is involved in the regulation of phosphatidic acid metabolism at a subdomain of the nuclear envelope in yeast. Biochimica et Biophysica Acta (BBA) - Molecular and Cell Biology of Lipids. 2015;*1851*:(1450-1464. https://doi.org/10.1016/j.bbalip.2015.08.003.
169. Han, G.-S., Kwiatek, J.M., Hu, K.S., and Carman, G.M. Catalytic core function of yeast Pah1 phosphatidate phosphatase reveals structural insight into its membrane localization and activity control. Journal of Biological Chemistry. 2024;*300*:(105560. 10.1016/j.jbc.2023.105560.

170. Han, G.-S., and Carman, G.M. Characterization of the Human LPIN1-encoded Phosphatidate Phosphatase Isoforms*. Journal of Biological Chemistry. 2010;*285*:(14628-14638. https://doi.org/10.1074/jbc.M110.117747.
171. Péterfy, M., Phan, J., Xu, P., and Reue, K. Lipodystrophy in the fld mouse results from mutation of a new gene encoding a nuclear protein, lipin. Nature Genetics. 2001;*27*:(121-124. 10.1038/83685.
172. Donkor, J., Sariahmetoglu, M., Dewald, J., Brindley, D.N., and Reue, K. Three mammalian lipins act as phosphatidate phosphatases with distinct tissue expression patterns. J Biol Chem. 2007;*282*:(3450-3457. 10.1074/jbc.M610745200.
173. Valente, V., Maia, R.M., Vianna, M.C.B., and Paçó-Larson, M.L. Drosophila melanogaster lipins are tissue-regulated and developmentally regulated and present specific subcellular distributions. The FEBS Journal. 2010;*277*:(4775-4788. 10.1111/j.1742-4658.2010.07883.x.
174. Golden, A., Liu, J., and Cohen-Fix, O. Inactivation of the C. elegans lipin homolog leads to ER disorganization and to defects in the breakdown and reassembly of the nuclear envelope. Journal of Cell Science. 2009;*122*:(1970-1978. 10.1242/jcs.044743.
175. Eastmond, P.J., Quettier, A.-L., Kroon, J.T.M., Craddock, C., Adams, N., and Slabas, A.R. PHOSPHATIDIC ACID PHOSPHOHYDROLASE1 and 2 Regulate Phospholipid Synthesis at the Endoplasmic Reticulum in Arabidopsis The Plant Cell. 2010;*22*:(2796-2811. 10.1105/tpc.109.071423.
176. Langner, C.A., Birkenmeier, E.H., Ben-Zeev, O., Schotz, M.C., Sweet, H.O., Davisson, M.T., and Gordon, J.I. The fatty liver dystrophy (fld) mutation. A new mutant mouse with a developmental abnormality in triglyceride metabolism and associated tissue-specific defects in lipoprotein lipase and hepatic lipase activities. J Biol Chem. 1989;*264*:(7994-8003.
177. Langner, C.A., Birkenmeier, E.H., Roth, K.A., Bronson, R.T., and Gordon, J.I. Characterization of the peripheral neuropathy in neonatal and adult mice that are homozygous for the fatty liver dystrophy (fld) mutation. J Biol Chem. 1991;*266*:(11955-11964.
178. Harris, T.E., Huffman, T.A., Chi, A., Shabanowitz, J., Hunt, D.F., Kumar, A., and Lawrence, J.C., Jr. Insulin controls subcellular localization and multisite phosphorylation of the phosphatidic acid phosphatase, lipin 1. J Biol Chem. 2007;*282*:(277-286. 10.1074/jbc.M609537200.
179. Huffman, T.A., Mothe-Satney, I., and Lawrence, J.C., Jr. Insulin-stimulated phosphorylation of lipin mediated by the mammalian target of rapamycin. Proc Natl Acad Sci U S A. 2002;*99*:(1047-1052. 10.1073/pnas.022634399.
180. Zhang, P., and Reue, K. Lipin proteins and glycerolipid metabolism: Roles at the ER membrane and beyond. Biochimica et Biophysica Acta (BBA) - Biomembranes. 2017;*1859*:(1583-1595. https://doi.org/10.1016/j.bbamem.2017.04.007.
181. Costanzo, M., VanderSluis, B., Koch, E.N., Baryshnikova, A., Pons, C., Tan, G., Wang, W., Usaj, M., Hanchard, J., Lee, S.D., et al. A global genetic interaction network maps a wiring diagram of cellular function. Science. 2016;*353*:(10.1126/science.aaf1420.
182. Garg, A. Acquired and inherited lipodystrophies. N Engl J Med. 2004;*350*:(1220-1234. 10.1056/NEJMra025261.
183. Smyth, S., and Heron, A. Diabetes and obesity: the twin epidemics. Nat Med. 2006;*12*:(75-80. 10.1038/nm0106-75.
184. Reue, K. The lipin family: mutations and metabolism. Curr Opin Lipidol. 2009;*20*:(165-170. 10.1097/MOL.0b013e32832adee5.

185. Meijer, I.A., Sasarman, F., Maftei, C., Rossignol, E., Vanasse, M., Major, P., Mitchell, G.A., and Brunel-Guitton, C. LPIN1 deficiency with severe recurrent rhabdomyolysis and persistent elevation of creatine kinase levels due to chromosome 2 maternal isodisomy. Molecular Genetics and Metabolism Reports. 2015;*5*:(85-88. https://doi.org/10.1016/j.ymgmr.2015.10.010.
186. Zeharia, A., Shaag, A., Houtkooper, R.H., Hindi, T., de Lonlay, P., Erez, G., Hubert, L., Saada, A., de Keyzer, Y., Eshel, G., et al. Mutations in LPIN1 cause recurrent acute myoglobinuria in childhood. Am J Hum Genet. 2008;*83*:(489-494. 10.1016/j.ajhg.2008.09.002.
187. Nadra, K., de Preux Charles, A.S., Médard, J.J., Hendriks, W.T., Han, G.S., Grès, S., Carman, G.M., Saulnier-Blache, J.S., Verheijen, M.H., and Chrast, R. Phosphatidic acid mediates demyelination in Lpin1 mutant mice. Genes Dev. 2008;*22*:(1647-1661. 10.1101/gad.1638008.
188. Hancock, L.C., Behta, R.P., and Lopes, J.M. Genomic analysis of the Opi- phenotype. Genetics. 2006;*173*:(621-634. 10.1534/genetics.106.057489.
189. Salas-Santiago, B., and Lopes, J.M. Saccharomyces cerevisiae essential genes with an Opi- phenotype. G3 (Bethesda). 2014;*4*:(761-767. 10.1534/g3.113.010140.
190. Aitken, J.F., van Heusden, G.P., Temkin, M., and Dowhan, W. The gene encoding the phosphatidylinositol transfer protein is essential for cell growth. J Biol Chem. 1990;*265*:(4711-4717.
191. Shi, L., and Tu, B.P. Acetyl-CoA and the regulation of metabolism: mechanisms and consequences. Curr Opin Cell Biol. 2015;*33*:(125-131. 10.1016/j.ceb.2015.02.003.
192. Srere, P.A. (1992). The Molecular Physiology of Citrate. In Current Topics in Cellular Regulation, E.R. Stadtman, and P.B. Chock, eds. (Academic Press), pp. 261-275. https://doi.org/10.1016/B978-0-12-152833-1.50020-4.
193. Wellen, K.E., and Thompson, C.B. A two-way street: reciprocal regulation of metabolism and signalling. Nat Rev Mol Cell Biol. 2012;*13*:(270-276. 10.1038/nrm3305.
194. Eisenberg, T., Schroeder, S., Andryushkova, A., Pendl, T., Küttner, V., Bhukel, A., Mariño, G., Pietrocola, F., Harger, A., Zimmermann, A., et al. Nucleocytosolic depletion of the energy metabolite acetyl-coenzyme a stimulates autophagy and prolongs lifespan. Cell Metab. 2014;*19*:(431-444. 10.1016/j.cmet.2014.02.010.
195. McGarry, J.D., and Foster, D.W. Regulation of hepatic fatty acid oxidation and ketone body production. Annu Rev Biochem. 1980;*49*:(395-420. 10.1146/annurev.bi.49.070180.002143.
196. Hsieh, W.-C., Sutter, B.M., Ruess, H., Barnes, S.D., Malladi, V.S., and Tu, B.P. Glucose starvation induces a switch in the histone acetylome for activation of gluconeogenic and fat metabolism genes. Molecular Cell. 2022;*82*:(60-74.e65. https://doi.org/10.1016/j.molcel.2021.12.015.
197. Wakil, S.J., and Abu-Elheiga, L.A. Fatty acid metabolism: target for metabolic syndrome. J Lipid Res. 2009;*50 Suppl*:(S138-143. 10.1194/jlr.R800079-JLR200.
198. Witters, L.A., and Watts, T.D. Yeast acetyl-CoA carboxylase: in vitro phosphorylation by mammalian and yeast protein kinases. Biochem Biophys Res Commun. 1990;*169*:(369-376. 10.1016/0006-291x(90)90341-j.
199. Brownsey, R.W., Boone, A.N., Elliott, J.E., Kulpa, J.E., and Lee, W.M. Regulation of acetyl-CoA carboxylase. Biochem Soc Trans. 2006;*34*:(223-227. 10.1042/bst20060223.
200. Kim, J., Kwon, J., Kim, M., Do, J., Lee, D., and Han, H. Low-dielectric-constant polyimide aerogel composite films with low water uptake. Polymer Journal. 2016;*48*:(829-834. 10.1038/pj.2016.37.

201. Tehlivets, O., Scheuringer, K., and Kohlwein, S.D. Fatty acid synthesis and elongation in yeast. Biochimica et Biophysica Acta (BBA) - Molecular and Cell Biology of Lipids. 2007;*1771*:(255-270. https://doi.org/10.1016/j.bbalip.2006.07.004.
202. Chirala, S.S., Zhong, Q., Huang, W., and Al-Feel, W. Analysis of FAS3/ACC regulatory region of Saccharomyces cerevisiae : identification of a functional UAS INO and sequences responsible for fatty acid mediated repression. Nucleic Acids Research. 1994;*22*:(412-418. 10.1093/nar/22.3.412.
203. Carman, G.M., and Han, G.S. Regulation of phospholipid synthesis in the yeast Saccharomyces cerevisiae. Annu Rev Biochem. 2011;*80*:(859-883. 10.1146/annurev-biochem-060409-092229.
204. Woods, A., Munday, M.R., Scott, J., Yang, X., Carlson, M., and Carling, D. Yeast SNF1 is functionally related to mammalian AMP-activated protein kinase and regulates acetyl-CoA carboxylase in vivo. J Biol Chem. 1994;*269*:(19509-19515.
205. Zhang, M., Galdieri, L., and Vancura, A. The yeast AMPK homolog SNF1 regulates acetyl coenzyme A homeostasis and histone acetylation. Mol Cell Biol. 2013;*33*:(4701-4717. 10.1128/mcb.00198-13.
206. Lu, J.Y., Lin, Y.Y., Sheu, J.C., Wu, J.T., Lee, F.J., Chen, Y., Lin, M.I., Chiang, F.T., Tai, T.Y., Berger, S.L., et al. Acetylation of yeast AMPK controls intrinsic aging independently of caloric restriction. Cell. 2011;*146*:(969-979. 10.1016/j.cell.2011.07.044.
207. Fridkin, A., Penkner, A., Jantsch, V., and Gruenbaum, Y. SUN-domain and KASH-domain proteins during development, meiosis and disease. Cell Mol Life Sci. 2009;*66*:(1518-1533. 10.1007/s00018-008-8713-y.
208. Mekhail, K., and Moazed, D. The nuclear envelope in genome organization, expression and stability. Nat Rev Mol Cell Biol. 2010;*11*:(317-328. 10.1038/nrm2894.
209. Huh, W.K., Falvo, J.V., Gerke, L.C., Carroll, A.S., Howson, R.W., Weissman, J.S., and O'Shea, E.K. Global analysis of protein localization in budding yeast. Nature. 2003;*425*:(686-691. 10.1038/nature02026.
210. Lusk, C.P., Blobel, G., and King, M.C. Highway to the inner nuclear membrane: rules for the road. Nat Rev Mol Cell Biol. 2007;*8*:(414-420. 10.1038/nrm2165.
211. Akhtar, A., and Gasser, S.M. The nuclear envelope and transcriptional control. Nat Rev Genet. 2007;*8*:(507-517. 10.1038/nrg2122.
212. Bâcle, J., Groizard, L., Kumanski, S., and Moriel-Carretero, M. Nuclear envelope-remodeling events as models to assess the potential role of membranes on genome stability. FEBS Letters. 2023;*597*:(1946-1956. 10.1002/1873-3468.14688.
213. Kabachinski, G., and Schwartz, T.U. The nuclear pore complex--structure and function at a glance. J Cell Sci. 2015;*128*:(423-429. 10.1242/jcs.083246.
214. Fabre, E., and Hurt, E. Yeast genetics to dissect the nuclear pore complex and nucleocytoplasmic trafficking. Annu Rev Genet. 1997;*31*:(277-313. 10.1146/annurev.genet.31.1.277.
215. Siniossoglou, S., Wimmer, C., Rieger, M., Doye, V., Tekotte, H., Weise, C., Emig, S., Segref, A., and Hurt, E.C. A Novel Complex of Nucleoporins, Which Includes Sec13p and a Sec13p Homolog, Is Essential for Normal Nuclear Pores. Cell. 1996;*84*:(265-275. https://doi.org/10.1016/S0092-8674(00)80981-2.
216. Molenaar, I., Smitt, W.W.S., Rozijn, T.H., and Tonino, G.J.M. Biochemical and electron microscopic study of isolated yeast nuclei. Experimental Cell Research. 1970;*60*:(148-156. https://doi.org/10.1016/0014-4827(70)90500-8.

217. Shenoy, N., Kessel, R., Bhagat, T.D., Bhattacharyya, S., Yu, Y., McMahon, C., and Verma, A. Alterations in the ribosomal machinery in cancer and hematologic disorders. Journal of Hematology & Oncology. 2012;*5*:(32. 10.1186/1756-8722-5-32.
218. Oakes, M., Aris, J.P., Brockenbrough, J.S., Wai, H., Vu, L., and Nomura, M. Mutational Analysis of the Structure and Localization of the Nucleolus in the Yeast Saccharomyces cerevisiae. Journal of Cell Biology. 1998;*143*:(23-34. 10.1083/jcb.143.1.23.
219. Walters, A.D., Amoateng, K., Wang, R., Chen, J.H., McDermott, G., Larabell, C.A., Gadal, O., and Cohen-Fix, O. Nuclear envelope expansion in budding yeast is independent of cell growth and does not determine nuclear volume. Mol Biol Cell. 2019;*30*:(131-145. 10.1091/mbc.E18-04-0204.
220. Jorgensen, P., Edgington, N.P., Schneider, B.L., Rupes, I., Tyers, M., and Futcher, B. The size of the nucleus increases as yeast cells grow. Mol Biol Cell. 2007;*18*:(3523-3532. 10.1091/mbc.e06-10-0973.
221. Neumann, F.R., and Nurse, P. Nuclear size control in fission yeast. J Cell Biol. 2007;*179*:(593-600. 10.1083/jcb.200708054.
222. Campbell, J.L., Lorenz, A., Witkin, K.L., Hays, T., Loidl, J., and Cohen-Fix, O. Yeast Nuclear Envelope Subdomains with Distinct Abilities to Resist Membrane Expansion. Molecular Biology of the Cell. 2006;*17*:(1768-1778. 10.1091/mbc.e05-09-0839.
223. Musacchio, A. The Molecular Biology of Spindle Assembly Checkpoint Signaling Dynamics. Current Biology. 2015;*25*:(R1002-R1018. https://doi.org/10.1016/j.cub.2015.08.051.
224. Meseroll, R.A., and Cohen-Fix, O. The Malleable Nature of the Budding Yeast Nuclear Envelope: Flares, Fusion, and Fenestrations. Journal of Cellular Physiology. 2016;*231*:(2353-2360. 10.1002/jcp.25355.
225. Witkin, K.L., Chong, Y., Shao, S., Webster, M.T., Lahiri, S., Walters, A.D., Lee, B., Koh, J.L., Prinz, W.A., Andrews, B.J., and Cohen-Fix, O. The budding yeast nuclear envelope adjacent to the nucleolus serves as a membrane sink during mitotic delay. Curr Biol. 2012;*22*:(1128-1133. 10.1016/j.cub.2012.04.022.
226. Walters, A.D., May, C.K., Dauster, E.S., Cinquin, B.P., Smith, E.A., Robellet, X., D'Amours, D., Larabell, C.A., and Cohen-Fix, O. The yeast polo kinase Cdc5 regulates the shape of the mitotic nucleus. Curr Biol. 2014;*24*:(2861-2867. 10.1016/j.cub.2014.10.029.
227. Webster, M.T., McCaffery, J.M., and Cohen-Fix, O. Vesicle trafficking maintains nuclear shape in Saccharomyces cerevisiae during membrane proliferation. J Cell Biol. 2010;*191*:(1079-1088. 10.1083/jcb.201006083.
228. Roberts, P., Moshitch-Moshkovitz, S., Kvam, E., O'Toole, E., Winey, M., and Goldfarb, D.S. Piecemeal Microautophagy of Nucleus inSaccharomyces cerevisiae. Molecular Biology of the Cell. 2003;*14*:(129-141. 10.1091/mbc.e02-08-0483.
229. Pan, X., Roberts, P., Chen, Y., Kvam, E., Shulga, N., Huang, K., Lemmon, S., and Goldfarb, D.S. Nucleus–Vacuole Junctions in Saccharomyces cerevisiae Are Formed Through the Direct Interaction of Vac8p with Nvj1p. Molecular Biology of the Cell. 2000;*11*:(2445-2457. 10.1091/mbc.11.7.2445.
230. Krick, R., Muehe, Y., Prick, T., Bremer, S., Schlotterhose, P., Eskelinen, E.L., Millen, J., Goldfarb, D.S., and Thumm, M. Piecemeal Microautophagy of the Nucleus Requires the Core Macroautophagy Genes. Molecular Biology of the Cell. 2008;*19*:(4492-4505. 10.1091/mbc.e08-04-0363.

231. Ostrowicz, C.W., Meiringer, C.T.A., and Ungermann, C. Yeast vacuole fusion: A model system for eukaryotic endomembrane dynamics. Autophagy. 2008;*4*:(5-19. 10.4161/auto.5054.
232. Starr, M.L., and Fratti, R.A. The Participation of Regulatory Lipids in Vacuole Homotypic Fusion. Trends in Biochemical Sciences. 2019;*44*:(546-554. 10.1016/j.tibs.2018.12.003.
233. Fratti, R.A., Jun, Y., Merz, A.J., Margolis, N., and Wickner, W. Interdependent assembly of specific regulatory lipids and membrane fusion proteins into the vertex ring domain of docked vacuoles. Journal of Cell Biology. 2004;*167*:(1087-1098. 10.1083/jcb.200409068.
234. Mima, J., Hickey, C.M., Xu, H., Jun, Y., and Wickner, W. Reconstituted membrane fusion requires regulatory lipids, SNAREs and synergistic SNARE chaperones. The EMBO Journal. 2008;*27*:(2031-2042. 10.1038/emboj.2008.139.
235. Mima, J., and Wickner, W. Complex Lipid Requirements for SNARE- and SNARE Chaperone-dependent Membrane Fusion. Journal of Biological Chemistry. 2009;*284*:(27114-27122. 10.1074/jbc.m109.010223.
236. Lawrence, G., Brown, C.C., Flood, B.A., Karunakaran, S., Cabrera, M., Nordmann, M., Ungermann, C., and Fratti, R.A. Dynamic association of the PI3P-interacting Mon1-Ccz1 GEF with vacuoles is controlled through its phosphorylation by the type 1 casein kinase Yck3. Molecular Biology of the Cell. 2014;*25*:(1608-1619. 10.1091/mbc.e13-08-0460.
237. Poteryaev, D., Datta, S., Ackema, K., Zerial, M., and Spang, A. Identification of the Switch in Early-to-Late Endosome Transition. Cell. 2010;*141*:(497-508. 10.1016/j.cell.2010.03.011.
238. Sherr, G.L., LaMassa, N., Li, E., Phillips, G., and Shen, C.-H. Pah1p negatively regulates the expression of V-ATPase genes as well as vacuolar acidification. Biochemical and Biophysical Research Communications. 2017;*491*:(693-700. https://doi.org/10.1016/j.bbrc.2017.07.127.
239. Manifava, M., Thuring, J.W.J.F., Lim, Z.-Y., Packman, L., Holmes, A.B., and Ktistakis, N.T. Differential Binding of Traffic-related Proteins to Phosphatidic Acid- or Phosphatidylinositol (4,5)- Bisphosphate-coupled Affinity Reagents. Journal of Biological Chemistry. 2001;*276*:(8987-8994. 10.1074/jbc.m010308200.
240. Miner, G.E., Starr, M.L., Hurst, L.R., Sparks, R.P., Padolina, M., and Fratti, R.A. The Central Polybasic Region of the Soluble SNARE (Soluble N-Ethylmaleimide-sensitive Factor Attachment Protein Receptor) Vam7 Affects Binding to Phosphatidylinositol 3-Phosphate by the PX (Phox Homology) Domain. Journal of Biological Chemistry. 2016;*291*:(17651-17663. 10.1074/jbc.m116.725366.
241. Hönscher, C., and Ungermann, C. A close-up view of membrane contact sites between the endoplasmic reticulum and the endolysosomal system: from yeast to man. Crit Rev Biochem Mol Biol. 2014;*49*:(262-268. 10.3109/10409238.2013.875512.
242. Eden, E.R. The formation and function of ER-endosome membrane contact sites. Biochim Biophys Acta. 2016;*1861*:(874-879. 10.1016/j.bbalip.2016.01.020.
243. Millen, J.I., Pierson, J., Kvam, E., Olsen, L.J., and Goldfarb, D.S. The luminal N-terminus of yeast Nvj1 is an inner nuclear membrane anchor. Traffic. 2008;*9*:(1653-1664. 10.1111/j.1600-0854.2008.00789.x.
244. Jeong, H., Park, J., Kim, H.I., Lee, M., Ko, Y.J., Lee, S., Jun, Y., and Lee, C. Mechanistic insight into the nucleus-vacuole junction based on the Vac8p-Nvj1p crystal structure. Proc Natl Acad Sci U S A. 2017;*114*:(E4539-e4548. 10.1073/pnas.1701030114.
245. Levine, T.P., and Munro, S. Dual targeting of Osh1p, a yeast homologue of oxysterol-binding protein, to both the Golgi and the nucleus-vacuole junction. Mol Biol Cell. 2001;*12*:(1633-1644. 10.1091/mbc.12.6.1633.

246. Kvam, E., and Goldfarb, D.S. Nvj1p is the outer-nuclear-membrane receptor for oxysterol-binding protein homolog Osh1p in Saccharomyces cerevisiae. J Cell Sci. 2004;*117*:(4959-4968. 10.1242/jcs.01372.
247. Kohlwein, S.D., Eder, S., Oh, C.S., Martin, C.E., Gable, K., Bacikova, D., and Dunn, T. Tsc13p is required for fatty acid elongation and localizes to a novel structure at the nuclear-vacuolar interface in Saccharomyces cerevisiae. Mol Cell Biol. 2001;*21*:(109-125. 10.1128/mcb.21.1.109-125.2001.
248. Kvam, E., Gable, K., Dunn, T.M., and Goldfarb, D.S. Targeting of Tsc13p to nucleus-vacuole junctions: a role for very-long-chain fatty acids in the biogenesis of microautophagic vesicles. Mol Biol Cell. 2005;*16*:(3987-3998. 10.1091/mbc.e05-04-0290.
249. Hariri, H., Rogers, S., Ugrankar, R., Liu, Y.L., Feathers, J.R., and Henne, W.M. Lipid droplet biogenesis is spatially coordinated at <scp>ER</scp> –vacuole contacts under nutritional stress. EMBO reports. 2018;*19*:(57-72. 10.15252/embr.201744815.
250. Kvam, E., and Goldfarb, D.S. Nucleus–vacuole junctions in yeast: anatomy of a membrane contact site. Biochemical Society Transactions. 2006;*34*:(340-342. 10.1042/BST0340340.
251. Wood, N.E., Kositangool, P., Hariri, H., Marchand, A.J., and Henne, W.M. Nutrient Signaling, Stress Response, and Inter-organelle Communication Are Non-canonical Determinants of Cell Fate. Cell Rep. 2020;*33*:(108446. 10.1016/j.celrep.2020.108446.
252. Hariri, H., Rogers, S., Ugrankar, R., Liu, Y.L., Feathers, J.R., and Henne, W.M. Lipid droplet biogenesis is spatially coordinated at ER-vacuole contacts under nutritional stress. EMBO Rep. 2018;*19*:(57-72. 10.15252/embr.201744815.
253. Wang, C.W., Miao, Y.H., and Chang, Y.S. A sterol-enriched vacuolar microdomain mediates stationary phase lipophagy in budding yeast. J Cell Biol. 2014;*206*:(357-366. 10.1083/jcb.201404115.
254. Kohler, V., and Büttner, S. Remodelling of Nucleus-Vacuole Junctions During Metabolic and Proteostatic Stress. Contact. 2021;*4*:(25152564211016608. 10.1177/25152564211016608.
255. Manik, M.K., Yang, H., Tong, J., and Im, Y.J. Structure of Yeast OSBP-Related Protein Osh1 Reveals Key Determinants for Lipid Transport and Protein Targeting at the Nucleus-Vacuole Junction. Structure. 2017;*25*:(617-629.e613. 10.1016/j.str.2017.02.010.
256. Liu, L.-K., Choudhary, V., Toulmay, A., and Prinz, W.A. An inducible ER–Golgi tether facilitates ceramide transport to alleviate lipotoxicity. Journal of Cell Biology. 2017;*216*:(131-147. 10.1083/jcb.201606059.
257. Hariri, H., Ugrankar, R., Liu, Y., and Henne, W.M. Inter-organelle ER-endolysosomal contact sites in metabolism and disease across evolution. Commun Integr Biol. 2016;*9*:(e1156278. 10.1080/19420889.2016.1156278.
258. Elbaz-Alon, Y., Eisenberg-Bord, M., Shinder, V., Stiller, S.B., Shimoni, E., Wiedemann, N., Geiger, T., and Schuldiner, M. Lam6 Regulates the Extent of Contacts between Organelles. Cell Rep. 2015;*12*:(7-14. 10.1016/j.celrep.2015.06.022.
259. Murley, A., Sarsam, R.D., Toulmay, A., Yamada, J., Prinz, W.A., and Nunnari, J. Ltc1 is an ER-localized sterol transporter and a component of ER-mitochondria and ER-vacuole contacts. J Cell Biol. 2015;*209*:(539-548. 10.1083/jcb.201502033.
260. Bean, B.D.M., Dziurdzik, S.K., Kolehmainen, K.L., Fowler, C.M.S., Kwong, W.K., Grad, L.I., Davey, M., Schluter, C., and Conibear, E. Competitive organelle-specific adaptors recruit Vps13 to membrane contact sites. J Cell Biol. 2018;*217*:(3593-3607. 10.1083/jcb.201804111.

261. Lang, A.B., John Peter, A.T., Walter, P., and Kornmann, B. ER-mitochondrial junctions can be bypassed by dominant mutations in the endosomal protein Vps13. J Cell Biol. 2015;*210*:(883-890. 10.1083/jcb.201502105.
262. Tosal-Castano, S., Peselj, C., Kohler, V., Habernig, L., Berglund, L.L., Ebrahimi, M., Vögtle, F.N., Höög, J., Andréasson, C., and Büttner, S. Snd3 controls nucleus-vacuole junctions in response to glucose signaling. Cell Rep. 2021;*34*:(108637. 10.1016/j.celrep.2020.108637.
263. Kvam, E., and Goldfarb, D.S. Nucleus-vacuole junctions and piecemeal microautophagy of the nucleus in S. cerevisiae. Autophagy. 2007;*3*:(85-92. 10.4161/auto.3586.
264. Ji, L., Zhao, L., Xu, K., Gao, H., Zhou, Y., Kornberg, R.D., and Zhang, H. Structure of the NuA4 histone acetyltransferase complex. Proc Natl Acad Sci U S A. 2022;*119*:(e2214313119. 10.1073/pnas.2214313119.
265. Pascual, F., Soto-Cardalda, A., and Carman, G.M. PAH1-encoded Phosphatidate Phosphatase Plays a Role in the Growth Phase- and Inositol-mediated Regulation of Lipid Synthesis in Saccharomyces cerevisiae. Journal of Biological Chemistry. 2013;*288*:(35781-35792. 10.1074/jbc.m113.525766.
266. Longtine, M.S., McKenzie, A., 3rd, Demarini, D.J., Shah, N.G., Wach, A., Brachat, A., Philippsen, P., and Pringle, J.R. Additional modules for versatile and economical PCR-based gene deletion and modification in Saccharomyces cerevisiae. Yeast. 1998;*14*:(953-961. 10.1002/(SICI)1097-0061(199807)14:10<953::AID-YEA293>3.0.CO;2-U.
267. Dicarlo, J.E., Norville, J.E., Mali, P., Rios, X., Aach, J., and Church, G.M. Genome engineering in Saccharomyces cerevisiae using CRISPR-Cas systems. Nucleic Acids Research. 2013;*41*:(4336-4343. 10.1093/nar/gkt135.
268. Li, Z., Vizeacoumar, F.J., Bahr, S., Li, J., Warringer, J., Vizeacoumar, F.S., Min, R., Vandersluis, B., Bellay, J., Devit, M., et al. Systematic exploration of essential yeast gene function with temperature-sensitive mutants. Nature Biotechnology. 2011;*29*:(361-367. 10.1038/nbt.1832.
269. Galarneau, L., Nourani, A., Boudreault, A.A., Zhang, Y., Héliot, L., Allard, S., Savard, J., Lane, W.S., Stillman, D.J., and Côté, J. Multiple Links between the NuA4 Histone Acetyltransferase Complex and Epigenetic Control of Transcription. Molecular Cell. 2000;*5*:(927-937. 10.1016/s1097-2765(00)80258-0.
270. Hashemi, H.F., and Goodman, J.M. The life cycle of lipid droplets. Current Opinion in Cell Biology. 2015;*33*:(119-124. 10.1016/j.ceb.2015.02.002.
271. Miller, K.E., Kim, Y., Huh, W.-K., and Park, H.-O. Bimolecular Fluorescence Complementation (BiFC) Analysis: Advances and Recent Applications for Genome-Wide Interaction Studies. Journal of Molecular Biology. 2015;*427*:(2039-2055. 10.1016/j.jmb.2015.03.005.
272. Mijaljica, D., Prescott, M., and Devenish, R.J. The intricacy of nuclear membrane dynamics during nucleophagy. Nucleus. 2010;*1*:(213-223. 10.4161/nucl.1.3.11738.
273. Tamura, Y., Kawano, S., and Endo, T. Organelle contact zones as sites for lipid transfer. The Journal of Biochemistry. 2019;*165*:(115-123. 10.1093/jb/mvy088.
274. Toulmay, A., and Prinz, W.A. A conserved membrane-binding domain targets proteins to organelle contact sites. Journal of Cell Science. 2012;*125*:(49-58. 10.1242/jcs.085118.
275. Millen, J.I., Krick, R., Prick, T., Thumm, M., and Goldfarb, D.S. Measuring piecemeal microautophagy of the nucleus inSaccharomyces cerevisiae. Autophagy. 2009;*5*:(75-81. 10.4161/auto.5.1.7181.

276. Rosado, C., Mijaljica, D., Hatzinisiriou, I., Prescott, M., and Devenish, R.J. Rosella: A fluorescent pH-biosensor for reporting vacuolar turnover of cytosol and organelles in yeast. Autophagy. 2008;*4*:(205-213. 10.4161/auto.5331.
277. Wang, X., and Hayes, J.J. Acetylation Mimics within Individual Core Histone Tail Domains Indicate Distinct Roles in Regulating the Stability of Higher-Order Chromatin Structure. Molecular and Cellular Biology. 2008;*28*:(227-236. 10.1128/mcb.01245-07.
278. Krick, R., Mühe, Y., Prick, T., Bredschneider, M., Bremer, S., Wenzel, D., Eskelinen, E.-L., and Thumm, M. Piecemeal microautophagy of the nucleus: Genetic and morphological traits. Autophagy. 2009;*5*:(270-272. 10.4161/auto.5.2.7639.
279. Tang, F., Peng, Y., Nau, J.J., Kauffman, E.J., and Weisman, L.S. Vac8p, an Armadillo Repeat Protein, Coordinates Vacuole Inheritance With Multiple Vacuolar Processes. Traffic. 2006;*7*:(1368-1377. 10.1111/j.1600-0854.2006.00458.x.
280. Mameri, A., and Côté, J. JAZF1: A metabolic actor subunit of the NuA4/TIP60 chromatin modifying complex. Frontiers in Cell and Developmental Biology. 2023;*11*:(10.3389/fcell.2023.1134268.
281. Yang, P., Xu, C., Reece, E.A., Chen, X., Zhong, J., Zhan, M., Stumpo, D.J., Blackshear, P.J., and Yang, P. Tip60- and sirtuin 2-regulated MARCKS acetylation and phosphorylation are required for diabetic embryopathy. Nature Communications. 2019;*10*:(282. 10.1038/s41467-018-08268-6.
282. Nordentoft, I., Jeppesen, P.B., Nielsen, A.L., Jorgensen, P., and Hermansen, K. Expression Analysis of cPLA2 Alpha Interacting TIP60 in Diabetic KKAy and Non-Diabetic C57BL Wild-Type Mice: No Impact of Transient and Stable TIP60 Overexpression on Glucose-Stimulated Insulin Secretion in Pancreatic Beta-Cells. Rev Diabet Stud. 2007;*4*:(147-158. 10.1900/rds.2007.4.147.
283. Fang, Z., Weng, C., Li, H., Tao, R., Mai, W., Liu, X., Lu, L., Lai, S., Duan, Q., Alvarez, C., et al. Single-Cell Heterogeneity Analysis and CRISPR Screen Identify Key β-Cell-Specific Disease Genes. Cell Rep. 2019;*26*:(3132-3144.e3137. 10.1016/j.celrep.2019.02.043.
284. Simha, V., and Garg, A. Phenotypic heterogeneity in body fat distribution in patients with congenital generalized lipodystrophy caused by mutations in the AGPAT2 or seipin genes. J Clin Endocrinol Metab. 2003;*88*:(5433-5437. 10.1210/jc.2003-030835.
285. Alzheimer, A., Stelzmann, R.A., Schnitzlein, H.N., and Murtagh, F.R. An English translation of Alzheimer's 1907 paper, "Uber eine eigenartige Erkankung der Hirnrinde". Clin Anat. 1995;*8*:(429-431. 10.1002/ca.980080612.
286. Moulton, M.J., Barish, S., Ralhan, I., Chang, J., Goodman, L.D., Harland, J.G., Marcogliese, P.C., Johansson, J.O., Ioannou, M.S., and Bellen, H.J. Neuronal ROS-induced glial lipid droplet formation is altered by loss of Alzheimer's disease-associated genes. Proc Natl Acad Sci U S A. 2021;*118*:(10.1073/pnas.2112095118.
287. Yamazaki, Y., Zhao, N., Caulfield, T.R., Liu, C.C., and Bu, G. Apolipoprotein E and Alzheimer disease: pathobiology and targeting strategies. Nat Rev Neurol. 2019;*15*:(501-518. 10.1038/s41582-019-0228-7.
288. Goldberg, I.J., Reue, K., Abumrad, N.A., Bickel, P.E., Cohen, S., Fisher, E.A., Galis, Z.S., Granneman, J.G., Lewandowski, E.D., Murphy, R., et al. Deciphering the Role of Lipid Droplets in Cardiovascular Disease: A Report From the 2017 National Heart, Lung, and Blood Institute Workshop. Circulation. 2018;*138*:(305-315. 10.1161/circulationaha.118.033704.

289. Anderson, E.J., Kypson, A.P., Rodriguez, E., Anderson, C.A., Lehr, E.J., and Neufer, P.D. Substrate-specific derangements in mitochondrial metabolism and redox balance in the atrium of the type 2 diabetic human heart. J Am Coll Cardiol. 2009;*54*:(1891-1898. 10.1016/j.jacc.2009.07.031.
290. Glass, C.K., and Witztum, J.L. Atherosclerosis. the road ahead. Cell. 2001;*104*:(503-516. 10.1016/s0092-8674(01)00238-0.
291. Cruz, A.L.S., Barreto, E.A., Fazolini, N.P.B., Viola, J.P.B., and Bozza, P.T. Lipid droplets: platforms with multiple functions in cancer hallmarks. Cell Death Dis. 2020;*11*:(105. 10.1038/s41419-020-2297-3.
292. Tirinato, L., Marafioti, M.G., Pagliari, F., Jansen, J., Aversa, I., Hanley, R., Nisticò, C., Garcia-Calderón, D., Genard, G., Guerreiro, J.F., et al. Lipid droplets and ferritin heavy chain: a devilish liaison in human cancer cell radioresistance. Elife. 2021;*10*:(10.7554/eLife.72943.
293. Singh, I., and Lele, T.P. Nuclear Morphological Abnormalities in Cancer: A Search for Unifying Mechanisms. Results Probl Cell Differ. 2022;*70*:(443-467. 10.1007/978-3-031-06573-6_16.
294. Shibahara, D., Akanuma, N., Kobayashi, I.S., Heo, E., Ando, M., Fujii, M., Jiang, F., Prin, P.N., Pan, G., Wong, K.K., et al. TIP60 is required for tumorigenesis in non-small cell lung cancer. Cancer Science. 2023;*114*:(2400-2413. 10.1111/cas.15785.
295. McGuire, A., Casey, M.C., Shalaby, A., Kalinina, O., Curran, C., Webber, M., Callagy, G., Holian, E., Bourke, E., Kerin, M.J., and Brown, J.A.L. Quantifying Tip60 (Kat5) stratifies breast cancer. Scientific Reports. 2019;*9*:(3819. 10.1038/s41598-019-40221-5.
296. Hong, Y.J., Park, J., Hahm, J.Y., Kim, S.H., Lee, D.H., Park, K.S., and Seo, S.B. Regulation of UHRF1 acetylation by TIP60 is important for colon cancer cell proliferation. Genes Genomics. 2022;*44*:(1353-1361. 10.1007/s13258-022-01298-x.
297. Judes, G., Rifaï, K., Ngollo, M., Daures, M., Bignon, Y.J., Penault-Llorca, F., and Bernard-Gallon, D. A bivalent role of TIP60 histone acetyl transferase in human cancer. Epigenomics. 2015;*7*:(1351-1363. 10.2217/epi.15.76.
298. Zhao, L.J., Loewenstein, P.M., and Green, M. Enhanced MYC association with the NuA4 histone acetyltransferase complex mediated by the adenovirus E1A N-terminal domain activates a subset of MYC target genes highly expressed in cancer cells. Genes Cancer. 2017;*8*:(752-761. 10.18632/genesandcancer.160.
299. Sekiguchi, M., and Matsushita, N. DNA Damage Response Regulation by Histone Ubiquitination. Int J Mol Sci. 2022;*23*:(10.3390/ijms23158187.
300. Deshpande, R.A., Myler, L.R., Soniat, M.M., Makharashvili, N., Lee, L., Lees-Miller, S.P., Finkelstein, I.J., and Paull, T.T. DNA-dependent protein kinase promotes DNA end processing by MRN and CtIP. Science Advances. 2020;*6*:(eaay0922. doi:10.1126/sciadv.aay0922.
301. Lashgari, A., Kougnassoukou Tchara, P.-E., Lambert, J.-P., and Côté, J. New insights into the DNA repair pathway choice with NuA4/TIP60. DNA repair. 2022;*113*:(103315. 10.1016/j.dnarep.2022.103315.
302. Schneiter, R., Hitomi, M., Ivessa, A.S., Fasch, E.-V., Kohlwein, S.D., and Tartakoff, A.M. A Yeast Acetyl Coenzyme A Carboxylase Mutant Links Very-Long-Chain Fatty Acid Synthesis to the Structure and Function of the Nuclear Membrane-Pore Complex. Molecular and Cellular Biology. 1996;*16*:(7161-7172. 10.1128/mcb.16.12.7161.
303. Mijaljica, D., Prescott, M., and Devenish, R.J. A Late Form of Nucleophagy in Saccharomyces cerevisiae. PLOS ONE. 2012;*7*:(e40013. 10.1371/journal.pone.0040013.

304. Noda, N.N., and Fujioka, Y. Atg1 family kinases in autophagy initiation. Cell Mol Life Sci. 2015;*72*:(3083-3096. 10.1007/s00018-015-1917-z.
305. Rahman, M.A., Kumar, R., Sanchez, E., and Nazarko, T.Y. Lipid Droplets and Their Autophagic Turnover via the Raft-Like Vacuolar Microdomains. Int J Mol Sci. 2021;*22*:(10.3390/ijms22158144.
306. Fairman, G., and Ouimet, M. Lipophagy pathways in yeast are controlled by their distinct modes of induction. Yeast. 2022;*39*:(429-439. 10.1002/yea.3705.
307. Barbosa, A.D., and Siniossoglou, S. Spatial distribution of lipid droplets during starvation: Implications for lipophagy. Communicative & Integrative Biology. 2016;*9*:(e1183854. 10.1080/19420889.2016.1183854.
308. Maeda, Y., Oku, M., and Sakai, Y. A defect of the vacuolar putative lipase Atg15 accelerates degradation of lipid droplets through lipolysis. Autophagy. 2015;*11*:(1247-1258. 10.1080/15548627.2015.1056969.
309. Lu, P.Y.T., Kirlin, A.C., Aristizabal, M.J., Brewis, H.T., Lévesque, N., Setiaputra, D.T., Avvakumov, N., Benschop, J.J., Groot Koerkamp, M., Holstege, F.C.P., et al. A balancing act: interactions within NuA4/TIP60 regulate picNuA4 function in Saccharomyces cerevisiae and humans. Genetics. 2022;*222*:(10.1093/genetics/iyac136.
310. Xiao, H., Chung, J., Kao, H.-Y., and Yang, Y.-C. Tip60 Is a Co-repressor for STAT3*. Journal of Biological Chemistry. 2003;*278*:(11197-11204. https://doi.org/10.1074/jbc.M210816200.
311. Sliva, D., Zhu, Y.X., Tsai, S., Kamine, J., and Yang, Y.C. Tip60 interacts with human interleukin-9 receptor alpha-chain. Biochem Biophys Res Commun. 1999;*263*:(149-155. 10.1006/bbrc.1999.1083.
312. Sapountzi, V., Logan, I.R., and Robson, C.N. Cellular functions of TIP60. The International Journal of Biochemistry & Cell Biology. 2006;*38*:(1496-1509. https://doi.org/10.1016/j.biocel.2006.03.003.

Appendices

Appendix A: Supplemental Figures and Tables from Manuscript #1

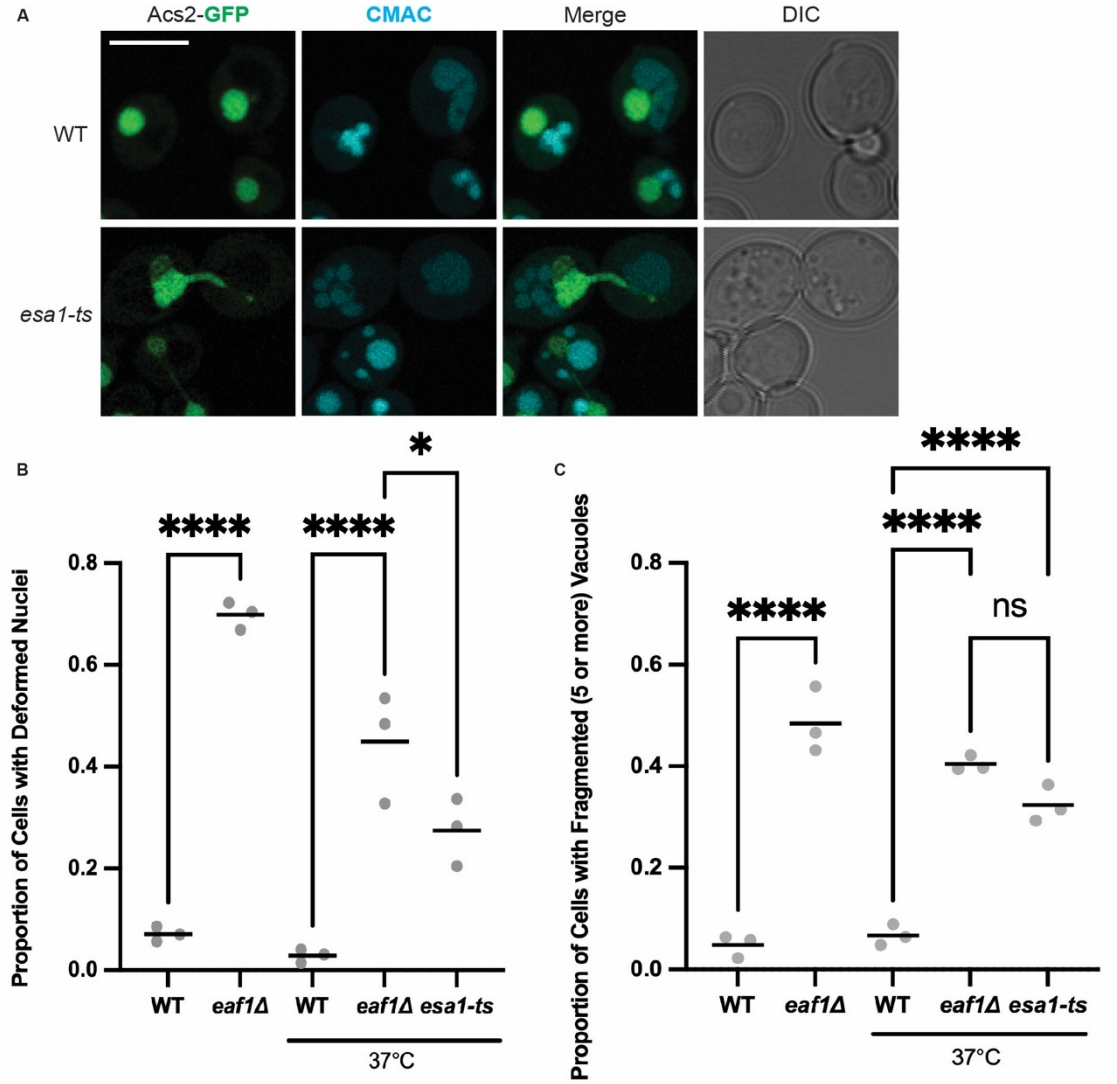

Supplemental Figure 2.1: Nuclear deformation and vacuole fragmentation in temperature sensitive *ESA1* mutants. (A) Single sliced Z-stack image showing the nucleus, marked by Acs2-GFP, and vacuoles, stained by CMAC, in WT (YKB 4972) and *esa1-ts* mutant (YKB 5125). Scale bar = 5 μm (B) Graphic representing the proportion of total cells with nuclear deformation that were quantified via visual analysis of the cells. (C) Graphic representing the proportion of total cells with fragmented vacuoles (i.e. having 5 or more vacuolar lobes) that were quantified through counting the number of vacuoles per cell. Analysis for B and C was repeated for three biological replicates, counting at least 100 cells for each. Grey and purple dots represent three biological replicates and horizontal bars represent the mean. Data for WT and *eaf1Δ* is repeated from Figure 2.1 for comparison with *esa1-ts* mutant. ANOVA analysis was performed using Tukey's multiple comparison test. *$p \leq 0.05$, ****$p < 0.0001$. ns = not significant, $p > 0.05$. Relevant statistical significance bars are shown, additional comparisons can be found in Supplemental Table 2.1.

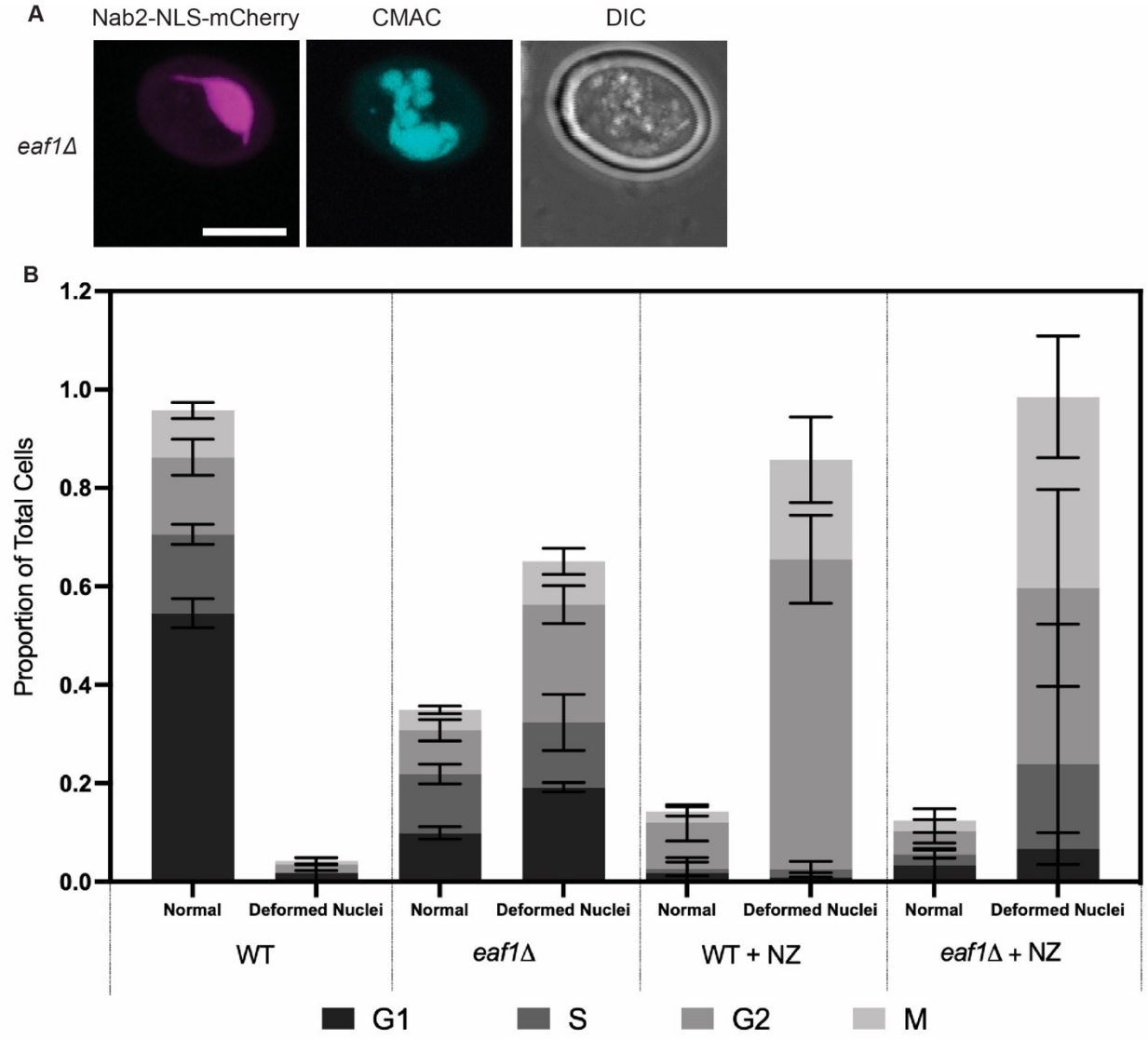

Supplemental Figure 2.2: Nuclear deformation in *eaf1*Δ occurs in all stages of the yeast cell cycle. (A) *eaf1*Δ cell (YKB 5187) is shown with Nab2-NLS-mCherry to visualize the nucleus and CMAC staining the vacuole. Cells were grown in SC-URA to maintain the Nab2-NLS-mCherry plasmid. This shows an example of nuclear deformations in *eaf1*Δ that occur in the G1 stage of the yeast cells cycle**. (B)** WT and *eaf1*Δ cells expressing *ACS2-GFP*, *NUP49-RFP* (YKB 4972 and YKB 4863) were grown to log phase in YPD or YPD + 15 µg/ml nocodazole (NZ) for three hours to initiate mitotic arrest. The proportion of total cells with normal or deformed nuclei were quantified for each cell cycle stage, which was determined by analyzing bud morphology. The analysis was repeated for three biological replicates, counting at least 100 cells for each. Error bars represent standard deviation. Each shade of grey in the bar represents a stage of the cell cycle as indicated in the legend.

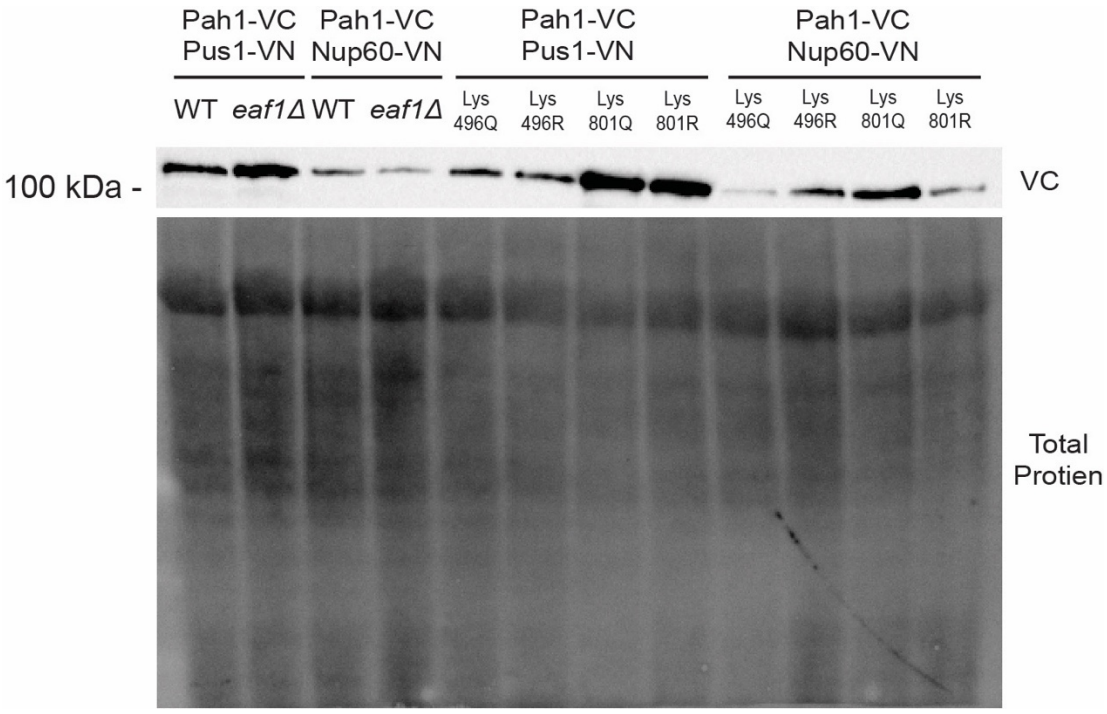

Supplemental Figure 2.3: Expression of Pah1-VC constructs used in BiFC assays. WT (YKB 1079) strains containing Pah1-VC, *Pah1-K496Q-VC*, *Pah1-K496R-VC*, *Pah1-K801Q-VC*, or *Pah1-K801R-VC* plasmids, in combination with Nup60-VN and Pus1-VN (YKB 4975 – YKB 4978, and YKB 5206 – YKB 5213) were analyzed via immunoblot of whole cell extracts with anti-GFP antibody (capable of detecting Venus fragment VC). Total protein is shown below via TGX blot activation.

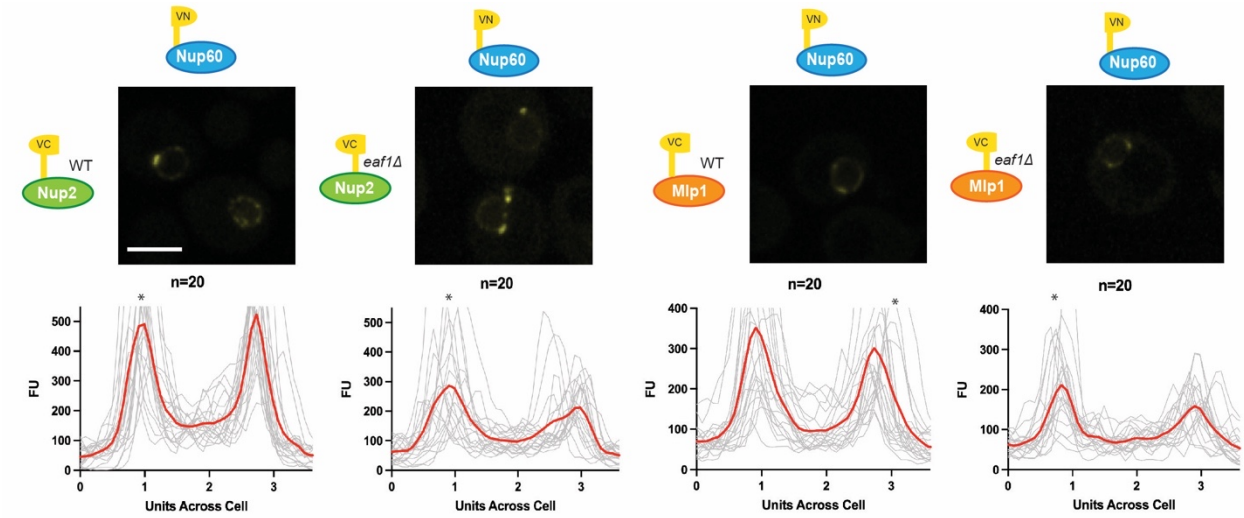

Supplemental Figure 2.4: Pah1-VC interacts with Nup2-VC and Mlp1-VC in both WT and *eaf1*Δ. BiFC experiment with WT or *eaf1*Δ cells expressing Nup60-VN with either Nup2-VC (YKB 5214 and YKB 5215) or Mlp1-VC (YKB 5216 and YKB 5217). Scale bar = 5 μm. Line graphs were generated by measuring the fluorescence intensity value of pixels across the nucleus of the cell, using Plot Profile in ImageJ software. Red lines indicate the average for the indicated number of cells, and the grey lines show each cell profile. n = the number of randomly selected cells. FU = Fluorescence Units. * Indicates that that y-axis has been cropped for easy comparison of strains.

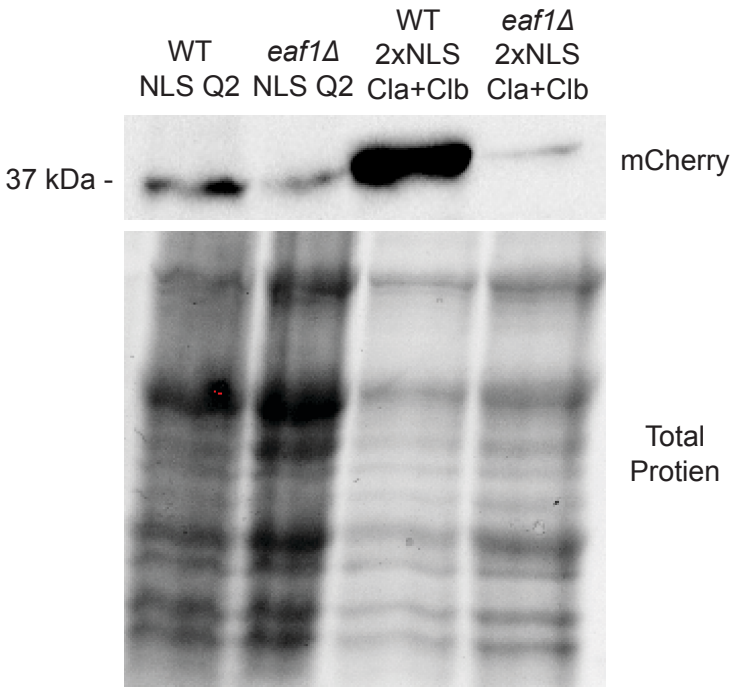

Supplemental Figure 2.5: Expression of NLS Q2 and 2xNLS Cla+Clb-mCherry constructs. WT and *eaf1*Δ strains containing NLS Q2 (YKB 5182 and YKB 5183) and 2xNLS Cla+Clb-mCherry (YKB 5184 and YKB 5185) were analyzed via immunoblot of whole cell extracts with an anti-mCherry antibody. Total protein is shown below via TGX gel activation.

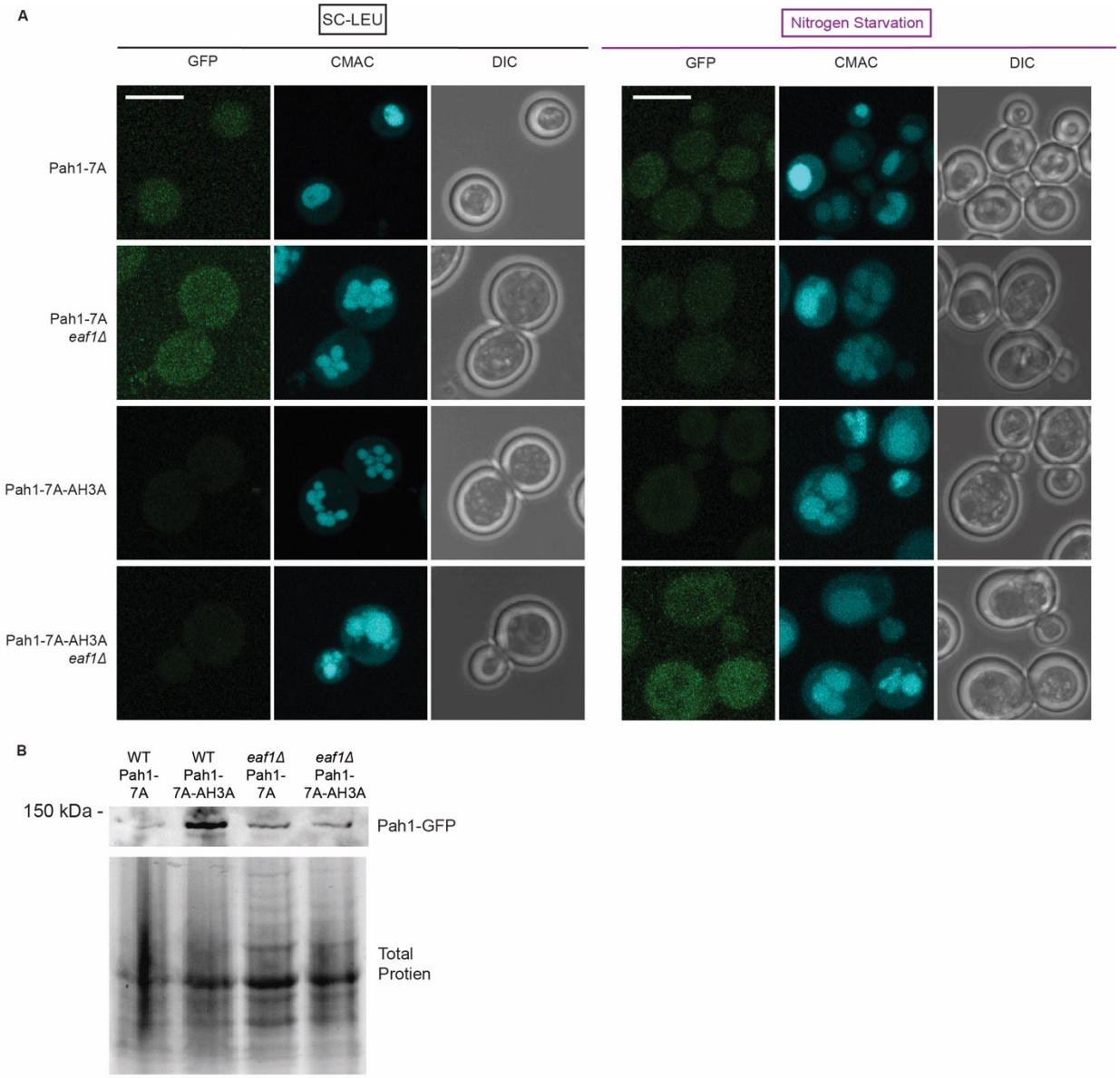

Supplemental Figure 2.6: Pah1-7A and Pah1-7A-AH3A-GFP localization in WT and *eaf1*Δ cells. (A) Merged Z-stack images of WT (YKB 5194 and YKB 5196) and *eaf1*Δ (YKB 5195 and YKB 5197) expressing Pah1-7A-GFP or Pah1-7A-AH3A-GFP. Vacuoles were stained with CMAC. Cells were grown in SC-Leu media or switched to nitrogen starvation (NS) media for four hours. (B) Western blot analysis of whole cell extracts to detect Pah1-7A-GFP and Pah1-7A-AH3A-GFP in both WT and *eaf1*Δ strains. Total protein is shown below via TGX gel activation.

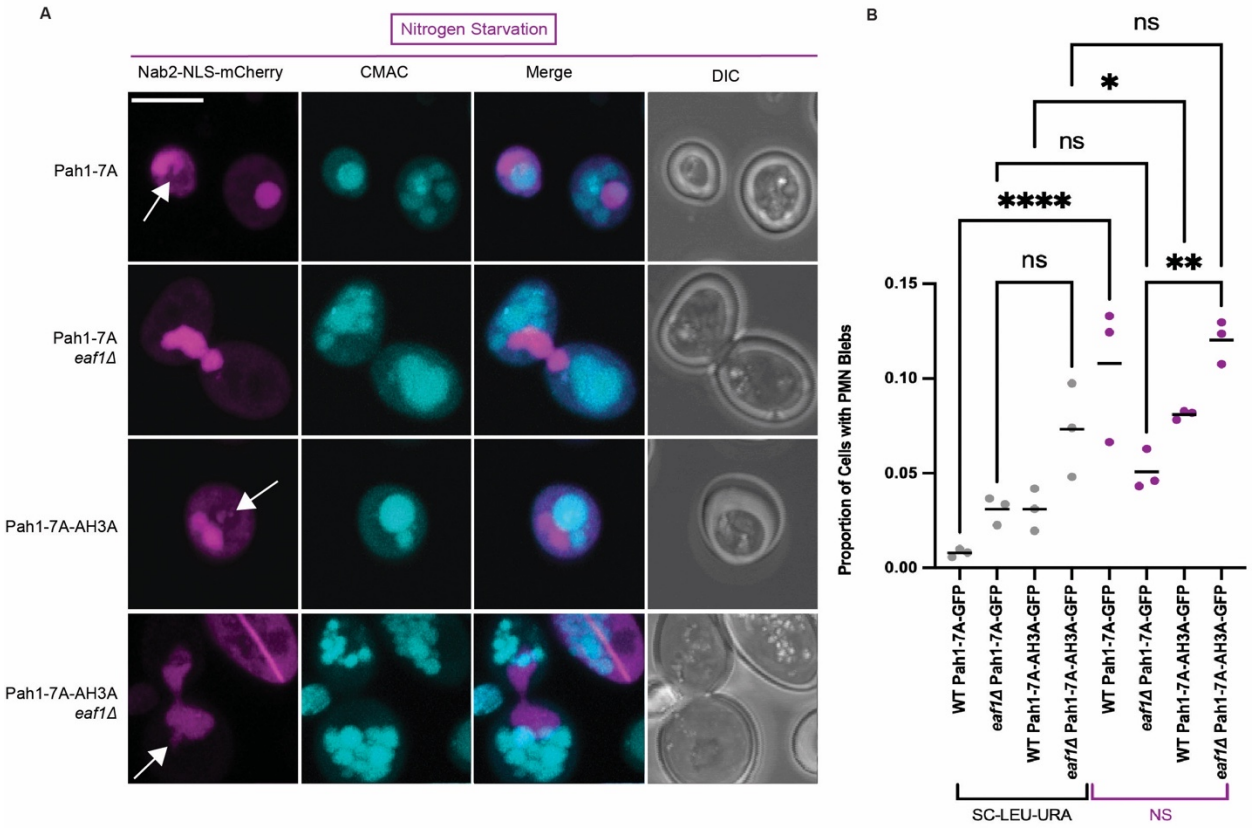

Supplemental Figure 2.7: Pah1-7A-GFP expression does not rescue PMN dysfunction in *eaf1*Δ cells. (A) Merged Z-stack images showing WT and *eaf1*Δ Pah1-7A-GFP (YKB 5198 and YKB 5199) as well as WT and *eaf1*Δ Pah1-7A-AH3A-GFP with Nab2-NLS-mCherry (YKB 5200 and YKB 5201) to visualize the nucleus, and the vacuole stained with CMAC. Cells were grown in nutrient rich media to log phase and then switched to NS for four hours. Merged Z-stack images show the formation of PMN structures after four hours of nitrogen starvation. (B) Quantification of the proportion of cells with PMN blebs. Cells were grown in SC-Leu-Ura media then switched to nitrogen starvation (NS) media for four hours. If there was a clear portion of Nab2-NLS-mCherry that entered the vacuole (CMAC), a cell was counted as having PMN. For B, an ANOVA analysis was performed using Tukey's multiple comparison test. Cells were counted by investigating the full Z-stack of cells which was repeated for three biological replicates, counting at least 100 cells for each. Each biological replicate is represented by a gray or purple dot. Horizontal bars represent the mean. *$p \leq 0.05$, **$p \leq 0.01$, ****$p < 0.0001$, ns = not significant, $p > 0.05$. Relevant statistical significance bars are shown, additional comparisons can be found in Supplemental Table 2.1.

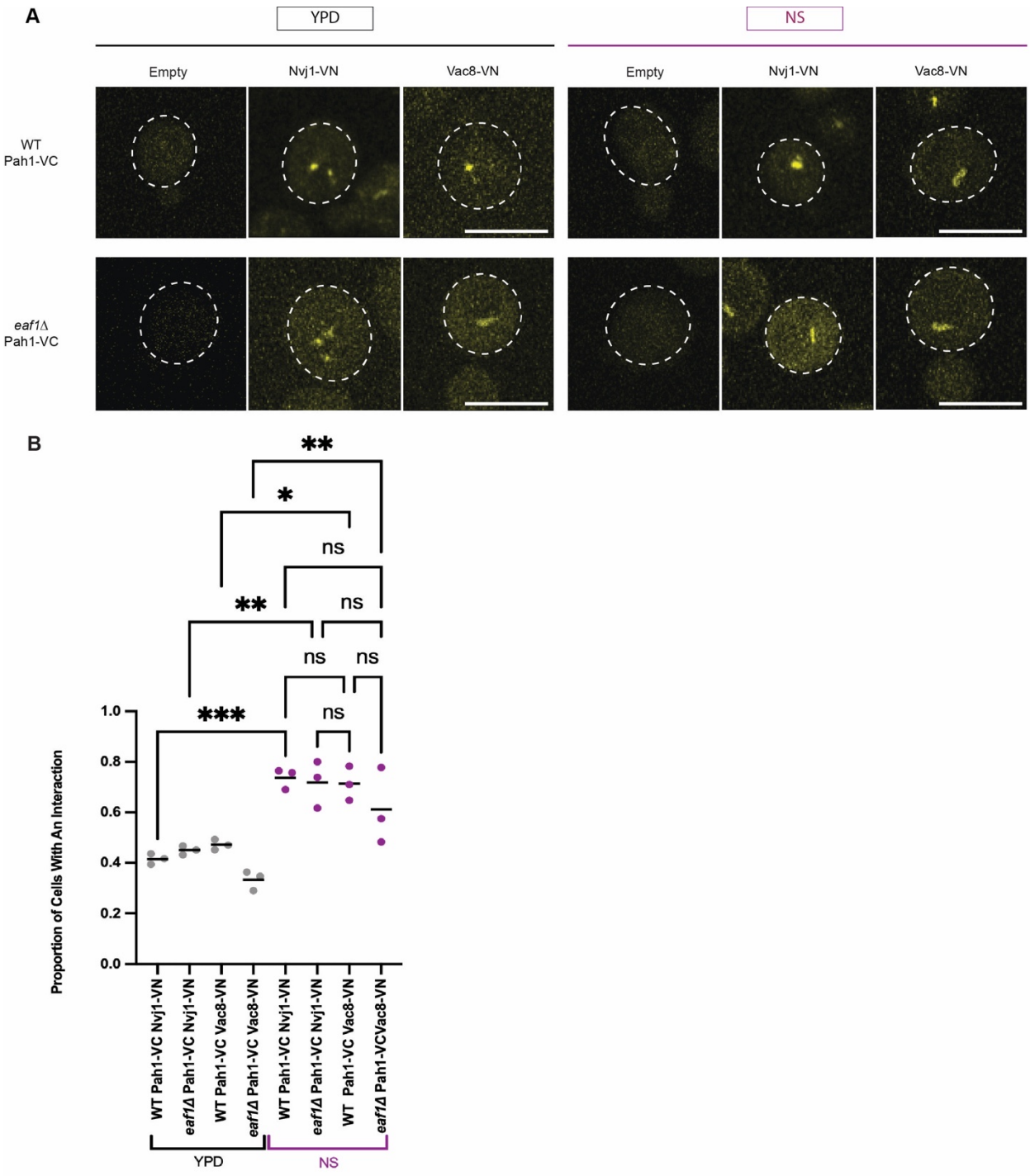

Supplemental Figure 2.8: Nvj1 and Vac8 remain in contact with Pah1 during nitrogen starvation in both WT and *eaf1*Δ. (A) Interaction of genomically integrated Nvj1-VN and Vac8-VN with Pah1-VC examined under YPD and nitrogen starvation (NS) conditions in both WT (YKB 5202 and 5204) and *eaf1*Δ (YKB 5203 and YKB 5205). First image of each WT and *eaf1*Δ is of cells expressing only Pah1-VC, showing that Nvj1-VN or Vac8-VN are necessary to provide a fluorescence signal. Representative images are merged Z-stacks. Scale bar = 5 μm. (B) Proportion of cells with an interaction were quantified by visually assessing the presence or absence of Venus punctae within the cell. At least 100 cells were measured for each strain and performed in triplicate. Each biological replicate is represented by a gray or purple dot. Horizontal bars represent the mean. An ANOVA analysis was performed using Tukey's multiple comparison test. *p≤0.05, **p≤0.01,

***p≤0.001. ns = not significant, p>0.05. Relevant statistical significance bars are shown, additional comparisons can be found in Supplemental Table 2.1.

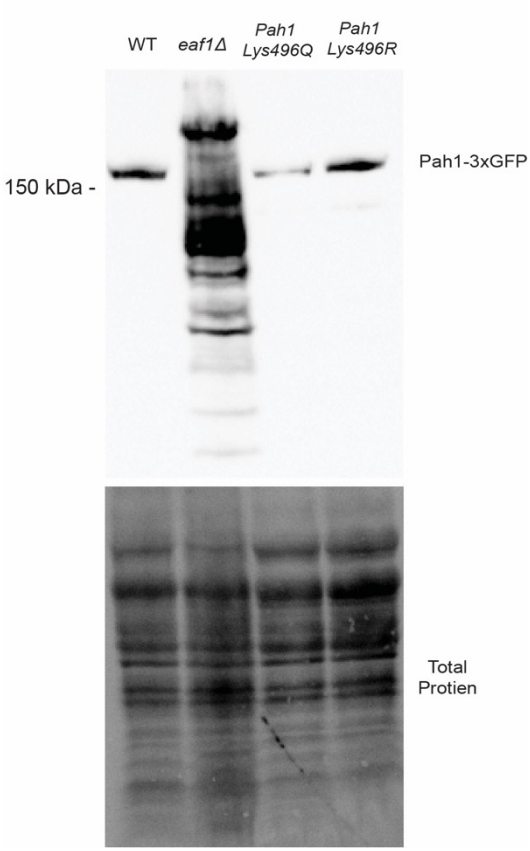

Supplemental Figure 2.9: Expression of Pah1-3xGFP. WT (YKB 4993), *eaf1*Δ (YKB 4994), *PAH1-K496Q* (YKB 5130) and *PAH1-K496R* (YKB 5131) were assessed via western blot analysis of whole cell extracts. Total protein is shown below via TGX blot activation.

Supplemental Table 2.1: Additional Statistical Analysis for Figures.
This table can be found Supplemental to Manuscript #1 at:
https://figshare.com/s/0448d63faeb05ded3d0b
It has been excluded here for conciseness and clarity of this body of work.

Supplemental Table 2.2: List of yeast strains and plasmids used in this work.

YKB Strain Number	Genotype	Background	Mat	Reference
1079	*WT BY4741*	*his3Δ1 leu2Δ0 met15Δ0 ura3Δ0*	MATa	[1]
4803	*eaf1Δ::HYG*	*his3Δ1 leu2Δ0 met15Δ0 ura3Δ0*	MATa	this study
4586	*esa1Δ::HIS3 esa1ts::URA3*	*his3Δ1 leu2Δ0 met15Δ0 ura3Δ0*	MATa	[2]
4972	*ACS2-GFP::HIS NUP49-RFP:URA*	*his3Δ1 leu2Δ0 met15Δ0 ura3Δ0*	MATa	this study
4863	*eaf1Δ::HYG ACS2-GFP::HIS NUP49-RFP::URA*	*his3Δ1 leu2Δ0 met15Δ0 ura3Δ0*	MATa	this study

4991	*ACS2-GFP::HIS NUP49-RFP::URA pah1Δ::KAN*	*his3Δ1 leu2Δ0 met15Δ0 ura3Δ0*	MATa	this study
4992	*ACS2-GFP::HIS NUP49-RFP::URA eaf1Δ::HYG pah1Δ::KAN*	*his3Δ1 leu2Δ0 met15Δ0 ura3Δ0*	MATa	this study
4883	*ACS2-GFP::HIS NUP49-RFP::URA dgk1Δ::KAN*	*his3Δ1 leu2Δ0 met15Δ0 ura3Δ0*	MATa	this study
4884	*ACS2-GFP::HIS NUP49-RFP::URA eaf1Δ::HYG dgk1Δ::KAN*	*his3Δ1 leu2Δ0 met15Δ0 ura3Δ0*	MATa	this study
4881	*ACS2-GFP::HIS NUP49-RFP::URA ino1Δ::KAN*	*his3Δ1 leu2Δ0 met15Δ0 ura3Δ0*	MATa	this study
4882	*ACS2-GFP::HIS NUP49-RFP::URA ino1Δ::KAN eaf1Δ::HYG*	*his3Δ1 leu2Δ0 met15Δ0 ura3Δ0*	MATa	this study
5128	*ACS2-GFP::NAT cds1-ts::URA*	*his3Δ1 leu2Δ0 met15Δ0 ura3Δ0*	MATa	this study, derived from [3]
5129	*ACS2-GFP::NAT cds1-ts::URA eaf1Δ::HYG*	*his3Δ1 leu2Δ0 met15Δ0 ura3Δ0*	MATa	this study
5124	*ACS2-GFP::NAT*	*his3Δ1 leu2Δ0 met15Δ0 ura3Δ0*	MATa	this study
5125	*ACS2-GFP::NAT esa1Δ::HIS3 esa1ts::URA3*	*his3Δ1 leu2Δ0 met15Δ0 ura3Δ0*	MATa	this study, derived from [2]
4973	*RS313-GPDprom-PAH1-5xGS-VC*	*his3Δ1 leu2Δ0 met15Δ0 ura3Δ0*	MATa	this study
4974	*eaf1Δ::HYG pRS313-GPDprom-PAH1-5xGS-VC*	*his3Δ1 leu2Δ0 met15Δ0 ura3Δ0*	MATa	this study
4975	*pRS313-GPDprom-PAH1-5xGS-VC pRS315-PUS1prom-PUS1-GS-VN*	*his3Δ1 leu2Δ0 met15Δ0 ura3Δ0*	MATa	this study
4976	*eaf1Δ::HYG pRS313-GPDprom-PAH1-5xGS-VC pRS315-PUS1prom-PUS1-GS-VN*	*his3Δ1 leu2Δ0 met15Δ0 ura3Δ0*	MATa	this study
4977	*pRS313-GPDprom-PAH1-5xGS-VC pRS315-NUP60prom-NUP60-GS-VN*	*his3Δ1 leu2Δ0 met15Δ0 ura3Δ0*	MATa	this study
4978	*eaf1Δ::HYG pRS313-GPDprom-PAH1-5xGS-VC pRS315-NUP60prom-NUP60-GS-VN*	*his3Δ1 leu2Δ0 met15Δ0 ura3Δ0*	MATa	this study
4979	*pRS315-PUS1prom-PUS1-GS-VN*	*his3Δ1 leu2Δ0 met15Δ0 ura3Δ0*	MATa	this study, plasmid from [4]
4980	*eaf1Δ::HYG pRS315-PUS1prom-PUS1-GS-VN*	*his3Δ1 leu2Δ0 met15Δ0 ura3Δ0*	MATa	this study, plasmid from [4]
4981	*pRS315-NUP60prom-NUP60-GS-VN*	*his3Δ1 leu2Δ0 met15Δ0 ura3Δ0*	MATa	this study, plasmid from [4]
4982	*eaf1Δ::HYG pRS315-NUP60prom-NUP60-GS-VN*	*his3Δ1 leu2Δ0 met15Δ0 ura3Δ0*	MATa	this study, plasmid from [4]
5182	*ACS2-GFP::HIS pRS316-CYC1prom-NUP60(1-24)-OPI1 Q2-mCh*	*his3Δ1 leu2Δ0 met15Δ0 ura3Δ0*	MATa	this study, plasmid from [4]
5183	*eaf1Δ::HYG ACS2-GFP::HIS pRS316-CYC1prom-NUP60(1-24)-OPI1 Q2-mCh*	*his3Δ1 leu2Δ0 met15Δ0 ura3Δ0*	MATa	this study, plasmid from [4]
5184	*ACS2-GFP::HIS pRS316-CYC1prom-NUP60(1-24)-C1a+C1b-mCh*	*his3Δ1 leu2Δ0 met15Δ0 ura3Δ0*	MATa	this study, plasmid from [4]
5185	*eaf1Δ::HYG ACS2-GFP::HIS pRS316-CYC1prom-NUP60(1-24)-C1a+C1b-mCh*	*his3Δ1 leu2Δ0 met15Δ0 ura3Δ0*	MATa	this study, plasmid from [4]
5123	*ACS2-GFP::NAT NVJ1-RFP::URA*	*his3Δ1 leu2Δ0 met15Δ0 ura3Δ0*	MATa	this study
5134	*eaf1Δ::HYG ACS2-GFP::NAT NVJ1-RFP::URA*	*his3Δ1 leu2Δ0 met15Δ0 ura3Δ0*	MATa	this study
5186	*pRS316- Nab2-NLS-mCherry*	*his3Δ1 leu2Δ0 met15Δ0 ura3Δ0*	MATa	this study, plasmid from [6]
5187	*eaf1Δ::HYG pRS316- Nab2-NLS-mCherry*	*his3Δ1 leu2Δ0 met15Δ0 ura3Δ0*	MATa	this study, plasmid from [6]

5188	*pAS1NB-NAB35-RG*	*his3Δ1 leu2Δ0 met15Δ0 ura3Δ0*	MATa	this study, plasmid from [7]
5189	*eaf1Δ::HYG pAS1NB-NAB35-RG*	*his3Δ1 leu2Δ0 met15Δ0 ura3Δ0*	MATa	this study, plasmid from [7]
4993	*PAH1-3xGFP::KAN*	*his3Δ1 leu2Δ0 met15Δ0 ura3Δ0*	MATa	this study
4994	*PAH1-3xGFP::KAN eaf1Δ::HYG*	*his3Δ1 leu2Δ0 met15Δ0 ura3Δ0*	MATa	this study
5130	*pah1-K496Q-3xGFP::KAN*	*his3Δ1 leu2Δ0 met15Δ0 ura3Δ0*	MATa	this study
5131	*pah1-K496R-3xGFP::KAN*	*his3Δ1 leu2Δ0 met15Δ0 ura3Δ0*	MATa	this study
5190	*PAH1-3xGFP::KAN pRS316- Nab2-NLS-mCherry*	*his3Δ1 leu2Δ0 met15Δ0 ura3Δ0*	MATa	this study, plasmid from [6]
5191	*PAH1-3xGFP::KAN eaf1Δ::HYG pRS316- Nab2-NLS-mCherry*	*his3Δ1 leu2Δ0 met15Δ0 ura3Δ0*	MATa	this study, plasmid from [6]
5192	*pah1-K396Q-3xGFP::KAN pRS316- Nab2-NLS-mCherry*	*his3Δ1 leu2Δ0 met15Δ0 ura3Δ0*	MATa	this study, plasmid from [6]
5193	*pah1-K496R-3xGFP::KAN pRS316- Nab2-NLS-mCherry*	*his3Δ1 leu2Δ0 met15Δ0 ura3Δ0*	MATa	this study, plasmid from [6]
5194	*YCplac111- PAH1-7A-GFP-LEU*	*his3Δ1 leu2Δ0 met15Δ0 ura3Δ0*	MATa	this study, plasmid from [5] and [6]
5195	*YCplac111- PAH1-7A-GFP-LEU eaf1Δ::HYG*	*his3Δ1 leu2Δ0 met15Δ0 ura3Δ0*	MATa	this study, plasmid from [5] and [6]
5196	*YCplac111-PAH1-AH3A-7A-GFP-LEU*	*his3Δ1 leu2Δ0 met15Δ0 ura3Δ0*	MATa	this study, plasmid from [5] and [6]
5197	*YCplac111-PAH1-AH3A-7A-GFP-LEU eaf1Δ::HYG*	*his3Δ1 leu2Δ0 met15Δ0 ura3Δ0*	MATa	this study, plasmid from [5] and [6]
5198	*YCplac111- PAH1-7A-GFP-LEU pRS316- Nab2-NLS-mCherry*	*his3Δ1 leu2Δ0 met15Δ0 ura3Δ0*	MATa	this study, plasmid from [5] and [6]
5199	*YCplac111- PAH1-7A-GFP-LEU pRS316- Nab2-NLS-mCherry eaf1Δ::HYG*	*his3Δ1 leu2Δ0 met15Δ0 ura3Δ0*	MATa	this study, plasmid from [5] and [6]
5200	*YCplac111-PAH1-AH3A-7A-GFP-LEU pRS316-Nab2-NLS-mCherry*	*his3Δ1 leu2Δ0 met15Δ0 ura3Δ0*	MATa	this study, plasmid from [5] and [6]
5201	*YCplac111-PAH1-AH3A-7A-GFP-LEU pRS316-Nab2-NLS-mCherry eaf1Δ::HYG*	*his3Δ1 leu2Δ0 met15Δ0 ura3Δ0*	MATa	this study, plasmid from [5] and [6]
5202	*PAH1-VC::HIS NVJ1-VN::KAN*	*his3Δ1 leu2Δ0 met15Δ0 ura3Δ0*	MATa	this study
5203	*eaf1Δ::HYG PAH1-VC::HIS NVJ1-VN::KAN*	*his3Δ1 leu2Δ0 met15Δ0 ura3Δ0*	MATa	this study
5204	*PAH1-VC::HIS VAC8-VN::KAN*	*his3Δ1 leu2Δ0 met15Δ0 ura3Δ0*	MATa	this study
5205	*eaf1Δ::HYG PAH1-VC::HIS VAC8-VN::KAN*	*his3Δ1 leu2Δ0 met15Δ0 ura3Δ0*	MATa	this study
5206	*pRS313-GPDprom-PAH1-Lys496Q-5xGS-VC pRS315-PUS1prom-PUS1-GS-VN*	*his3Δ1 leu2Δ0 met15Δ0 ura3Δ0*	MATa	this study, plasmid modified from [4]
5207	*pRS313-GPDprom-PAH1-Lys496Q-5xGS-VC pRS315-NUP60prom-NUP60-GS-VN*	*his3Δ1 leu2Δ0 met15Δ0 ura3Δ0*	MATa	this study, plasmid modified from [4]
5208	*pRS313-GPDprom-PAH1-Lys496R-5xGS-VC pRS315-PUS1prom-PUS1-GS-VN*	*his3Δ1 leu2Δ0 met15Δ0 ura3Δ0*	MATa	this study, plasmid modified from [4]
5209	*pRS313-GPDprom-PAH1-Lys496R-5xGS-VC pRS315-NUP60prom-NUP60-GS-VN*	*his3Δ1 leu2Δ0 met15Δ0 ura3Δ0*	MATa	this study, plasmid modified from [4]
5210	*pRS313-GPDprom-PAH1-Lys801Q-5xGS-VC pRS315-PUS1prom-PUS1-GS-VN*	*his3Δ1 leu2Δ0 met15Δ0 ura3Δ0*	MATa	this study, plasmid modified from [4]
5211	*pRS313-GPDprom-PAH1-Lys801Q-5xGS-VC pRS315-NUP60prom-NUP60-GS-VN*	*his3Δ1 leu2Δ0 met15Δ0 ura3Δ0*	MATa	this study, plasmid modified from [4]

5212	*pRS313-GPDprom-PAH1-Lys801R-5xGS-VC pRS315-PUS1prom-PUS1-GS-VN*	*his3Δ1 leu2Δ0 met15Δ0 ura3Δ0*	MATa	this study, plasmid modified from [4]
5213	*pRS313-GPDprom-PAH1-Lys801R-5xGS-VC pRS315-NUP60prom-NUP60-GS-VN*	*his3Δ1 leu2Δ0 met15Δ0 ura3Δ0*	MATa	this study, plasmid modified from [4]
5214	*pRS313-GPDprom-NUP2-5xGS-VC pRS315-NUP60prom-NUP60-GS-VN*	*his3Δ1 leu2Δ0 met15Δ0 ura3Δ0*	MATa	this study, plasmid modified from [4]
5215	*eaf1Δ::HYG pRS313-GPDprom-NUP2-5xGS-VC pRS315-NUP60prom-NUP60-GS-VN*	*his3Δ1 leu2Δ0 met15Δ0 ura3Δ0*	MATa	this study, plasmid modified from [4]
5216	*pRS313-GPDprom-MLP1-5xGS-VC pRS315-NUP60prom-NUP60-GS-VN*	*his3Δ1 leu2Δ0 met15Δ0 ura3Δ0*	MATa	this study, plasmid modified from [4]
5217	*eaf1Δ::HYG pRS313-GPDprom-MLP1-5xGS-VC pRS315-NUP60prom-NUP60-GS-VN*	*his3Δ1 leu2Δ0 met15Δ0 ura3Δ0*	MATa	this study, plasmid modified from [4]

PKB Number	**Name in Paper**	**Plasmid**	**Yeast Selection**	**Reference/Source**
357	Pah1-VC	*pRS313-GPDprom-PAH1-5xGS-VC*	HIS	[4]
358	Pus1-VN	*pRS315-PUS1prom-PUS1-GS-VN*	LEU	[4]
359	Nup60-VN	*pRS315-NUP60prom-NUP60-GS-VN*	LEU	[4]
360	NLS Q2-mCherry	*pRS316-CYC1prom-NUP60(1-24)-OPI1 Q2-mCh*	URA	[4]
361	Cla+Clb-mCherry	*pRS316-CYC1prom-NUP60(1-24)-C1a+C1b-mCh*	URA	[4]
362	Pah1-7A-GFP	*YCplac111- PAH1-7A-GFP*	LEU	[5]
363	Pah1-AH3A-7A-GFP	*YCplac111-PAH1-AH3A-7A-GFP*	LEU	[5]
364	Nab2-NLS-mCherry	pRS316- Nab2-NLS-mCherry	URA	[6]
365	Nuclear Rosella Plasmid	pAS1NB-NAB35-RG	LEU	[7]
366	Pah1-Lys496Q-VC	pRS313-GPDprom-PAH1-Lys496Q-5xGS-VC	HIS	this study, modified from [4]
367	Pah1-Lys496R-VC	pRS313-GPDprom-PAH1-Lys496R-5xGS-VC	HIS	this study, modified from [4]
368	Pah1-Lys801Q-VC	pRS313-GPDprom-PAH1-Lys801Q-5xGS-VC	HIS	this study, modified from [4]
369	Pah1-Lys801R-VC	pRS313-GPDprom-PAH1-Lys801R-5xGS-VC	HIS	this study, modified from [4]
370	Nup2-VC	pRS313-GPDprom-NUP2-5xGS-VC	HIS	this study, modified from [4]
371	Mlp1-VC	pRS313-GPDprom-MLP1-5xGS-VC	HIS	this study, modified from [4]

References for Supplemental Table 2.2:

1 Brachmann CB, Davies, A, Cost GJ, Caputo E, Li J, Hieter P, and Boeke JD. Designer deletion strains derived from Saccharomyces cerevisiae S288C: a useful set of strains and plasmids for PCR-mediated gene disruption and other applications. Yeast. 1998; 14(2):115-32

2 Dacquay L, et al. NuA4 Lysine Acetyltransferase Complex Contributes to Phospholipid Homeostasis in Saccharomyces cerevisiae. G3. Dacquay L, Flint A, Butcher J, Salem D, Kennedy M, Kaern M, et al. NuA4 lysine acetyltransferase complex contributes to phospholipid homeostasis in Saccharomyces cerevisiae. G3 Genes, Genomes, Genet. 2017;7[6]:1799–809 7(6):1799-1809

3 Li, T.Y., L. Song, Y. Sun, J. Li, C. Yi, S.M. Lam, D. Xu, L. Zhou, X. Li, Y. Yang, C.-S. Zhang, C. Xie, X. Huang, G. Shui, S.-Y. Lin, K. Reue, and S.-C. Lin. 2018. Tip60-mediated lipin 1 acetylation and ER translocation determine triacylglycerol synthesis rate. Nature Communications. 9.

4 Romanauska A, Köhler A. The Inner Nuclear Membrane Is a Metabolically Active Territory that Generates Nuclear Lipid Droplets. Cell. 2018 Jul 26;174(3):700-715.e18. doi: 10.1016/j.cell.2018.05.047. Epub 2018 Jun 21. PMID: 29937227; PMCID: PMC6371920.
5 Karanasios, E., G.-S. Han, Z. Xu, G.M. Carman, and S. Siniossoglou. 2010. A phosphorylation-regulated amphipathic helix controls the membrane translocation and function of the yeast phosphatidate phosphatase. Proceedings of the National Academy of Sciences. 107:17539-17544.
6 Jonathan I. Millen, Roswitha Krick, Tanja Prick, Michael Thumm & David S. Goldfarb (2009) Measuring piecemeal microautophagy of the nucleus in Saccharomyces cerevisiae, Autophagy, 5:1, 75-81, DOI: 10.4161/auto.5.1.7181
7 Rosado CJ, Mijaljica D, Hatzinisiriou I, Prescott M, Devenish RJ. Rosella: a fluorescent pH-biosensor for reporting vacuolar turnover of cytosol and organelles in yeast. Autophagy. 2008 Feb;4(2):205-13. doi: 10.4161/auto.5331. Epub 2007 Nov 21. PMID: 18094608.

All Supplemental Videos can be found at: https://figshare.com/s/0448d63faeb05ded3d0b

S2.1 Video: Nuclear and vacuole structure in WT cells. WT (YKB 4972) yeast cells were grown to log phase in YPD media and images were captured using a Laser Scanning, Zeiss LSM880 confocal microscope equipped with Airyscan processing. Z-stacks were taken at 0.2 µm and projected into 3D surfaces using Imaris 9.8. Image is a 3D model of Z-stack images shown in **Figure 2.1**. Green represents Acs2-GFP fluorescence and shows the nucleus of the cell. Blue represents the vacuolar lumen stained with CMAC.

S2.2 Video: Nuclear deformation and vacuole fragmentation in *eaf1*Δ cells. *eaf1*Δ (YKB 4863) cells were grown to log phase in YPD media and images were captured using a Laser Scanning, Zeiss LSM880 confocal microscope equipped with Airyscan processing. Z-stacks were taken at 0.2 µm and projected into 3D surfaces using Imaris 9.8. Image is a 3D model of Z-stack images shown in **Figure 2.1**. Green represents Acs2-GFP fluorescence and shows the nucleus of the cell. Blue represents the vacuolar lumen stained with CMAC.

S2.3 Video: Nuclear deformation and vacuole fragmentation in *eaf1*Δcells. *eaf1*Δ (YKB 4863) cells were grown to log phase in YPD media and images were captured using a Laser Scanning, Zeiss LSM880 confocal microscope equipped with Airyscan processing. Z-stacks were taken at 0.2 µm and projected into 3D surfaces using Imaris 9.8. Image is a 3D model of Z-stack images shown in **Figure 2.1**. Green represents Acs2-GFP fluorescence and shows the nucleus of the cell. Blue represents the vacuolar lumen stained with CMAC.

S2.4 Video: WT Nab2-NLS-mCherry CMAC: WT cells expressing a Nab2-NLS-mCherry construct (YKB 5186) to visualize the nucleus (shown in purple) with the vacuole (shown in blue) stained with CMAC. Cells were grown to log phase in YPD media and then transferred into nitrogen starvation media. Images were captured using a Laser Scanning, Zeiss LSM880 confocal microscope equipped with Airyscan processing. Z-stacks were taken at 0.2 µm and projected into 3D surfaces using Imaris 9.8. Image is a 3D model of Z-stack images shown in **Figure 2.5**. PMN blebs, seen as projections of the nucleus, entering the vacuole can be seen.

S2.5 Video: *eaf1*Δ Nab2-NLS-mCherry CMAC: *eaf1*Δ cells expressing Nab2-NLS-mCherry (YKB 5187) to visualize the nucleus (shown in purple) with the vacuole (shown in blue) stained with CMAC. Cells were grown to log phase in YPD media and then transferred into nitrogen starvation media. Images were captured using a Laser Scanning, Zeiss LSM880 confocal microscope equipped with Airyscan processing. Z-stacks were taken at 0.2 µm and projected into 3D surfaces using Imaris

9.8. The image is a 3D model of Z-stack images shown in **Figure 2.5**. Nuclear extensions can be seen pushing between vacuolar lobes.

S2.6 Video: *eaf1*Δ Nab2-NLS-mCherry CMAC: *eaf1*Δ cells expressing Nab2-NLS-mCherry (YKB 5187) to visualize the nucleus (shown in purple) with the vacuole (shown in blue) stained with CMAC. Cells were grown to log phase in YPD media and then transferred into nitrogen starvation media. Images were captured using a Laser Scanning, Zeiss LSM880 confocal. microscope equipped with Airyscan processing. Z-stacks were taken at 0.2 μm and projected into 3D surfaces using Imaris 9.8. Image is a 3D model of Z-stack images shown in **Figure 2.5**. Nuclear extensions wrapping around vacuolar lobes can be seen.

Appendix B: Co-Authored Paper (Bcy1 regulation by NuA4)

Phenomic screen identifies a role for the yeast lysine acetyltransferase NuA4 in the control of Bcy1 subcellular localization, glycogen biosynthesis, and mitochondrial morphology

Elizabeth A. Walden [1,2], Roger Y. Fong [1,2], Trang T. Pham [1,2], Hana Knill [1,2], Sarah Jane Laframboise [1,2], Sylvain Huard [1,2], Mary-Ellen Harper [1,2], Kristin Baetz [1,2]*

[1]Department of Biochemistry, Microbiology and Immunology, Faculty of Medicine, University of Ottawa, Ottawa, Canada
[2]Ottawa Institute of Systems Biology, Ottawa, Canada

B. 1 Abstract

Cellular metabolism is tightly regulated by many signaling pathways and processes, including lysine acetylation of proteins. While lysine acetylation of metabolic enzymes can directly influence enzyme activity, there is growing evidence that lysine acetylation can also impact protein localization. As the *Saccharomyces cerevisiae* lysine acetyltransferase complex NuA4 has been implicated in a variety of metabolic processes, we have explored whether NuA4 controls the localization and/or protein levels of metabolic proteins. We performed a high-throughput microscopy screen of over 360 GFP-tagged metabolic proteins and identified 23 proteins whose localization and/or abundance changed upon deletion of the NuA4 scaffolding subunit, *EAF1*. Of the identified proteins, three proteins were required for glycogen synthesis and 14 proteins were associated with the mitochondria. We determined that in *eaf1*Δ cells the transcription of glycogen biosynthesis genes is upregulated resulting in increased proteins and glycogen production. Further, in the absence of *EAF1*, mitochondria are highly fused, increasing in volume 3-fold, and are chaotically distributed but remain functional. Both the increased glycogen synthesis and mitochondrial elongation in *eaf1*Δ cells are dependent on Bcy1, the yeast regulatory subunit of PKA. Surprisingly, in the absence of *EAF1*, Bcy1 localization changes from being nuclear to cytoplasmic and PKA activity is altered. We found that NuA4-dependent localization of Bcy1 is dependent on a lysine residue at position 313 of Bcy1. However, the glycogen accumulation and mitochondrial elongation phenotypes of *eaf1Δ,* while

dependent on Bcy1, were not fully dependent on Bcy1-K313 acetylation state and subcellular localization of Bcy1. As NuA4 is highly conserved with the human Tip60 complex, our work may inform human disease biology, revealing new avenues to investigate the role of Tip60 in metabolic diseases.

B. 2 Author Summary

Metabolism, how cells process nutrients and energy substrates, is dramatically altered in many diseases. For example, during tumorigenesis, changes in cellular metabolism allow for the rapid cellular growth and division. One way to control metabolism is by moving the proteins involved in metabolism to different parts of the cell. Similar to an assembly line, when all the "parts" (metabolic proteins) are brought together, efficiency can be increased. In contrast, if one or more parts are shipped to the wrong place (mislocalized), production is decreased, and an alternative production process may even be necessary to meet demands. Here we ask whether Tip60, a protein complex implicated in many diseases, affects the location of metabolic proteins in the cell. We use budding yeast as a model system to assess the effect of disrupting yeast Tip60 on the location of over 360 metabolic proteins. We found that Tip60 controls the location of many metabolic proteins and in the absence of Tip60 there is an increase in the mitochondria and in cellular carbohydrate storage (the metabolic 'hubs' of the cell). This work suggests that yeast Tip60 functions as a "brake" on cellular metabolism and provides novel potential roles of Tip60 in metabolic diseases.

B. 3 Introduction

Lysine acetylation is one of the most common post-translational modifications (PTM) in the cell. Lysine acetylation has been historically characterized as a PTM occurring on histones, however, in the last 10 years, thousands of non-histone acetylation sites have been identified through global screens for protein acetylation, establishing lysine acetylation as a conserved and dynamic PTM

[48,82,152–155]. It is therefore not surprising that lysine acetylation plays diverse roles in the regulation of cellular processes and that it is deregulated in many human diseases [61,156–158].

Lysine acetylation is catalytically controlled by two opposing classes of enzymes: Lysine acetyltransferases (KATs) and lysine deacetylases (KDACs). Our work focuses on the *Saccharomyces cerevisiae* KAT complex NuA4, the yeast homolog of the human Tip60 complex, which has been associated with many diseases including cancer, developmental issues, and neurodegenerative disease [51,61–65]. Given the exceptional conservation of KAT function across eukaryotes, the study of the homologous NuA4 complex may provide insight into further understanding the biological roles of Tip60 and the cellular consequences of its deregulation in disease [51].

NuA4 contains 13 subunits, six of which are essential genes for viability, including the gene for the catalytic subunit *ESA1* [58,66–68]. Though non-essential, the *EAF1* subunit is a critical scaffolding protein required to maintain the complete NuA4 complex [66,68]. Yeast cells deficient for Eaf1 are viable but lose much of the targeting of the catalytic Esa1 subunit, making the *eaf1Δ* mutant an excellent genetic model system to identify the biological roles and protein targets of NuA4 [66,67,79,80]. Alternatively, NuA4 function can be probed using the temperature sensitive mutation, *esa1-ts* (*esa1-L245P*), which reduces the acetylation activity of Esa1 at increased temperatures [58,81,82].

Given its essential role, it is not surprising that NuA4 has been implicated in a myriad of biological processes, including metabolism. Indeed, lysine acetylation, which neutralizes the positive lysine side chain charge, has been suggested to be an ideal "switch" to turn off and on enzymes. For example, NuA4 dependent acetylation of phosphoenolpyruvate carboxykinase (Pck1) is important for activating its function in the rate controlling step of gluconeogenesis [59,112,121]. Acetylation has also been implicated in controlling protein-protein interactions. NuA4 yeast mutants have replicative lifespan defects caused by impairments in the NuA4-dependent acetylation of Sip2 [60]. Sip2 acetylation increases its interaction with Snf1 decreasing Snf1 activity [60]. Sip2 is one of the three inhibitory β subunits of the Snf1 complex (AMPK in humans) [122,123]. The Snf1 kinase responds to changes in cellular AMP levels and plays an important role in the adaptation of yeast cells to glucose limiting conditions as its kinase activity leads to the derepression of many glucose repressed genes [60,122,123,159,160]. Similarly, work by Filteau and colleagues suggests that the protein-protein interactions which control the activity of the Protein Kinase A (PKA), also referred to as cAMP-dependent protein kinase, are regulated through NuA4-dependent acetylation of the PKA regulatory subunit Bcy1 [52]. PKA is a central metabolic kinase and has been extensively linked to many cellular processes including stress response and mitochondrial processes [161–164].

In yeast, the PKA complex is a heterotetrameric complex containing two Bcy1 regulatory subunits bound to two catalytic subunits, of the three partially redundant Tpk1, Tpk2, and Tpk3 [125,127,165,166]. The study by Filteau and colleagues suggests that the unacetylated form of Bcy1 can interact with and inhibit the catalytic PKA subunits Tpk1/2/3, but when Bcy1 is acetylated the Bcy1-Tpk interaction is disrupted leading to PKA activation [52]. In humans, PKA activity can be regulated through being anchored to different parts of the cell including the mitochondria by A-Kinase Anchoring Proteins (AKAPs) [167]. While AKAPs have not been identified in yeast, the localization of the Tpks and Bcy1 are regulated in response to environmental factors which is likely also associated

with changes in activity or substrates [163,168,169]. One key downstream effect of Tpk activity is the regulation of the localization of the functionally redundant Msn2 and Msn4 (Msn2/4) stress response transcription factors which are phosphorylated and sequestered in the cytoplasm [131,170]. Upon stress or inhibition of PKA activity, Msn2/Msn4 phosphorylation decreases allowing for translocation into the nucleus where they bind to stress response elements (STREs) and activate transcription of genes related to β oxidation of fatty acids, glycolysis, and stress response [132,171,172]. Interestingly, Msn2/4-dependent transcription is de-repressed in NuA4 mutants [79]. While this transcriptional de-repression may be associated with PKA activity, it is also possible that there is direct regulation as NuA4 can co-IP with Msn2 and Msn4 [79,131]. Finally, PKA activity and transcriptional activation of Msn2/4 targets have also been linked to another target of NuA4, the oxysterol binding protein Kes1 [134]. Kes1 functions as a lipid exchange protein in the cell and its acetylation has been demonstrated to regulate cell cycle arrest in response to nutrient stress [134]. Yeast with impaired NuA4 activity showed increased Kes1 activity with an associated increase in Msn2/4 transcriptional activity in addition to the metabolic characteristics of quiescence [134]. Overall, many preliminary links of NuA4 to metabolism have begun to be uncovered.

In addition to regulating enzyme activities and protein-protein interactions directly, lysine acetylation has also been associated with contributing to protein subcellular localization. For example, in mammalian cells, Tip60 acetylation of lipin drives its localization to the endoplasmic reticulum [53]. Indeed, the role of acetylation in regulating protein subcellular localization may be far reaching. Chong and colleagues used synthetic genetic array (SGA) technology coupled with high content screening to assess the impact of the deletion of the KDAC *RPD3* on over 4000 GFP fusions [41]. *RPD3* deletion led to a large number of proteins that increased in abundance but more intriguingly, the subcellular localization of more than 30 proteins were altered upon deletion of *RPD3* [41].

Given that NuA4 is implicated in the regulation of a variety of metabolic proteins [59,173], and the global impact of Rpd3 on protein abundance and localization [41], here we ask if NuA4 impacts the subcellular localization or abundance of metabolic proteins. We identified 23 proteins that displayed altered localization or abundance upon deletion of *EAF1* and of these, 14 were associated with mitochondria and three were associated with glycogen synthesis. We determined that the mitochondrial elongation and increased glycogen detected in *eaf1Δ* cells are partially due to the yeast PKA regulatory subunit, Bcy1, and that NuA4 is regulating the subcellular localization of Bcy1.

B.4 Results

***EAF1* dependent remodeling of the metabolic proteome**

To identify metabolic protein localization and abundance changes between wild type (WT) and the NuA4 mutant *eaf1Δ* we performed a focused phenomic screen. Using synthetic genetic array technology [174,175], both WT and *eaf1Δ* strains were crossed to 407 C-terminal GFP-fusion proteins from the GFP collection [42] with known or implicated roles in metabolism. Due to attrition of strains during mating, this resulted in a pair matched single (X-GFP) and double (X-GFP *eaf1Δ*) mutant set consisting of 368 genes (Screen outlined in S6.1 Fig).

The localization and protein abundance of the 368 GFP-tagged metabolic proteins was assessed in the WT and *eaf1Δ* background by high-throughput microscopy. In total, manual classification identified 70 proteins whose protein level and/or localization is impacted by deletion of *EAF1*. Additionally, the GFP intensity between WT and *eaf1Δ* cells for each strain was compared using ImageJ to assess changes in protein abundance, many of which corresponded with the manual classifications (S6.1 Table and S6.2 Fig). Of the approximately 70 potential changes identified (manually and by Image J), we selected 23 GFP fusions that had dramatic observable changes in localization upon deletion of *EAF1* to reassess. The identity of the selected GFP fusions were confirmed by PCR in both WT and *eaf1Δ* backgrounds and secondary microscopy was performed

(Figure 6.1, S6.3 Fig, and S6,1 Table). The 23 confirmed changes were categorized into six categories: mitochondrial elongation, cytoplasm to punctate, nucleus to cytoplasm, cytoplasm to nucleus, cell periphery to cytoplasm, and increased abundance (Figure 6.1A, S6.3 Fig, and S6.2 Table). Two categories of localization changes particularly stood out, the cytoplasm to punctate phenotype and the mitochondrial elongation phenotype. The cytoplasm to increased punctate phenotype (represented by Gsy2-GFP in Figure 6.1B) was of interest because all three proteins within this category are part of the glycogen regulation pathway. The second striking feature of this screen were the 14 GFP-tagged mitochondrial proteins, which displayed elongated mitochondrial phenotype (represented by Aco2-GFP in Figure 6.1B). Our screen shows that deletion of *EAF1* results in remodeling of a subset of the yeast metabolic proteome.

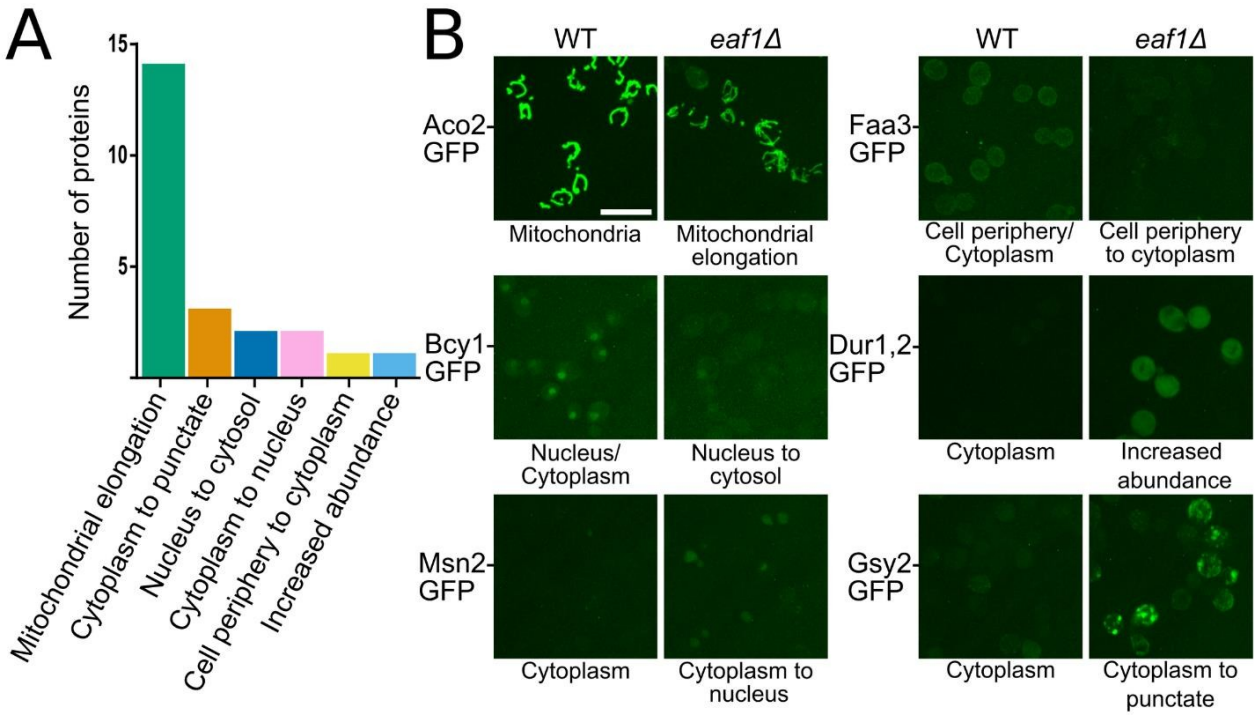

Figure 6.1. Summary of impact of *EAF1* deletion on metabolic protein localization and signal. (A) A phenomic screen for changes in protein localization and abundance between WT and *eaf1Δ* yeast was performed using SGA technology and high throughput microscopy. 23 confirmed changes in GFP signal localization or abundance were identified and categorized (S6.2 Table). (B) Six representative images of the change in GFP-fusion proteins identified in the phenomic screen (images of all confirmed changes available in S6.3 Fig). WT localization of proteins as previously reported at https://thecellvision.org/cyclops/ are listed under the WT image and the change category is listed under the *eaf1Δ* image. Some of these proteins also had changes in abundance in the *eaf1Δ* relative to WT. Fold changes outside our cut-off were: Aco2=0.51, Dur1, 2 = 3.77, and Gsy2 = 1.65. Scale bar = 10 μm.

NuA4 regulation of glycogen biosynthesis is dependent on PKA and Msn2/Msn4

Our screen identified three GFP-tagged glycogen biosynthesis proteins (Gdb1, Gsy1, and Gsy2) that in *eaf1Δ* cells increased in GFP signal and were concentrated into punctate structures (Figure 6.1B, S6.3 and S6.4A Figs). These proteins are responsible for glycogen synthesis (Gsy1 and Gsy2) and glycogen debranching (Gdb1) [176]. Glycogen is a large polysaccharide molecule made of repeating and branching glucose molecules [176] (Figure 6.2A). It is an important energy storage molecule for mammals and yeast [176–178]. Iodine staining to assess glycogen content confirmed that *eaf1Δ* cells have a higher level of glycogen (darker staining) than WT cells [179] (Figure 6.2B). Additionally, at the semi-restrictive temperature of 30ºC the temperature sensitive *ESA1* mutant $esa1^{L254P}$ *(esa1-ts*) also demonstrated an increase in iodine staining (S6.4 Fig).

We next sought to determine mechanistically how deletion of *EAF1* causes an increase in glycogen biosynthesis proteins. Given the similar induction in protein levels observed by microscopy and western blot (Figure 6.2C and 6.2D and S6.4 Fig) and that *GDB1*, *GSY1*, and *GSY2* genes are all associated with stress response element (STRE) activated transcription [172,180–182], we performed further characterization using only Gsy2, the predominant glycogen synthase in yeast [183]. As both the PKA-Msn2/Msn4 axis and Snf1 have been implicated in the transcriptional regulation of glycogen biosynthesis genes [180,181,184,185] (Figure 6.2A) we asked if the increased glycogen level seen in *eaf1Δ* cells is dependent on *MSN2/MSN4, BCY1*, or *SNF1* (Figure 6.2B). We found that *eaf1Δ* cells have a much darker iodine staining than WT cells, suggesting an accumulation of glycogen (Figure 6.2B). While *snf1*Δ cells displayed less iodine staining than WT cells, suggesting less glycogen accumulation, *snf1Δeafδ* cells displayed iodine staining similar to *eaf1Δ* cells. In contrast, deletion of both *MSN2* and *MSN4* (*msn2/4Δ)* or deletion of *BCY1* (*bcy1Δ)* suppressed glycogen accumulation in *eaf1Δ* cells when analyzed by iodine staining (Figure 6.2B). This suggests that NuA4-dependent

regulation of the PKA-Msn2/4 pathway contributes to the control of glycogenesis, while NuA4-dependent regulation of AMPK/Snf1 does not.

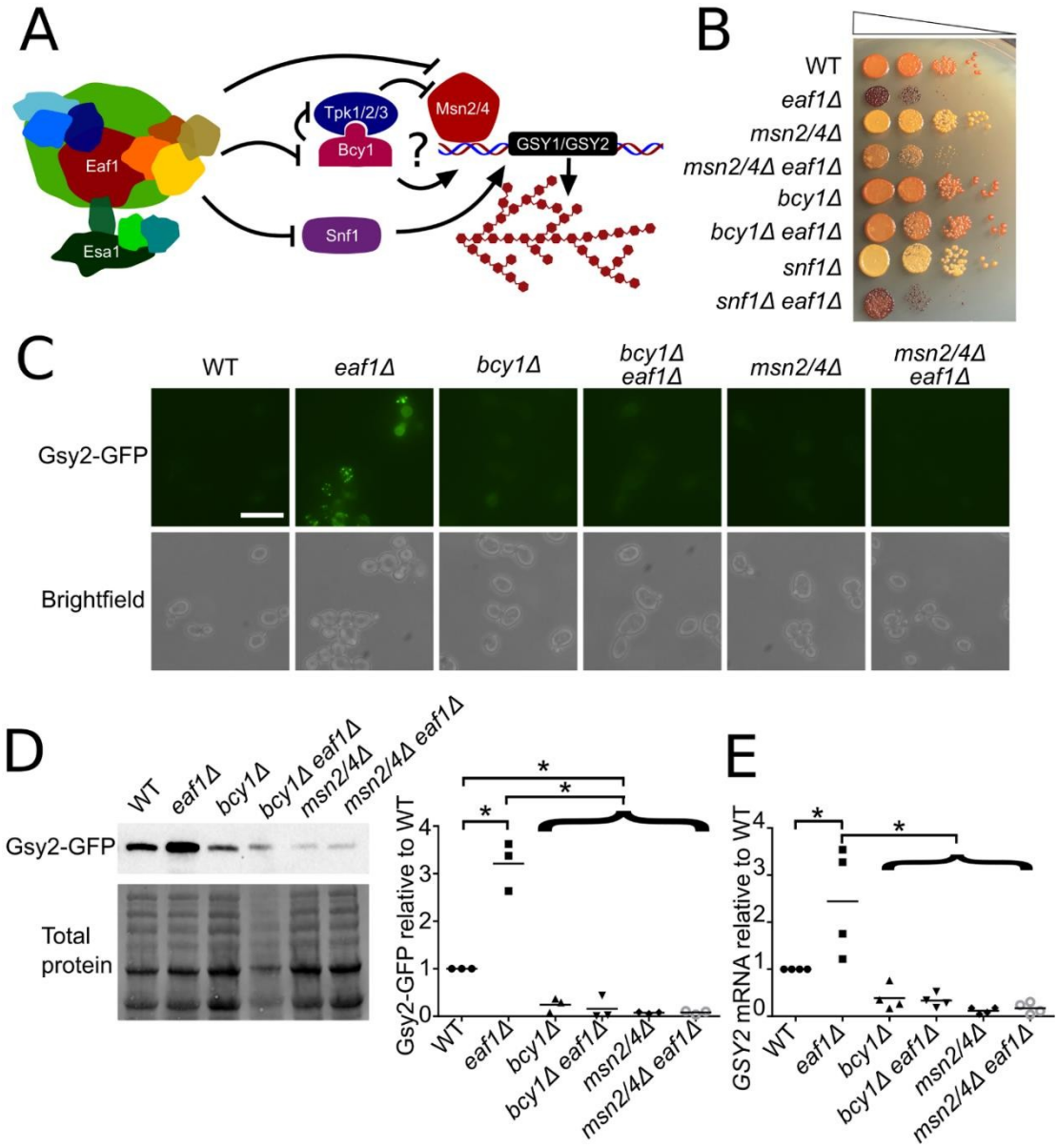

Figure 6.2. NuA4 regulation of glycogen biosynthesis proteins is mediated by PKA-Msn2/4 pathway. (A) Schematic model of NuA4 regulation of glycogen biosynthesis genes. (B) Increased glycogen levels in *eaf1Δ* cells is suppressed by *bcy1Δ* and *msn2Δ msn4Δ*. The indicated strains were serially diluted on to YPD plates, grown at 30ºC for 24 hours prior to exposure to iodine crystal vapours. Darker color corresponds to more glycogen storage. (C) Gsy2-GFP expression and localization were assessed in the indicated strain backgrounds by microscopy. Images are representative of three independent biological replicates. Scale bar = 10 µm. (D) Gsy2-GFP protein levels were assessed by quantitative western blot analysis using whole cell extracts from the indicated strains expressing Gsy2-GFP. Panel to the left is representative anti-GFP western and total protein blot; panel to the right is the quantification of western blots for three independent biological replicates where the Gsy2-GFP band intensity was normalized to total protein. (E) *GSY2* mRNA was measured using RT-qPCR relative to the *TDH3* gene for indicated yeast strains using four biological replicates. For D and E, ANOVA

analysis was performed with a Tukey's multiple comparison test comparing pairs of means. *= $p < 0.05$, relevant significance bars shown. Horizontal bar in data represents the mean.

Further, we were surprised to see that deletion of *BCY1* suppressed the slow growth defects of *eaf1Δ* cells, where *msn2Δmsn4Δ* did not (Figure 6.2B). The *bcy1Δ* suppression of *eaf1Δ* slow growth was confirmed by OD-based growth curve analysis and calculation of doubling time for each strain (S6.5 Fig). This suggests that derepression of Msn2/Msn4-dependent transcription is not contributing to slow growth of *eaf1Δ*, rather other targets of PKA are likely contributing to its slow growth. The dependence of the glycogen content on Msn2/4 signalling was of additional interest to us as our screen also identified Msn2 to move from the cytoplasm to the nucleus upon deletion of *EAF1* (Figure 6.1B). Parallel analysis of the Gsy2-GFP signal by microscopy and quantitative western blot confirmed that Gsy2-GFP protein expression is induced upon deletion of *EAF1* and demonstrated that this is dependent on Msn2/Msn4 and Bcy1 (Figure 6.2C and 6.2D). qRT-PCR determined that the increase in Gsy2 protein was at least partially due to a significant increase in *GSY2* mRNA expression in *eaf1Δ* cells relative to WT (Figure 6.2E). Finally, the increase in protein abundance of Gsy2-GFP and mRNA levels of *GSY2* seen in *eaf1*Δ cells were suppressed upon deletion with *msn2Δmsn4*Δ or *bcy1Δ* (Figure 6.2C, 6.2D, and 6.2E). Together this work is consistent with the conclusion that the increase in glycogen biosynthetic proteins identified in our screen are at least partially due to NuA4 regulation of PKA and Msn2/Msn4 activity.

Mitochondrial volume increases in the absence of NuA4

Our screen identified 14 mitochondrial proteins that had a change in GFP signal between WT and *eaf1Δ* (Figure 6.1A and S6.3 Fig.). As all of the 14 proteins are resident mitochondrial proteins, rather than proteins that are relocalizing to the mitochondria, it suggests that mitochondrial elongation is occurring in *eaf1Δ* cells. To confirm this hypothesis we assessed 3 common markers of the mitochondria in both WT and *eaf1Δ* cells: Cit1-GFP, Aco2-GFP and MitoLoc [186], a plasmid

expressing a mitochondrial localized GFP peptide (Figure 6.3 and S6.6 Fig.). In each case, we detected hyperelongated mitochondria with increased branching in *eaf1Δ* cells. Despite the fact that *eaf1Δ* cells are almost 2x larger than WT cells (Figure 6.3 and S6.7 Fig.), when the change in the mitochondrial volume is normalized to the increased cell size of the *eaf1Δ*, there is still a significant 1.7-fold increase in the mitochondrial volume relative to cell size (mitochondrial fraction) (Figure 6.3). When cell size is not accounted for, the mitochondrial volume of the *eaf1Δ* strain was found to be approximately three times larger than WT (S6.8 Fig). The mitochondrial morphology of the *esa1-ts* was also assessed after 2 hours at a semi-permissive temperature of 33ºC and there was a slight change in mitochondrial morphology and but no significant change in mitochondrial fraction was identified (S6.9 Fig). The difference in the penetrance of the mitochondrial phenotype between the *eaf1Δ* and the *esa1-ts* may be explained by the difference in the mutation type. The *esa1-ts* is functional when grown at 25ºC and the short 2-hour incubation at 33ºC decreases NuA4 catalytic activity however extended temperature shift dramatically decreases viability. In contrast, deletion of *EAF1* disrupts the NuA4 complex, including substrate targeting, but the catalytic activity remains intact. It is also possible that Eaf1 plays a role outside of the NuA4 complex and Esa1 targeting, but that remains as a speculation, and the small effect of the *esa1-ts* on mitochondrial morphology seen in our experiments would suggest that this is not the case. Altogether, this indicates that a reduction in NuA4 activity results in altered mitochondrial morphology (a fused phenotype) and increased mitochondrial content per cell (mitochondriogenesis).

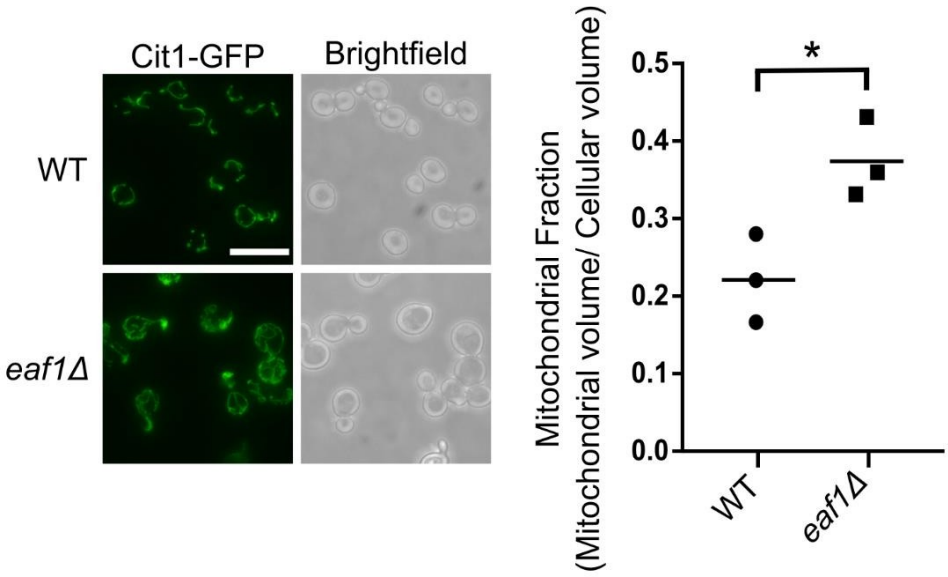

Figure 6.3. Mitochondrial morphology and volume are altered in NuA4 mutants. Cit1-GFP was used as a marker of the mitochondria to compare WT and *eaf1Δ* mitochondrial morphology by fluorescent microscopy. The mitochondrial volume was quantified based on the Cit1-GFP fluorescence using the MitoMap plugin for ImageJ which was then divided by the average total cellular volume of the strain to give the Mitochondrial Fraction (Raw cellular and mitochondrial volume measurements can be found in S2.7 and S2.8 Figs). Images are representative of 3 independent biological replicates and at least 50 cells per replicate were analyzed for quantification Scale bar = 10 μm. An unpaired T-test was run. *= $p < 0.05$. Horizontal bar in data represents the mean.

While chaotic and elongated, the mitochondria in *eaf1Δ* cells are functional

The structure of the mitochondria is important to its function [187]. Therefore, we sought to test if mitochondrial function was intact in *eaf1Δ* cells using three different assays. First, a Seahorse Extracellular Flux Analyzer (XF; Agilent) was used to measure mitochondrial bioenergetics. WT and *eaf1Δ* yeast were prepared overnight in YPD and then diluted in the morning into YPD or YPE (Ethanol), a non-fermentable carbon source that forces mitochondrial oxidative reactions over glycolysis. The oxygen consumption rate (OCR) of the mutant was compared to the control in YPD and YPE media and in both cases the *eaf1Δ* consumed significantly more oxygen than the WT yeast (Figure 6.4A and 6.4B).

The oxygen consumption was confirmed to be mitochondrial dependent as the addition of sodium azide, an electron transport chain inhibitor, significantly reduced the OCR in both cases. As a second measure of mitochondrial activity, we compared the viability of WT and *eaf1Δ* cells to treatment with a mitochondrial inhibitor. We anticipated that if *eaf1Δ* cells had increased functional mitochondria, they would be less sensitive to antimycin A, an inhibitor of the electron transport chain complex III. As expected, through dot assay analysis we found that both WT and *eaf1Δ* cells are able to survive antimycin A treatments in the presence of glucose (YPD) when cells do not require mitochondrial function to survive. However, when grown on a non-fermentable carbon source such as glycerol (YPG) mitochondrial function is essential and WT cells were hyper-sensitive to antimycin A treatment compared to *eaf1Δ* cells (Figure 6.4C). Together with the mitochondrial bioenergetics assays, this suggests that not only do *eaf1Δ* cells have more mitochondria but that the mitochondria are functional. Finally, as the elongated mitochondria seen in *eaf1Δ* cells could reflect excessive mitochondrial fusion, or alternatively increased biogenesis, we next performed biogenesis and fragmentation assays. We first assessed the mitochondrial fission response upon exposure to hydrogen peroxide. Similar to WT cells, the mitochondria of *eaf1Δ* cells were able to fragment under hydrogen peroxide stress, indicating that mitochondrial fission is intact in *eaf1Δ* cells (Figure 6.4D). We then tested the ability of the *eaf1Δ* cells to undergo mitochondriogenesis in the non-fermentable condition of ethanol, where the mitochondria are required for ATP production and cell growth [188]. Both WT and *eaf1Δ* cells increased mitochondrial content upon ethanol treatment to a similar extent suggesting mitochondrial biogenesis is intact in *eaf1Δ* cells (Figure 6.4D). Consistent with this observation we determined that the increased mitochondrial volume of *eaf1Δ* cells is not reversed upon deletion of *HAP4*, the activator member of the Hap complex important for mitochondrial biogenesis (S6.10 Fig) [189]. Together our work shows that *eaf1Δ* cells not only have increased mitochondrial volume and are

more fused and elongated, but that their mitochondria are functional and can respond to environmental stresses.

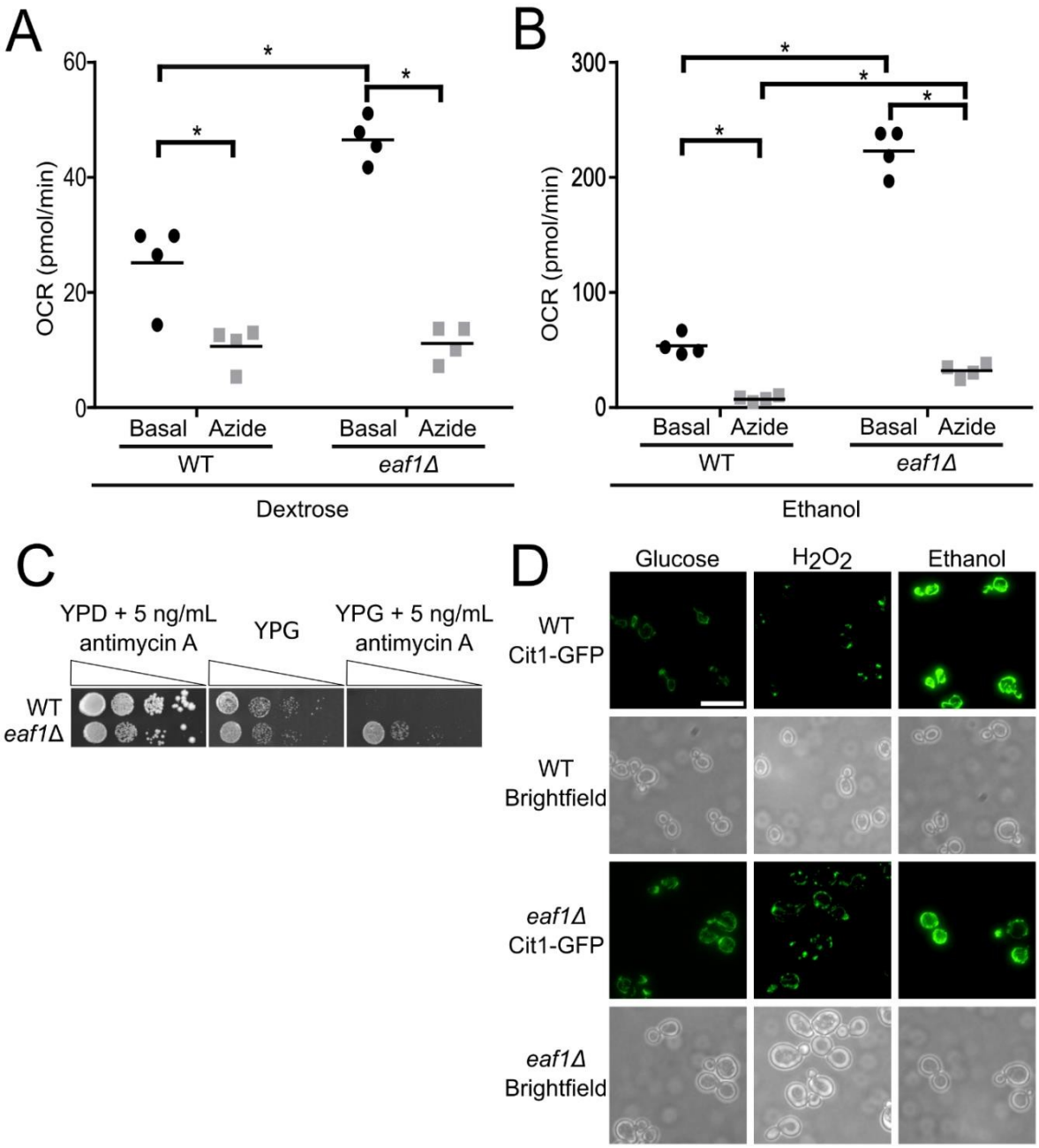

Figure 6.4. *eaf1Δ* mutants have functional mitochondria and are able to respond to biogenesis and fission signals. The oxygen consumption rate (OCR) of either WT or *eaf1Δ* cells was measured using the Seahorse Extracellular Flux Analyzer. After basal measurements, sodium azide was injected into the wells to shut off mitochondrial oxygen consumption and an additional set of measurements were taken. This was performed for (A) cells grown in dextrose media and (B) for cells grown in ethanol media for four biological replicates. ANOVA analysis was performed with a Tukey's multiple comparison test comparing pairs of means. *= $p < 0.05$. Horizontal bars in the data represents the mean. (C) WT and *eaf1Δ* cells were serially diluted onto YP plates containing glucose (YPD) or the nonfermentable glycerol (YPG) in the presence of the mitochondrial complex III inhibitor antimycin A. (D) Mitochondrial responsiveness to environmental stressors was assessed by growing WT and *eaf1Δ* cells in the presence of ethanol to assess biogenesis or H_2O_2 to assess stress induced fission. Scale bar = 10 μm.

Mitochondrial elongation in *eaf1Δ* cells can be partially reversed upon deletion of *BCY1*

We next sought to determine a mechanism by which NuA4 may regulate mitochondrial morphology and volume. We first focused our attention on the AMPK/Snf1 and PKA-Msn2/Msn4 axis as they have both been implicated in mitochondrial dynamics [161,190–193]. Snf1 is a key kinase in yeast metabolic signalling [123]. In response to stress or low availability of glucose, and therefore high AMP, Snf1 kinase is activated and phosphorylates transcription factors leading to the transcription of glucose repressed genes[123]. Snf1 has also been more directly associated with mitochondria by regulating fission, mitophagy, and mitochondrial biogenesis [60,122,194]. The transcription factors Msn2 and Msn4 are activators of glycolysis [172], and they have also been linked to autophagy and mitochondrial respiration [191,195].

Finally, PKA activity has been closely linked to the control of mitochondrial processes through multiple targets [196–202]. Therefore, we assessed the structure of the mitochondria using Cit1-GFP in WT and *eaf1Δ* backgrounds in combination with *snf1Δ*, *msn2msn4Δ*, and *bcy1Δ* (hyperactive PKA) (Figure 6.5). Though the morphology or mitochondrial fraction (mitochondrial volume divided by cellular volume) were not significantly changed in *snf1Δ* or *msn2Δmsn4Δ* cells, there was a slight increase in mitochondrial fraction in *bcy1Δ* cells, however the morphology of the mitochondria was similar to WT (Figure 6.5A). The elongated and branched structure and increased mitochondrial fraction in *eaf1Δ* cells was not impacted by the deletion of *SNF1* or *MSN2/4*. In contrast, mitochondrial structure in *bcy1Δ eaf1Δ* cells did not appear different from *bcy1Δ* cells (Figure 6.5A).

Similarly, there was no significant increase in the mitochondrial fraction in *bcy1Δ eaf1Δ* cells compared to *bcy1Δ* cells (Figure 6.5B and S6.8 Fig.). Our work suggests that NuA4 regulates mitochondrial morphology and volume through a mechanism dependent on the regulatory subunit of PKA, Bcy1, which is independent of Msn2/Msn4.

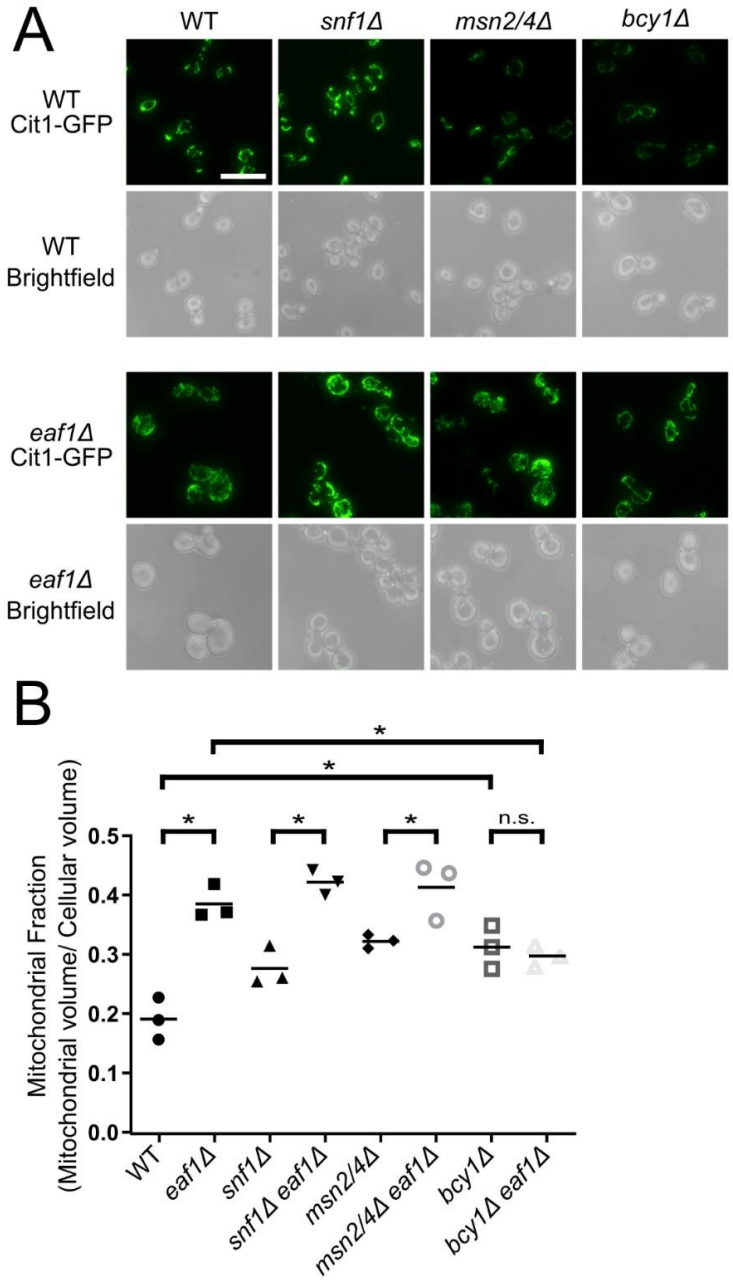

Figure 6.5. The increase in mitochondrial volume in an *eaf1Δ* is partially dependent on Bcy1. (A) Mitochondrial morphology was assessed in the indicated strains expressing the mitochondrial marker Cit1-GFP. Images are representative of three independent biological replicates. Scale bar = 10 μm. (B) The mitochondrial volume was quantified based on the Cit1-GFP fluorescence using the MitoMap plugin for ImageJ which was then divided by the average total cellular volume of the strain to give the Mitochondrial Fraction (Raw cellular

and mitochondrial volume measurements can be found in S6.7 and S6.8 Figs). Images are representative of 3 independent biological replicates and at least 50 cells were quantitated per each biological replicate. ANOVA analysis was performed with a Tukey's multiple comparison test comparing pairs of means. *= $p<0.05$, n.s. = $p> 0.05$, select relevant significance bars shown. Horizontal bars in the data represent the mean.

Bcy1-GFP localization to the nucleus is dependent on NuA4

The glycogen synthesis and mitochondrial content phenotypes identified in the screen are partially, if not fully, dependent on Bcy1, the regulatory subunit of yeast PKA (catalytic subunits are Tpk1/2/3). Additionally, the deletion of *BCY1* appears to reverse the growth defect of an *eaf1Δ* (Figure 6.2B). Interestingly, Bcy1 was also one of the 23 hits from our phenomic screen. While our screen and other studies [163,168] have determined that Bcy1-GFP is enriched in the nucleus in log phase WT cells grown in glucose, upon the deletion of *EAF1* in the same conditions, Bcy1-GFP nuclear signal decreases with an increase in cytoplasmic localization (Figs 6.1B, 6.6A, and 6.6B). Fluorescent intensity profile plots of Bcy1-GFP signal across the whole cell centred on the nucleus indicate that within the population there is an accumulation of Bcy1-GFP in the nucleus of WT cells, however this signal is spread more evenly across *eaf1Δ* cells indicative of dispersion of Bcy1-GFP throughout the cell (Figure 6.6A). The proportion of cells with prominent nuclear localization of Bcy1-GFP was also quantified demonstrating that nuclear localization of Bcy1-GFP is reduced in an *eaf1Δ* (Figure 6.6B). While the localization of at least Tpk1 has been suggested to be associated with Bcy1 localization [163,168], we did not find any associated changes in the localization of Tpk1, 2, or 3 upon deletion of *EAF1* in our screen or in follow up analysis (S6.11 Fig).

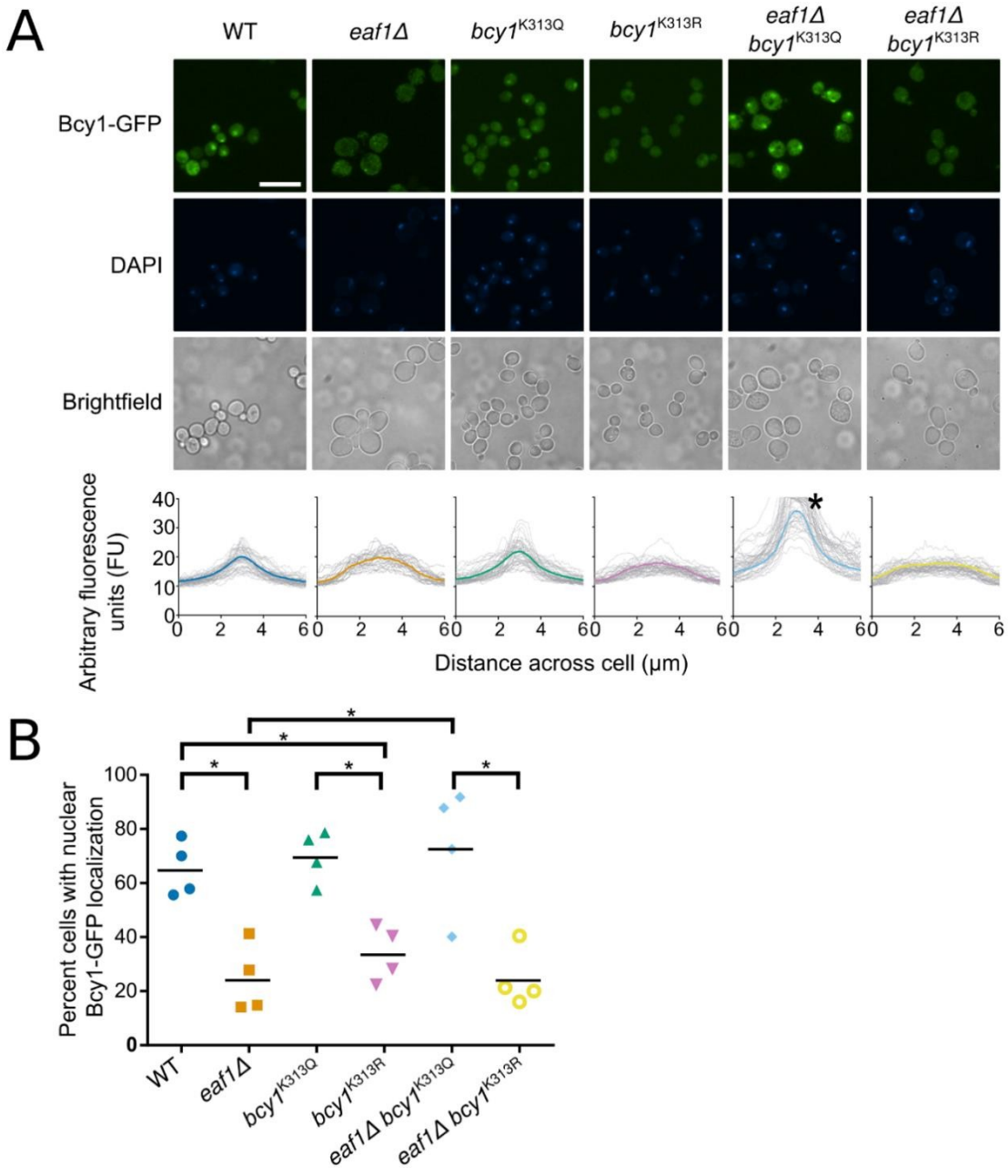

Figure 6.6. Bcy1 nuclear localization is dependent on NuA4 and the acetylation state of Bcy1-K313. (A) The localization of Bcy1-GFP, Bcy1^{K313Q}-GFP and Bcy1^{K313R}-GFP was assessed in WT and *eaf1Δ* yeast. Scale bar = 10 μm. Fluorescent intensity plots of Bcy1-GFP were derived by measuring the fluorescent intensity value of pixels across a nucleus-centered line using Plot Profile in ImageJ Software (Lower panel). The coloured line is the mean of three biological replicates for each strain, and profiles for 50 cells are shown in dotted lines. * For *eaf1Δ bcy1^{K313Q}* the y-axis has been cropped at 40 for comparison. The height of the peak corresponds with the pixel intensity maximum of the nucleus and therefore approximates the abundance of Bcy1-GFP in the nucleus. (B) The percentage of cells with nuclear localization of Bcy1-GFP was calculated for each strain indicated. A minimum of 50 cells were counted for each of the four biological replicates. ANOVA analysis was performed with a Tukey's multiple comparison test comparing pairs of means. *= $p<0.05$, relevant significance bars shown. Horizontal bars in the data represent the mean.

Previous work has suggested that Bcy1 binding to the catalytic subunits of PKA may be regulated through NuA4-dependent acetylation of lysine K313 [52]. It has been proposed that the unacetylated form of Bcy1 can interact with and inhibit PKA subunits, Tpk1/2/3, but when Bcy1 is acetylated by NuA4 the Bcy1-TPK interaction is disrupted leading to activation of PKA. Our work suggests that NuA4 is also regulating Bcy1 localization. Hence, we sought to establish if the acetylation state of Bcy1-K313 affects its localization. We used CRISPR-Cas9 to create the Bcy1^{K313Q}-GFP and Bcy1^{K313R}-GFP mutations in the yeast genome to assess the impact of K313 lysine acetylation on the localization of Bcy1. The structure and electron distribution of arginine (R) is a good resemblance for a lysine residue in the unacetylated state while glutamine (Q) resembles the acetylated form of lysine [203]. We first assessed the nuclear localization of these mutations using DAPI stain as a marker for the nucleus and quantified cells with an enrichment of Bcy1-GFP in the nucleus. The nuclear enrichment is maintained in the Bcy1^{K313Q}-GFP acetylated mimic mutant but not in the Bcy1^{K313R}-GFP unacetylated mimic (Figure 6.6). This suggests that mislocalization of Bcy1-GFP in *eaf1Δ* cells is potentially due to a lack of acetylation on Bcy1-K313. If this hypothesis is correct, we would anticipate that Bcy1^{K313Q}-GFP expressed in *eaf1Δ* cells would restore localization to the nucleus. As expected, the Bcy1^{K313Q}-GFP expressed in *eaf1Δ* background is enriched in the nucleus while the non-acetylatable lysine mimic Bcy1^{K313R}-GFP expressed in *eaf1Δ* is dispersed across the cell (Figure 6.6A and 6.6B). Together our results suggest that the Eaf1-dependent localization of Bcy1 is regulated by the acetylation state of K313.

Bcy1-K313 mutation affects mitochondrial morphology and glycogen content

We next asked whether the Bcy1-K313 dependent change in localization of Bcy1 in *eaf1Δ* cells is contributing to either the increase in glycogen or mitochondrial content. We first assessed mitochondrial morphology and determined that there is slight but not significant increase in the mitochondrial fraction and mitochondrial elongation in both the *bcy1^{K313R}* and *bcy1^{K313Q}* mutants

similar to that of *bcy1*Δ mitochondria (Figure 6.7A and 6.7B, and S6.8 Fig.). Further, both the *bcy1*^{K313Q} and *bcy1*^{K313R} could both slightly suppress the increase in the mitochondrial fraction and the mitochondrial elongation in *eaf1Δ* cells (Figure 6.7A and 6.7B, and S6.8 Fig.) a phenotype similar to the mitochondria of the *bcy1Δ eaf1Δ* (Figs 6.5 and 6.7). As mitochondrial morphology is not significantly different in *bcy1*^{K313R} and *bcy1*^{K313Q} mutants, it suggests that K313 is important for Bcy1 function and is not necessarily acetylation state specific. Therefore, there may also be an additional level of Bcy1 regulation by NuA4 outside of direct K313 acetylation.

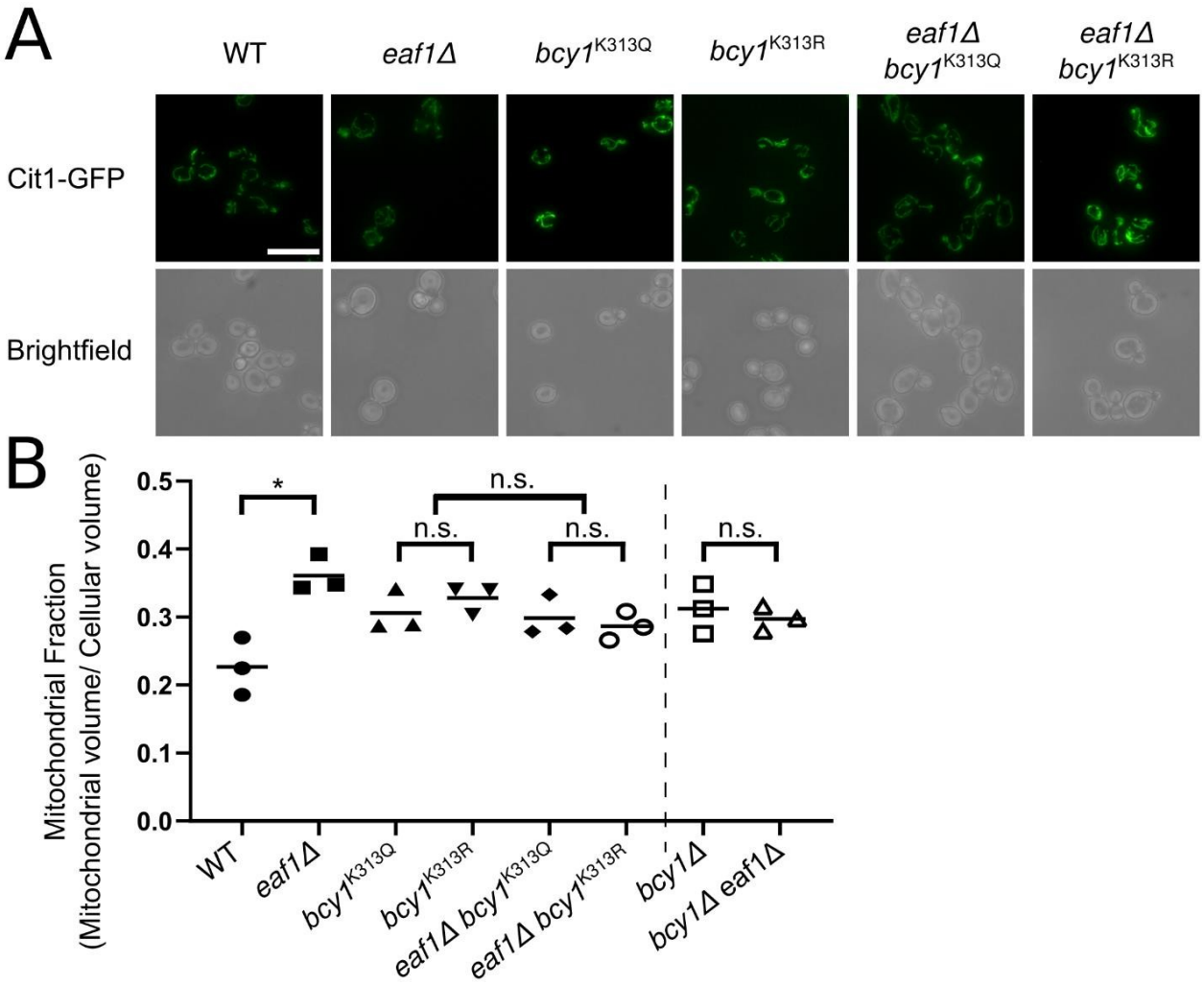

Figure 6.7. Assessment of mitochondrial volume in Bcy1-K313Q/R mutants. (A) The mitochondrial structure and volume were assessed in the indicated strains expressing the mitochondrial marker Cit1-GFP. Scale bar = 10 μm. (B) The mitochondrial volume was quantified based on the Cit1-GFP fluorescence using the MitoMap plugin for ImageJ which was then divided by the average total cellular volume of the strain to give the Mitochondrial Fraction (Raw cellular and mitochondrial volume measurements can be found in S6.7 and S6.8 Figs). Images are representative of 3 independent biological replicates and at least 50 cells per replicate were

analyzed for quantification. This volume was compared to previously calculated *bcy1Δ* and *bcy1Δ eaf1Δ* mitochondrial volume measurements (x-axis break represents experiments previously shown in Figure 6.5). ANOVA analysis was performed with a Tukey's multiple comparison test comparing pairs of means. *= $p<0.05$, n.s. = $p>0.05$, relevant significance bars shown. Horizontal bars in the data represent the mean.

To assess the impact of the *bcy1* mutants on glycogen, we performed both iodine staining of cells and measured glucose released from the hydrolyzed cellular glycogen [185,204]. As expected, the *bcy1*^{K313R} cells displayed higher glycogen levels (darker iodine staining) than WT, *bcy1*^{K313Q}, and *bcy1Δ* cells, yet lower than the *eaf1Δ* cells (Figure 6.8A). However, *bcy1*^{K313Q} cells were also stained darker compared to WT cells, suggesting glycogen levels are increased in both mutants. This may be the result of the inability of a glutamine residue to perform all functionality of an acetylated lysine. The intermediate effects of the *bcy1* mutants were also seen in the suppression of glycogen accumulation in *eaf1Δ* cells. The *bcy1*^{K313Q} *eaf1*Δ appeared consistently slightly lighter in iodine staining that *bcy1*^{K313R} *eaf1*Δ, however the *bcy1*^{K313Q} mutant does not fully suppress glycogen accumulation in *eaf1*Δ cells (Figure 6.8A) [52].

Similar trends were detected by hydrolyzation of cellular glycogen. There was approximately a 15-fold increase in glucose released from *eaf1Δ* cells relative to WT cells (Figure 6.8B). This increase was suppressed by the deletion of *BCY1* in the *eaf1Δ* strain. Consistent with the iodine staining, the glucose released from all of the Bcy1-K313 mutants was closer to the WT cells than the *eaf1Δ* cells. However, while not significant there was a small increase in the glucose released by hydrolyzation in *bcy1*^{K313R} cells compared to the *bcy1*^{K313Q} cells and the *eaf1Δ bcy1*^{K313R} cells did show a significant increase in glucose release relative to the *eaf1Δ bcy1*^{K313Q} cells. This suggests that the accumulation of glycogen in *eaf1*Δ cells is only partially due to decreased acetylation on K313 and mislocalization of Bcy1. Together this suggests that while acetylation state of Bcy1-K313 may regulate its subcellular localization, the acetylation of this target site alone is not fully responsible for NuA4-dependent regulation of mitochondrial morphology or PKA-regulation of glycogen biosynthesis.

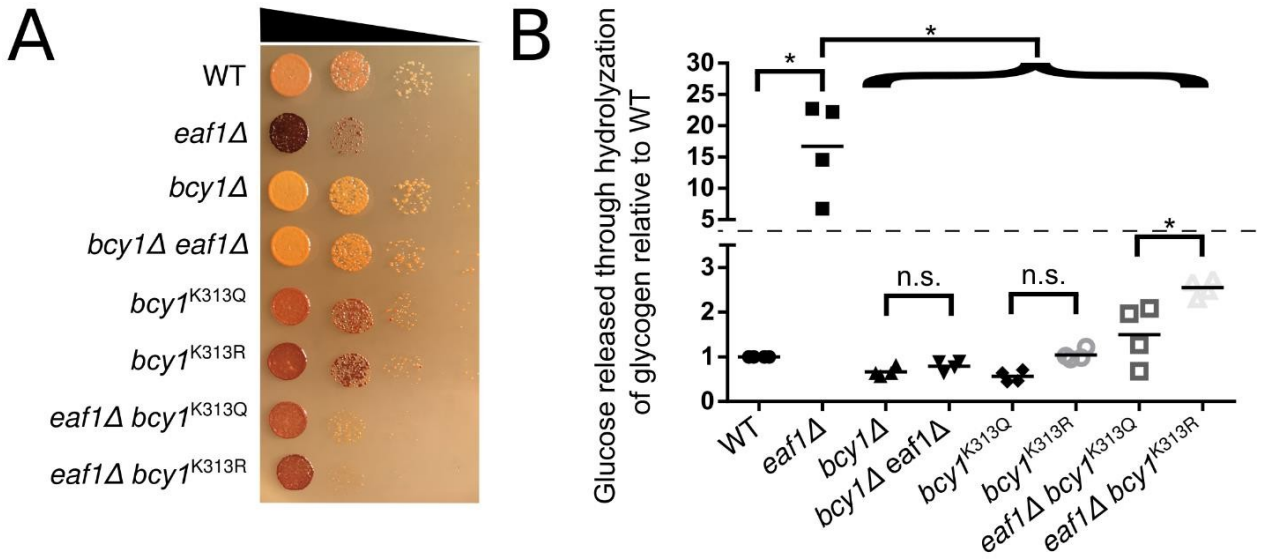

Figure 6.8. Bcy1-K313Q/R mutants partially suppress glycogen accumulation of *eaf1Δ* cells **(**A) Cellular glycogen levels was assessed using iodine staining. The indicated strains were serially diluted on to YPD plates, grown at 30°C for 24 hours prior to exposure to iodine crystals. Darker staining represents more glycogen within the cell. Image is representative of three independent dot assays. (B) Cellular glycogen content was assessed by measuring glucose released from hydrolyzation of glycogen. Cellular glycogen was extracted and treated with amyloglucosidase to break down glycogen into glucose. Glucose was then measured directly using the Glucose Colorimetric/Fluorometric assay kit (Biovision, K606). The amount of glucose released through the hydrolyzation of glycogen in each replicate was normalized to that of the WT strain. The Y-axis is broken (horizontal dotted line) in order to best show the data. ANOVA analysis was performed with a Tukey's multiple comparison test comparing pairs of means. *= $p<0.05$, n.s. = $p>0.05$, relevant significance bars shown. Horizontal bars in the data represent the mean.

PKA phosphorylation substrates are impacted by deletion of *EAF1*

Though mutations that mimic the acetylated and un-acetylated state of Bcy1-K313 impact its interaction with Tpk1/2/3 [52] and its subcellular distribution (Figure 6.6), our work suggests NuA4-regulation of PKA activity maybe more complex than simply acting as an on or off switch through Bcy1 acetylation. Therefore, we next asked if deletion of *EAF1* affects global PKA activity or if only a subset of PKA substrates are impacted. Overall activity of the yeast PKA catalytic subunits (Tpks) was assessed by blotting whole cell extracts from WT and *eaf1Δ* cells with a Phospho-PKA Substrate (RRXS*/T*) antibody, which is commonly used to assess PKA activity [205–207]. Interestingly, in glucose-rich conditions there was no significant difference in total phosphorylation between WT and *eaf1Δ* cells, but there are reproducible distinct changes in substrates detected by the anti-phospho-PKA antibody (Figure 6.9A).

One protein at approximately 100 kDa reproducibly appeared as an increased phosphorylation target in the *eaf1Δ* strains while a protein at 25 kDa appeared to have slightly reduced phosphorylation (Figure 6.9A). As PKA activity is affected by glucose abundance, we also assessed phosphorylation of PKA targets in the WT and *eaf1Δ* cells after 1 hour of glucose starvation. Under glucose starvation the *eaf1Δ* cells had approximately a 30% reduction in total phosphorylation compared to WT cells, including complete loss of some phospho-PKA substrates (Figure 6.9B). These results suggest that NuA4 is not simply turning on or off PKA activity but is playing a potential role in regulating PKA substrates.

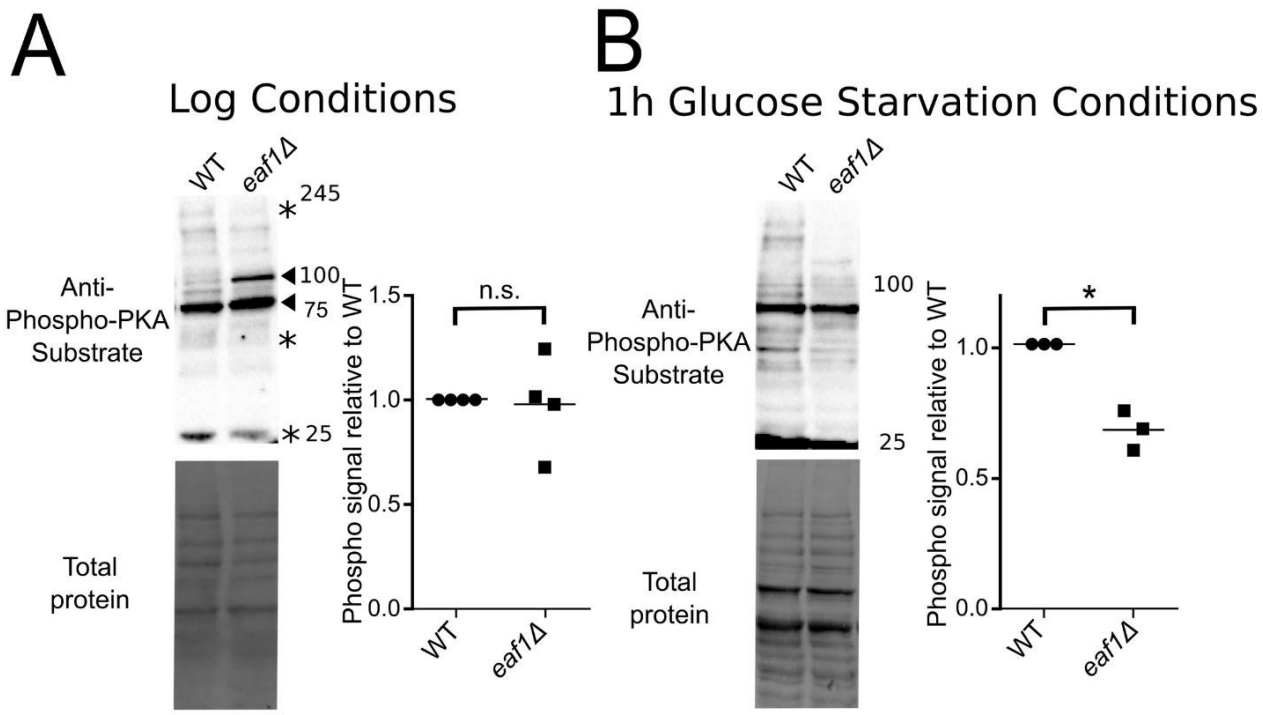

Figure 6.9. PKA activity is altered in an *eaf1Δ.* (A) PKA substrate phosphorylation under glucose rich conditions was assessed by quantitative western blot analysis using whole cell extracts from WT and *eaf1Δ* strains. Panel to the left is a representative of a total phosphorylation and a total protein blot (Stars highlight bands that decreased, and arrows highlight bands that increase in *eaf1Δ* extracts); panel to the right is the quantification of western blots for four independent biological replicates where the total phosphorylation signal intensity was normalized to total protein. (B) PKA substrate phosphorylation under glucose starvation conditions was assessed by quantitative western blot analysis using whole cell extracts from WT and *eaf1Δ* strains that were starved for glucose for 1 hour. Panel to the left is a representative total phosphorylation and total protein blot; panel to the right is the quantification of western blots for three independent biological replicates where the total phosphorylation signal intensity was normalized to total protein.

B. 5 Discussion

We found that 23 metabolic proteins change localization and/or abundance upon disruption of the NuA4 complex (Figure 6.1 and S6.3 Fig.). Remarkably, we determined that the majority of the detected changes, including induction of the glycogen biosynthesis pathway and mitochondrial elongation, were at least partially dependent on NuA4-target Bcy1 (Figs 6.2 and 6.5). Given the well-established role of Bcy1 in regulating the PKA catalytic subunits (Tpk1/2/3), this suggests that many of the cellular impacts of NuA4 on metabolism are likely mediated through regulation of PKA.

How is NuA4 impacting PKA activity? Contrary to many other metabolic enzymes where acetylation is acting as an "on" or "off" switch, our work suggests that NuA4-dependent regulation of PKA is more subtle. Our work suggest a model that in the absence of *EAF1* or NuA4 activity, acetylation of Bcy1-K313 is decreased allowing for Bcy1 to translocate to the cytoplasm altering the inhibition of some or all of the yeast PKA enzymes, Tpk1/2/3 (Figure 6.10). Indeed, upon deletion of *EAF1*, under glucose rich and replete conditions, we demonstrated that substrates detected by the phospho-PKA substrate antibody are not simply globally decreased, but rather altered.

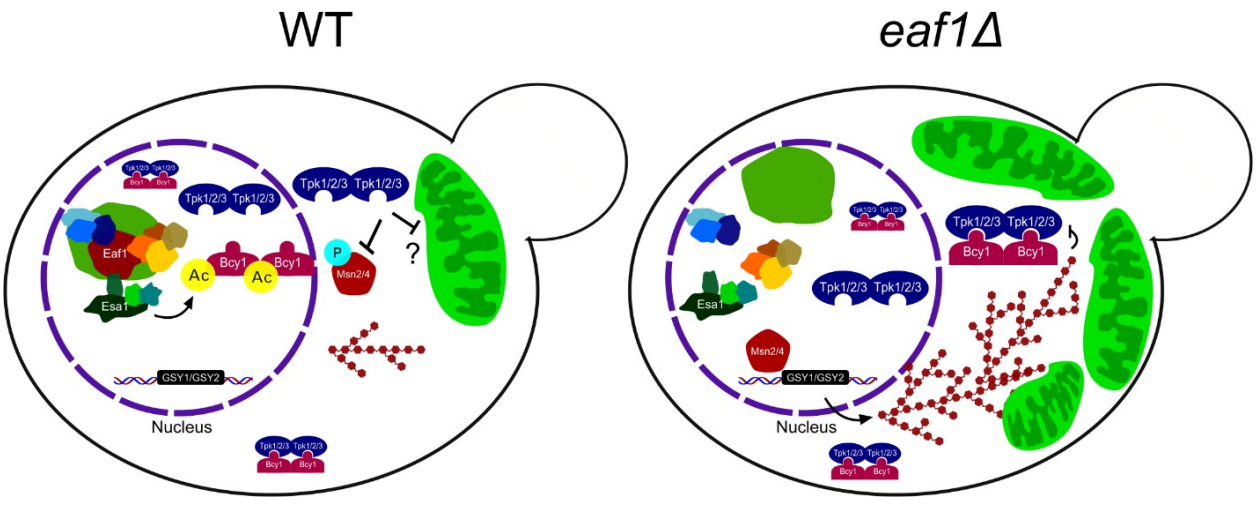

Figure 6.10. Model for regulation of mitochondrial morphology and glycogen synthesis by NuA4. We propose that NuA4 regulates Bcy1 acetylation and subcellular distribution leading to a change in Tpk activity downstream, thereby affecting regulation of mitochondrial volume and glycogen synthesis gene transcription.

NuA4 regulation of glycogen synthesis

Our screen determined that glycogen synthesis pathway proteins are increased in *eaf1Δ cells*, leading to increased glycogen content (Figs 6.2B and 6.8). The small differences between the glycogen content results of the iodine staining and hydrolyzation by amyloglucosidase may be accounted for by difference in the chemistry of these methods [204]. Iodine binds to endogenous glycogen to produce the red/brown colour in the cell while glycogen must be extracted for hydrolyzation then glycogen is indirectly measured through the amount of glucose released [204]. Each have limitations, but together they strongly support that *eaf1Δ* cells have significantly more glycogen than WT. This fits well with the literature demonstrating that *GSY1*, *GSY2*, and *GDB1* are established transcriptional targets of Msn2/Msn4 [172,180,181] and that other Msn2/Msn4-dependent genes are derepressed in NuA4 mutants [79,208]. As the deletion of *EAF1* results in the reduction of nuclear Bcy1-GFP, enriched nuclear Msn2-GFP, and an induction of Gsy2-GFP, a simple explanation is that NuA4 is regulating PKA activity simply through regulation of Bcy1 localization. However, this is not the case as *bcy1^{K313R}* cells do not accumulate glycogen to similar levels of *eaf1Δ* cells (Figure 6.8), despite the fact that Bcy1^{K313R}-GFP has a similar decrease in nuclear enrichment as Bcy1-GFP in *eaf1Δ* cells (Figure 6.6). Even more surprisingly, although the *eaf1Δ bcy1^{K313R}* cells have more glycogen than the *eaf1Δ bcy1^{K313Q}* cells, both have far less glycogen accumulation than the *eaf1Δ* alone. This suggests that NuA4 may also regulate the PKA- Msn2/Msn4 axis through additional mechanisms outside of Bcy1-K313 acetylation.

NuA4 regulation of mitochondrial morphology

How is deletion of *EAF1* resulting in elongation of the mitochondria? A simple explanation could have been that NuA4 regulates transcription of genes required for mitochondrial biogenesis and fusion. However, we determined that Eaf1-dependent mitochondrial changes are not mediated by Msn2/4 (Figure 6.5) or Hap4 (S6.10 Fig). Indeed, transcriptome studies do not indicate any up-

regulation of genes involved in mitochondrial biogenesis, fusion, or fission upon deletion of *EAF1* [67], suggesting NuA4's impact on mitochondrial morphology is not due to transcriptional defects.

We found that the mitochondrial defects in *eaf1*Δ cells can be partially rescued by deletion of *BCY1* (Figure 6.5), which suggests that altered PKA activity in NuA4 mutants contributes to mitochondrial elongation. However, deletion of *BCY1* or mutation of Bcy1-K313 to either R or Q resulted in increases in the mitochondrial fraction per cell, albeit not as high as seen in *eaf1Δ* cells (Figs 6.5 and 6.7). This suggests that both K313 mutants have compromised Bcy1 function that results in increased mitochondrial function.

At first, this seems counter intuitive. How could *bcy1*Δ cells with increased PKA activity and *eaf1Δ* cells that we show have altered PKA activity and many hallmarks of decreased PKA activity, both lead to increased mitochondrial content? Our work suggests that NuA4 and acetylation of Bcy1 is not simply acting as an on or off switch for PKA activity. Rather, we show that under glucose rich conditions, deletion of *EAF1*, and presumably the collapse of NuA4, alters the PKA-substrate profile, with some phospho-PKA substrates increasing while others decreasing (Figure 6.9). Though one cannot rule out the possibility that deletion of *EAF1* is impacting the protein levels of PKA substrates, indeed our high content screen does detect changes in protein levels (Figure 6.1 and S6.2 Fig), overall the impact of *EAF1* on global transcription is minor [67]. Future studies will be needed to identify the extent by which NuA4 impacts PKA activity and substrate selection, including through acetylation of Bcy1 or other mechanisms.

Interestingly, PKA has been extensively linked to various aspects of mitochondrial regulation, including biogenesis and disassembly. PKA activity has been generally demonstrated to promote mitochondrial fusion and function, explaining why the deletion of *BCY1* alone may result in slightly more mitochondria than in WT cells [164]. Studies have shown that PKA phosphorylates Drp1, a key mitochondrial fission protein, inhibiting its function and promoting fusion [209,210]. Similarly, PKA phosphorylates MIC60 reducing PINK1 presence at the mitochondria, preventing mitochondrial degradation [211]. Additionally, deleting *BCY1* and high cAMP conditions, both of which should increase PKA activity, each led to an increase in mitochondrial content in yeast, while deletion of *TPK3* (one of the yeast PKA catalytic subunits) was associated with a decrease in cytochrome C content [161,212]. Outside of overall mitochondrial structure and content regulation PKA also directly phosphorylates members of the electron transport chain as well as translocase of the outer membrane (TOM) proteins responsible for mitochondrial protein import [199–201]. Finally, PKA activity has been associated with mitochondriogenesis through phosphorylation and activation of CREB leading to transcription of PGC1α, a key cotranslational activator of mitochondriogenesis [167,213].

Given this research, it is clear that NuA4 is regulating mitochondrial elongation through PKA, but the mechanism(s) remain to be established. There are complex nuances associated with PKA signalling, and perhaps it is not as cut and dry as increased versus decreased PKA activity affecting mitochondrial regulation. For example, PKA dependent phosphorylation of two different apoptotic proteins Bad and Bim has opposite functions, preventing and promoting apoptosis respectively [214–216]. While we did not see large scale changes in the localization of any of the Tpk subunits in an *eaf1Δ* when compared to WT (S6.11 Fig), we cannot rule out that NuA4 is modulating distinct pools of PKA (e.g., Tpk1 vs Tpk2, or different compartmentalized

groups) that have different effects on mitochondrial biology. Indeed, due to functional redundancies, the biological roles of individual PKA subunits in yeast have yet to be discerned in detail.

NuA4 dependent regulation of Bcy1 subcellular localization

Previous high throughput protein-fragment complementation assay (PCA) studies identified a role for NuA4 in regulating PKA [52]. In particular, this study determined that upon deletion of *EAF1* or *EAF7* the Tpk1-Bcy1 (PKA1) interaction is increased under both glucose and galactose conditions, however Tpk2-Bcy1 (PKA2) was not impacted, supporting the idea that NuA4 may differentially regulate the individual PKA subunits. Further, through PCA-based assay in mammalian cells they showed that increasing acetylation through either overexpression of KATs or inhibition of KDACs results in a reduction of PKA type II interactions. Though not directly tested, it was proposed that acetylation of Bcy1-K313 reduced its interaction with Tpk1, hence relieving inhibition of PKA. While this may be the case, our work shows that Eaf1 (and presumably NuA4) and acetylation are regulating the subcellular localization of Bcy1. Bcy1-GFP is predominantly nuclear in glucose grown cells [163] while in the absence of *EAF1,* Bcy1-GFP is present in both nuclear and cytoplasmic compartments (Figs 6.1 and 6.6). Further, Bcy1^{K313R}-GFP, which mimics the unacetylated state, displays a similar disperse cellular signal as seen for Bcy1-GFP in *eaf1Δ* cells, and the Bcy1^{K313Q} -GFP mutant maintains a nuclear localization even when *EAF1* is deleted (Figure 6.6).

The subcellular localization of Bcy1 is extremely important as the compartmentalization of PKA components plays a role in regulating its activity [169]. For example, in the mammalian system, specific A- Kinase anchor proteins (AKAPs) have evolved to localize PKA to different areas of the cell [169,217]. While mammalian AKAP homologs have not been identified in yeast, the

localization of yeast PKA members is dependent on carbon source availability and environmental stresses and many interacting proteins have been identified [163,169,218]. In glucose, Bcy1 is predominantly nuclear [163,169], however upon glucose starvation or when grown in non-fermentable Ethanol or Glycerol media, Bcy1 has a nucleo-cytoplasmic distribution [163,169]. In contrast, each TPK subunit has distinct subcellular distribution, while Tpk2 is predominantly nuclear, Tpk1 and Tpk3 are evenly distributed between nucleus and cytoplasm under logarithmic growth in glucose. Interestingly, when cells enter stationary phase, while Tpk1 and Bcy1 are distributed across the cytoplasm and nucleus, Tpk2 and Tpk3 are enriched in P-bodies that are largely devoid of Bcy1 [169]. In the absence of nuclear localized Bcy1, others have shown that nuclear Tpk1 is also reduced, suggesting Bcy1 may not only regulate PKA activity but sequester PKA catalytic subunits to specific locations [163]. Interestingly, while we determined that upon deletion of *EAF1,* Bcy1-GFP nuclear localization is reduced (Figs 6.1 and 6.6), we did not see a change in Tpk1-GFP subcellular distribution (S6.11 Fig). The fact that Tpk1 localization is not dramatically altered in an *eaf1Δ* cell suggests that enough Bcy1 remains in the nucleus to maintain pools of Tpk1 in the nucleus. Alternatively, while our screen and direct analysis did not detect any dramatic changes in the localization or abundance of the Tpks, we cannot rule out if subtle changes in Tpk1, Tpk2, and Tpk3 subcellular localization are regulated by NuA4 through Bcy1-K313 acetylation or other means. Further exploration will require detailed temporal and spatial analysis of subcellular localization and activity of individual PKA subunits upon modulation of NuA4 activity.

As the disperse localization of Bcy1-GFP in *eaf1Δ* cells grown in glucose conditions (Figure 6.6) looks similar to localization of Bcy1-GFP upon glucose deprivation [163,168], one

simple explanation is that *eaf1Δ* cells are defective for glucose sensing resulting in the mislocalization of Bcy1-GFP indirectly.

However, our work suggests that subcellular localization is dependent on the acetylation state of Bcy1- K313 (Figure 6.6), which suggests NuA4 is directly regulating Bcy1 localization through acetylation. Presently it is not known if NuA4 activity changes upon starvation or glucose deprivation, however NuA4 is implicated in regulating stress granule formation upon glucose deprivation [173] and glucose-starvation apoptosis in cancer cells [88]. Therefore, it will be interesting to determine if the acetylation state of Bcy1 changes upon glucose deprivation and if so, if this is dependent on NuA4.

Regulation of Bcy1 localization by post-translational modification is not new. The Yak1-dependent phosphorylation of the N-terminal domain of Bcy1 drives its localization to the cytoplasm where it is retained by Zds1 [163,168]. Interestingly the Bcy1-K313 site is not within the established N- terminal clusters required for interaction with Zds1 and cytoplasmic localization of Bcy1. This suggest that other proteins may be interacting with the acetylated or unacetylated versions of Bcy1 aiding in changing its subcellular distributions. Though we or others have yet to establish if acetylation of Bcy1 is also impacting the physical interaction with TPKs, what is clear is that deleting *EAF1* decreases Bcy1 nuclear localization and results in phenotypes that suggest PKA activity is decreased, including increased glycogen production, Msn2 relocalization to the nucleus, and mitochondriogenesis (Figs 6.1, 6.2, and 6.7). However, localization of Bcy1 is clearly not the only contributor of NuA4-dependent regulation of PKA activity, as $bcy1^{K313R}$ and $bcy1^{K313Q}$ mutants, despite having strong separation of Bcy1 localization (Figure 6.6), have similar impacts on mitochondria morphology and only small differential impacts on glycogen accumulation (Figs 6.7 and 6.8). One possibility that should be considered is that while K to R

and K to Q are used as mimics for acetylation states *in vivo*, these are in fact not ideal. For example, NuA4 has been shown to regulate the oxysterol binding protein Kes1 *in vivo*, but the Kes1 acetylated and unacetylated mimics proteins do not fully replicate Kes1 acetylated and unacetylated proteins *in vitro* biochemical assays [134]. The limitation of these acetylation state mimics may explain why the *bcy1*^{K313R} and *bcy1*^{K313Q} mutants appear to act similarly to each other in some cases. However, their additional similarity to *bcy1*Δ and differences from WT and *eaf1Δ* in terms of mitochondrial morphology and glycogen content does support an important function of the K3l3 position of Bcy1, although how NuA4 dependent acetylation of this residue is involved awaits further study.

B. 6 Conclusions

Our results clearly demonstrate that NuA4 is regulating the localization of a master regulator of cellular metabolism, Bcy1, the regulatory subunit PKA. Additionally, both the increased glycogen synthesis proteins and mitochondrial elongation of *eaf1*Δ cells identified in our screen are dependent on Bcy1, and PKA activity is altered upon deletion of *EAF1*, supporting our proposed PKA regulation.

Finally, our screen suggests that NuA4 may be regulating multiple metabolic pathways through the localization of proteins. Taken together, our work indicates that human homolog of NuA4, Tip60, may play a key role in controlling cellular metabolism, perhaps explaining how aberrant Tip60 function may be important in the development of human disease.

B. 7 Materials and Methods

Strains and culturing conditions

The BY4741 (S288C) strain was used throughout this work. A list of yeast strains used in this study can be found in S6.3 Table. The GFP collection was used for the phenomic screening [42]. Additional GFP-tag and deletion mutants were taken from the GFP collection [42] or deletion mutant array (DMA) (GE, CAT# YSC1053) or were made by PCR-mediated insertion/deletion [219]. All strains listed (S2.3 Table) were confirmed by PCR. Yeast were cultured at 30°C in YPD, unless otherwise specified. Yeast cultures were grown by shaking in YPD (1% yeast extract, 2% peptone, 2% dextrose) at 30°C unless otherwise stated. In preparation for experiments, yeast were grown overnight in YPD before being diluted to an OD600 of 0.1 (or 0.15 for *eaf1Δ*) in the morning and grown to mid log (OD600 = 0.5-0.8).

High content screen

A focused mini array of 407 metabolic-associated GFP-tagged genes were extracted from the GFP library (*MATa* ORF-GFP::HIS) [42]. The genes were selected based on literature review and the Saccharomyces Genome Database (SGD) (List of Genes in S6.1 Table) and fell into categories relating to metabolic processes, gluconeogenesis, changes in regulation dependent on glucose, glucose import, cAMP, and AMPK. Using synthetic genetic array technology [175] and the Singer HTP robotic platform, the GFP fusion metabolic strain mini array was mated to a WT (*ura3Δ:*:NAT) or *eaf1Δ* (*eaf1Δ*::NAT) query strains to create both WT and *eaf1*Δ GFP fusion arrays as previously described [41].

Strains generated for the focused high throughput microscopy screen were grown overnight and diluted to 0.1 in the morning. Once they had reached log-phase (OD600 =0.4-0.7), the cells were collected and diluted in SC media before being plated onto concavalin A-treated 96-well imaging plates. Plated cells were centrifuged and washed twice with SC media. Fluorescent images were taken using a CellVoyager CV1000 disk confocal microscope

(Yokogawa Electric Corporation, Musashino Tokyo, Japan). All images were initially captured at a 300 ms exposure for the GFP channel, 30 z-stacked images were taken using the GFP signal with 30 corresponding brightfield images. Two fields of view with at least 35 cells each were captured for each strain (most fields had in the range of 75-200 cells). Images were manually compared for differences in GFP signal between the WT and *eaf1Δ* backgrounds of each GFP-tagged protein by three independent researchers. Each WT- *eaf1Δ* pair was assessed for changes in where the GFP signal was localized and for obvious abundance differences based on GFP intensity in the cell. Additionally, the overall intensity of the WT and *eaf1Δ* images were compared using an in house macro-based batch analysis in ImageJ comparing mean grey value per cell. Two fields of view were analyzed for each strain. Cells were highlighted as regions of interest (ROIs) using the brightfield image to define the cell limits and those ROIs were used to measure the GFP signal intensity per cell. The mean grey value per cell was measured as it removed issues with differences in cell size between the WT and *eaf1Δ* strains. The mean grey value of the measured cells was then averaged for each image and the average mean cell intensity of the *eaf1Δ* image was divided by the average mean cell intensity of a paired WT image. This gave a measurement of the change in the intensity of the GFP signal of each protein in an *eaf1Δ* cell relative to WT cell. Changes in intensity were ranked and primary hits were selected as strains having a greater than 1.3-fold increase or 0.7-fold decrease in intensity in the *eaf1Δ* relative to WT. The top 70 ranked images from the manual analysis were also reanalyzed a second time using the same batch analysis comparison of the mean GFP intensity per cell. If changes were detected through the manual scoring or the intensity measurements, they were reconfirmed in another round of microscopy, and top consistent changes were selected resulting in the confirmed set. Localization of the proteins and their associated changes were categorized

based on the well characterized WT localization of GFP-tagged proteins in the CYCLoPs database and literature review [41,220].

Microscopy

All additional microscopy was done using a Leica fluorescent microscope (DMI6000; Leica Microsystems) equipped with a high-performance camera (Hamamatsu), DG4 light source (Sutter Instruments) and Volocity 4.3.2 software (PerkinElmer). Strains were grown to mid log, spun down to collect live cell pellet and resuspended in SC media containing glucose for live GFP and brightfield imaging. As indicated, cells were stained with DAPI (Sigma) prior to spinning down culture. DAPI was added to the liquid culture at a concentration of 1 μg/mL plus 0.1% Triton X-100 (CSH protocols).

Mitochondrial volume was assessed using the MitoMap plugin for ImageJ [186]. Images were corrected to scale dimensions using SetScale. Individual cells were selected and analyzed with the MitoMap plugin [186]. This plugin identifies pixels highlighted with the Cit1-GFP signal and quantifies the volume and surface area of the input mitochondria, for our analysis volume was used. For all quantifications, a minimum of 50 cells were analyzed per replicate.

To test mitochondrial response to ethanol, yeast were grown overnight, diluted to OD600 of 0.1 in Yeast Peptone media supplemented with 3% ethanol, a non-fermentable carbon source, and grown to mid log phase before imaging by microscopy. For the fragmentation assay, Hydrogen peroxide was added to mid log day cultures at a final concentration of 4 μM and the cultures were returned to the incubator for 30 minutes before analysis by fluorescent microscopy as described above.

Bcy1-GFP fluorescence was first quantified manually by percent cells with prominent nuclear localization. Additionally, a profile of Bcy1-GFP intensity was measured using ImageJ

Software and compressed z-stack images [221]. A 60 unit (6.23 μm) long line was placed across the nucleus of the cell (centred on the nucleus), and Plot Profile analysis was performed to give the fluorescent intensity value of pixels along the line. This was repeated for three biological replicates of 25 cells for each sample. The mean of all replicates was plotted on a representative graph for sample comparison.

Serial dilution spot assays

Cultures were grown to mid log in YPD before being diluted to an OD600 of 0.1 and three 10- fold serial dilutions (0.01, 0.001, 0.0001). 5 μL of the serial dilutions were spotted onto the indicated plates. To make drug plates, a stock solution of antimycin A (Sigma) was created in 95% Ethanol and was used to create final plates with a concentration of 5 ng/mL. Iodine staining was performed after dot assay growth as described below.

Glycogen Assays

For analysis by iodine staining, spot assays were prepared as above and iodine glycogen assays were performed as previously described [222]. After 24 hours of growth on plain YPD, plates were inverted over iodine crystals for 3-5 minutes, exposing the yeast to the vapours and causing them to stain relative to the abundance of glycogen.

Quantitative measurements of glycogen were assessed by extracting glycogen from cells and treating extracts with amyloglucosidase. This enzyme breaks down glycogen into glucose which can then be measured directly. Cultures of yeast were grown in 100 mL to mid log and a volume of yeast equivalent to 25 ODs was spun down to collect a yeast pellet. Pellets were washed twice in water prior to being flash frozen in liquid nitrogen and stored at -80^{o}C. Pellets were thawed in 500 uL of 0.25 M Na_2CO_3, vortexed, and boiled at 95^{o}C for 4h. Glycogen (Sigma) was used as a control. The pH of the samples was adjusted by adding 300ul of 1M acetic

acid and 1200 ul 0.2M NaOAc pH 5.2. Half of the sample was kept as the no enzyme control and to the other half 20 ul of 20mg/ml amyloglucosidase (Sigma, 10115, 70U/mg protein) was added prior to an overnight incubation at 57^{o}C overnight.

The digested samples were centrifuged, and supernatants were collected. The glucose released by digestion in each sample was diluted and analyzed using the Glucose Colorimetric/Fluorometric assay kit (Biovision, K606) according to the manufacturer's protocol.

Growth curve analysis

Cultures were grown to mid log in YPD before being diluted to an OD600 of 0.1 in YPD. 200uL of this dilution was plated into a BioScreen C honeycomb plate. The plate was incubated at 30^{o}c for 48h in a BioScreen C plate reader which collected OD600 readings every 15 minutes. Growth curve data was averaged for 3 technical replicates then 3 biological replicates and plotted for the first 24 hours. The doubling time for each strain was calculated based on the slope of the log (OD600) curve during log growth of the strain (between 3 and 7.5 hours). Doubling time = Δ t*Log (2)/ (Log (OD600@t2/OD600@t1)).

Quantitative Western blot

Yeast strains were grown overnight in YPD and diluted into 50 mL cultures in the morning to an OD600 of 0.1. Cells were harvested at mid log and whole cell extracts were collected as previously described [79]. Briefly, cells were collected by centrifugation and pellets were flash frozen in liquid nitrogen and stored at -80^{o}C. The cell pellets were thawed in 3x the pellet volume of lysis buffer (20 mM HEPES, pH 7.4, 0.1% Tween 20, 2 mM $MgCl_2$, 300 mM NaCl, protease inhibitor cocktail [P-8215; Sigma]) and lysed using bead beating 6 times for 1 minute with an equal volume of glass beads (Fisher 35-5350).

Whole cell extracts were collected by centrifugation and quantified using a Bradford assay. In the case of glucose starvation, cultures were grown to mid log, spun down and washed 2x in YP (glucose free) media and resuspended in YP for 1 hour of growth at 30^{o}C before collecting pellets and freezing as above.

A standard curve for each protein was performed to determine the optimal amount of protein to be loaded on TGX quantitative gels for western blot [223]. For Gsy2-GFP, 40 µg of protein was found to be optimal, so this was loaded onto TGX gels, run, and a standard western blot protocol for TGX gels was followed. Following electrophoresis, the gel was activated and visualized by UV before being transferred onto nitrocellulose (Bio-Rad 1620112). Total protein was imaged using UV. For GFP blots, the blots were blocked in 5% skim milk in PBS-T (phosphate buffered saline + 1% Tween 20) before incubation overnight with a 1: 500 dilution of anti-GFP primary antibody (Sigma-Aldrich 11874460000) in 5% milk PBS-T. Next blots were washed 3X in PBS-T, incubated for 1h with goat-anti-mouse secondary antibody (BioRad; cat. # 170–6516) at 1: 2500 in 5% milk PBS-T and washed 3 times. A similar procedure was followed for the PKA assay but blocking and antibodies were done in 3% Bovine Serum Albumin (BSA Sigma-Aldrich A7906). For PKA activity 80 µg of protein was run and the Phospho-PKA Substrate (RRXS*/T*) (Cell Signaling 100G7E) primary was used followed by a goat-anti-rabbit secondary antibody (BioRad; cat. # 170-6515). Finally, blots were incubated with Clarity Western ECL substrate (Bio-Rad 170-5061) and imaged using the Bio-Rad ChemiDoc imaging system. Relative protein abundance of our proteins of interest was quantified using the Image Lab software (Bio-Rad) and each band was normalized to the total protein signal of the lane then calculated relative to the WT signal of the protein.

qPCR

Yeast were prepared in YPD, and 30 mL of OD600 = 0.5 cells were pelleted and washed with water before flash freezing in liquid nitrogen. Cell pellets were thawed in an equal volume of lyticase reaction solution (1.2 M sorbitol + 1 mg/mL lyticase (Sigma)) then incubated at 30ºC for 30 min. Cell lysis and RNA purification were then performed using the Ambion PureLink RNA Mini Kit according to manufacturer's instructions. Briefly, cells were lysed by vortexing in lysis buffer with 2-mercaptoethanol and extracts collected following centrifugation. Ethanol was added to disrupt enzymatic function and RNA was purified and collected using a spin cartridge. RNA extracts were then treated with DNase I for 1 h at 37oC before performing a phenol/chloroform/isoamyl extraction and measuring RNA concentration by nanodrop. At this point the quality of the RNA was assessed by agarose gel. 2 μg of the mRNA was reverse transcribed using the High-Capacity cDNA Reverse Transcription Kit (Applied Biosystems).

Serial dilutions of the cDNA product were performed and a pooled standard curve to determine optimal dilution for each transcript type. mRNA transcript levels were measured using the SsoFast EvaGreen Supermix for qPCR (Bio-Rad) with the appropriate primer pairs (S2.4 Table). The data for each experiment was normalized to the chosen internal control (*TDH3* mRNA) and then compared to WT using the ΔΔCt method.

Seahorse Assays

Seahorse assays were performed as previously described [224]**.** Briefly**,** Yeast cultures were grown overnight in YPD and in the morning they were split and diluted to an OD600 of 0.1 in YPD or 0.25 in YPE (Yeast Peptone Ethanol 3%), grown to mid log (OD600 of 0.5- 0.7) prior to cells being pelleted (3000 RPM for 3 min) and resuspended into yeast seahorse assay media (0.167% yeast nitrogen base, 0.5% ammonium sulfate, and 3% ethanol or 2% dextrose respectively). Cells were counted and diluted to a concentration of 2.8 x 10^6 cells/mL in yeast

seahorse media. 180 µL of the cell dilutions were used to seed the wells of a Seahorse XF96 cell culture microplate (Agilent) that had been pre-treated with poly-l- lysine to enable cell adhesion (MilliporeSigma). A minimum of 8 technical replicates were performed for each experiment. The seeded plate was centrifuged at 500 RPM for 3 min to promote yeast adhesion and the plate was rested for 30 min at 30°C. A soaked and calibrated Seahorse XF96 Sensor Cartridge was prepared with 0.5% sodium azide (Sigma) injection in chamber A before loading into the Seahorse XF96 analyzer (Agilent) and measurement of oxygen consumption rate (OCR) of the yeast in the cell culture microplate. Measurements were performed at 30°C. Three basal OCR measurements were taken for 3 minutes each with 1.5 minutes of mixing between measurements. Sodium azide was then programmed to be injected and three additional OCR measurements were performed for 3 min with 1.5 minutes of mixing between.

Acetylation mimics/CRISPR-Cas9

Point mutations on Bcy1 at the lysine 313 (K313) site were performed by targeting with CRISPR- Cas9 to cut the DNA and introducing a homologous strand of DNA with the mutation of interest. The lysine 313 site of Bcy1 was mutated to a Glutamine (Q) or Arginine (R) to represent an unacetylated and an acetylated form of Bcy1 (K313Q and K313R).

The general DiCarlo *et. al*. protocol was followed with minor adjustments. Briefly, the Cas9 plasmid, p414-TEF1p-Cas9-CYC1t [225], was transformed using lithium acetate into the Bcy1-GFP, Bcy1- GFP *eaf1Δ*, Cit1-GFP, and cit1-GFP *eaf1Δ* strains and maintained by growth on SC-LEU. In parallel to account for problems with off target effects, two different PAM sequences targeting the Bcy1-K313 area were cloned into the guide RNA plasmid, p426-SNR52p-NotI (gRNA)-SUP4t by PCR amplification.

These sequences were selected from DiCarlo and colleague's list [225]. Following PCR, the resulting plasmid was treated with DPN1, transformed into DH5α *E. coli* for amplification, and sent for sequencing at the TCAG facility (SickKids) to confirm guide RNA incorporation. Double stranded DNA homologous to the area to be cleaved but containing the mutations to the K313 and the NGG PAM site was prepared by ordering single stranded oligos and annealing them at 100^{o}C and slowly ramping down the temperature. The dsDNA for homologous repair and the corresponding guide RNA plasmid were transformed using lithium acetate into the strains pre-prepared with the Cas9 expression plasmid.

Transformed cells were selected on SC-LEU-URA and positive colonies were collected, genomic DNA extracted, and a PCR of the area of interest was performed, which was then sent for sequencing at the TCAG Facility (SickKids, Toronto) to confirm the mutation in the genome.

Statistical Analyses information

Statistical analyses were performed using GraphPad Prism. When comparing two groups a student's t-test was performed. In the case of more than two groups a 2-way ANOVA was performed, and individual pairs were compared by a Tukey's multiple comparison test comparing each mean to the mean of every other group. For all analyses, a $p < 0.05$ to define significance was used.

Acknowledgements

We thank Brenda Andrews and Christian Landry for providing strains and plasmids.

Appendix C: First Author Paper (Graduate Student Finances in Canada)

Analysis of financial challenges faced by graduate students in Canada

Sarah Jane Laframboise,[1,2] Thomas Bailey, [1,2] Anh-Thu Dang, [1,2] Mercedes Rose, [1,2] Zier Zhou, [1,2] Matthew D. Berg, [3] Stephen Holland, [1,2] Sami Aftab Abdul, [1,2] Kaela O'Connor, [1,2] Sara El-Sahli, [1,2] Dominique M. Boucher, [1,2] Garrett Fairman, [1,2] Jacky Deng, [1,2] Katherine Shaw, [1,2] Nathaniel Noblett, [1,2] Alexa D'Addario, [1,2] Madelaine Empey, [1,2] and Keaton Sinclair[1,2]

[1]University of Ottawa, Ottawa, ON, Canada
[2]Ottawa Science Policy Network, University of Ottawa, Ottawa, ON, Canada
[3]Canadian Society of Molecular Biosciences, Ottawa, ON, Canada

C. 1 Author contributions

S.J.L. Author Contributions: Conceptualization, Data curation, Formal analysis, Investigation, Methodology, Project administration, Resources, Supervision, Validation, Visualization, Writing – original draft, and Writing – review & editing.

C. 2 Abstract

Graduate students are vital to the creation of research and innovation in Canada. The National Graduate Student Finance Survey was launched in 2021 by the Ottawa Science Policy Network to investigate the financial realities of Canadian graduate students. Closing in April 2022, the survey received 1305 responses from graduate students representing various geographical locations, years of study, fields of education, and demographic backgrounds. The results capture a snapshot into graduate student finances, including an in-depth analysis of stipends, scholarships, debt, tuition, and living expenses. In its entirety, we found that the majority of graduate students are facing serious financial concerns. This is largely due to stagnant funding for students both from federal and provincial granting agencies and from within their institutions. This reality is even worse for international students, members of historically underrepresented communities, and those with dependents, all of whom experience additional challenges that impact their financial security. Based on our findings, we propose several recommendations to the Tri-Council agencies (Natural Sciences and Engineering Research Council, Social Science and Humanities Research Council, and Canadian Institute for Health Research) and academic institutions to strengthen graduate student finances and help sustain the future of research in Canada.

C. 3 Introduction

Graduate students play a large role in the research and innovation ecosystem in Canada. These students have already completed a bachelor's degree and are enrolled in a master's or doctoral degree. Most graduate degrees include full-time, independent research in collaboration with a Principal Investigator or supervisor, who is a faculty member at a university. This work requires laborious training and creates the foundation of research in Canada. Research has shown that one-third of publications feature PhD students as either authors or co-authors (Lariviére 2012), exemplifying the crucial role that graduate students play in research and academic publications.

Since graduate students are often enrolled in full-time studies, many receive a stipend intended to offset living costs so that they can focus on their studies. The source of this funding for graduate students can be complex. In Canada, funding comes from two main sources: (1) directly through scholarships, such as those provided by the three federal granting agencies, known as the Tri-Council (Natural Sciences and Engineering Research Council (NSERC), Social Science and Humanities Research Council (SSHRC), and the Canadian Institute for Health Research (CIHR)) or (2) indirectly through their supervisor's research grants and(or) department funding. As such, graduate student pay is often referred to as a stipend, since it is often a fixed pay, independent from work performed. Stipends can vary among graduate students and depend on many factors. For example, some students may be required to complete teaching assistantships (TAs) in which they assist a professor with instructional responsibilities or research assistantships (RAs) in which they assist a professor or instructor with additional research activities such as performance of clerical, laboratory, or technical tasks as part of their stipend.

The value of graduate student stipends can be set by universities, faculties, departments, and supervisors. It appears that, in the absence of any other government guidance, federal Tri-Council scholarship values have set the precedent for stipend values. However, it is important to acknowledge that these scholarships have not changed in value since 2003. Additionally, there has been little increase in the number of available Canadian scholarships over the years. A 2018 report from the Science and Policy Exchange (SPE) revealed that 91% of graduate students were largely displeased with the number of Tri-Council scholarships available for graduate students (Science and Policy Exchange 2020). Furthermore, 79% replied that they would like to see an increase in the value of the awards. This 2018 report eloquently displayed the dissatisfaction among graduate students in regard to the value and number of federal scholarships, as well as the perceived financial security that comes with obtaining these scholarships.

During the COVID-19 pandemic, financial concerns of graduate students became even more prominent, with Statistics Canada reporting that over two-thirds of continuing postsecondary students were very or extremely concerned about the financial impacts of the pandemic (Wall 2020). The Toronto Science Policy Network's *COVID-19 Graduate Student Report* has also revealed that finances were at the forefront of worries for graduate students during the pandemic (Toronto Science Policy Network 2020).

These financial concerns for graduate students have continued, with inflation recently hitting a 40-year high, causing an increase in everyday expenses (Scherer and Smith 2022). While inflation affects all those in Canada, graduate students can be considered a particularly vulnerable group because their stipend values do not reflect average living costs. The Canadian housing market has also witnessed a large increase in real-estate prices. While the majority of

graduate students are not in a position to purchase their own homes, rental prices across Canada are increasing at unprecedented rates (Chen 2022).

Given these pressures, graduate students have been actively advocating for increases to graduate student scholarships and funding in Canada. Most notably, our fellow student-led science policy networks have been advocating for increased financial support for graduate students for many years. In response to the release of the *Fundamental Science Review in 2017,* commonly known as the Naylor Report (Advisory Panel for the Review of Federal Support for Fundamental Science 2017), the SPE started a campaign called #Students4TheReport that urged the government to implement the report's 32 recommendations. The SPE then launched a survey entitled *Rethinking Federal Research Funding* that investigated the opinions of graduate students and postdoctoral fellows on federal awards from the Tri-Council Agencies (SSHRC, NSERC, and CIHR). This report became a key piece of evidence in the formation of the Canadian Council of Academies' *Degrees of Success* Report that investigated barriers for PhD students when transferring into the labour market (Council of Canadian Academies 2021).

Despite this work, there is a lack of national data on graduate student finances, especially for the vast majority of graduate students who do not hold a federal scholarship. This survey aimed to investigate the state of graduate student finances in Canada. From 1305 responses of graduate students representing various geographical locations, years of study, fields of education, and demographic backgrounds, we examined costs, tuition, debt, sources of funding, reported financial struggle, and other financial indicators. As a result of these analyses, we propose six recommendations to better support graduate students and enable them to more fully focus on research. Our findings will be essential in implementing changes to support the Canadian

research ecosystem. In addition, by sharing and bringing awareness to the stories and financial struggles of graduate students, we hope to humanise this issue.

C. 4 Materials and methods

Survey development

The “National Graduate Students Finance Survey" was conceptualised and designed by members of the Ottawa Science Policy Network (OSPN) in collaboration with additional authors. The goal of the survey was to generate a comprehensive report on graduate student finances to use this information as leverage following the 2021 Federal Election and to launch a campaign to improve the well-being of graduate students in Canada. We aimed to report on the current status of stipends for master’s and doctoral students as funded through the Tri-Council Agencies: the CIHR, NSERC, and SSHRC. Survey questions were carefully designed and best efforts were made to frame the questions objectively. The survey questions can be found in the supplementary file. According to the Tri-Council Policy Statement (TCPS-2), ethics review/approval was deemed unnecessary as “ethics review/approval is not required for projects that are considered Quality assurance and quality improvement studies, as these don't typically meet the purpose of research.” Article 2.5 of the TCPS-2 states “Quality assurance and quality improvement studies, program evaluation activities, and performance reviews, or testing within normal educational requirements when used exclusively for assessment, management or improvement purposes, do not constitute research for the purposes of this Policy, and do not fall within the scope of REB review.”

Survey distribution

From October to December 2021, using a list of all Canadian universities, we collected emails from graduate student associations, societies, departmental groups, and clubs that were

accessible online. The survey was sent out by email between 10 December 2021 and 14 December 2021, with follow-up emails sent in the following weeks. The survey was open from 10 December 2021 until 14 April 2022. To reach a broad audience, the survey was advertised on social media platforms, including Twitter and Instagram. In line with our organisation's commitment to bilingualism, our survey was accessible in both of Canada's official languages (English and French).

Data policy

Responses to the survey are held as confidential by the OSPN, a student organisation at the University of Ottawa. Aggregated, anonymous, or de-identified data may be shared with representatives of student associations, university administrations, advocacy groups, legislatures, and governments across Canada, including data subsets where appropriate.

Although we did not collect identifying information (e.g., respondent names), individuals may still be identifiable by combining data. To protect anonymity, we will only publish or share subsets of data generated by combining responses of two or more questions when there are at least five responses in all categories. Any numerical data will only be published or shared as summary statistics (for example, mean and standard deviation) or as binned data (such as a histogram). Responses will never be shared or published in such a way that links together all an individual's responses.

Raw data collected in the survey will be retained for a period of seven years after which it will be deleted. Any data published or shared with other organisations will be retained indefinitely. Once the analysis of the data has concluded, access will only be granted to the OSPN president (or other OSPN members that the OSPN president determines are responsible for data custody).

Data preprocessing

Data preprocessing occurred prior to analysis. Based on the unique identifiers provided for each survey entry and demographic information, 14 respondents were determined to be duplicates (i.e., the same individual filled in the survey twice) and were removed. As data analysis was performed in English, all French responses were translated into English. Numerical data were transformed into a consistent format (e.g., removing comma separators and $ symbols), but no numerical values were changed. In cases where the authors felt there was an obvious entry error or possible misunderstanding of the question, the responses were excluded from the analyses.

For some questions, where a free-form response was an option, responses were classified into groups to better enable comparisons. This was done for the following survey sections: current level of study Q2, ethnic identities Q8, gender identity Q9, field of study Q14, living environment (urban, suburban, rural) Q23, ownership status of accommodation Q24, who else the respondent lived with Q25, and sources of financial support Q27. In these classifications, effort was taken to retain the meaning of a response, especially for demographic information, and reclassification was based on all information available and best judgement. A copy of the unprocessed survey answers has been retained.

Statistics and data visualization

Throughout this report we used a significance threshold of 5% (i.e., $P < 0.05$). This means that for findings to be claimed significant, there is a greater than 95% probability that any difference detected is not solely due to random variation in sampling. However, it does not provide any information about why two (or more) groups may differ and does not take into account possible underlying factors—only that the difference is unlikely to be due to statistical

chance alone. For comparing categorical data, the χ^2 test was performed using the categories presented in the plot or other summary data. For numerical data comparisons, a two-sample Kolmogorov–Smirnov (KS) test or Kruskal–Wallis (KW) test was used to compare the means when more than two categories existed. When comparing more than two categories, the statistical test does not provide information about how or which categories differ—only that the total extent of differences seen are unlikely to be due to randomness of sampling.

For data visualisation, bar graphs were created using GraphPad Prism 9.5.0; donut charts using R 4.2.1 (R Core Team 2022) and the lessR package (Gerbing 2021); and violin and QQ-plots were created using Python 3.8.10 with the statsmodels package (Seabold and Perktold 2010).

B. 5 Results and discussion

Demographics of survey respondents

One aim of our survey was to assess the financial situation of graduate students across Canada, including students from varying programs, fields of study, and ages. We received a total of 1305 responses, 1030 of which were in English and 275 in French. Nearly all respondents were registered as full-time students (96.7%), with only a small percentage registered in part-time programs (2.3%). Students that resided in QC and ON made up 78.6% of respondents, with 484 respondents from ON and 541 from QC (Fig. 7.1A). This is consistent with Statistics Canada data from the National Graduates Survey that showed QC and ON made up 73.8% and 73.7% of master's and PhD graduates, respectively (Statistics Canada 2019). Additionally, over 70% of respondents were between the ages of 24 and 33 (Fig. 7.1B). Again, this is consistent with the Statistics Canada data that showed an average graduate student's age was 31 and 35 upon graduation from master's and PhD programs, respectively (Statistics Canada 2019). This

provides confidence that the conclusions made in this survey are a valid representation of the overall graduate student profile in Canada.

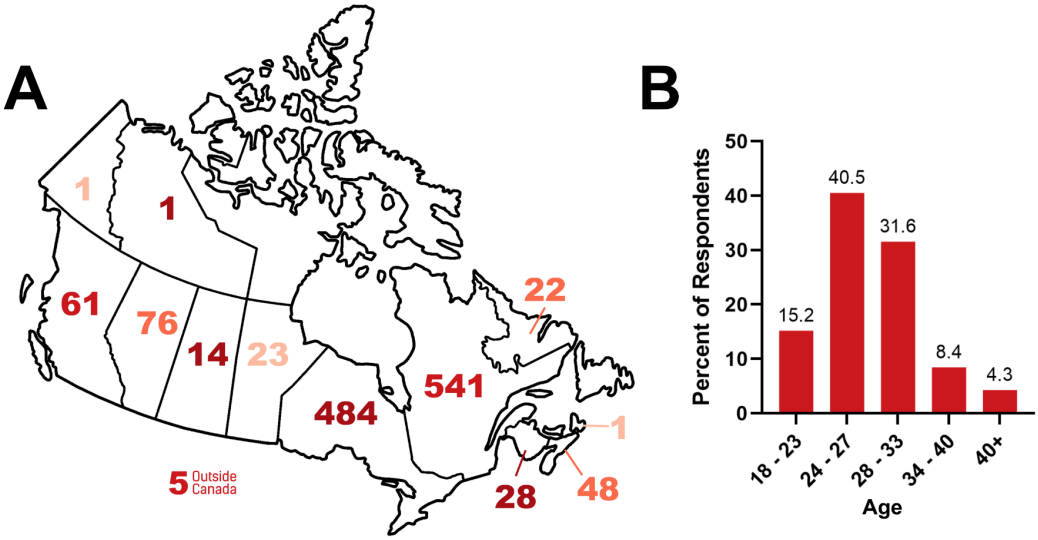

Figure 7.1. Geographic Location and Age. ***A*** *Number of respondents from each province and territory (n=1305).* ***B*** *Age category of respondents by percent (n=1305).*

A majority of respondents (57.6%) were pursuing a doctoral degree and nearly all were in a research-stream program (Fig. 7.2A). Similarly, the majority (60.9%) of master's student respondents were in the research stream, while the remaining were in course-based (19.8%) and professional master's programs (19.3%) (Fig. 7.2A). Responses across years of study were evenly dispersed (Fig. 7.2B). Survey respondents were primarily in science-based programs, including physical science (26.3%), medical sciences (23.8%), life sciences (23.5%), and social sciences (16.4%) (Fig. 7.3). Arts and humanities students comprised 7.7% of respondents (Fig. 7.3). A small percentage of business students (1.6%) and law students (0.5%) also responded to the survey (Fig. 7.3). As such, our overall findings are most representative of graduate students in STEM-related fields, which encompassed 73% of our respondents. This is higher than the 46.4% of students in science-related graduate degrees, as shown in the Canadian Association for Graduate Studies 2019 survey. This survey also estimated that there were about

63 000 graduate students in Canada. Additional demographic data can be found in Supplementary Table 7.1.

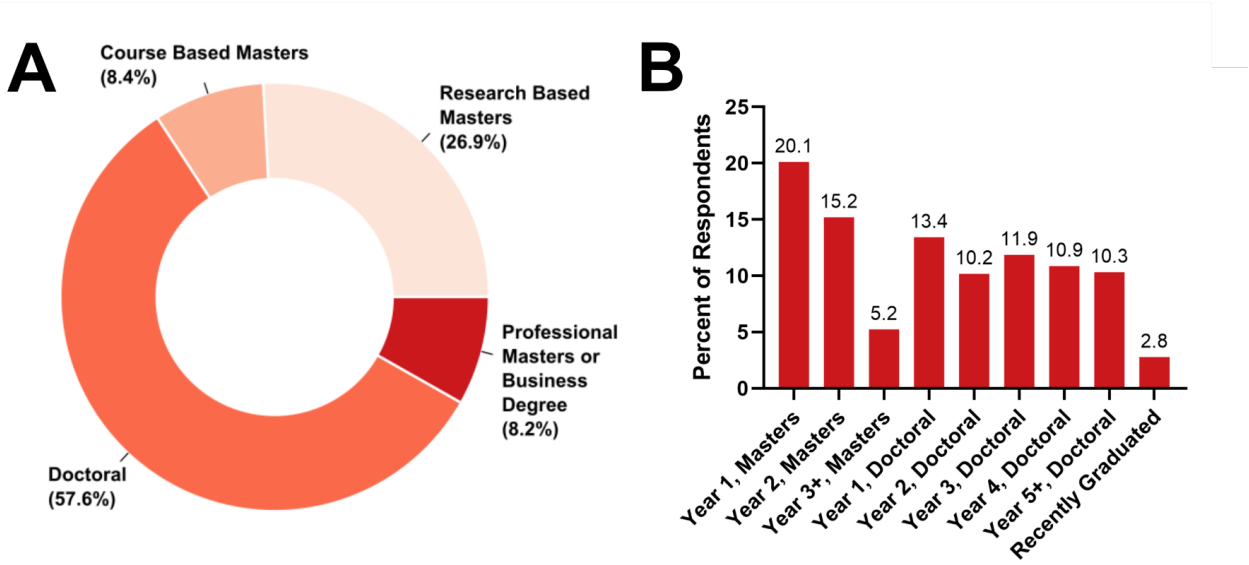

Figure 7.2. Level and Year of Study. ***A*** *Current type and level of study by percent (n=1303). The Doctoral category includes Professional Doctoral (ex. EdD, PharmD, DBA), Research Stream Doctoral (PhD), Course Based Doctoral and MD PhD* ***B*** *Current year of study by percent (n=1297).*

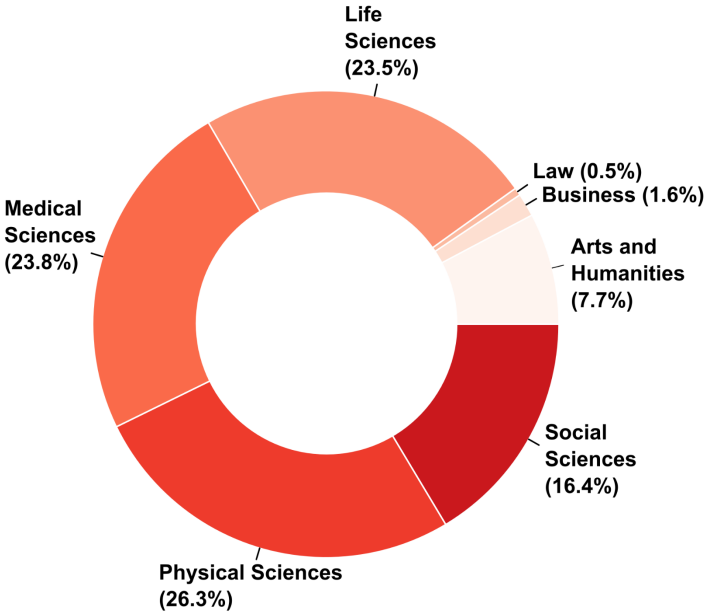

Figure 7.3. Field of Study. *Respondents self-reported their field of study from 7 categories: Arts and Humanities, Business, Law, Life Sciences, Medical Sciences, Physical Sciences (Engineering, Physics, Mathematics, etc.) and Social Sciences (n=1305). If respondents indicated multiple fields of study or an option not listed in the survey, they were categorised into one of the seven categories based on their answers for analysis purposes.*

Tuition remains a large financial burden for graduate students

Tuition is one of the largest expenses for graduate students in Canada and is primarily regulated by provincial governments. According to Statistics Canada, the average tuition for Canadian graduate students is about $7437 per year (up 1.7% from last year) (Statistics Canada 2022*a*). NS graduate students have the highest tuition, on average $10 591 per year, with ON ($9385) and BC ($9994) close behind. Comparatively, QC has the lowest average tuition for graduate students, at an average of $3582 per year (Statistics Canada 2022*a*).

Universities can use different tuition fee structures, with various opportunities for tuition rebates and waivers. Tuition freezes, which were implemented in ON during the COVID-19 pandemic, can also affect the rising tuition costs across the country. In addition to tuition fees, students are required to pay ancillary fees throughout their education. These can include fees for fitness or athletic services, technology use, public transit, health and dental plans, etc.

To assess the financial situation of graduate students, we investigated tuition variance among students. We found that the average annual tuition paid by respondents across Canada was $7518 for domestic students (see the analysis of international student costs below). The lowest average cost of tuition was reported in NL at $5016.27 per year, while the highest average was reported in ON at $8972.46 per year, with NS following behind at $7770 (Fig. 7.4). The highest tuitions were among four provinces in both our survey and the Statistics Canada data: ON, NS, NB, and BC.

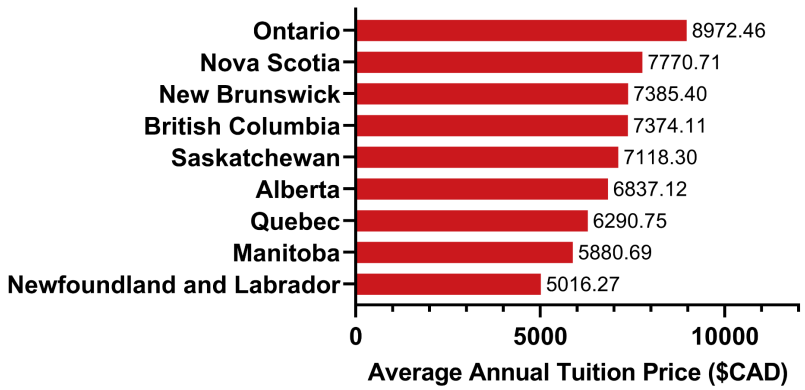

Figure 7.4. Annual Tuition Fees. *Average annual tuition in CAD dollars by province (n=886). Categories with less than 5 responses were excluded (Prince Edward Island, Northwest Territories, Yukon and Outside of Canada).*

Tuition remains a large burden on graduate student finances, though it is questionable whether these costs are factored into university funding packages. For example, one respondent stated "My stipend total this year (including additional TA work) was $29 000. From that, ~$6000 was deducted for tuition. $23 000/year is not enough to live on—this is below the low income threshold that qualifies you for assistance program (ex: Leisure Access Pass) in Edmonton. Except as students we are exempt from these programs."

To further characterise tuition distribution among respondents, we asked graduate students to report their out-of-pocket payments. This accounts for students' tuition waivers, which are offered through universities to subsidise the cost of tuition. Across domestic students, the average out-of-pocket tuition was $3226. Our results reflect a bimodal distribution, with the vast majority of respondents either paying 0%–10% or 90%–100% (Fig. 7.5), where 82.6% of domestic graduate students either pay less than 10% or more than 90% of their tuition out of pocket, highlighting an all-or-none approach to tuition finances. This variation in out-of-pocket tuition payments could partly be attributed to money that some students receive through scholarships. When broken down by scholarship status, we found that domestic respondents who held a government award paid significantly less tuition out of pocket (KS test, $P < 10^{-5}$), with

70% of award holders paying 10% or less of their tuition out of pocket compared with 37.3% for those who did not hold a government award (Fig. 7.6). However, it is important to note that the bimodal distribution was still seen for students who do not hold a government award, suggesting that other factors also contribute.

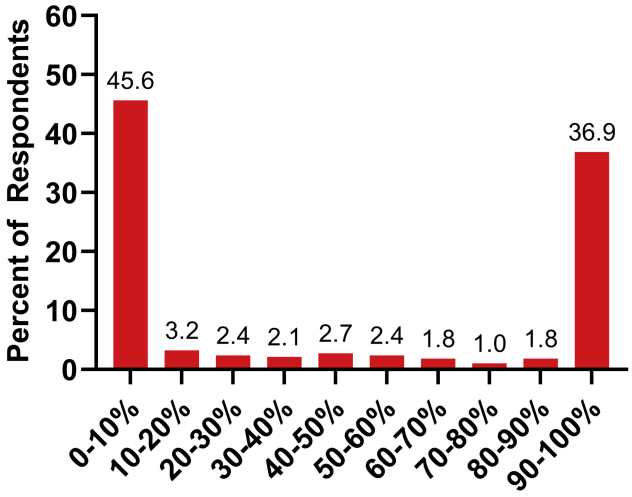

Figure 7.5. Percent Tuition Paid out of Pocket (Domestic Only). *Percent of tuition paid out of pocket after any applicable scholarships for domestic respondents (n=885). Tuition paid out of pocket was divided by total annual tuition fees to calculate the percentage.*

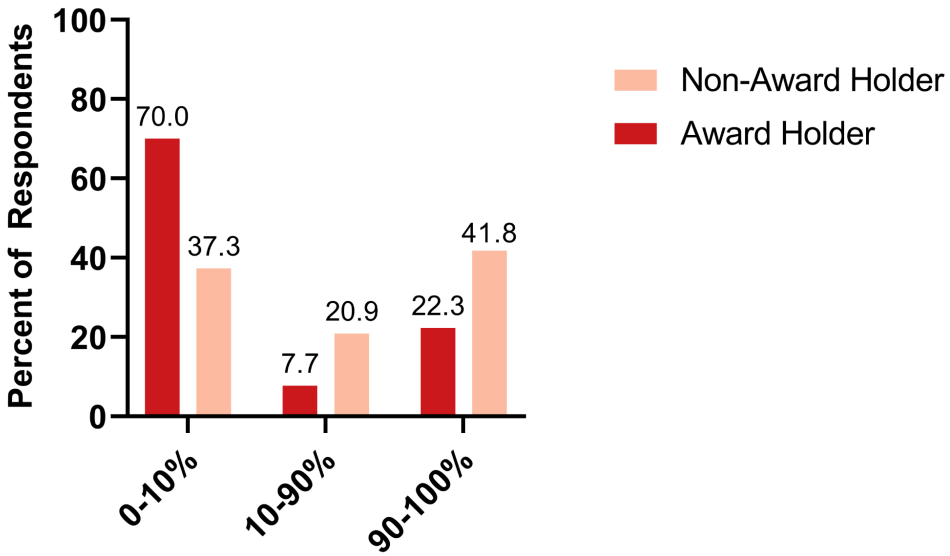

Figure 7.6. Percent Tuition Paid Out of Pocket by Award Holder Status (Domestic Only) *Percent of tuition paid out of pocket after any applicable scholarships for domestic students with a government award (n=220) and without a government award (n=665). Tuition paid out of pocket was divided by the total annual tuition fees for each respondent to calculate the percentage.*

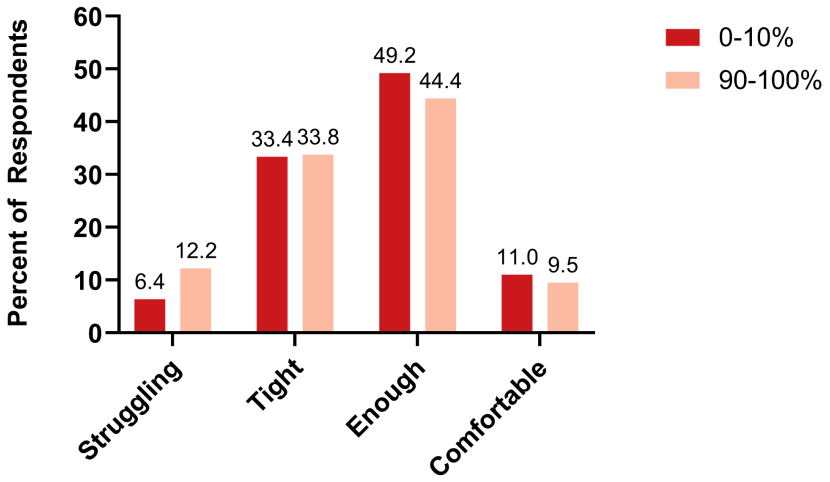

Figure 7.7. *Financial Situation of Low (0-10%) vs. High (90-100%) Percent Tuition Paid out of Pocket (n=1,004)*

Graduate students in Canada struggle to pay many costs of living

As described in the introduction, Canada is currently experiencing a 40-year inflation high, resulting in higher costs of living for all Canadians. In combination with the lingering effects of the COVID-19 pandemic, graduate students are particularly financially vulnerable, considering slow and inflexible funding models. To better understand how graduate students are spending their finances, we investigated their housing costs, area of residence, living situation, and monthly expenses.

Our findings show that over 80% of respondents were renting, with less than 10% owning homes (Fig. 7.8A). This is concerning compared to recent Statistics Canada data profiling home ownership. For young adults aged 25–29 years, 36.5% owned their homes. For those aged 30–34 years, home-ownership rates were 52.3% (Statistics Canada 2022*b*). This indicates a large financial burden experienced by graduate students compared to their peers. One respondent remarked: "I had to take cash advances on my credit card and borrow money from family to get by… As such I am still paying off debts which has delayed accomplishing milestones (like buying a house and starting a family) that others my age are currently doing.

Bottom line graduate students should be paid at least a minimum wage full-time salary as taking on secondary jobs to supplement income is just not possible if we want to graduate on time" and another respondent noted that "after groceries and rent, [their] funding leaves [them] with a negative cashflow position." While others age-matched are building wealth and investing in their future, graduate students are subjected to the insecurity of the rental market.

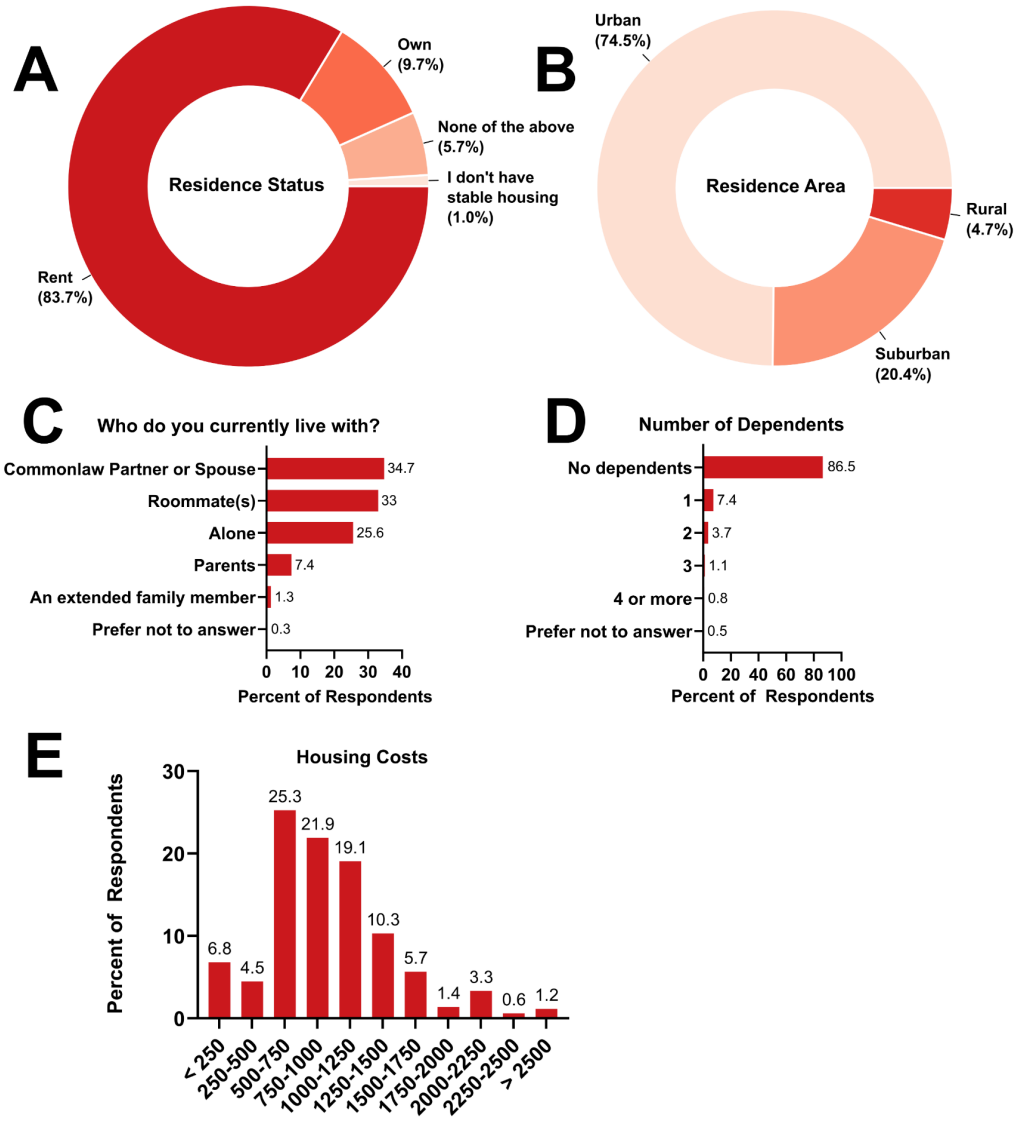

Figure 7.8. Residence Situation. ***A*** *Residence status of respondents by percent (n=1,305).* ***B*** *Area of residence by percent (n=1,305). Respondents who listed areas other than Urban, Rural or Suburban were re-categorized into one of the three.* ***C*** *Current living arrangements of respondents (multiple selections possible) by percent (n=1,305).* ***D*** *Number of dependents reported by respondents by percent (n=1,305).* ***E*** *Monthly Housing Costs ($CAD) by percent of respondents (n=1,291).*

Three-quarters of respondents lived in urban areas (74.5%), while the remainder lived in suburban areas (20.4%) and in rural areas (4.7%) (Fig. 7.8B). Most respondents lived with other people, such as a partner, roommate(s), or family (Fig. 7.8C), while 25% lived alone. A large majority of our respondents did not have dependents (Fig. 7.8D), while the remaining 13% had one or more dependents (further analysis of those with dependents can be found further below). Based on those who paid rent, a quarter of respondents (25.3%) paid $500–$750 monthly (Fig. 7.8E). Most respondents paid between $500–$1500 in rent, a wide range that depends on location, roommate situation, and other factors. One percent of respondents (14/1305) did not have stable housing.

Monthly expenses for respondents were surveyed across different categories (Fig. 7.9). The highest expense, aside from rent (Fig. 7.8E), were groceries, with $100–$400 spent monthly by over 70% of respondents.

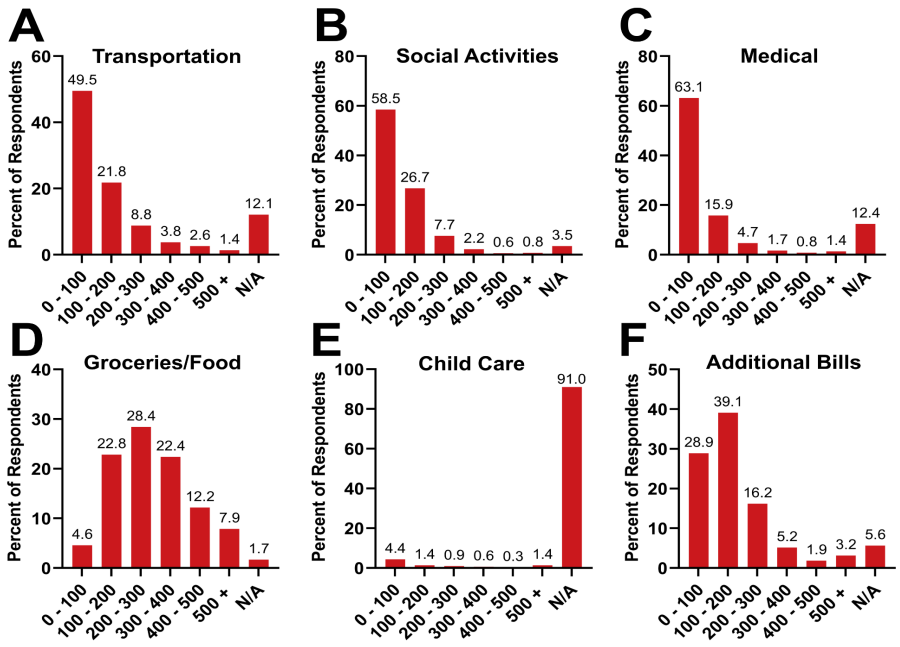

Figure 7.9. Monthly Expenses. Respondents were asked to share their average monthly expenses in each category within a range: **A** Transportation (n=1,305), **B** Social Activities (n=1,305), **C** Medical (n=1,305), **D** Groceries/Food (n=1,305), **E** Child Care (n=1,305), **F** Additional Bills (n=1,297). Data are shown by the percent of respondents for each category.

Canadian graduate students are experiencing financial stress

Between low pay, increasing costs of living, and accumulating debt, it is clear that financial stress is a major concern for many graduate students. Not only does financial stress impact graduate students' well-being and ability to complete their studies, but insufficient savings and outstanding debt can impact their future financial security. This has become a dominant narrative across research ecosystems as many students are speaking out on these financial struggles in Canada (Marhnouj 2022) and in other countries (Woolston 2022).

To investigate this question in graduate students across Canada, we asked survey respondents to identify their comfort levels with their current financial situation. Our team examined how concerned students were about various financial stresses, including living expenses, debt, and emergency funds. To investigate students' financial status, we asked participants to choose which most appropriately defined their current financial situation: *comfortable* (I am very comfortable financially. I have enough money that I do not need to worry about monthly expenses and spend as I would like.), *enough* (I have enough. My finances are a bit tight but I live within my means and can afford to provide for myself.), *tight* (every month is tight, but I am getting by. I am often making sacrifices to pay for necessities.), and *struggling* (I am struggling financially. I often do not have enough to make ends meet.) Nearly half of all respondents (43.4%) identified that they were either frequently struggling to make ends meet or that their tight finances forced them to make sacrifices to afford necessities (Fig. 7.10A). Less than 10% of students stated that they were very comfortable with their current financial situation (Fig. 7.10A). Unsurprisingly, those who identified as struggling to make ends meet generally had the lowest stipend values, whereas those who identified as being very comfortable with their financial situation had the highest (Fig. 7.10B). One student even stated that they had to "drop

out of [their] Masters program due to finances and having to work full time to afford the cost of living." This student also highlighted how the "faculty [they were] in did not support students working externally yet offered very few alternatives to afford both tuition, living expenses, and debt payments."

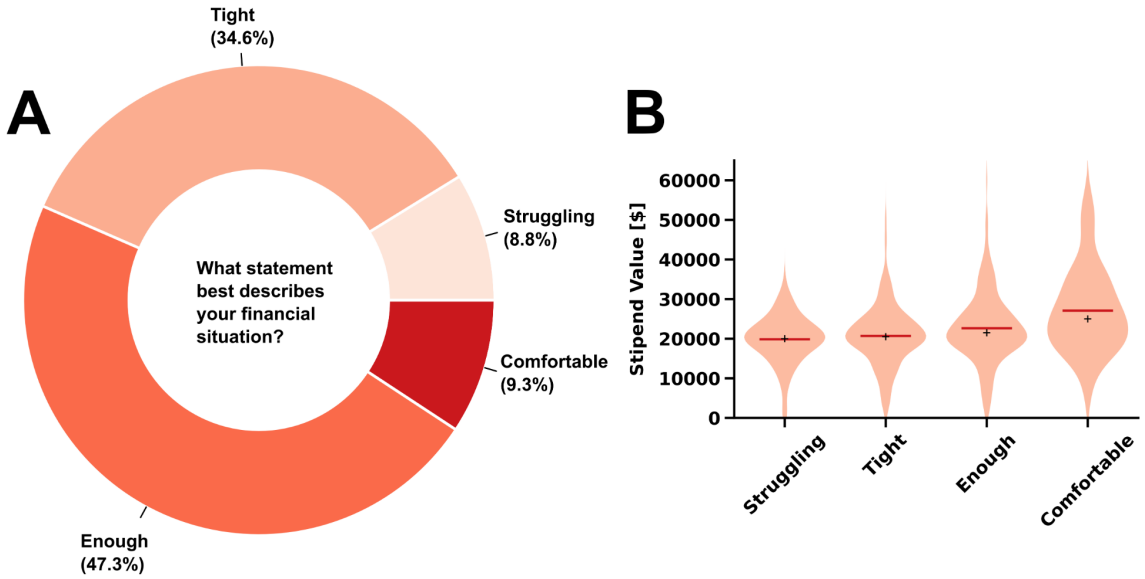

Figure 7.10. Financial Situation. **A** Respondents were asked what best describes their financial situation: Comfortable (I am very comfortable financially. I have enough money that I do not need to worry about monthly expenses and spend as I would like.), Enough (I have enough. My finances are a bit tight but I live within my means and can afford to provide for myself.), Tight (Every month is tight, but I am getting by. I am often making sacrifices to pay for necessities.) and Struggling (I am struggling financially. I often do not have enough to make ends meet.). Data are shown by percent (n=1,303). **B** Violin plot of respondents' financial situation and their stipend value (n=1,303).

The majority of respondents (85.7%) expressed experiencing stress/anxiety about finances at some point during their graduate studies. Meanwhile, 54.7% experienced difficulty budgeting, and 30.7% have considered leaving their studies due to financial struggles alone (Fig. 7.11A). Concern about insufficient funds for living expenses was common among respondents, with over 30% having experienced concern about rent and food (Fig. 7.11A) and 27.2% either "always" or "often" worrying about their ability to pay for bills (Fig. 7.11B).

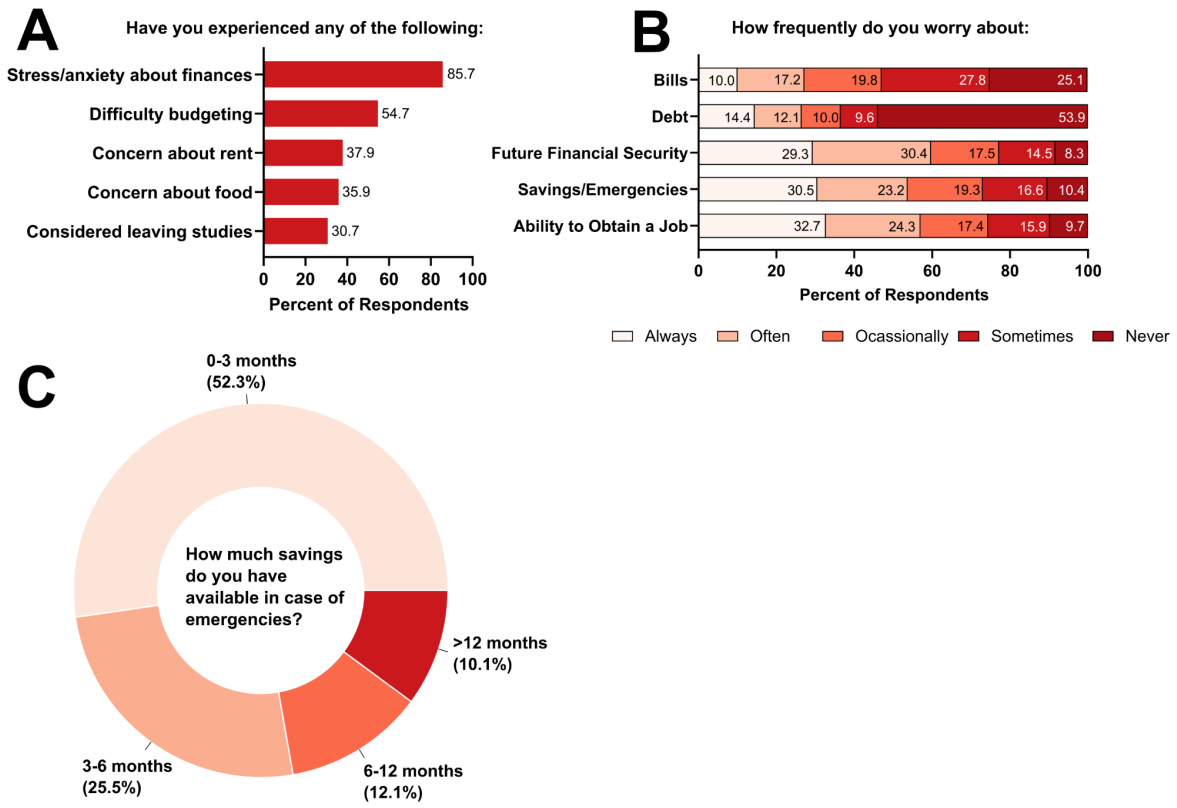

Figure 7.11. Financial Stressors. **A** Concerns and stress experienced by respondents (multiple selections possible) by percent (n=1,178). **B** Respondents were asked how frequently they worry about their ability to obtain a future job in their chosen field, savings/ability to pay for emergency expenses, future financial security, ability to pay back debt, and ability to pay bills. Data are shown by percent in each category (n=1,305). **C** Amount of savings, measured by months of living expenses, that respondents have available for emergencies, by percent (n=1,264).

The standard advice from financial experts and the recommendation by the Financial and Consumer Agency of Canada is to ideally have at least 3–6 months of savings for living expenses (Financial Consumer Agency of Canada 2022). Only half of our survey respondents met this recommendation, with 52.3% having only 0–3 months of living expenses saved (Fig. 7.11C) and 53.7% of students either "always" or "often" worrying about their ability to pay for emergency expenses (Fig. 7.11B). These findings highlight that graduate students are vulnerable to unexpected financial challenges.

As an expected consequence, graduate students worry about their future financial security. Nearly 60% of respondents indicated that they either "always" or "often" worry about

future financial security, and a similar number (57%) indicated “always” or “often” worrying about their ability to obtain a job in the future (Fig. 7.11B). A key contributor to this may be the accumulation of debt throughout one’s university studies, as over half of respondents (52.2%) had some outstanding debt, the majority of which had over $10 000 owed (Fig. 7.12A). Indeed, respondents with outstanding debt reported worrying about future financial security more often than respondents with no outstanding debt ($P < 10^{-5}$, χ^2 test) (Fig. 7.12B). A higher percentage of respondents with outstanding debt also reported struggling financially compared to those with no outstanding debt ($P < 10^{-5}$, χ^2 test) (Fig. 7.12C). Reliance on debt seems to partly stem from a lack of parental support, as only 20% of students with debt received financial support from parents, compared to 30% of students with no debt having received parental support ($P = 0.000028$, χ^2 test) (Fig. 7.12D). Additionally, doctoral students had a higher amount of debt on average than master’s students ($34 370 for doctoral vs. $29 272, $24 942, and $28 903 for course-based, research-based, and professional and business master’s students, respectively; Fig. 7.13A). This is unsurprising given the increased length of study, but note that master’s students and doctoral students still reported similar responses regarding their financial situations (Fig. 7.13B).

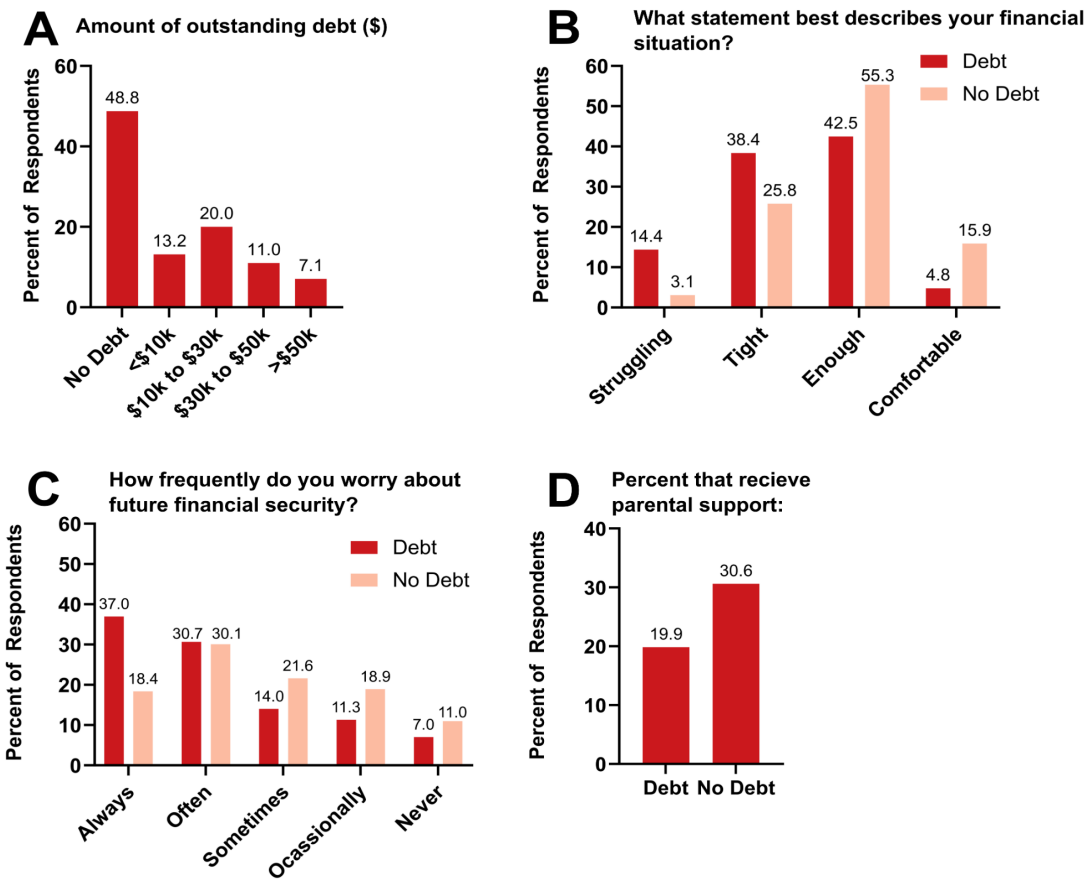

Figure 7.12. Financial Situation by Debt Status. **A** Amount of outstanding debt of respondents in ranges, by percent (n=1,130). **B** Financial situation of respondents with debt (n=584) or no debt (n=555) by percent. **C** Financial situation of respondents with debt (n=584) or no debt (n=555). Data are shown by the percent of respective debt status. **D** Parental support of respondents with debt (n=584) or no debt (n=555) by percent.

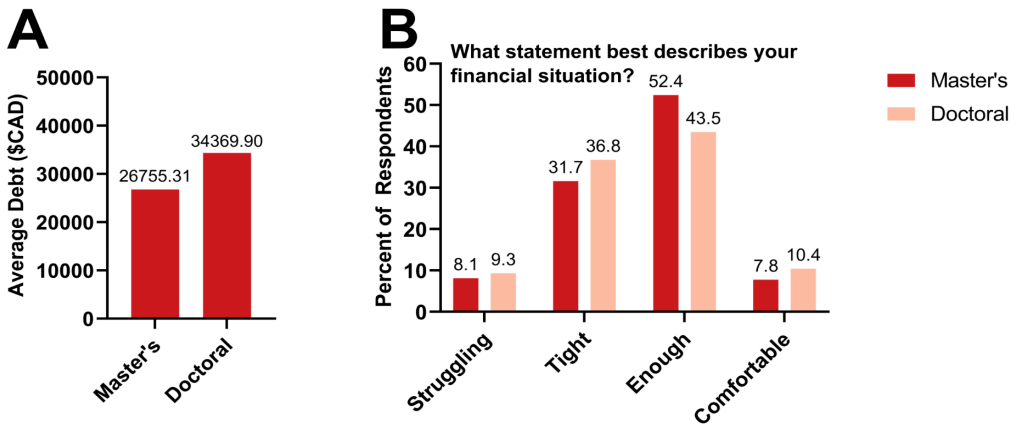

Figure 7.13. Financial Situation by Level of Study. **A** Average debt of Master's (n=553) and Doctoral respondents (n=750) in CAD dollars. **B** Financial situation of Master's (n=553) and Doctoral (n=750) respondents. Data are shown by the percent of the respective level of study.

Graduate students in Canada often have to work outside of their studies

Non-academic work completed outside of a graduate student's studies, to supplement income, is often considered taboo as it can be frowned upon or, in some cases, is against university regulations. Academic institutions can prevent graduate students from accessing alternative forms of income by restricting the number of hours they are permitted to work outside of their studies. For example, McGill University allows graduate students up to a maximum of 12 h work per week outside of their studies to maintain full-time status (McGill University 2022). In 1994, the Ontario Council on Graduate Studies, of which 21 universities across ON are members, implemented the 10 h rule, which restricts the number of hours graduate students can work outside of their studies to 10 h per week (Ontario Council on Graduate Studies 2021). Scholarships issued by the Ontario Government also adhere to this rule and regulate the amount of time another establishment can employ a student. There is growing awareness of the problems arising from the 10 h rule. For example, the University of Waterloo recently cited that there was a "strong desire to provide greater flexibility in employment hours" and changed the requirements of the 10 h rule to now allow for a student to work up to 20 h per week (University of Waterloo 2022). In our survey, one respondent noted that "[m]ost graduate students in our department work full-time jobs on top of completing their studies AND TA [teaching assistant] or RA [research assistant] positions. The department complains about students not finishing their programs within a short amount of time, yet they won't pay us more and strongly advise against/look down on students who work over the 10 hour/week 'limit'." Abolishing the 10 h rule has increasingly become a topic of conversation concerning financial struggle among graduate students. In provinces outside of ON, this is less of an issue as many

universities/provinces have higher limits on work outside of studies (for example, the University of Winnipeg has a limit of 35 h per week).

To investigate external employment of graduate students and gain insight into their work–study balance, we asked respondents whether they were externally employed (or get paid for a service) outside of their graduate studies. This included any money that is made in addition to their stipend. Many graduate students work as TAs, and this was counted as additional work if the payment was not included or required as part of their stipend.

More than half of all respondents (55.6%) worked in addition to their studies (Figs. 7.14A, 7.14B). Of this majority, nearly half worked less than 10 h per week, while the other half worked over 10 h per week. This includes 18.5% who worked between 5 and 10 h/week and 17.8% who worked between 10 and 20 h/week (Fig. 7.14C). A small % of respondents (6.5%) worked over 30 h per week. Additionally, when looking at financial struggles, respondents who worked were significantly more worried about their ability to pay back student debt compared to those who did not work (χ^2 test, $P = 0.036$) (Fig. 7.15). Other financial concerns were similar between the working and non-working groups.

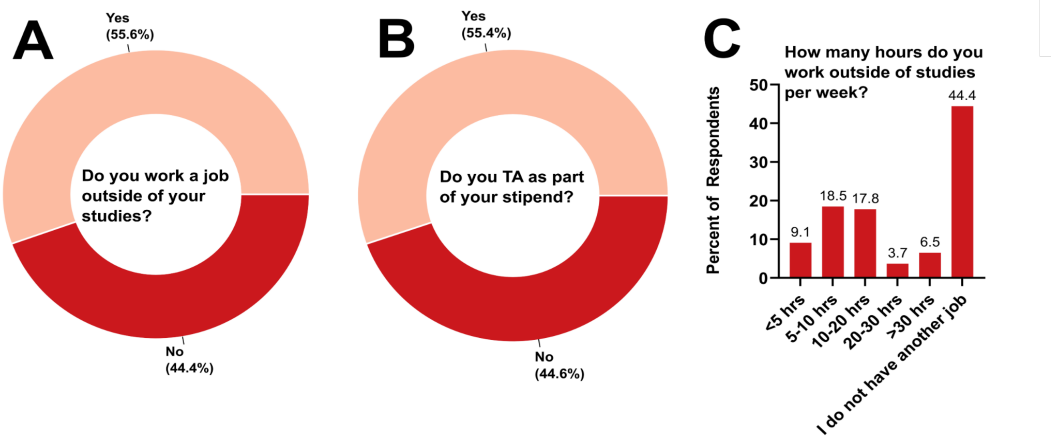

Figure 7.14. Work outside of studies. ***A*** *Respondents were asked if they work a job outside their studies, by percent (n=1305).* ***B*** *Respondents indicated if being a Teaching Assistant (TA) was a condition of their stipend (n=914).* ***C*** *Number of hours respondents worked outside of studies per week, by percent (n=1305).*

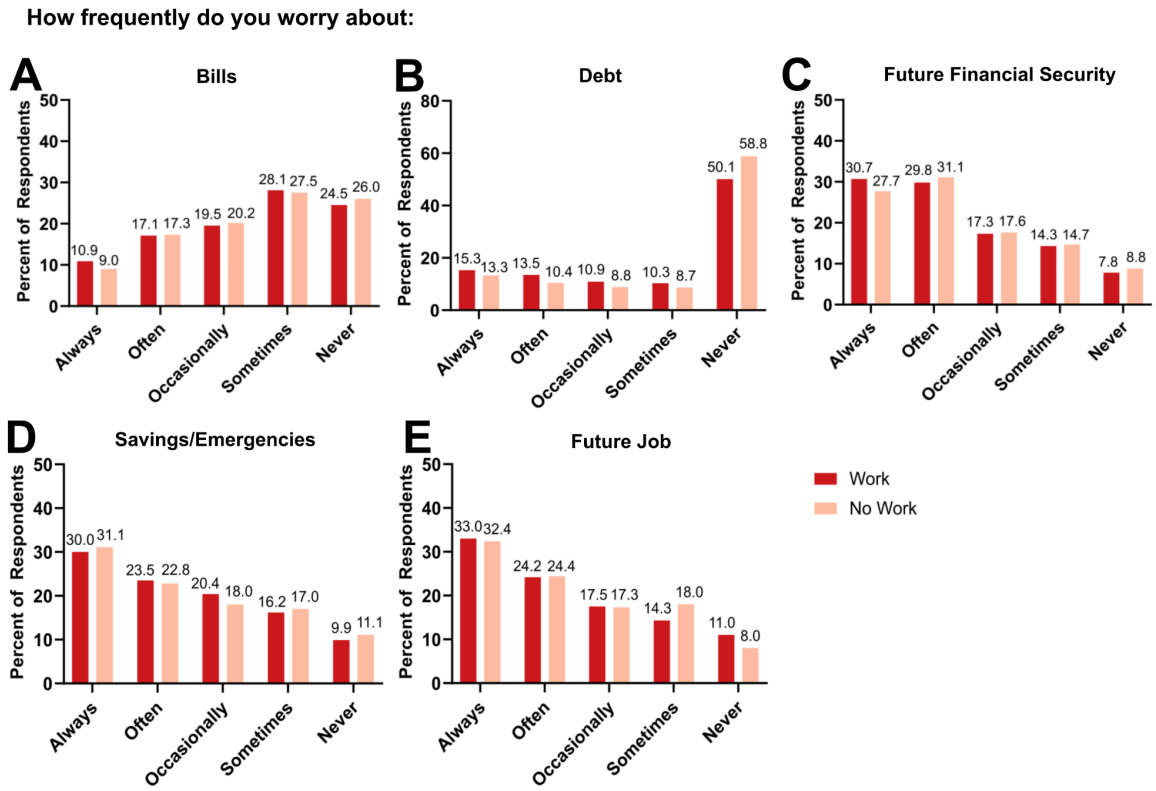

Figure 7.15. Work outside of studies - Financial Situation. How frequently respondents who work or don't work worry about their **A** ability to pay bills, **B** ability to pay back their student debt, **C** future financial security, **D** savings/ability to pay for emergency expenses and **E** ability to obtain a future job in their chosen field. Data are shown by percent in each category: Work (n=727) and No Work (n=578).

Graduate students experience errors in stipend payments

Graduate students depend on their stipends for living costs; however, some graduate students have experienced "stipend errors," defined as a disruption in the regularly scheduled payment of a stipend. Our survey sought to understand the stipend errors experienced by graduate students using questions based on a study conducted by the Dalhousie Working for Inclusion in Chemical Sciences Group (Dalhousie Working for Inclusion in Chemical Sciences Group 2021).

When asked whether survey respondents experienced any errors regarding stipend payments, over 60% of respondents indicated they had not experienced any errors (Fig. 7.16A). In contrast, 27% of respondents stated they received late stipend payments. Students also had

errors in getting paid too little, too much, or had their stipend payments put towards a university expense/fee (Fig. 7.16A). More than one in three respondents (36.4%) have experienced at least one error in stipend payments (Fig. 7.16B).

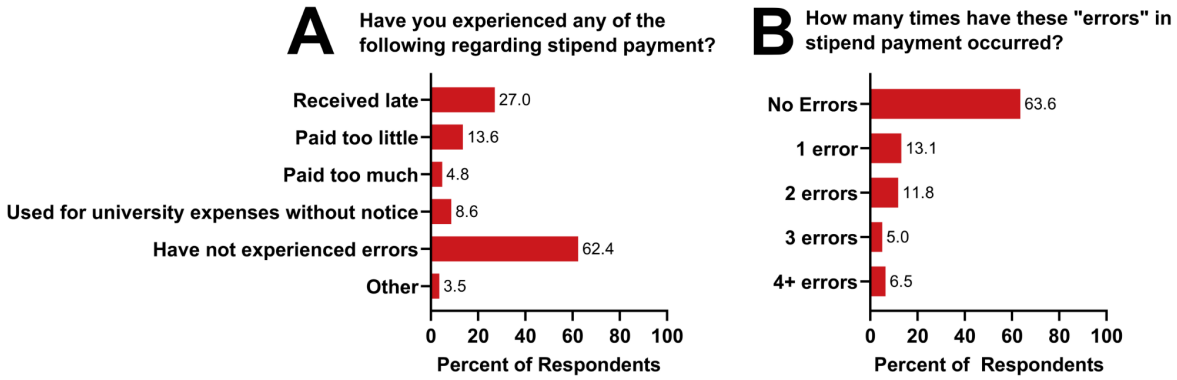

Figure 16. Stipend Errors. **A** Respondents were asked if they ever experienced any errors regarding stipend payments (multiple selections possible) by percent (n=914). An "error" was defined as a *disruption in the regular scheduled payment of your stipend.* **B** Number of times respondents experienced an "error" in stipend payments, by percent (n=914).

Personalized responses demonstrated that stipend errors can seriously affect graduate students' finances, time, and energy. For example, one student noted they were "not enrolled by the financial department to receive payment for over two months," while other students had stipend payments that were anywhere from 8 weeks to 3 months late. One student said their stipend was "mistakenly cancelled" and it took "a lot of back and forth with profs and admin" to receive it. Students also stated that their "stipend payment was put towards a university expense/fee without [their] prior knowledge."

Since this process largely depends on the university administration that is responsible for stipend payments, these analyses will need to be assessed on a university and(or) department level basis to properly determine the impacts of stipend errors. While our results show that stipend errors occur, future work should identify why this is happening and how this can be improved to alleviate student financial stress in this area.

Graduate students are not always reimbursed in a timely manner for out-of-pocket research costs

While the cost of living continues to increase at record rates and stipends remain stagnant, many graduate students are not equipped to deal with unexpected expenses. With only 9.3% of respondents having felt comfortable financially (Fig. 7.10A), we were concerned about the impact of upfront research expenses paid by graduate students for their financial security. These types of expenses can include purchasing lab equipment and paying for trips related to field work, software, parking, and academic conferences. Field work and conferences, in particular, can incur hundreds of dollars in expenses for travel fees. Additionally, these costs may require payment months in advance of a specific date. A delay in reimbursement, or absence of one, could lead to increased interest on credit card charges and(or) lack of money to pay for standard living expenses.

To determine the extent to which this situation may occur, we surveyed respondents on out-of-pocket academic expenses and the timing of their reimbursement. Over 50% of respondents, in doctoral (73.6%) or research-based master's degrees (52.5%), have previously paid for academic expenses upfront (Fig. 7.17A). For graduate students in course-based professional and business master's degrees, the percentage of respondents was lower at 34.81%. Within these proportions, we focused on expenses that needed to be paid out of pocket. Approximately 10%–15% of graduate students in a research-based master's (10.6%) or doctoral degree (14.6%) were required to pay these expenses. A higher proportion of students in course-based professional and business master's degrees (26.1%) were required to do the same. On average, students in course-based programs paid less in upfront academic expenses but were required to do so largely out of pocket or without reimbursement. As there may be some overlap

in respondents who answered that they paid out-of-pocket expenses and those who answered that they failed to be reimbursed, further examination may be required for these concerns.

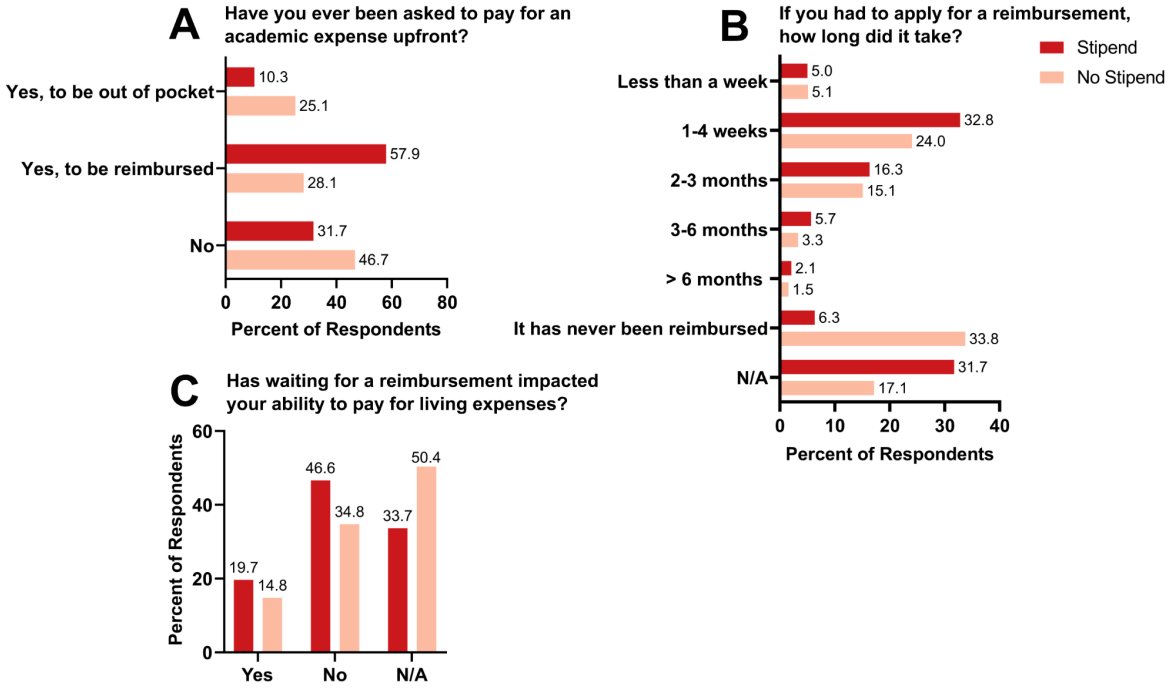

Figure 7.17. Reimbursements. **A** Respondents who receive a stipend (n=832) or do not (n=366) indicated if they have been asked to pay for an academic expense upfront. **B** Length of time to receive expense reimbursement. Data are shown by percent in each category: Stipend (n=914) and No Stipend (n=391). **C** Impact of reimbursement on living expenses.

The vast majority of students waited longer than a week for reimbursements (Fig. 7.17B). Only 35.9% of students in research-based master's degrees, 39.9% of students in doctoral degrees, and 27% of students in course-based professional or business master's degrees were reimbursed within 4 weeks. Between 4% and 9% of respondents were required to wait more than 3 months to be reimbursed. Having to wait periods of over a month can impact financial security, as students have regular monthly expenses such as rent, utilities, credit card bills, etc. One student commented that "for conferences and plane tickets, [they] could only request a reimbursement after the conference has actually happened. This means I pay the conference fee and 6 months later I can get it reimbursed." Thus, waiting for reimbursements is likely to have

impacted the ability of the survey's respondents to pay for their living expenses. Of these, 23.1% of students in course-based master's degrees, 13.4% of students in doctoral degrees, and 9.4% of students in course-based professional and business master's degrees have indicated this was the case (Fig. 7.17C).

This survey provides a cursory overview of the effects of upfront academic expenses on graduate students and has highlighted this as a real issue. Future work should aim to provide a more detailed picture of this issue and how it impacts students. For example, while we did not ask about the nature of these expenses, it may be valuable to delve further into the expenses students were asked to pay for, such as whether the expense was considered mandatory or not? Did students feel like they had a choice in the decision? What is the total amount of expenses students have paid for? Additionally, one of the risks with waiting for expenses is that if a student paid for it through a credit card and doesn't receive their reimbursement on time, then interest will begin to increase. This interest will not be covered by the eventual reimbursement.

Analysis of graduate student funding and support

Funding for graduate students in Canada is complex as it comes from various sources and is regulated on multiple levels. While some universities set minimum funding levels for student stipends, this can vary greatly between departments and even faculty within a university. Over 70% of respondents declared that they received a stipend (Fig. 7.18A). The remaining 30% reported that they did not receive a stipend at all. Of these, 73% felt that they should receive a stipend (Fig. S3).

The average stipend reported was $23 750 for doctoral students, $19 725 for research-based master's students, $16 813 for course-based master's students, and $13 113 for business and professional master's students (Fig. 7.18B). If we consider the context of a typical 40 h work

week, this becomes an average hourly pay of $9.18/h for a master's student and $11.43/h for a PhD student. This is well below the $15/h minimum wage implemented by the federal government (Employment and Social Development Canada 2022*a*) and does not account for the many graduate students who work over the average 40 h standard.

Based on the Likert scale of satisfaction (1 as very unhappy and 5 as very happy) (Likert 1932), almost half the respondents (46%) felt unhappy about their stipend value, which highlights an issue with current stipend values (Fig. 7.19). When asked about their ideal stipend values, respondents reported an average of $33 619 for doctoral students, $29 213 for research-based master's students, $26 912 for course-based master's students, and $22 705 for business and professional master's students (Fig. 7.20). The SPE's *Rethinking Federal Research Funding Report* found that respondents' ideal value of federal scholarships was $21 000 for a master's student and $35 000 for a PhD student (Science and Policy Exchange 2020). In our results, master's students reported a much higher ideal stipend value compared to their current average funding, which puts them well below the poverty line (Statistics Canada 2022*c*). Further, the ideal value of $21 000 from the SPE survey would still fall below the poverty line in the vast majority of the country.

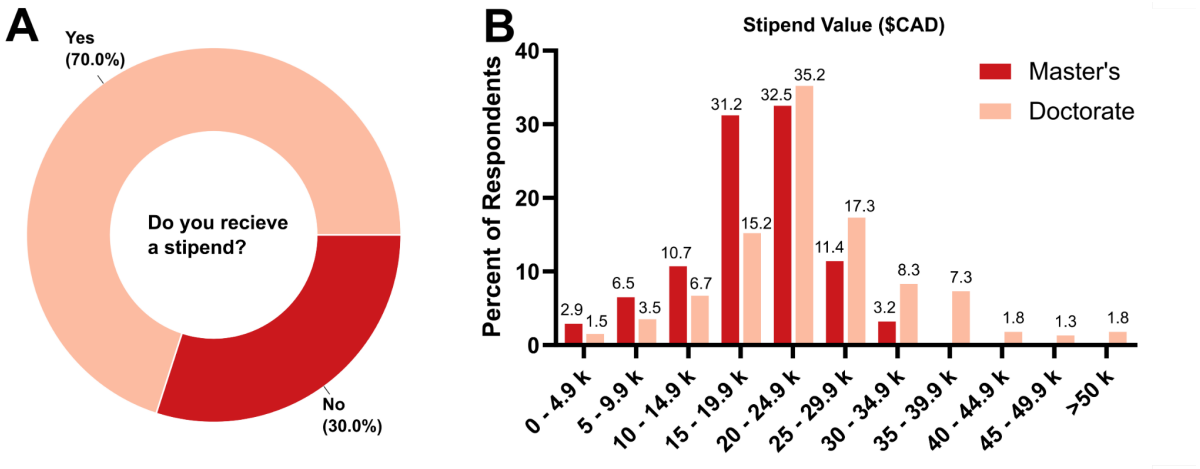

C

	MASTER'S	DOCTORATE
Average	$19,094.26	$23,765.10
Standard Deviation	$6,789.55	$9,194.01
Median	$19,500.00	$22,000.00

Figure 7.18. Stipend Status. **A** Respondents were asked if they receive a stipend, by percent (n=1305). **B** Stipend value of respondents in their Master's (n=308) or Doctorate (n=600) studies. Data are shown by the percentage of students in the respective level of study. **C** Average and Median stipend value of respondents in their Master's (n=308) or Doctorate (n=600) studies.

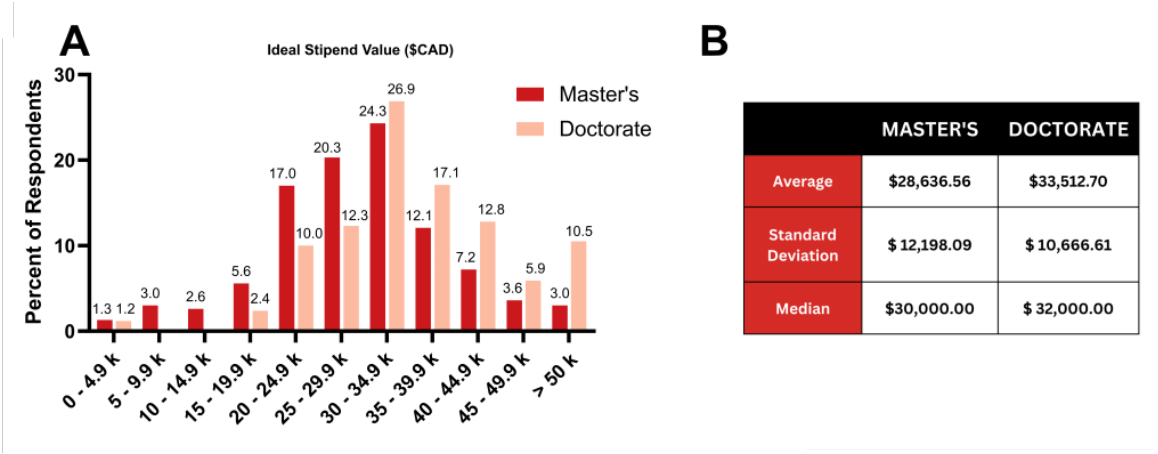

B

	MASTER'S	DOCTORATE
Average	$28,636.56	$33,512.70
Standard Deviation	$ 12,198.09	$ 10,666.61
Median	$30,000.00	$ 32,000.00

Figure 7.19. Ideal Stipend. **A** The ideal stipend value shared by respondents in their Master's (n=305) or Doctorate (n=592) studies. Data are shown by the percentage of students in the respective level of study. **B** Average and Median of ideal stipend value of respondents in their Master's (n=308) or Doctorate (n=600) studies.

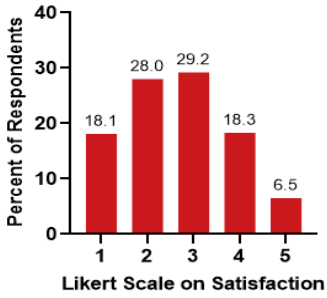

Figure 7.20. Stipend Satisfaction. Respondents were asked if they were happy with the value of their stipend based on the Likert scale of satisfaction (1 as Very Unhappy and 5 as Very Happy) by percent (n=914).

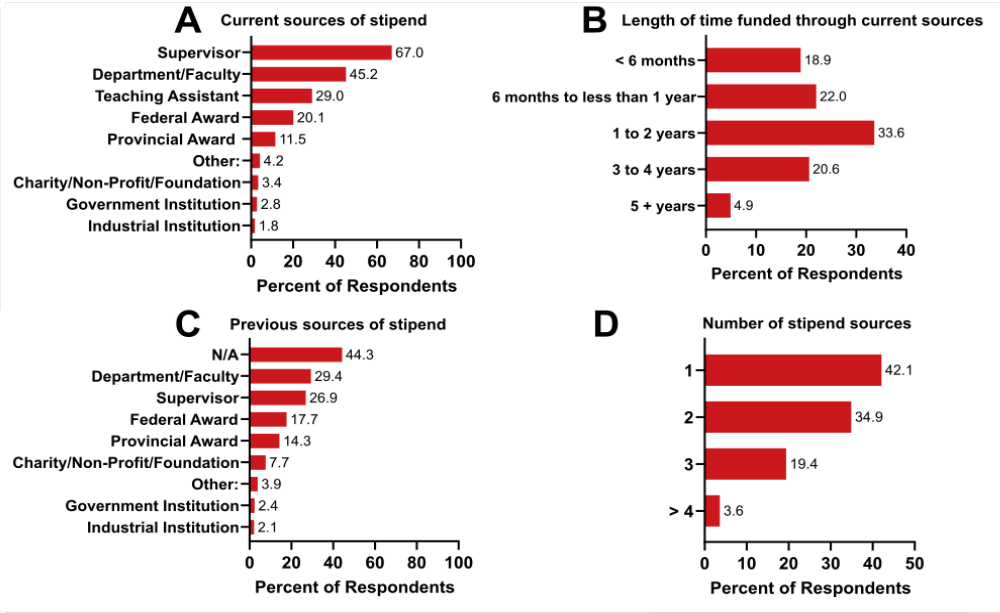

Figure 7.21. Stipend Sources. **A** Current sources of stipend of respondents (multiple selections possible) (n=914). "Other" includes institutional scholarships, research assistantships, and university scholarships. **B** Length of time funded through current sources of stipend (n=914). **C** Previous sources of stipend, not including current stipend sources (multiple selections possible) (n=914). "Other" includes Mitacs and institutional scholarships. **D** Number of current stipend sources (n=914). Data are shown by percentage.

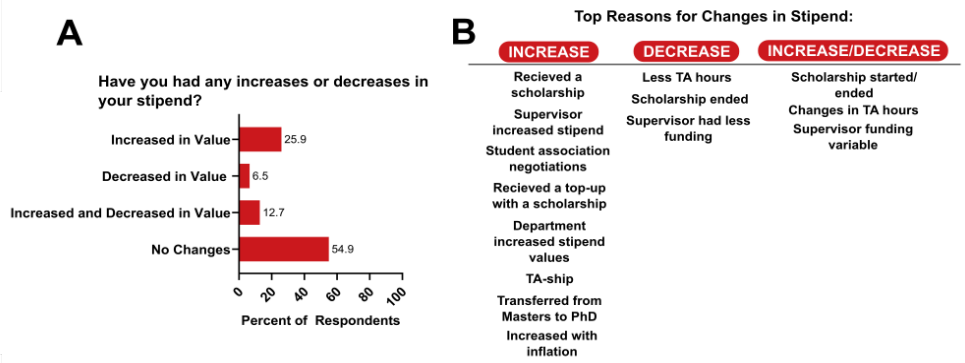

Figure 7.22. Stipend Changes **A** Reported increases and decreases in student stipend values (n=914). **B** Top reasons for the reported change in stipend values, broken down increase, decrease or both an increase and a decrease.

We asked respondents to share the source of their stipend. The majority of respondents (67%) were funded through their supervisor (Fig. 7.21A). Less than half (45.2%) were funded from their department/faculty. While national and provincial awards exist, only 20% were funded through federal awards, and 11.5% of respondents were funded through provincial awards. Most respondents (77%) reported only having 1–2 funding sources (Fig. 7.21D). The length of funding also varied from under 6 months to 4 years (Fig. 7.21C). About 45.1% of students have experienced either an increase or decrease in their stipend value: 25.9% have received an increase, 6.5% have received a decrease, and 12.7% have received both an increase and a decrease at some point in their studies (Fig. 7.22A). The top-reported cause of a stipend increase was that the respondent received a scholarship (further information about scholarships can be found below). Otherwise, respondents reported that their supervisor gave a stipend raise or their student association negotiated to increase student stipends (Fig. 7.22B). Conversely, the top reasons for students' stipends decreasing were a change in TA hours, their scholarship ending, or their supervisors decreasing their funding (Fig. 7.22B). In general, scholarships, TA hours, and the supervisor's financial status were the largest determinants of student stipend values.

Inadequate finances affect graduate students in all fields of study

Graduate student experiences, especially regarding financial situations, vary greatly depending on the field of study due to differences in tuition prices, stipend values, work expectations, and scholarship access. Statistics Canada reported in 2022/2023 that students' tuition varied substantially across degrees. For example, those studying business, management, and public administration paid the highest tuition, averaging $14 272 per year. Graduate students in STEM fields, such as computer and information sciences and engineering, were on the higher

end of tuition costs, paying an average of $8902 and $7454 per year, respectively. Comparatively, humanities graduate students had lower tuition on average at $4753 per year (Statistics Canada 2022*b*).

We were interested in exploring how tuition, stipend payments, and work varied among graduate students in different fields of study and whether these contributed to differences in financial struggle. We asked students to report their annual tuition fees, including ancillary fees. Unsurprisingly, business students had the highest annual tuition (Fig. 7.23), which was similar to what was reported by Statistics Canada. Physical sciences, medical sciences, and law students reported annual tuition costs above $9000, while social sciences, life sciences, and arts and humanities students paid over $8000 per year (Fig. 7.23).

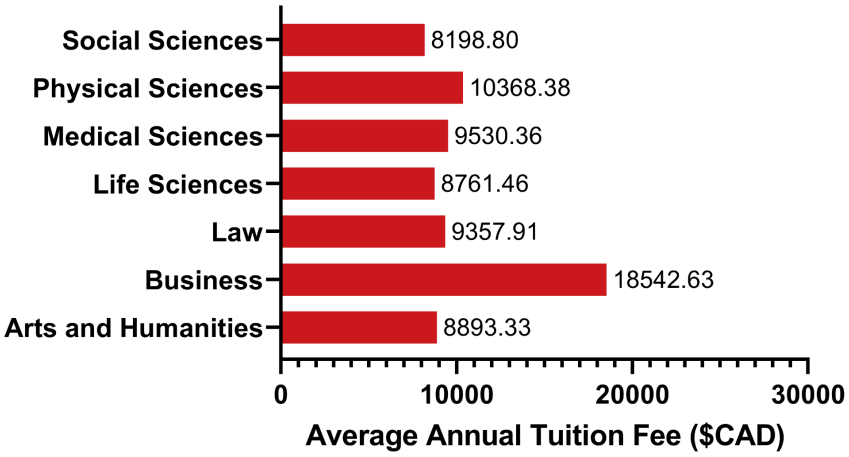

Figure 7.23. Tuition Fee by Field of Study. Average annual tuition in CAD dollars by field of study (n=1305). Respondents self-reported their field of study from 7 categories. If respondents indicated multiple fields of study or an option not listed in the survey, they were categorized into one of the six categories based on their answers for analysis purposes.

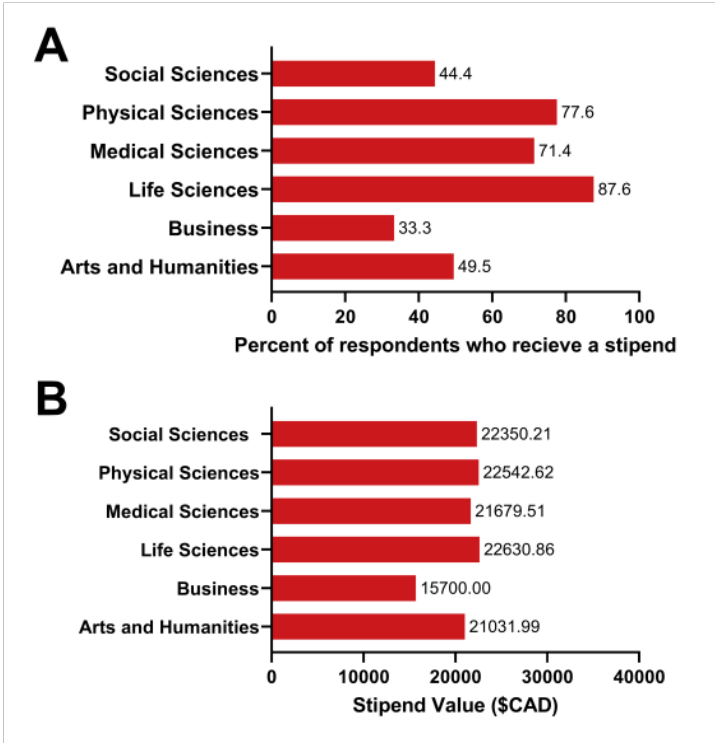

Figure 7.24. Field vs. Stipend. **A** Respondents were asked if they receive a stipend, categorized by field of study. Responses are shown as a percent of respondents who responded yes to receiving a stipend (n=914). **B** Average stipend value of respondents by their field of study. Arts and Humanities (n=101), Business (n=21), Life Sciences (n=307), Medical Sciences (n=311), Physical Sciences (Engineering, Physics, Mathematics, etc) (n=344) and Social Sciences (n=214). Law was excluded due to less than 5 responses.

Whether students receive a stipend depends on the program and degree type. The majority of students in the life sciences, physical sciences, and medical sciences reported receiving a stipend: 87.6%, 77.6%, and 71.4%, respectively (Fig. 7.24A). In comparison, only 49.5% and 44.4% of students in the arts and humanities and social sciences, respectively, receive a stipend. Business students were least likely to receive a stipend, with only 33.3% reporting receiving one. This disparity between programs is likely a consequence of stipends typically only being granted to students in research-based programs, which tend to be more common in the natural sciences. While the average stipend value was consistent across programs (Fig. 7.24B), the most common sources for stipends differed. Funding by supervisors was the most common stipend source for life sciences, physical sciences, and medical sciences students, followed by

funding from the department/faculty and then TAs (life sciences and physical sciences) or federal awards (medical sciences) (Table 7.1). In contrast, for arts and humanities and social sciences students, the department/faculty was the most common stipend source, followed by TAs and then federal awards (arts and humanities) and supervisors (social sciences).

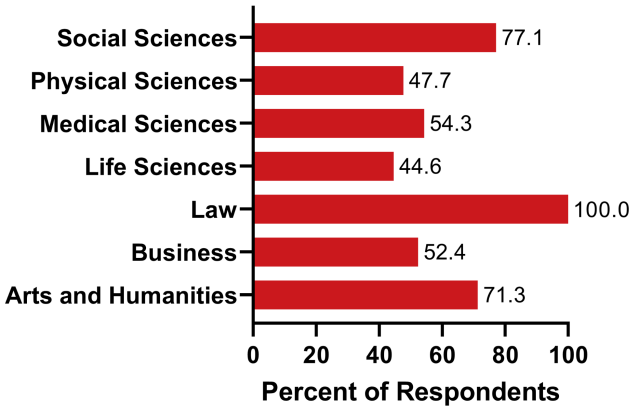

Figure 7.25. Work by Field of Study. Respondents were asked if they work a job outside of their studies, categorised by field of study: Arts and Humanities (n=101), Business (n=21), Law (n=7), Life Sciences (n=307), Medical Sciences (n=311), Physical Sciences (Engineering, Physics, Mathematics, etc) (n=344) and Social Sciences (n=214). Data are shown as a percent of respondents who responded yes to working outside of their studies.

FIELD OF STUDY	RANKING	FUNDING SOURCE	PERCENT OF RESPONDENTS
Arts and Humanities	1	Department/Faculty	64.00%
	2	Teaching Assistant	46.00%
	3	Federal Award (Tri-Councils - NSERC, CIHR, SSHRC, etc)	22.00%
Life Sciences	1	Supervisor	75.09%
	2	Department/Faculty	44.61%
	3	Teaching Assistant	31.60%
Medical Sciences	1	Supervisor	74.77%
	2	Department/Faculty	30.63%
	3	Federal Award (Tri-Councils - NSERC, CIHR, SSHRC, etc)	17.57%
Physical Sciences (Engineering, Physics, Mathematics, etc)	1	Supervisor	90.99%
	2	Department/Faculty	55.86%
	3	Teaching Assistant	34.68%
Social Sciences	1	Department/Faculty	67.37%
	2	Teaching Assistant	50.53%
	3	Supervisor	33.68%

Table 7.1. Top Funding Sources by Field of Study. Top three funding sources by field of study (multiple selections possible): Arts and Humanities (n=50), Business (n=21), Life Sciences (n=269), Medical Sciences (n=222), Physical Sciences (Engineering, Physics, Mathematics, etc) (n=267) and Social Sciences (n=95). Business and Law were excluded due to fewer than 5 responses. Data are shown as a percent of respondents by field of study.

As expected, a larger percentage of students in programs receiving fewer stipends, particularly arts and humanities and social sciences, reported working outside of their studies (71.3% and 77.1%, respectively) (Fig. 7.25). In comparison, students in programs that more frequently receive stipends (e.g., life sciences, medical sciences, and physical sciences) were less likely to report working outside of their studies (44.6%, 54.3%, and 47.7%, respectively).

Financial awards support graduate student research

As previously outlined, graduate students fund their studies through different sources, including federal/provincial/institutional scholarships, bursaries/grants, federal/provincial student

loans, bank loan/line of credit, family/spousal/partner support, employment pay, employer support, institutional stipends, and personal savings. Though the list of potential monetary support for students may initially appear extensive, the amount of available funding for a given student depends on their living situation and varies greatly.

In Canada, awards are granted to students who display a high level of academic achievement and are intended to encourage graduate students to dedicate more time to their studies (Table 7.2). The awards are primarily distributed by three federal research funding groups: the NSERC, the SSHRC, and the CIHR, which together form the Tri-Councils Agency. In addition to federal research awards, there are also provincial awards for graduate students. For example, the Ontario Graduate Scholarship is allocated through a merit-based program and available for application by students of varying academic disciplines across the province. Each award is jointly funded by the Province of Ontario (66%) and the university offering the award (33%). Fonds de recherche du Québec (FRQ) is another provincial organisation known to recognize excellence in research. Every year, FRQ provides financial support to many students by offering awards, from master's training scholarships to doctoral scholarships. Similar provincial graduate scholarships are offered in BC (BC Gov News 2021), AB (Government of Alberta n.d.), and NS (Communications Nova Scotia 2023).

Of 1305 survey respondents, 17.2% of doctoral and 13.4% of research-based master's students reported receiving a federal award, while 11.2% of doctoral and 5.0% of research-based master's students reported receiving a provincial award (Fig. 7.26). These award recipients represent high-calibre students who have not only achieved acceptance into competitive graduate research programs but have also been identified as the top scholars within this strong research categorization. In surveying graduate students in Canada, we wanted to identify whether the

intended goals of federal and provincial awards were being achieved by the current 2021 award values (Canadian Institutes of Health Research 2014) and how the financial well-being of award and non-award holders varied.

AWARD TITLE	FEDERAL RESEARCH FUNDING AGENCY	VALUE ($CAD), MAXIMUM DURATION & TENURE	ELIGIBILITY*
Canadian Graduate Scholarships-Master's (CGS-M)	Tri-Agency	$17,500/yr. for 1 yr. Eligible Canadian institution	Canadian Citizen, Permanent Resident of Canada, or a Protected person under subsection 95(2) of the Immigration and Refugee Protection Act (Canada) Completed between 0-12 months in program
Vanier Canada Graduate Scholarships	Tri-Agency	$50,000/yr. for 3 yrs. Eligible Canadian institution	Canadian Citizen, Permanent Resident of Canada, Foreign Citizens Completed <20 months in program Completed <32 months in program****
Canadian Graduate Scholarships-Doctoral (CGS-D)	Tri-Agency	$35,000/yr. for 3 yrs. Eligible Canadian institution	Canadian Citizen, Permanent Resident of Canada, or a Protected person under subsection 95(2) of the Immigration and Refugee Protection Act (Canada) Completed <24 months in program** Completed <36 months in program***
NSERC Postgraduate Scholarships-Doctoral (PGS-D)	NSERC	$21,000/yr. for 3 yrs. Eligible Canadian institution or eligible foreign institution	Canadian Citizen, Permanent Resident of Canada, or a Protected person under subsection 95(2) of the Immigration and Refugee Protection Act (Canada) Completed <24 months in program** Completed <36 months in program***
SSHRC Doctoral Fellowships	SSHRC	$20,000/yr. for 1-4 yrs. Eligible Canadian institution or eligible foreign institution	
Doctoral Foreign Study Award (DFSA)	CIHR	$30,000/yr. for 3 yrs. Eligible foreign institution	Canadian Citizen, Permanent Resident of Canada, or a Protected person under subsection 95(2) of the Immigration and Refugee Protection Act (Canada) Completed <24 months in program** Completed <36 months in program***

Table 7.2. Summary of Federal Tri-Council Awards. A summary of NSERC, SSHRC and CIHR awards for master and PhD students, including the funding agency, value and eligibility requirements.

In comparing responses of the financial concerns of award and non-award holders, awardees reported having less financial concern for bills (significant difference at $P < 10^{-5}$ level using a χ^2 test) and savings/emergencies (significant difference at $P = 0.032$ level using a χ^2 test) than non-award holders (Fig. 7.27). When asked how much savings students have available in

case of emergencies, award holders were significantly more likely than non-award holders to have 6+ months of living expenses saved (χ^2 test, $P = 0.00011$), though we note that less than 30% of respondents in both categories claimed to have these funds available (Fig. 7.28). The survey revealed that award holders have less outstanding student debt compared to non-award holders, at $14 260 and $17 977, respectively (Fig. 7.29). Furthermore, when asked to describe their current financial situation, award holders were less than half as likely to respond as "struggling" and more than twice as likely to respond as "comfortable" compared to non-award holders, a significant difference at the $P < 10^{-5}$ level (χ^2 test) (Fig. 7.30). Overall, 48.4% of non-award holders and 38% of award holders responded as either "struggling" or "tight" to describe their current financial situation. These survey findings are not surprising, considering that awards can help guarantee an income for graduate students that may or may not be provided to non-awardees.

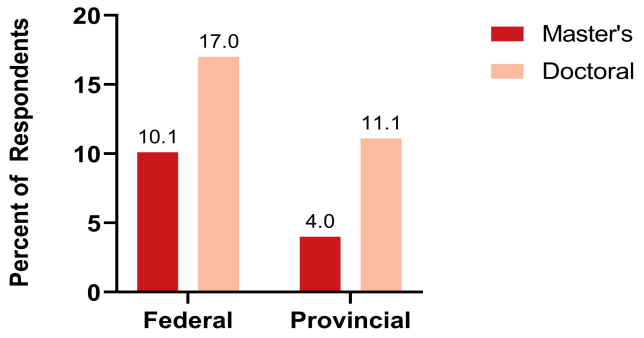

Figure 7.26. Federal and Provincial Award Holders. Percent of respondents who have received an award based on level of study: Master's (n=547) and Doctoral (n=758). Award holder status is defined as being selected to receive a federal or provincial award. This does not include any other awards that were indicated (admission scholarships, institutional scholarships, etc.).

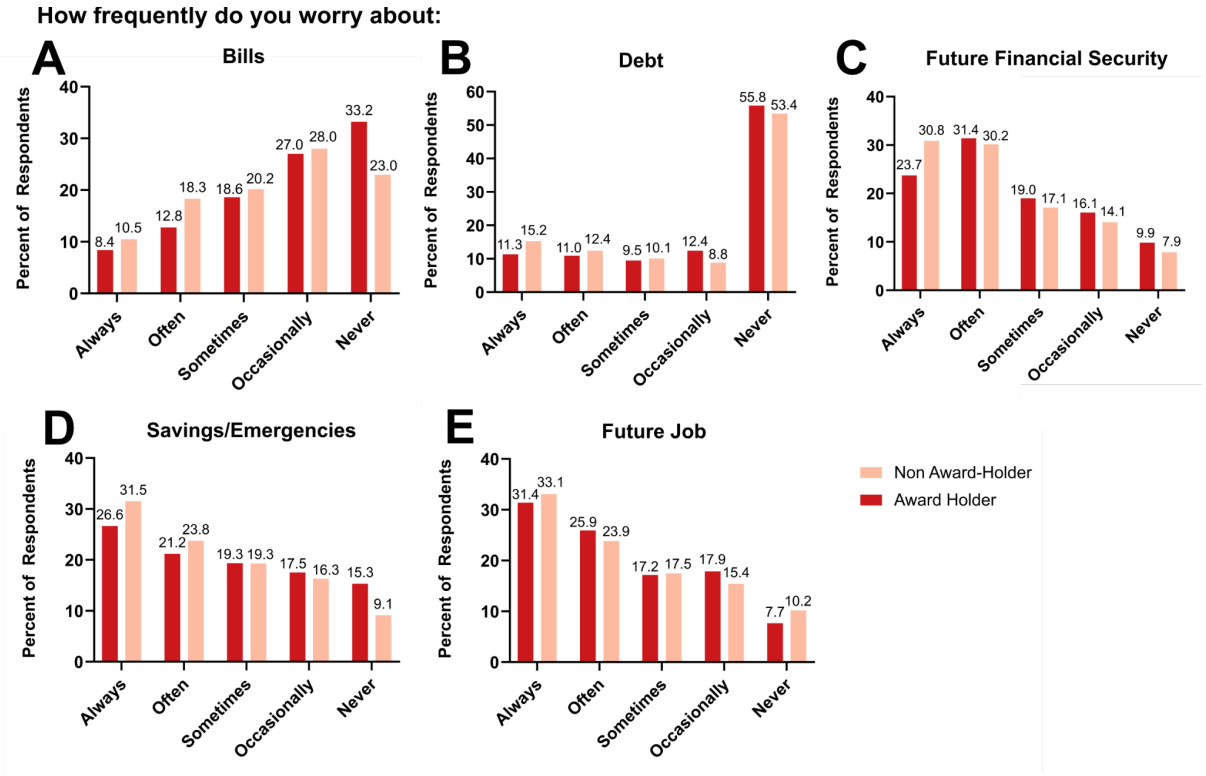

Figure 7.27. Financial Situation by Award Holder Status. How frequently respondents, based on award holder status, worry about their **A** ability to pay bills, **B** ability to pay back their student debt, **C** future financial security, **D** savings/ability to pay for emergency expenses and **E** ability to obtain a future job in their chosen field. Data are shown by percent in each category: Non Award-Holder (n=1031) and Award-Holder (n=274). Award holder status is defined as being selected to receive a federal or provincial award. This does not include any other awards that were indicated (admission scholarships, institutional scholarships, etc.).

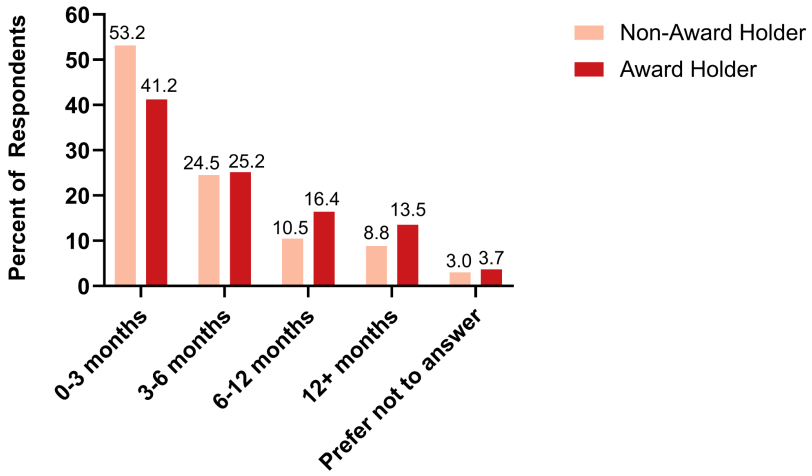

Figure 7.28. Amount of Savings by Award Holder Status. Amount of savings, measured by months of living expenses, that respondents have available for emergencies, by award holder status. Data are shown by percent in each category: Non Award-Holder (n=1031) and Award-Holder (n=274). Award holder status is defined as being selected to receive a federal or provincial award. This does not include any other awards that were indicated (admission scholarships, institutional scholarships, etc.).

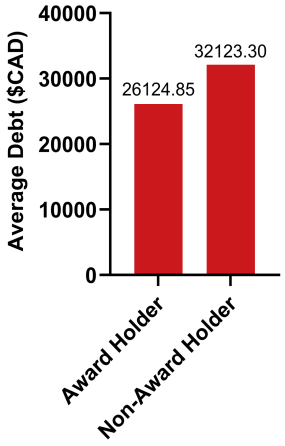

Figure 7.29. Average Debt by Award Holder Status. Average debt of respondents by award holder status. Data are shown by percent in each category: Non Award-Holder (n=1031) and Award-Holder (n=274). Award holder status is defined as being selected to receive a federal or provincial award. This does not include any other awards that were indicated (admission scholarships, institutional scholarships, etc.).

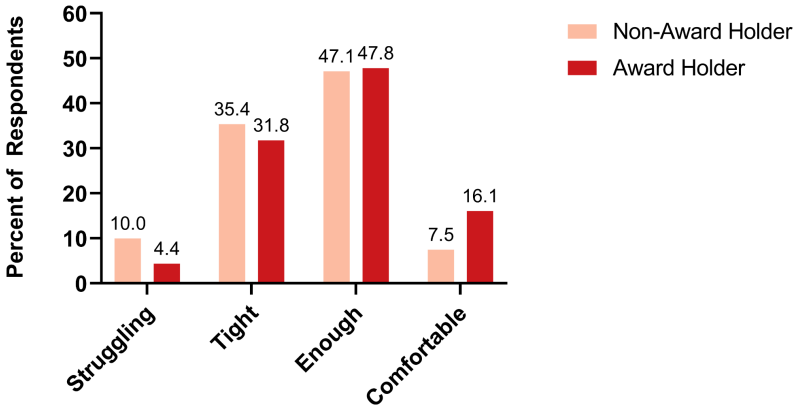

Figure 7.30. Financial Situation by Award Holder Status. Financial situation of non award-holding (n=1031) and award-holding (n=274) respondents. Data are shown by the percent of respective award statuses. Award holder status is defined as being selected to receive a federal or provincial award. This does not include any other awards that were indicated (admission scholarships, institutional scholarships, etc.).

Surprisingly, however, the survey responses demonstrated that awardees are nonetheless preoccupied with financial concerns during their graduate program. For example, when asked how frequently they worry about financial concerns including bills, savings/emergencies, and future financial security, over 66% of award holders responded having financial concern through responses of "always," "often," or "sometimes." Over 44% of award holders responded having concerns for financial debt (Fig. 7.27). These findings highlight the inability of current federal

and provincial award values to effectively enable graduate award holders to fully concentrate on their studies. When graduate students were asked what their ideal stipend value would be, 26% of respondents stated $30 000–$34 999 (Fig. 7.20). This value range falls close to the value of the current Canadian Graduate Scholarships-Doctoral (CGS-D) award at $35 000 per year. Additionally, we examined financial incentives received by graduate students after receiving an award (Fig. 7.31). The most popular incentive was an additional "top-up" of their stipend (27% of respondents), typically from their supervisor. This is typically granted to the student in cases where the scholarship replaces a stipend previously paid by their supervisor. Since the supervisor no longer needs to pay the student's stipend, some will choose to pay the student a smaller additional amount on top of their award. Additionally, 17% of respondents reported receiving a scholarship meant to cover their tuition fully, and 14% received a scholarship meant to cover their tuition partially. This is often granted by the student's department/university in the form of an "Excellence Scholarship" or "Tuition Waiver."

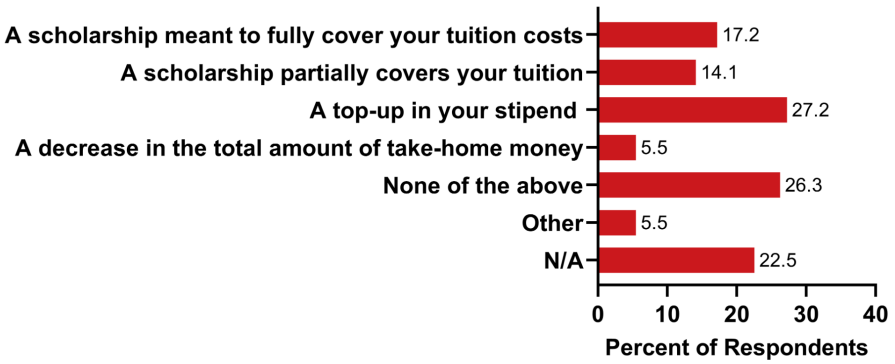

Figure 7.31. Scholarship Incentives. Respondents were asked if they received additional incentives or changes after receiving their scholarships (n=941). Other includes: scholarship is subtracted from stipend (no top-up) and funding caps.

Interestingly, 5.5% of award holders reported a decrease in their total amount of take-home money. This could be due to specific situations where the value of awards is less than the stipend value they were previously receiving. An additional concern is that these awards are

defined for a period of time that often does not cover the entirety of their studies. Although not fully captured in this study, future efforts should identify what happens to students' financial situations following the end of their award. It was noted various times in the personalized responses that students often did not have guaranteed funding after their scholarship ended. For example, one student comments "For example, [my scholarship] will end in August 2022, and my stipend for my research assistantship will not be adjusted to compensate for the $13 000 net loss in my annual compensation. For myself and others in my position, this will be an extremely large financial burden as we attempt to complete the final years of our graduate studies."

Graduate students from underrepresented groups are more likely to struggle financially

Diversity is essential among graduate students to foster generations of scientists with diverse perspectives and ideas. This will be vital to innovation as we tackle future challenges in society. Per the Dimensions charter: "equity, diversity and inclusion strengthen the research community, the quality, relevance and impact of research, and the opportunities for the full pool of potential participants." (Government of Canada 2019). A 2019 *Survey of Postsecondary Faculty and Researchers* from Statistics Canada showed that postdoctoral fellows and PhD students are increasingly more diverse than the previous generation of researchers. In fact, 50% of postdoctoral fellows and 39% of PhDs who responded to the survey reported belonging to a visible minority group.

Despite the presence and increasing prevalence of diverse groups, women, Indigenous peoples, and visible minorities still face inequities and barriers to inclusion in graduate programs, including lack of representation among those who receive federal doctoral and master's level scholarships (Baskaran et al. 2021). Additionally, it has been found that those who identified as women, visible minorities, individuals with disabilities, and Indigenous were all less likely to

receive research funding (Statistics Canada 2020). Factors such as eligibility, duration of awards, and evaluation criteria are significant barriers to promoting equity, diversity, and inclusion (EDI) in graduate programs. While targeted investments, such as new funding in Budget 2022 for Black Scholars (Department of Finance Canada 2022), and recent changes to evaluation criteria, such as NSERC's New Guidelines on Contributions to Research, Training, and Mentoring, which expands the definition of "excellence" (National Sciences and Engineering Research Council of Canada 2022), are steps in the right direction, there is still work to be done to ensure accessibility of graduate degrees.

This lack of support can lead to a lack of diversity in academia, and this concern was recognized by respondents in our survey. One respondent remarked that they "think that paying students such low stipends (i.e., below the poverty line) is really discouraging EDI in academia and is ensuring that already privileged people are the only ones that have access to higher education." From the data we collected, we aimed to understand the financial struggles of underrepresented groups of graduate students to further identify barriers of entry into graduate degrees in Canada.

Gender-based analysis

Women composed the majority of the survey sample (63.2%), followed by men (32.8%) and respondents who identified as non-binary, gender-fluid, agender, genderqueer, trans, two-spirit, or gender non-conforming (4.0%; category definitions in Supplementary file) (Fig. 7.32). There were no significant differences in average stipend values among gender groups (KW test, $P = 0.78$) (Fig. 7.33). Across all gender groups, approximately half viewed their financial situations as "Struggling" or "Tight," with slightly higher numbers among men; however, the differences between groups were not significant (χ^2 test, $P = 0.053$) (Fig. 7.35). It appears that

respondents who identified as either non-binary, gender-fluid, agender, genderqueer, trans, two-spirit, or gender non-conforming were less likely to have received a government award compared to those who did, though again this difference was not significant (χ^2 test, $P = 0.058$) (Fig. 7.34).

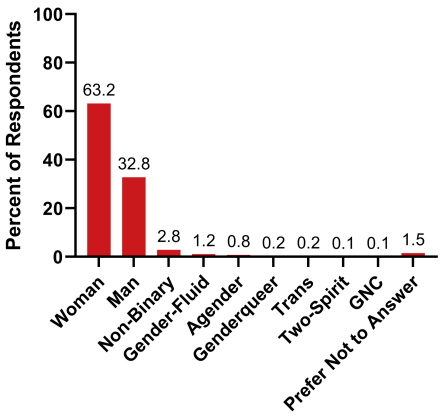

Figure 7.32. Gender Identity. Gender identity of all respondents by percent (n=1305) (multiple selections possible). Definitions are located in Appendix C. GNC = gender non-conforming.

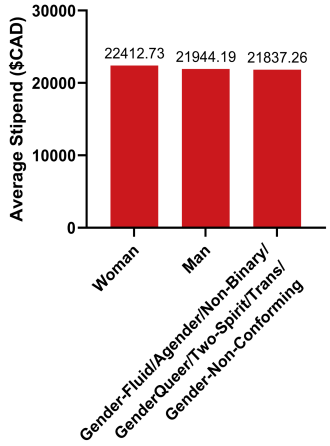

Figure 7.33. Average Stipend by Gender Identity. Average stipend value of respondents by their gender identity: Woman (n=547), Men (n=328) and Gender-Fluid/Agender/ Non-binary/ GenderQueer/ Two-Spirit/ Trans/ Gender-Non-Conforming (n=37).

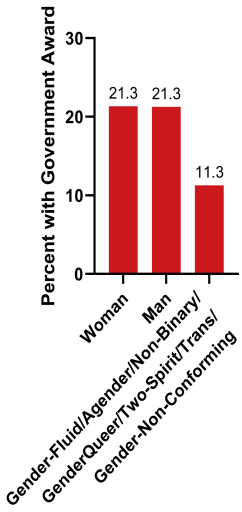

Figure 7.34. Award Holder Status by Gender Identity. Percent of respondents who have received an award by their gender identity: Woman (n=825), Men (n=428) and Gender-Fluid/ Agender/ Non-binary/ GenderQueer/ Two-Spirit/ Trans/ Gender-Non-Conforming (n=62). Award holder status is defined as being selected to receive a federal or provincial award. This does not include any other awards that were indicated (admission scholarships, institutional scholarships, etc.).

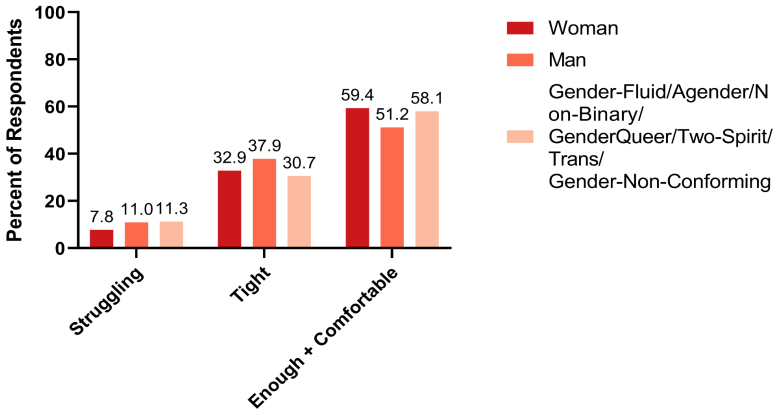

Figure 7.35. Financial Situation by Gender Identity. Financial situation of respondents by their gender identity: Woman (n=825), Men (n=428) and Gender-Fluid/Agender/Non-binary/GenderQueer/Two-Spirit/Trans/Gender-Non-Conforming (n=62). Enough and Comfortable responses were grouped to ensure more than 5 responses in this category.

With the low sample size of gender-diverse individuals in this study, cross-analyses for these metrics were not conclusive. Future efforts should target to better understand the specific financial struggles of these graduate students.

Respondents largely identified as White (66.5%) (Fig. 7.36). There were no significant differences (χ^2 test, $P = 0.73$) seen in the proportion of domestic students that received a government award (Fig. 7.38). No significant differences in average stipend values were found

for domestic students (KW test, $P = 0.35$) (Fig. 7.37). There were significant differences (χ^2 test, $P = 0.043$) in the reported level of financial struggle of domestic students with Black, Latin American, Middle Eastern, and South Asian students more likely to report struggling or feeling tight financially than East Asian, Southeast Asian, or White students (Fig. 7.39). Among international students, there were also significant differences (χ^2 test, $P = 1.7 \times 10^{-4}$), with Middle Eastern, South Asian, and Southeast Asian (not shown in the figure due to small sample size) students reporting financial struggle at a much higher rate. The discrepancy between the financial stress of domestic and international Southeast Asian students may be due to a small sample (with only 17 students and 11 international students).

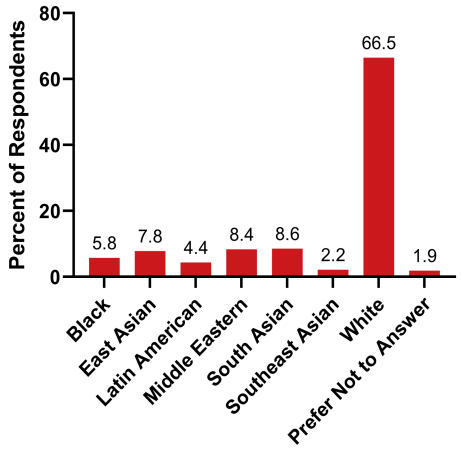

Figure 7.36. Ethnic Identity. Percent of respondents reporting selected ethnic identity (multiple selections possible) (n=1300).

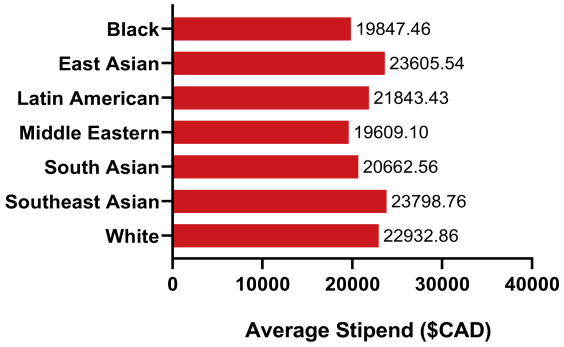

Figure 7.37. Average Stipend by Ethnic Identity. Average stipend value of respondents by their ethnic identity: Black (n=48), East Asian (n=78), Latin American (n=46), Middle Eastern (n=77), South Asian (n=91), Southeast Asian (n=21), White (n=588).

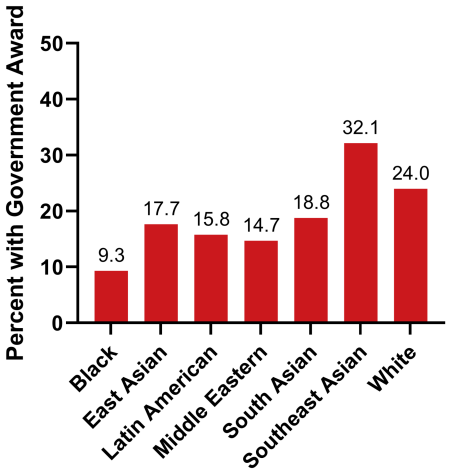

Figure 7.38. Award Holder Status by Ethnic Identity. Percent of respondents who have received an award by their ethnic identity: Black (n=75), East Asian (n=102), Latin American (n=57), Middle Eastern (n=109), South Asian (n=112), Southeast Asian (n=28), White (n=868). Award holder status is defined as being selected to receive a federal or provincial award. This does not include any other awards that were indicated (admission scholarships, institutional scholarships, etc.).

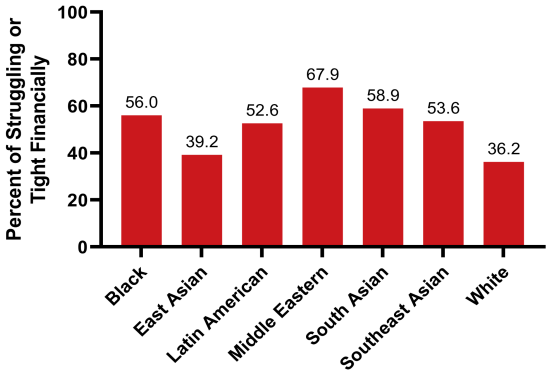

Figure 7.39. Financial Situation by Ethnic Identity. Financial situation of respondents by their ethnic identity: Black (n=75), East Asian (n=102), Latin American (n=57), Middle Eastern (n=109), South Asian (n=112), Southeast Asian (n=28), White (n=868). Enough/Comfortable and Tight/Struggling responses were combined to ensure more than 5 responses in the grouped categories.

Indigenous students

The 2021 Census reported that 1.8 million Indigenous peoples reside in Canada. Of these 1.8 million Indigenous individuals, approximately 1.048 million people identify as First Nation, 625 000 identify as Metis, and 70 000 identify as Inuit, representing the three main categories of Indigenous peoples in Canada (Statistics Canada 2022*d*). Indigenous participation in graduate programs surveyed was low. Indigenous respondents consisted of only 1.2% of our survey

population, while 0.8% of individuals preferred not to answer this question (Fig. 7.40). Proportionally, this is consistent with a 2020 Statistics Canada report showing that 1.7% of PhD students identified as indigenous (Statistics Canada 2020). While Indigenous peoples in Canada belong to three broad groups: Inuit, Metis, and First Nations, our survey did not collect any further identifying information among the Indigenous respondents.

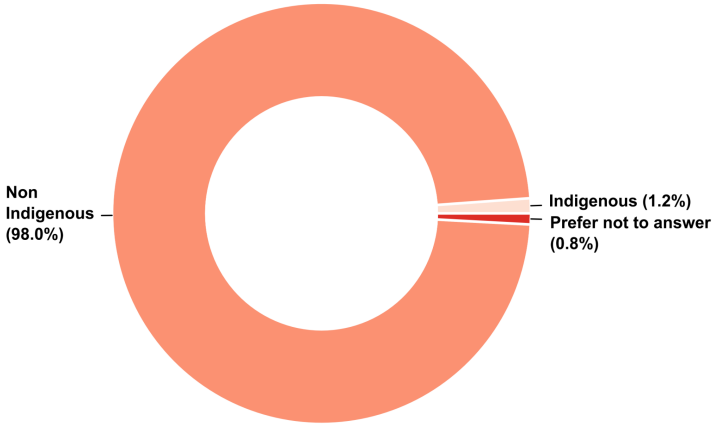

Figure 7.40. Indigenous Identity. Percent of respondents who identified as Indigenous (First Nations, Métis or Inuit) (n=1305).

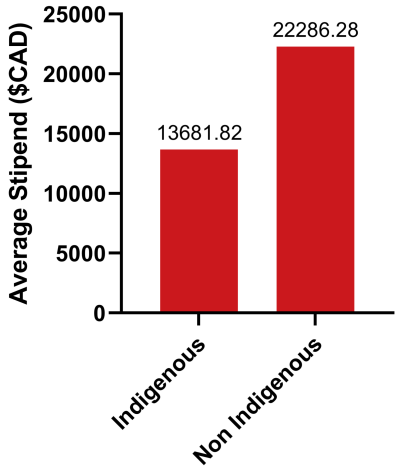

Figure 7.41. Average Stipend by Indigenous Identity. Average stipend value of respondents who identify as Indigenous: Indigenous (n=11) and Non Indigenous (n=890).

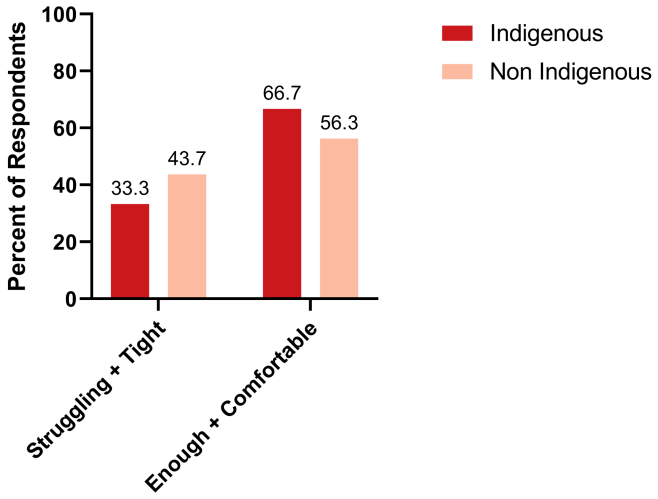

Figure 7.42. Financial Situation by Indigenous Identity. Financial situation of respondents who identify as Indigenous: Indigenous (n=15) and Non Indigenous (n=1279). Enough/Comfortable and Tight/Struggling responses were combined to ensure more than 5 responses in the grouped categories.

Some concerning trends could be seen between Indigenous and non-Indigenous graduate students in the findings. There was a significant reduction (KS test, $P = 0.0012$) in the average stipend value for Indigenous respondents ($13 682) compared to non-Indigenous respondents ($22 286) (Fig. 7.41). There was no significant difference (χ^2 test, $P = 0.42$) in the responses of Indigenous (33.3%) and non-Indigenous (43.7%) individuals that their financial situation was struggling or tight (Fig. 7.42). The small sample in our dataset indicates that it could be important for a more detailed investigation into these discrepancies.

Individuals with dependents

A dependent is an individual who relies on others, such as parents and family members, for financial support. We assessed the relevance of graduate students having dependents for their financial struggles. Survey data revealed that the majority of respondents have no dependents (86.5%), while having one dependent (7.4%) or more than one dependent was less common (5.7%) (Fig. 7.43). In general, having dependents corresponded with increased financial struggle, as more respondents with dependents classified their financial situation as struggling (15%) or

tight (42.4%), in comparison to those without dependents (7.8% and 33.6%, respectively) (Fig. 7.44). This could potentially be a consequence of the struggle of older graduate students with dependents to access need-based funding. One respondent noted that "awards and bursary applications are geared to young students and not at all applicable to adult homeowners of students with families/children. Adult learners are effectively excluded from needs-based support."

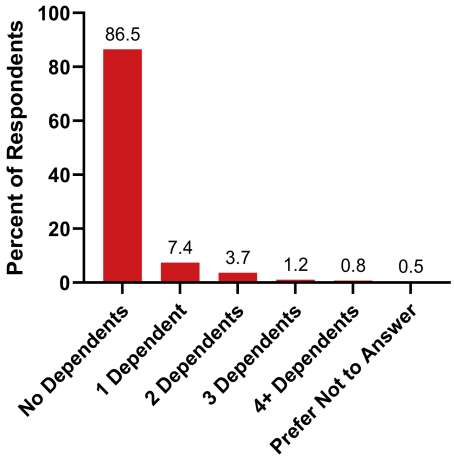

Figure 7.43. Dependents The percentage of respondents with each number of dependents.

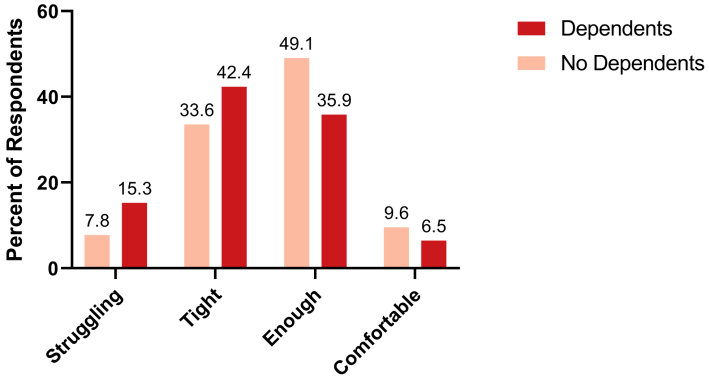

Figure 7.44. Dependents and Financial Situation. Financial situation of respondents with or without dependents: Dependents (n=170) and No Dependents (n=1129). Dependents include 1 or more dependents, and were combined to ensure more than 5 responses in the grouped categories.

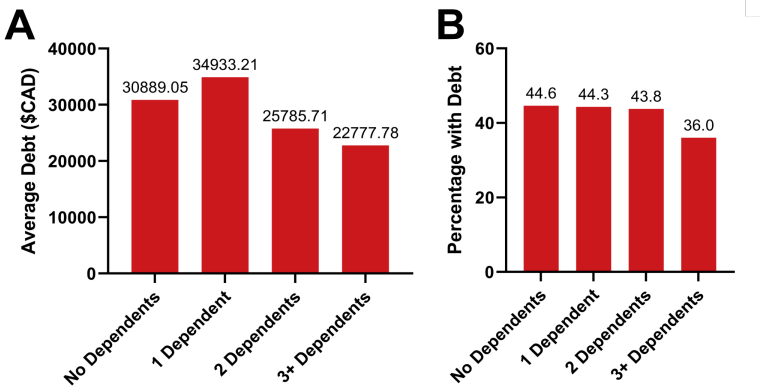

Figure 7.45. Dependents and Debt **A** The average student debt for those respondents who have student debt conditional on the number of dependents. **B** The proportion of respondents who have student debt conditional on the number of dependents.

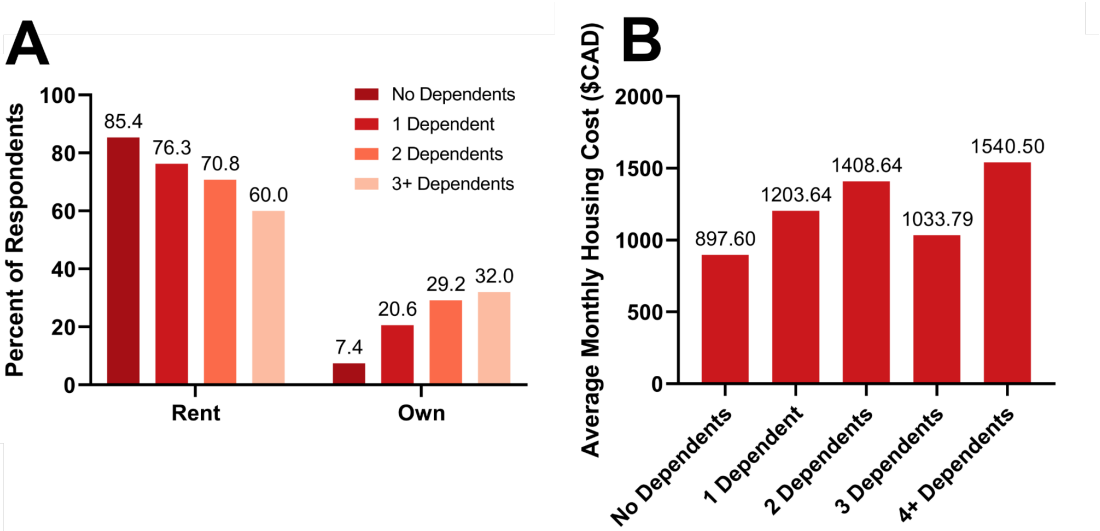

Figure 7.46. Dependents and Housing **A** The percentage of respondents who rent or own (does not add up to 100% due to other living statuses) conditional on the number of dependents they have. **B** The average monthly cost of housing for respondents conditional on the number of dependents.

Whether a graduate student has dependents or not, they have some contribution to the average debt accumulated in graduate studies. Respondents without dependents accumulated an average debt of $30 889, while those with one dependent averaged $34 933 debt (Fig. 7.45). As the number of dependents increased, the average debt decreased to below $26 000 (Fig. 7.45). The majority of graduate students, whether they have dependents or not, have rental accommodations. As the number of dependents increased, there was a slight decrease in the

average number of respondents that lived in rental properties and an increase in respondents who owned their homes (Fig. 7.46A).

We also surveyed respondents on their average monthly housing costs (mortgage or rent). On average, the monthly housing costs tend to be higher for graduates with more dependents, which could be attributed to the requirements of a larger living space. While graduate students with no dependents had an average monthly housing cost of $898, the average monthly housing costs also increased as the number of dependents increased (one dependent—$1204, two dependents—$1439, three dependents—$1034, and four or more dependents $1541) (Fig. 7.46B).

Individuals living with disabilities

A disability is defined by the Canadian Government as a physical, mental, intellectual, cognitive, sensory, learning, and communication impairment or a functional limitation, whether visible or not and permanent, temporary, or episodic in nature, which hinders a person's full and equal participation in society when they face a barrier. According to the 2017 Canadian Survey on Disability, 22% of the Canadian population aged 15 years or older (approximately 6.2 million individuals) had one or more disabilities (Statistics Canada 2018). It has been well documented that individuals with a disability face numerous obstacles and challenges in society. Some government aid programs for students with disabilities exist. For example, the Canada Student Grant for Students with Disabilities enables students to apply for grants up to $4000 per academic year through provincial granting agencies (Employment and Social Development Canada 2022*a*). In addition, local funding opportunities exist with grants and bursaries for individuals with disabilities at each academic institution. In addition to government funding, the National Education Association of Disabled Students (NEADS) is an organisation founded in

1986 designed to support full access to education and employment for post-secondary students and graduates across Canada. NEADS offers disabled students services such as student debt reduction, increased campus involvement, experience, and help with postgraduate employment. Academic institutions can provide and accommodate services for individuals with disabilities through means such as note-taking, visual language interpretation, captioning for virtual learning, accessibility in campus/classroom, testing/exam accommodation, and tutoring services designed for each disability and learning requirement.

We collected data on whether respondents identified as having a disability and whether it impacted their graduate school success and financial status. Overall, the majority of respondents (87.4%) stated that they did not identify with a disability, 10.3% identified as having a disability, and 2.3% of respondents preferred not to answer this question (Fig. 7.47). Respondents with a disability had an average stipend value similar to those without a disability ($23 134.83 vs. $22 120.41, respectively) (Fig. 7.48). In addition, graduate students with a disability received an award/scholarship at similar proportions individuals without a disability, 21.5% and 20.9%, respectively (Fig. 7.49). While not significant, a larger percentage of students with a disability indicated that they are financially "struggling" or "tight" compared to those without a disability. Our survey reported that 10.4% of graduate students with a disability were "struggling," while only 8.4% of graduate students without a disability were struggling (Fig. 7.50). In addition, 38.5% of graduate students with a disability were feeling "tight" on their finances, while only 34.0% of graduate students without a disability responded similarly (Fig. 7.50). Results showed that 51.1% of respondents with a disability were comfortable with their financial status, while 57.4% of respondents without a disability were comfortable with their finances. Respondents noted that things like "counselling, physical therapy, and prescription medications are both not

accounted for in stipend values and not covered by public insurance here in Canada," which can disproportionately affect graduate students with disabilities. Another student noted that "disability also increases costs by extending the length of people's programs, costing them many thousands of dollars in tuition and fees." Certainly, academic institutions have made progress with maintaining accessibility and offering support/services, but our survey highlights that individuals with disabilities are struggling or are tight with their finances, thus identifying a need for more governmental support.

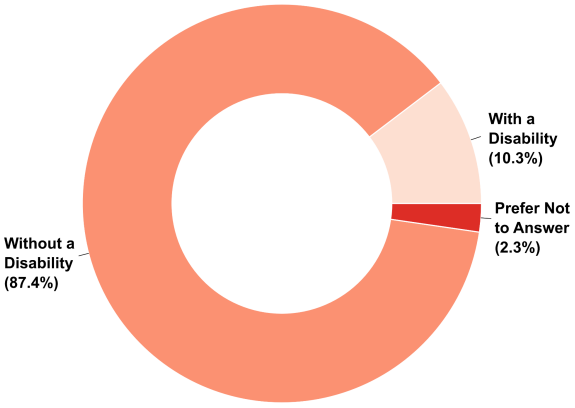

Figure 7.47. Disability Status The percentage (%) of respondents (n = 1305) who identify with a disability.

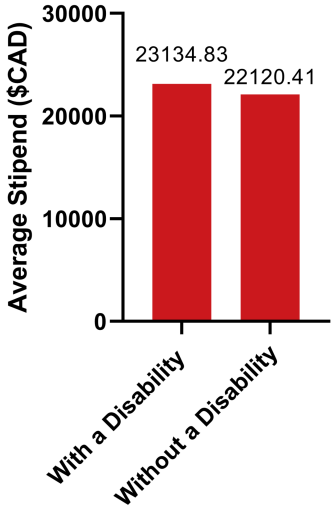

Figure 7.48. Average Stipend by Disability Status The average stipend ($) of respondents with (n = 93) or without (n = 794) a disability.

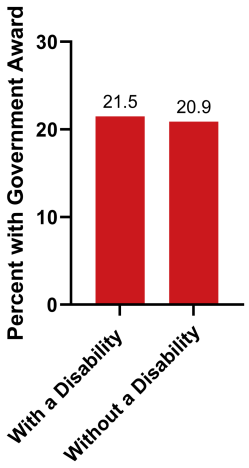

Figure 7.49. Award Holder Status by Disability Status The percentage (%) of respondents with (n = 135) or without (n = 1140) a disability who indicated receiving a Government award.

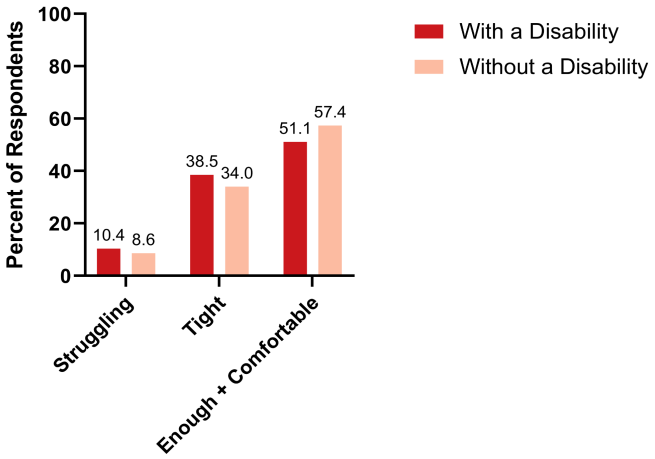

Figure 7.50. Financial Struggle by Disability Status The percentage (%) of respondents with (n = 135) or without (n = 1140) a disability who identified their financial status as being either "struggling", "tight" or "enough + comfortable".

International graduate students face larger financial struggles than domestic students

International students composed 21% of master's and 37% of doctoral students in Canada, with this proportion rising to nearly 50% for those studying in STEM (Statistics Canada 2022*e*). This is comparable to the 31.6% of survey respondents to our survey who were international students (Supplementary Table 7.1).

International students can face additional challenges compared to domestic students, such as legal limits on the number of hours they can work off campus, which has recently been

suspended until the end of 2023 (Immigration, Refugees and Citizenship Canada 2022), ineligibility for most Canadian government scholarships, as well as other struggles. One notable difference between international and domestic graduate students is the amount they pay in tuition, with 39% of international students reporting annual fees over $15 000 compared to only 3% of domestic students (Fig. 7.51). While 28% of international students have their tuition entirely covered by additional scholarships or higher stipends, over 66% must pay for at least part of their tuition out of pocket (Fig. 7.52).

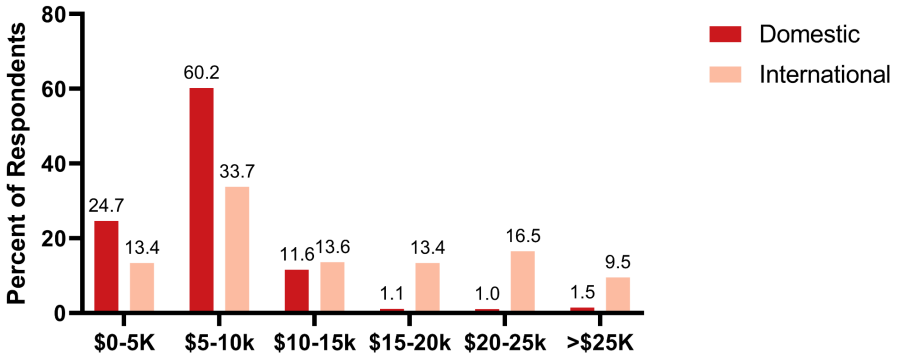

Figure 7.51. Tuition Fees The annual tuition and other mandatory fees for domestic (n=892) vs. international (n=412) students.

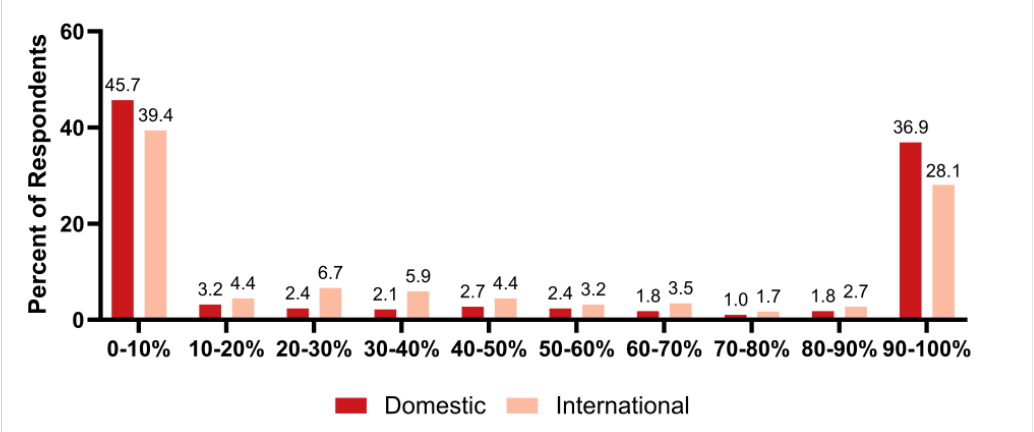

Figure 7.52. Tuition paid out of pocket The percentage of tuition paid out of pocket for domestic (n=886) vs. international (n=406) students.

International students were found to be significantly (χ^2 test, $P < 10^{-5}$) more likely to report that they are "struggling" to make ends meet or that their finances are "tight," with over

50% falling into these categories (Fig. 7.53). Concerns over one's ability to pay for bills, financial security, and emergency expenses were also significantly higher (χ^2 test, P values of $<10^{-5}$, 0.002, and $<10^{-5}$, respectively). The survey reported 44% of international students were "always worried" about their ability to pay for emergency expenses compared to 24% of domestic students (Fig. 7.54). The amount of emergency savings held by international students was also significantly different (χ^2 test, $P < 10^{-5}$), with 70% of international students having less than three months of expenses saved compared to 44% of domestic students (Fig. 7.55). This is despite international students generally paying less in rent (Fig. 7.56).

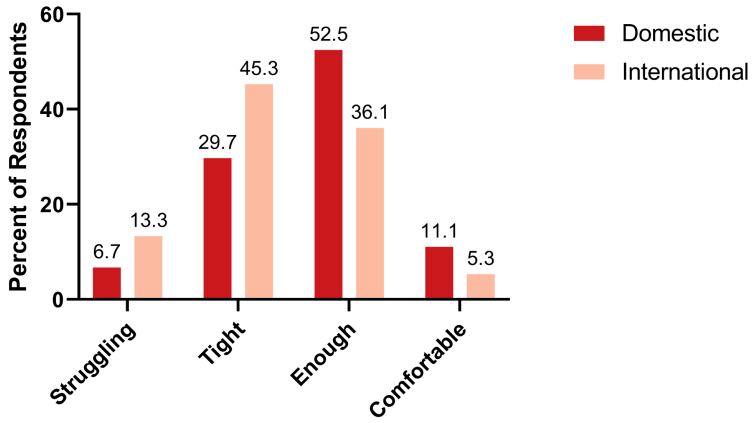

Figure 7.53. Financial Situation - Domestic vs. International The percent of respondents who are struggling financially and often do not have enough to make ends meet; every month is tight and often making sacrifices to pay for necessities; have enough and able to afford to provide for themselves or very comfortable and can spend as they like for domestic (n=892) vs. international (n=413) students.

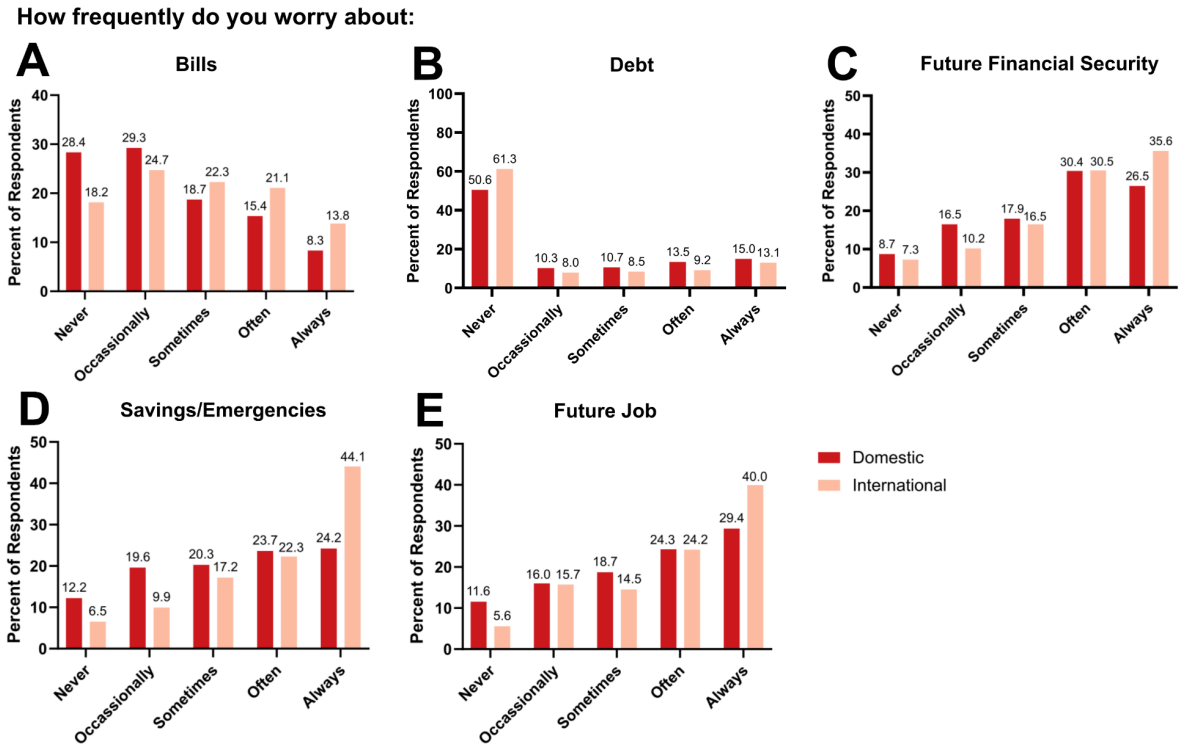

Figure 7.54. Financial Stresses - Domestic vs. International The responses for domestic (n=892) vs. international (n=413) students on how frequently they worry about their **A** ability to pay bills **B** ability to pay back their student debt **C** future financial security **D** savings/ability to pay for emergency expenses **E** ability to obtain a future job in their chosen field. Data are shown by percent in each category.

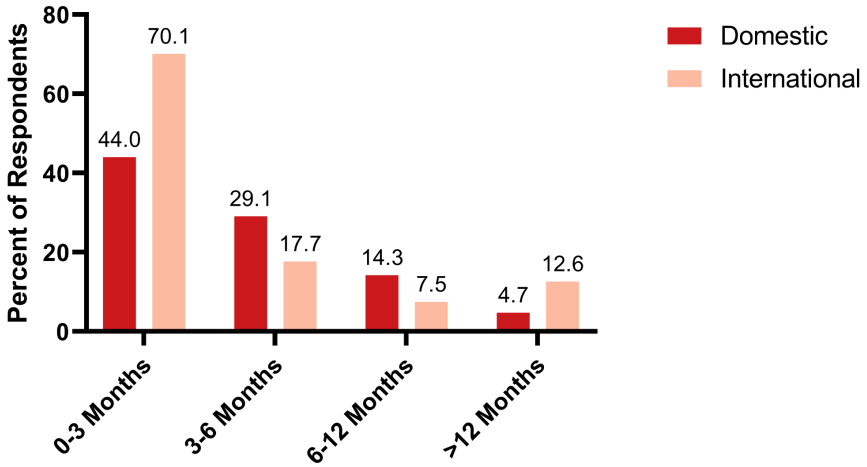

Figure 7.55. Savings - Domestic vs. International The number of months of living expenses respondents have as savings for domestic (n=863) vs. international (n=401) students.

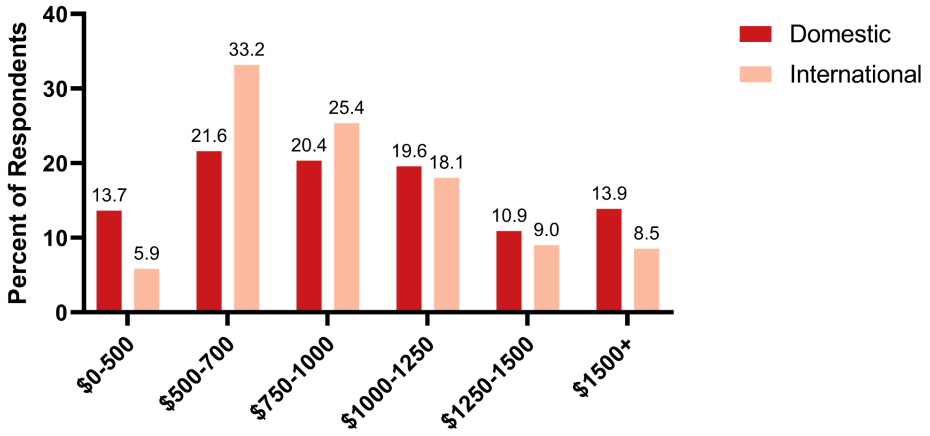

Figure 7.56. Housing costs - Domestic vs. International The monthly cost of housing of respondents for domestic (n=879) vs. international (n=410) students.

Additionally, there were large differences in how international graduate students received funding. Only 13% of international students received government scholarships compared to 26% of domestic students (Fig. 7.57). This is likely due to the lack of eligibility of international students for many federal and provincial scholarships. In fact, the only federal scholarship that international students can apply for is the prestigious Vanier Scholarship. An evaluation report of the Vanier Scholarship shows that only 13% of Vanier awardees are international scholars (Canadian Institutes of Health Research 2014). Since these awards, valued at $50 000, are much higher than other federal awards, they are highly competitive and have since failed at their original objective of attracting and recruiting prestigious students from outside of Canada (Canadian Institutes of Health Research 2014).

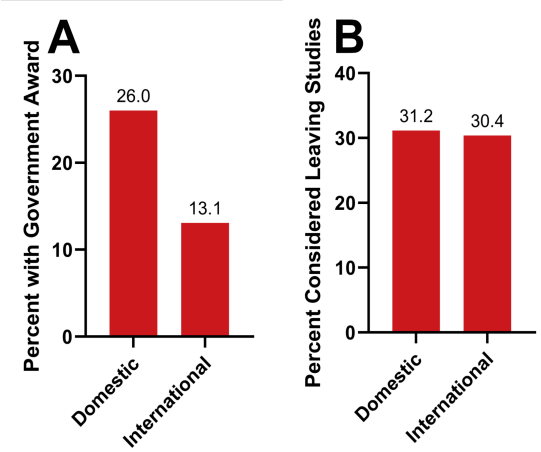

Figure 7.57. Government Awards and Leaving Studies **A** The percentage of respondents who receive a federal or provincial award for domestic (n=982) vs. international (n=413) students. **B** The percentage of respondents who have considered leaving studies due to concern over finances for domestic (n=889) vs. international (n=408) students.

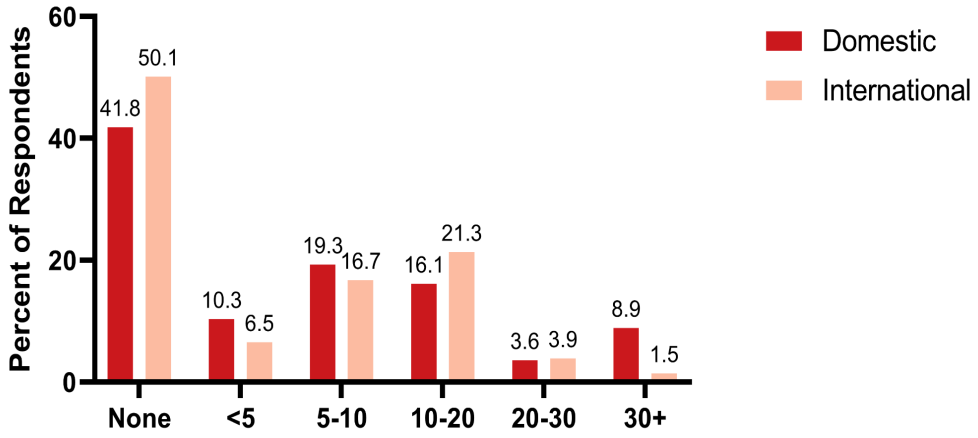

Figure 7.58. Hours outside work - Domestic vs. International The number of hours worked per week outside of graduate studies for domestic (n=892) vs. international (n=413) students.

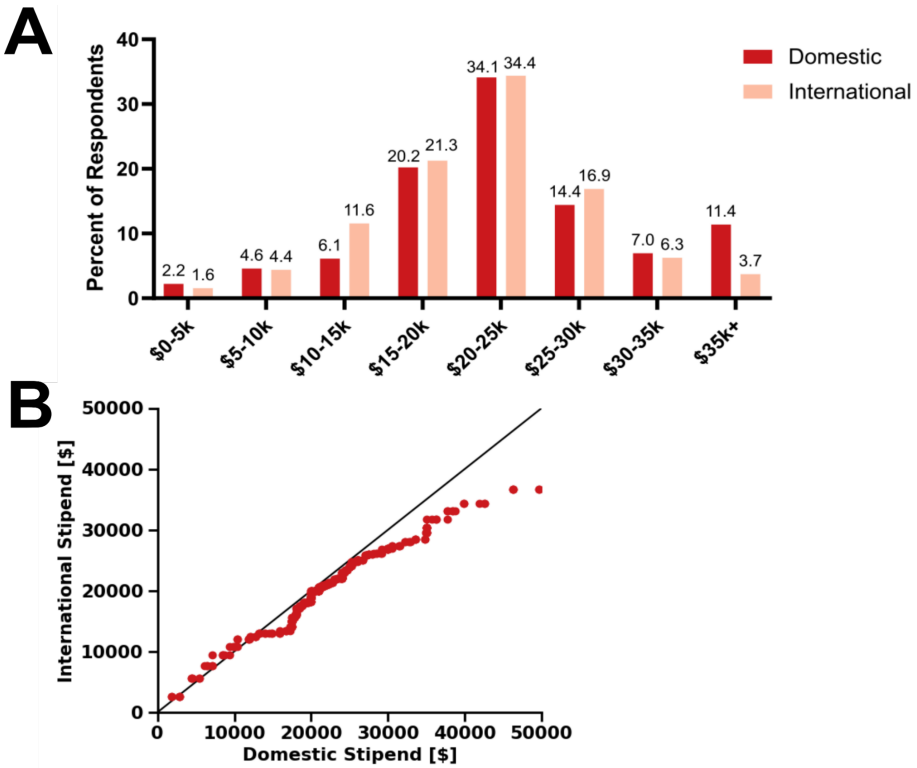

Figure 7.59. Stipend levels - Domestic vs. International The annual stipend received by respondents who were domestic (n=589) vs. international (n=320) students. **a** The percentage of respondents in each category who receive a stipend of this amount. **b** A Q-Q plot (binned into groups of 5 to maintain de-identification) showing how the distribution of stipends for domestic and international students differ. A Q-Q plot is such that the same quantile for each data set is plotted against each other (eg. the 5th percentile of both distributions is one point). If the two distributions were the same they would follow the line indicated.

Further, at the time this survey was conducted, there were limitations on the number of hours international students were allowed to work outside of their studies. This hinders the ability for students to supplement their income and puts them at increasing risk of financial insecurity. International student respondents worked less outside of their studies compared to domestic students (Fig. 7.58). Recently these limits have been suspended (Immigration, Refugees and Citizenship Canada 2022). The restriction for international students to work less than 20 h per week during school semesters has been temporary removed to allow for more additional income and to supplement labour shortages. Similarly, far fewer international student respondents indicated receiving stipends larger than $27 000 compared to domestic students, which may be due to the lack of access to federal scholarships (Fig. 7.59).

B. 6 Next steps and recommendations

1. Increase federal funding (through the Tri-Councils) for graduate students in the form of research grants and scholarships

The conclusions of this survey support the current recommendation of the Support Our Science campaign (Support our Science 2022). Put simply, we advocate for an increase in the *value* and *number* of graduate student scholarships at academic institutions across Canada to account for increased inflation and enrolment into graduate programs since 2003 (i.e., the last time these awards were increased):

a. **Increase in the *value* of Tri-Council scholarships—**we recommend harmonising all federal Tri-Council scholarships to a *minimum* of $25 000 for master's students and $35 000 for PhD students. This aligns with the ideal stipend values declared by our survey respondents (Fig. 7.19). Careful consideration should go into this decision as it can set the standard for stipends at the university level.

b. **Increase in the *number* of Tri-Council scholarships—**our survey has found that about 20% of students are funded through federal scholarships, while 12% are funded through provincial scholarships (Fig. 7.21). We recommend increasing the number of students who are funded through these scholarships by 50% annually to account for increased enrolment into graduate programs (Statistics Canada 2022*f*). While the number of graduate students in Canada has doubled between 2002 and 2019, we have seen decreases in the number of Tri-Council scholarships available resulting in increased competition and lower success rates for these competitions. By increasing the number of these awards, it would increase the overall percentage of graduate students funded and remove

some financial burden from supervisors and principal investigators to fund these students out of their grant funding.

c. **Increase the value of Tri-Council *research grants*—**we recommend a specific increase in research grants (e.g., discovery grants, etc.) that will allow for supervisors to increase the stipends of graduate students. Our survey shows that the majority of students (67%) are funded through their supervisors (Fig. 7.21). Future work should investigate the structural and policy changes needed to ensure that the increases in monetary value of research grants are directly funding and supporting graduate students. Careful consideration should be taken to ensure that financial support for students is increased and not simply being put towards funding for additional students at the current low pay rates.

2. Implement a standard for stipends in Canada and establish transparency practices for university departments

Many survey respondents cited confusion in variation and inconsistencies in aspects of stipends. In many ways, this confusion has contributed to the challenges faced by groups advocating for stipend increases. From university and department websites, it is often unclear what funding packages are available for graduate students, and this information can often be buried under policy jargon in academic regulations. Transparency of this information is vital to allow students to make informed decisions about their graduate school pursuits.

Additionally, we recommend developing a standardised approach to defining a stipend for graduate students. This includes shifting terminology to more effectively communicate the "take-home" value of stipends to ensure that students can live above the poverty line. Specifically, this means the amount of a students' stipend that remains *after* paying tuition and

mandatory expenses. This distinction is important as tuition remains one of the largest costs for students, and students who pay tuition out of pocket have increased financial struggles (Fig. 7.7). This goes in hand with increasing transparency of stipends, including stipulations, requirements, timelines, and limitations for graduate students.

As such, we propose the following calculation for universities to establish a minimum stipend for their students:

$$\text{Minimum stipend} = \text{Tuition} + \text{average cost of rent} + \$550/\text{month for additional fees} + \$500/\text{month for a PhD student}$$

In this case, tuition would include any ancillary, program, or incidental fees associated with the student's tuition (i.e., all cumulative mandatory tuition fees for the student). This would also account for an increased stipend need for international students and would compensate if the department provided any tuition waivers for international students. The average cost of rent can be calculated for a one-bedroom apartment within the city where the university is located. We recommend using a resource that regularly publishes these data (such as Zumper: https://www.zumper.com/blog/rental-price-data-canada/) to get the most accurate up-to-date data. Additionally, we recommend an average of $550/month for additional living expenses such as groceries, transportation, medical expenses, and more. The value of this number was calculated in our survey as the average additional monthly expenses seen from students (Fig. 7.9). We then recommend an additional $500/month for a PhD student as these students have increased financial needs and often have more dependents and responsibilities.

Here, we have provided an example of this equation at work for a domestic (in province, on campus) thesis-based graduate student attending a U15 university in Canada (Table 7.3). Full details on these numbers and sources can be found in Supplementary files.

Table 3. Recommended stipends for Canadian universities.

University	Total tuition	Rent (one-bedroom) per month	Master's minimum stipend	PhD minimum stipend
University of Alberta	$7086.54	$1020.00	$25 926.54	$31 926.54
University of British Columbia	$5777.02	$2500.00	$42 377.02	$48 377.02
University of Calgary	$7895.83	$1610.00	$33 815.83	$39 815.83
Dalhousie University	$11 060.24	$1800.00	$39 260.24	$45 260.24
Université Laval	$3187.44	$1100.00	$22 987.44	$28 987.44
University of Manitoba	$5011.86	$1090.00	$24 691.86	$30 691.86
McGill University	$6389.50	$1500.00	$30 989.50	$36 989.50
McMaster University	$8389.02	$1640.00	$34 669.02	$40 669.02
Universitié de Montreal	$5207.91	$1500.00	$29 807.91	$35 807.91
University of Ottawa	$7850.76	$1720.00	$35 090.76	$41 090.76
Queen's University	$9110.10	$1700.00	$36 110.10	$42 110.10
University of Saskatchewan	$5873.97	$1020.00	$24 713.97	$30 713.97
University of Toronto	$7997.28	$2300.00	$42 197.28	$48 197.28
University of Waterloo	$8414.33	$1800.00	$36 614.33	$42 614.33
University of Western Ontario	$9088.19	$1680.00	$35 848.19	$41 848.19

Note: Recommended values for minimum master's and PhD stipends at 15 Canadian universities, based on tuition fees, average rent prices for a one-bedroom apartment in corresponding cities, plus an additional $550 per month for expenses and additional $500 for PhD students per month. Additional details on calculations, sources, etc. can be found in Supplementary Table 3.

3. Expand the eligibility of Tri-Council graduate student scholarships to help provide better funding for international students and underrepresented groups

Current eligibility for Tri-Council graduate student scholarships, namely the CGS and PGS awards (Table 7.2), excludes international students. While the Vanier scholarship aims to attract and retain international scholars, this award fails to achieve these goals (Canadian Institutes of Health Research 2014). We recommend that the Tri-Council re-evaluate the key priorities of the Vanier scholarship and consider creating separate scholarship allocations for international students as our data indicate that they are less likely to receive these scholarships (Figs. 7.34 and 7.38). We further amplify the recommendations of Baskaran et al. (2021), which suggest harmonising the duration eligibility for Tri-Council CGS and PGS awards to increase the time in which a student is eligible to apply for the awards. We also recommend continuing efforts to expand the definition of "excellence" to include diverse forms of work, volunteering, and mentoring. All of these recommendations will assist with removing barriers of entry for foreign scholars and underrepresented groups.

4. Index and evaluate graduate student funding on a regular basis to ensure the sustainability of research infrastructure in Canada

To ensure the long-term sustainability of research in Canada and appropriately retain and attract top students, we recommend indexing the value of stipends and Tri-Council scholarships to the consumer price index (Statistics Canada 2023). This is already done in countries like Australia, which index all graduate student scholarships annually to adjust for inflation (Khoo 2021). This will better ensure in future that we do not reach a financial crisis among graduate students such as that we are experiencing now. The costs of living have continued to increase over time, including the cost of tuition for graduate students, which has increased by 38% since 2006 (Statistics Canada 2022*a*). It is therefore important to recognize the issue that federal awards have not changed in value since 2003, and financial support for graduate students has remained stagnant over the past 20 years.

5. Remove limits on work outside of studies for graduate students

We have highlighted the limitations of working outside of full-time graduate studies. We recommend the removal of certain work limitations (e.g., the 10 h rule), which severely impedes graduate students from obtaining needed supplemental income. To be clear, we *do not* suggest removing these limitations as a way of resolving graduate student financial struggle, as this would merely provide a band-aid solution to a much larger problem that is outlined in this report. Instead, this recommendation should be interpreted as a chance for students with increased financial needs to have the option to seek work outside of their studies while still maintaining their commitment to full-time studies.

6. Further investigate the role of EDI factors in financial struggle

One limitation of our survey is that we did not have sufficient demographic data to provide tangible and targeted EDI-centred recommendations. Future work should investigate the financial status of graduate students who identify as members of historically underrepresented groups, including women, Indigenous peoples (First Nations, Inuit, and Métis), persons with disabilities, members of visible minority/racialized groups, and members of LGBTQ2+ communities This will enable a more diverse understanding of students' needs depending on their demographic background and the subsequent development of effective, equitable, and evidence-based programs and(or) policies to support students from historically underrepresented groups.

B. 7 Acknowledgements

We would like to acknowledge all of the graduate students across Canada who participated in our survey, as well as the various student associations, organisations, and individuals who helped distribute the survey. We would also like to thank Amy Johnston for assistance with analysis of demographic cross-sections, as well as all those from the Science Policy Exchange and Toronto Science Policy Network providing insight during the initial development of the survey.

Appendix D: Sarah Laframboise CV

Education

PhD Biochemistry (September 2018- PRESENT), **University of Ottawa -** *Ottawa, Canada*

Supervisor: Dr. Kristin Baetz
Project Title: Uncovering the Role of NuA4 in Regulating Lipid Metabolism and Nuclear Morphology in *Saccharomyces cerevisiae*

- Successfully passed Transfer/Comprehensive Examination in February 2020
- Extensive development of lab techniques such as PCR, western blots, fluorescent microscopy, cell culturing, flow cytometry, electron microscopy, and more.

Bilateral Exchange (January 2018- June 2018), **Stockholm University** - *Stockholm, Sweden*

Supervisor: Dr. Marie Öhman
Project Title: Identifying A to I RNA Editing in Differentiated Sh-SH5Y Cells.

- Worked 40+ hours/week on a full-time intensive 6-month research project.
- Learned several lab techniques, such as human cell culturing, fluorescent microscopy, sectioning and staining of tissue, mice dissections, western blots, and more.

BSc. Hons. Biology (2013-2018), **York University** - *Toronto, Canada*

- Participated in a summer research project at the University of Windsor's Great Lakes Institute for Environmental Research (Dr. Subba Rao Chaganti) investigating water contamination in the Great Lakes. Assisted in a community led water collection and assisted with all sample analyzation and preparation and developed extensive knowledge on bacteria extractions and qPCR analysis of water samples.
- Member of the York Lions Varsity Women's Hockey Team

Awards

- York University's Top 30 Alumni Under 30 (2022)
- University of Ottawa's Faculty of Medicine Leadership Award (2021 and 2022)
- NSERC – CGS-D Alexander Graham Bell (2021-Present)
- Father Roger Guindon Scholarship Fund (2020)
- NSERC-Create SynBioApps Program Bursary (2018)
- York University's Student Award for Outstanding Global Engagement (2018)
- Swedish Woman for Education Toronto Scholarship (2018)
- York Mobility Award (2018)

Peer-Reviewed Publications

1. Bailey, T, Rohden, F, **Laframboise, SJ*.** ***20 years of choices: A fight for increased funding for graduate students and postdocs.*** (August 2024) *Biochemistry and Cell*

Biology. (Support Our Science Advocacy Work): https://cdnsciencepub.com/doi/full/10.1139/bcb-2024-0029

2. **Laframboise, SJ*,** Deneault, LD, Denoncourt, A, Downey, M, Baetz, K,. (2024) ***Uncovering the role of the yeast lysine acetyltransferase NuA4 in the regulation of nuclear shape and lipid metabolism.*** (July 2024) *Molecular and Cellular Biology*. (PhD Work): https://www.tandfonline.com/doi/full/10.1080/10985549.2024.2366206
3. Bailey, T, Holland, S, Rose, M, **Laframboise, SJ*,** D'Addario, A, Sinclair, K, Hakoum, M**.** ***International Mobility of Canadian Graduate Students: An Investigation into Brain Drain.*** Accepted. *Confluences: uOttawa Press*. (OSPN Work)
4. **Laframboise, SJ*,** Bailey, T, Dang, A, Rose, M, Zhou, Z, Berg, M, Holland, S, Abdul, SA, El-Sahli, S, Boucher, DM, Fairman, G, Deng, J, Shaw, K, Noblett, N, D'Addario, A, Empey, M, Sinclair, K. (April 2023) ***Analysis of financial challenges faced by graduate students in Canada****. Biochemistry and Cell Biology*. (OSPN Work): https://cdnsciencepub.com/doi/10.1139/bcb-2023-0021
5. Walden, EA, Fong, RY, Pham, TT, Knill, H, **Laframboise, SJ*,** Huard, S, Harper, ME, Baetz, K. (2020) ***Phenomic screen identifies a role for yeast lysine acetyltransferase NuA4 in the control of Bcy1 subcellular localization, glycogen biosynthesis, and mitochondrial morphology.*** *PLOS Genetics*. (PhD Work): https://journals.plos.org/plosgenetics/article?id=10.1371/journal.pgen.1009220

Selected Non-Peer-Reviewed Publications

1. ***Investing in the Future of Science: The Urgent Need to Fund Graduate Students and Postdoctoral Scholars in Canada.*** **Sarah Laframboise*.** (2023; Canadian Science Policy Centre Editorial Series; https://sciencepolicy.ca/posts/investing-in-the-future-of-science-the-urgent-need-to-fund-graduate-students-and-postdoctoral-scholars-in-canada/)
2. ***Canada's graduate students and post-doc experts need much more support than we give them.*** **Sarah Laframboise*,** Senator Stan Kutcher (2023; The Ottawa Citizen: https://ottawacitizen.com/opinion/laframboise-and-senator-stan-kutcher)
3. ***Intersections Between Next Generation Researchers and Science Policy in Canada - Past, Present and Future.*** Sivani Baskaran, Dhanyasri Maddiboina, Jina Kum, **Sarah Laframboise*,** Paalini Sathiyaseelan, Madison Rilling, Farah Qaiser, Anh-Koi Trinh, Shawn McGuirk. (2021; Canadian Science Policy Centre Magazine; https://drive.google.com/file/d/1prVOPVXW0IpLIMSdJMAXNBWT72-8OZvK/view)
4. ***Discovering the Breast Cancer Gene.*** **Laframboise, S*** (2021; Gairdner Foundation; https://gairdner.org/wp-content/uploads/2021/10/Discovering-the-Breast-Cancer-Gene.pdf/)
5. ***Yeast could soon make psilocybin cheaper than their magic mushroom cousins can.*** **Laframboise, S*** (2020; Massive Science; https://massivesci.com/articles/psilocybin-yeast-magic-mushrooms-psychedelics/)
6. ***Blurred Lines: Studying Concussions with a Concussion.*** **Laframboise, S*** (2020; Health Science Inquiry; https://www.healthscienceinquiry.com/index.php/hsi/article/view/316/294)

7. ***In the ruling against Caster Semenya, bogus science is being used to stifle the vulnerable.*** **Laframboise, S*** (2019; Massive Science; https://massivesci.com/articles/caster-semenya-track-field-iaaf-olympics-testosterone-hyperandrogenism/)
8. ***Bioengineered yeast can produce the active ingredients of marijuana better than the plant.*** **Laframboise, S*** (2019; Massive Science; https://massivesci.com/articles/yeast-weed-marijuana-thc-cbd-canabidiol-tetrahydrocannabinol-genetic-engineering/)

Oral Presentations

1. **BMI Seminar Day** (2024, Institutional; PhD Work, Oral Presentation) **Laframboise, S***, Baetz, K. Uncovering the Role of *EAF1* in the Regulation of Pah1 and Nuclear Flares in *Saccharomyces cerevisiae.*
2. **Ottawa Institute of Systems Biology Conference** (2022, Institutional; PhD Work, Oral Presentation, **1st Place Award)** **Laframboise, S***, Baetz, K. Uncovering the Role of *EAF1* in the Regulation of Pah1 and Nuclear Flares in *Saccharomyces cerevisiae.*
3. **BMI Seminar Day** (2022, Institutional; PhD Work, Oral Presentation, **1st Place Award)** **Laframboise, S***, Baetz, K. Uncovering the Role of *EAF1* in the Regulation of Pah1 and Nuclear Flares in *Saccharomyces cerevisiae.*
4. **BMI Seminar Video Day** (2020, Institutional; PhD Work, Video Presentation, **1st Place Award)** **Laframboise, S***, Baetz, K. Uncovering the Role of *EAF1* in the Regulation of Pah1 and Nuclear Flares in *Saccharomyces cerevisiae.*
5. **Cell Biology Student Seminar Series** (2019; Institutional; MSc/PhD work, Oral Presentation) **Laframboise, S***, Baetz, K. Uncovering the Role of *EAF1* in the Regulation of Pah1 and Nuclear Flares in *Saccharomyces cerevisiae.*
6. **Stockholm University Public Defence** (2018; Institutional; BSc work; Defence Oral Presentation) **Laframboise, S*,** Karlström, V, Öhman, K. (2018) Identifying A to I RNA Editing in Differentiated SH-SH5Y Cells.

Poster Presentations

Title: Uncovering the Role of *EAF1* in the Regulation of Pah1 and Nuclear Flares in *Saccharomyces cerevisiae.* **Laframboise, S***, Baetz, K. (MSc/PhD work)

1. **Canadian Society of Molecular Biosciences Conference** (2023; International; PhD work; Poster)
2. **BMI Symposium** (2023; Institutional; PhD work; **1st Place Prize;** Poster)
3. **Canadian Society of Molecular Biosciences Conference** (2022; International; PhD work; Poster)
4. **BMI Symposium** (2022; Institutional; PhD work; Poster)
5. **The Allied Genetics Conference** (2020; International; PhD Work, Video Poster and Poster Preview**, Travel Grant**)

6. **Faculty of Medicine Research Day** (2020; Institutional; PhD Work, Video Poster)
7. **Synthetic Biology Symposium 2.0** (2019; National; MSc work; Poster; **Travel Grant**)
8. **BMI Graduate Student Research Day** (2019; Institutional; **3rd Place Prize;** MSc work; Poster)
9. **Canadian Society of Molecular Biosciences Conference** (2019; International; MSc work; Poster)
10. **Ottawa Institute of Systems Biology Conference** (2019; Institutional; MSc work; Poster)

Speaking Engagements and Media Appearances

A. News:

1. *"Trudeau's science funding feint angers Canadian researchers".* September 1st, 2023. Times Higher Education: https://www.timeshighereducation.com/news/trudeaus-science-funding-feint-angers-canadian-researchers
2. *Canada's Graduate Students Crippled by Wages That Haven't Risen Since 2003*. February 17th, 2023. Chemistry World Magazine: https://www.chemistryworld.com/news/canadas-graduate-students-crippled-by-wages-that-havent-risen-since-2003/4017008.article
3. *"Have Canada Lost It's Science Game".* January 18th, 2023. TVO's The Agenda with Steve Paikin: https://www.tvo.org/video/has-canada-lost-its-science-game
4. *"Canada's grants for master's, PhD students haven't increased since 2003. These researchers want that changed"* December 24th, 2022. CBC News: https://www.cbc.ca/news/science/graduate-student-research-funding-nserc-sshrc-cihr-1.6692545?fbclid=IwAR3tJGbKpOHUvEjG92vwGm6Ph4AQe6A2crB9AXSijfDjcyBeJZMVpEHOLkQ
5. *"Ottawa grad students, postdocs facing 'huge financial burden'"* August 20th, 2022. CBC News: https://www.cbc.ca/news/canada/ottawa/graduate-students-affordability-living-costs-1.6551913
6. *"Mécontents du financement accordé aux jeunes chercheurs"* August 11th, 2022. Le Droit: https://www.ledroit.com/2022/08/10/mecontents-du-financement-accorde-aux-jeunes-chercheurs-d4f4fa2df730bec7864b24690ea0fd18
7. *"Scientists march on Parliament Hill with 60-metre-long open letter demanding pay raises"* August 11th, 2022. The National Post: https://nationalpost.com/news/canada/scientists-to-present-60-metre-long-open-letter-to-federal-government-demanding-raise
8. *"Despite love for her program, this grad student says the financial strain weighs on her"* August 11th, 2022. CBC Atlantic: https://www.cbc.ca/player/play/2062933571612
9. *"The "Support our Science" movement pushes to boost funding for young scientists"* August 11th, 2022. Ottawa Morning Radio with Robyn Bresnahan; https://www.cbc.ca/listen/live-radio/1-100-ottawa-morning/clip/15930177-grad-students-postdocs-rally-increased-funding
10. *"Scientists urge Ottawa to boost grant funding so researchers can earn 'living wage'"* Global News: https://globalnews.ca/news/9053816/canadian-scientists-urge-grant-funding-increase/

11. *"Better Support for Scientists"* CTV National News: https://www.supportourscience.ca/post/nightly-news-ctv-national-news-better-support-for-scientists-2-05
12. *"Politics Briefing: Canadian researchers and scientists march for better compensation"* Globe and Mail: https://www.theglobeandmail.com/politics/article-politics-briefing-canadian-researchers-and-scientists-march-for-better/

B. Government Engagements:

1. **Press Conference** – Hosted by Research Canada. October 5th 2023. https://www.cpac.ca/headline-politics/episode/coalition-of-research-orgs-hold-a-news-conference--october-5-2023?id=a1cd6c5b-d89c-47af-a4df-f51190633a87
2. **Witness** - *House of Common's Standing Committee on Science and Research, Graduate Student and Postdoctoral Scholars Funding*. May 2023. (Record: https://www.ourcommons.ca/documentviewer/en/44-1/SRSR/meeting-43/minutes - Final Report here: https://www.ourcommons.ca/DocumentViewer/en/44-1/SRSR/report-8/)
3. **Press Conference** – Hosted by MP Maxime Blanchette Joncas. May 1st 2023
4. **Guest** – *Senate appearance and introduction in the Chambers with Senator Stan Kutcher*, November 2022.
5. **Witness** - *Advisory Panel on the Federal Research Support System*. November 2022.
6. **Advisor** - *Our Visions for Science: Perspectives from the Chief Science Advisor of Canada's Youth Council* (Final Report here: https://science.gc.ca/site/science/en/office-chief-science-advisor/ocsas-youth-council-csa-yc/our-vision-science-perspectives-chief-science-advisor-canadas-youth-council)
7. **Witness** - *House of Common's Standing Committee on Science and Research, Top Talent.* May 2022. (Record: https://www.ourcommons.ca/DocumentViewer/en/44-1/SRSR/meeting-11/minutes - Final Report here: https://www.ourcommons.ca/Committees/en/SRSR/StudyActivity?studyActivityId=11578584)

C. Podcasts:

1. **The Science Pawdcast** - *Season 5 Episode 43: Horned Snakes, Wolf Microbes, and Sarah Laframboise on Yeast Power* – December 14, 2023: https://www.buzzsprout.com/413041/14151521-season-5-episode-43-horned-snakes-wolf-microbes-and-sarah-laframboise-on-yeast-power
2. **Canadian Science Policy Centre** - *SciPol Digest: A Deep Dive into the Advisory Panel on the Federal Research Support Systems.* July 24, 2023: https://open.spotify.com/episode/4ZikYZvfDNbraElyjRfBZP
3. **Quirks and Quarks with Bob McDonald** - *The "Support our Science" movement pushes to boost funding for young scientists.* Oct. 8, 2022: https://www.cbc.ca/listen/live-radio/1-51-quirks-and-quarks/clip/15941238-the-support-science-movement-pushes-boost-funding-young
4. **Metaphorigins Podcast:** *S3E2 - Handy Hindrances & Academic Ghostwriting With Sarah Laframboise.* 2021: https://metaphorigins.buzzsprout.com/949765/7943878-s3e2-handy-hindrances-academic-ghostwriting-with-sarah-laframboise-phd-student

D. Panels and Non-Academic Presentations (up until November 2023):

1. "Impact of Science and Innovation on Society" **Canadian Science Policy Centre.** November 2023
2. *"Science Policy and Evidence Based Decision Making"* Featuring Senator Stan Kutcher. **Canadian Society for Molecular Biology Conference**. June 2023.
3. *"Ethical Considerations for SciComm"* **SciCommCon Canada.** July 2023.
4. *"How to pursue a career in Science Policy?"* **Faculty of Medicine, University of Ottawa Career Day.** February 2023.
5. *"Funding for the Future of Science and Research."* Featuring Senator Stan Kutcher. **University of Ottawa, Faculty of Medicine.** September 2022.
6. *"The Bromley Memorial Event"* Student Respondent to Dr. Mona Nemer, Canada's Chief Science Advisor. **Institute for Science, Society and Policy.** April 2022.

Work Experience

Executive Director / Evidence for Democracy - *November 2023 to Present*

- Serve the public face and internal leader of Evidence for Democracy (E4D) is the leading non-partisan, not-for-profit organization championing evidence in government decision-making in Canada. Through original research, skills training, and advocacy campaigns, we foster public demand for transparent and evidence-informed policy-making. By equipping the science community with tools and knowledge, we empower them to take an active role in democracy and bridge the gap between science and policy.
- Manage a team of 5 employees in the execution of over $500,000 in operating funding, grants, projects and fundraising,
- Regularly provide training and public speaking to a variety of audiences, ranging from next generation researchers and the general public.
- Perform lobbying activities in direct support of the research ecosystem in Canada, advocating to transparency and scientific integrity amongst the federal government.

Freelance Writer and Science Communicator / Sarahlaframboise.ca - *April 2020 to Present*

- Write pieces related to science and technology for various media outlets, and internal content for companies.
- Provide graphic design for social media, websites, newsletters, and more.
- Develop compiled reports, documents, journals, and magazines for companies.

Part-Time Student, Office of VP Research, Grants and Scholarships / Natural Sciences and Engineering Research Council (NSERC) - *February 2022 to May 2023*

- Assisted the VP of Research, Grants and Scholarship by delivering speaking notes and assistance during presentations.
- Assisted in the implementation of NSERC's Leaders meetings, featuring nearly 100 representatives from Canadian Universities.
- Worked with a team to develop a video competition for the International Year for Basic Science for Sustainable Development.

Program and Communications Manager / Canadian Science Policy Centre (CSPC) - *February 2022 to May 2023*

- Managed all CSPC volunteer committees and worked alongside Chairs to develop CSPC programs throughout the year and delivered the Canadian Science Policy Conference.
- Managed CSPC's social media accounts, including X (Twitter), LinkedIn, and Facebook.
- Developed branded advertisements, infographics, newsletters, and graphics.
- Managed several of CSPC's stakeholders and partners, through delivery of partner advertisements.

Significant Volunteer Experience

Co-Founder, Executive Director and Member of the Board of Directors/ Support Our Science - *May 2022 to Current*

- Serve as the public face of Support Our Science and represent the organization in media, government relations and stakeholder meetings.
- Developed a website, blog and resource database for the Support Our Science movement.
- Developed governance, internal structure, financial plans, budgets and organizational plans for Support Our Science.
- Successfully executed two walkout/rallies in Ottawa on Parliament Hill, as well a Nationwide Walkout on May1st at 46 different institution in Canada with over 10,000 participants.
- Collaborated with various organizations, students, and faculty to deliver an official petition to the House of Commons which received over 3500 signatures in 2022. Subsequently completed 3 additional petitions through the summer of 2023 with cross party support.
- Represented Support Our Science in several meetings with MPs and Minister's, including Minister Champagne and Minister Freeland.

Member / Canada's Chief Science Advisor's Youth Council - *June 2023 to November 2023*

- Provide a youth perspective to the intersection of science, society and policy as it pertains to providing advice and recommendations to Canada's Chief Science Advisor, Dr. Mona Nemer.
- Meet with members of the youth council to develop relevant policies, reports and briefings on topical issues in Canada.

Founder and President / Ottawa Science Policy Network - *March 2021 – June 2023*

- Coordinated and managed a team of 50 students passionate about science policy, running bi-weekly meetings and creating yearly reports on OSPN.
- Developed and launched a national survey investigating graduate student finances which received over 1300 responses from graduate students across Canada.
- Hosted workshops and events to train students in science policy, advocacy, and diplomacy.
- Formed an institutional partnership with the Institute for Science, Society and Policy (ISSP) at the University of Ottawa, and now serve on the leadership committee for ISSP.

Editor-In-Chief / Co-Chair, Editorial Committee Member / Canadian Science Policy Centre - *March 2018 to November 2023*

- Chief editorial staff for the Canadian Science Policy Centre (CSPS) magazine, website and editorials. This includes logistical coordination of over 30 web editorials, 25 magazine articles, and more, every year.
- Oversee the volunteer editorial team by coordinating bi-weekly meetings and training opportunities for members.
- Developed 4 editions of the highly successful Canadian Science Policy magazine, including recruitment of authors, editing written pieces, and full graphic design of the magazine.

President / Biochemistry, Microbiology and Immunology Graduate Student Association (BMIGSA) - *May 2019 to September 2022*

- Coordinated all academic and social activities within the Department, while managing a team of 10+ executive members.
- Represented and advocated for graduate students in Faculty of Medicine and Department of Biochemistry, Microbiology and Immunology.
- Previously, served as a student representative organizing outreach activities for our students to get more involved in our community.

Production Director / University of Ottawa Journal Of Medicine - *September 2019 to September 2021*

- Compiled all graphic design elements, articles, and advertisements for 3-5 issues per year, publishing over 15 issues.
- Served on the executive committee for the journal and contributed to the development of production schedules and procedure.

Volunteer Teacher and Mentor / Let's Talk Science - *September 2018 to September 2021*

- Participated in 3 classroom visits a semester for local schools, providing science related programing and experiments.
- Participated in a week long Northern Aboriginal teaching trip to Deer Lake, ON. Provided 5 hours of programing each day.
- Provided mentorship through the Aboriginal Mentorship Program (AMP) helping students from local Indigenous communities develop science fair projects through a 5-month mentorship program.

Professional Development

Conferences

- Attendee. **Better Evidence Conference. (2024)**
- Attendee. **Bromley Memorial Lecture, Institute for Science, Society and Policy and George Washington University.** (2022, 2023)
- Attendee. **Science Writer and Communicators of Canada Conference.** (2023)
- Attendee. **Research Money Conference.** (2022, 2023, 2024)
- Attendee. **Canadian Science Policy Centre Conference**. (2019, 2020, 2021, 2022, 2023)
- Attendee. **ComSciCon Canada.** (2021)

Certificates and Courses

- Zeiss Microscopy Course (2019)
- Created Science Communication Videos on Yeast and Research (2018, 2019)
- Science advocacy training for CSMB members by Evidence for Democracy (2018)
- Bench, Biz, and Beyond: The Basics of Research Commercialization series participant
- Community Outreach and Media Relations in the Sciences (2019)
- Bioethics: The Law, Medicine, and Ethics of Reproductive Technologies and Genetics (2019)